LAMINAR HEAT TRANSFER TO NON-NEWTONIAN FLUIDS IN PIPES WITH ABRUPT CHANGES IN DIAMETER

by

ENYINNA.H. OHUONU, B.Sc., M.Eng.

A Thesis submitted in fulfilment of
the requirements for the degree of
Doctor of Philosophy

The University of Aston in Birmingham
Faculty of Engineering
Department of Mechanical Engineering

1975

ACKNOWLEDGEMENTS

The author wishes to express his sincere thanks to Professor A. J. Ede for the opportunity, guidance and encouragement in carrying out this investigation.

He is also much indebted to the Director of the National Engineering Laboratory, East Kilbride, (Department of Trade and Industry) for the financial support, loan of equipment and advice on technical problems.

The author also wishes to express his gratitude to the Senate and staff of the University of Aston in Birmingham for providing the facilities and very cooperative technical assistance without which this work would not have been possible.

Last but not least, many thanks are due to Professor Fujii (Visiting Professor) whose private communication on many aspects of this work proved very valuable.

..... to my mother Nwannediya

SUMMARY

In this thesis the results of experimental work performed to determine local heat transfer coefficients for non-Newtonian fluids in laminar flow through pipes with abrupt discontinuities are reported. The fluids investigated were water-based polymeric solutions of time-indpendent, pseudoplastic materials, with flow indices 'n' ranging from 0.39 to 0.9. The tube configurations were a 3.3 : 1 sudden convergence, and a 1 : 3.3 sudden divergence. The condition of a prescribed uniform wall heat flux was considered, with both upstream and downstream tube sections heated.

Radial temperature traverses were also undertaken primarily to justify the procedures used in estimating the tube wall and bulk fluid temperatures and secondly to give further insight into the mechanism of heat transfer beyond a sudden tube expansion.

A theoretical assessment of the influence of viscous dissipation on a non-Newtonian pseudoplastic fluid of arbitrary index 'n' was carried out. The effects of other secondary factors such as free convection and temperature-dependent consistency were evaluated empirically. In the present investigations, the test conditions were chosen to minimize the effects of natural convection and the estimates of viscous heat generation showed the effect

to be insignificant with the polymeric concentrations tested here.

The final results have been presented as the relationships between local heat transfer coefficient and axial distance downstream of the discontinuities and relationships between dimensionless wall temperature and reduced radius. The influence of Reynolds number, Prandtl number, non-Newtonian index and heat flux have been indicated.

NOMENCLATURE

a	General constant defined in text	[-]
a_i	Eigenvalues in equation (220)	[-]
A	General constant defined in text	[-]
B	General constant defined in text	[-]
B_i	Coefficients in equation (220)	[-]
B'_i	Coefficients in equation (224)	[-]
Br_m	Modified Brinkman number = $(R\tau_w^N/\dot{Q}_w K_N^{N-1})$	[-]
C, c	General constant defined in text	[-]
Cp	Specific heat capacity at constant pressure	[kJ/kg ^oK]
D	Diameter of tube	[m]
f	Frictional factor	[-]
F	Body force	[N]
g	Gravitational acceleration	[ms^{-2}]
G_o	Constant defined in equation (55)	[-]
Gr	Grashof number = $(D^3 g\rho^2(t_w - t_b)/\mu^2)$	[-]
Gz	Graetz number = (WC_p/kL)	[-]
h	Coefficient of heat transfer	[W/m^2 ^oK]
h_m	Mean value of h	[W/m^2 ^oK]
h_z	Local value of h	[W/m^2 ^oK]
h_∞	Value of h at large axial distances	[W/m^2 ^oK]
H	Specific enthalpy or	[kJ/kg]
	Heat generation parameter defined by equation (59)	[W/m^3]
I_m	Modified Bessel function in equation (76)	[-]
k	Thermal conductivity	[$W/m\,^oK$]

k_l	Thermal conductivity of suspending medium	[W/m^oK]
k_p	Thermal conductivity of dispersed particles	[W/m^oK]
k_s	Thermal conductivity of overall suspension	[W/m^oK]
K	Absolute temperature (Kelvin)	[^oK]
K_N	Fluid consistency	[NS^n/m^2]
K'_N	Fluid consistency = $(K_N(3n+1/4n)^n)$	[NS^n/m^2]
L	Axial length of tube	[m]
Leq	Equivalent length	[diameters]
Leff	Effective increase in tube length = $\left(\frac{1}{L}\int_0^L h\ dz\right)$	[diameters]
$\dot{m}$	Mass flow rate	[kg/s]
M	The ratio of two viscosities (μ_o/μ_∞)	[-]
n	Non-Newtonian flow behaviour index as defined by equation (4)	[-]
n '	Non-Newtonian flow behaviour index as defined by equation (23)	[-]
N	Non-Newtonian flow behaviour index as defined by equation (189)	[-]
Nu	Nusselt number	[-]
Nu_{fd}	Nusselt number under fully developed conditions	[-]
Nu_m	Mean Nusselt number	[-]
Nu_l	Local Nusselt number	[-]
Nu_q	Nusselt number as defined by equation (120)	[-]
Nu_z	Local Nusselt number	[-]

N'_u	Nusselt number corrected for variable viscosity	[-]
Nu^*	Ratio of Nusselt numbers = Nu (gradual entry theory) / Nu (contracted flow experiment)	[-]
p	Static pressure	[N/m^2]
Pr	Prandtl number = (μ Cp/k)	[-]
Pr'	Generalised Prandtl number = (γ Cp$(U_m/D)^{n-1}$/k)	[-]
q	Rate of heat flow through insulation to outside of pipe wall, per unit area of latter	[W/m^2]
$\dot{q}$	Heat flux in equation (82)	[W/m^2]
Q	Volumetric flow rate	[kg/m^3s]
$\ddot{Q}$	Rate of heat generation in pipe wall, per unit volume	[W/m^3]
$\dot{Q}$	Constant wall heat flux	[W/m^2]
r	Radial coordinate	[m]
R	Radius of tube	[m]
Re	Reynolds number = ($\rho U_m D/\mu$)	[-]
Re_{cr}	Critical Reynolds number in equation (51)	[-]
Re'	Generalized Reynolds number = $(8U_m^{2-n}D^n\rho/K_N(6n+2/n)^n)$	[-]
S	Diameter ratio = (D_2/D_1)	[-]
t	Dimensionless temperature as defined by equation (78)	[-]
T	Temperature	[^oC]
u, U	z-component of velocity	[m/s]
U_m	Mean axial velocity	[m/s]

V	Applied voltage (volts)	[V]
W	Mass flow rate	[kg/s]
$\dot{W}$	Rate of viscous energy generation per unit volume = ($2\tau_w U_m/R$)	[W/m^3]
x_v	Volume fraction of dispersed particles	[-]
x_{vb}	Volume fraction of solid particles in a sedimented bed	[-]
y	Radial distance from tube wall = $(r-r_w)$	[m]
	or dimensionless distance from pipe wall as defined by equation (77)	[-]
z, Z	Axial distance from the tube entrance	[m]
Z^+	Dimensionless distance parameter = $(N\alpha z/R^2 U_m(N+2)$	[-]
Z_o	Dimensionless distance = $(2z/D_i\ Re)$	[-]
Z_1	Axial distance with reference to upstream tube	[m]
Z_2	Axial distance with reference to downstream tube	[m]
Z'	Stability criterion as defined by equation (51)	

GREEK SYMBOLS

α	Thermal diffusivity = $(k/\rho Cp)$	[-]
β	Contraction ratio; or as defined by equation (78)	[-]
β_v	Velocity gradient at the wall	[sec^{-1}]
δ	Correction for non-Newtonian behaviour = $(3n'+1/4n')$	[-]
ξ	Dimensionless radius = (r/R)	[-]

λ	Coefficient of thermal expansion	[$1/^{o}K$]
θ	Dimensionless temperature = $(T-T_{bi}/\dot{Q}R/k)$	[-]
$\psi(H)$	Temperature factor as defined by equation (188)	[-]
η	Apparent viscosity as defined by equation (50)	[NS/m^2]
ρ	Density	[kg/m^3]
τ	Shear Stress	[N/m^2]
μ	Dynamic viscosity	[kg/ms]
ν	Kinematic viscosity	[m^2/s]
γ	Fluid consistency parameter = $8K_N^{n-1}\Delta^n$	[Ns^{2-n}/m^2]
$\dot{\gamma}$	Rate of shear	[sec^{-1}]
Δ	Correction for non-Newtonian behaviour = $(3n+1/4n)$	[-]
ΔP	Pressure difference	[-]
ΔT	Temperature difference between tube wall and fluid	[^{o}K]
δT	Temperature difference between the top and the bottom surface of tube	[^{o}K]

SUBSCRIPTS

1	Upstream of change of tube diameter
2	Downstream of change of tube diameter
b	Bulk
f	Film
fd	Fully developed
i	Inlet
m	Mean

max	Maximum
min	Minimum
o	Outlet
r	Radial
w	Wall
z	Local (at axial position z)

N.B.

Notations, other than the above, have been defined wherever they have been used in the text.

CONTENTS

CHAPTER ONE

INTRODUCTION

The present investigation on heat transfer in non-Newtonian liquids has been carried out in the Department of Mechanical Engineering of the University of Aston in Birmingham, under the terms of an Extra Mural Research Agreement with the Department of Trade and Industry. In common with all such contract-based investigations, the scope of work and the choice of equipment has been greatly influenced not only by the terms of the contract, but also, by the time and finance available.

The initiation of this project is a further recognition of the odd fact that, although in most chemical and process industries the so-called anomalous or "non-Newtonian" fluids are the most frequently encountered, the special problems involved have so far received scant attention, at least, from the point of view of a heat transfer engineer. This neglect becomes significant when it is realised that, as reported in some recent surveys, a breakdown of capital expenditure on process plant indicates that for the average large project, heat exchangers as such account for some 6½% of capital invested. This figure is

7-12% for petroleum refinery plants. For those industries involved in processing viscous materials, capital has to be invested in heat exchangers dealing with such materials and since the size of the exchanger will be almost completely dictated by heat transfer between the viscous medium and an adjacent wall, it becomes of paramount importance that accurate design procedures should be readily available.

A large number of studies have already been devoted to the investigation of the process of heat transfer during the movement of a Newtonian fluid in tubes. This is one of the most important aspects of the subject of heat transfer, and often plays a fundamental part in the operation of plant and machinery in engineering processes.

The greater part of existing and available data relates to flow of such fluids in straight continuous pipes, whereas, in practice, most flows would have to be controlled by valves and directed through elbows and other such passages in the circuit. These give rise to discontinuities in the flow which in some ways affect the local heat-transfer coefficients of the fluid.

Most of the Newtonian fluids studied have been air and water and little work has been done using viscous fluids.

Not until quite recently has there been any serious attempt to study the effects of abrupt discontinuities on heat transfer characteristics of fluids flowing through heated conduits. The scarcity of data on this aspect of heat transfer applies to both the most commonly studied air and water and the more viscous liquids such as oils.

The foregoing picture reflects very clearly the uniqueness of the experimental investigations, which is reported here. One of the main objectives of this research is the correlation of data regarding the effects of abrupt changes in diameter on local heat transfer coefficients for non-Newtonian systems. The results to be presented will therefore not only furnish much needed data on the effects of abrupt discontinuities on heat transfer processes between fluid and pipes, but also further our knowledge in the hitherto scantily explored field of non-Newtonian heat transfer.

CHAPTER TWO

STATEMENT OF BROAD OBJECTIVES

This work represents part of a wider project initiated at the National Engineering Laboratory, East Kilbride, to investigate those little explored areas of the heat-transfer field in which distrubed regions of flow arise, or where fluids of viscous or non-Newtonian nature occur - particularly in piped flows.

The main objective is the measurement of local heat transfer coefficients in pipes downstream of discontinuities, especially abrupt changes of diameter, in fluids having significant non-Newtonian properties.

It is also intended, if the time is available, to make temperature and velocity traverses across the flow.

The investigation will be specifically concerned with the class of non-Newtonian fluids known as pseudoplatics or "power law" fluids. A pseudoplastic fluid generally is defined as one which has a viscosity that decreases reversibly with increasing shear rate, which has no yield value, and which undergoes no time-dependent change in consistency.

Non-Newtonian behaviour in liquids is characterised by two parameters: (i) the flow behaviour index 'n' and

(ii) the consistency factor 'K_N'.

The series of liquids to be considered will have flow behaviour indices ranging from n = 0.4 to 0.9. For Newtonian fluids n = 1.0 and $K_N = \mu$; where μ is the coefficient of viscosity.

The flow regime contemplated is the Laminar Region, that is, with Reynolds Numbers in the range 1 to 2100.

The configurations to be considered are, (i) a tube having a sudden increase in diameter, the proposed diameter ratio being 1:3 and (ii) a tube having a sudden decrease in diameter, the proposed ratio being 3:1.

These investigations will include an assessment of the way in which the rate of heat transfer is affected by the variation in fluid consistency with temperature and the viscous dissipation of mechanical energy in the fluid. Attempts will be made to eliminate the effects of natural convection but where free convection becomes significant, suitable corrections will be made to the experimental data.

CHAPTER THREE

PHENOMENON OF NON-NEWTONIAN BEHAVIOUR IN FLUIDS

A brief review of the rheology of non-Newtonian fluids will be very useful in the understanding of the nature of this project, and the special features of practical engineering interest.

3.1 FLUID CLASSIFICATION

In the familiar Newtonian fluids, shear stress is directly proportional to the velocity gradient (in laminar flow).

This equation may be written as

$$\tau = \mu \, du/dy = \mu\dot{\gamma} \qquad (1)$$

where the constant of proportionality, μ, is called the Newtonian viscosity.

The Newtonian viscosity, μ, depends only on temperature and pressure and is independent of the rate of shear. The diagram relating shear stress and rate of shear for Newtonian fluids, the so-called "flow curve", is therefore a straight line of slope μ as in Fig.1 (Appendix 1) and the single constant, μ, completely characterizes the fluid.

Newtonian behaviour is exhibited by fluids in which the dissipation of viscous energy is due to the collision of comparatively small molecular species. All gases and liquids and solutions of low molecular weight come into this category. Notable exceptions are colloidal suspensions and polymeric solutions where the molecular species are large. These fluids show marked deviations from Newtonian behaviour.

3.1.1 NON-NEWTONIAN FLUIDS

In laminar Newtonian flow the material may be considered as laminae which slide over one another with no internal strain. Non-Newtonian characteristics arise when elements within the fluid interact resulting in an additional energy dissipation which is a function of the rate of shearing strain and which depends occasionally on the previous history. The flow curve for such fluids is therefore not linear, i.e. the "viscosity" of a non-Newtonian fluid is not a constant at a given temperature and pressure but depends on other factors such as the rate of shear in the fluid, the apparatus in which the fluid is contained or even on the previous history of the fluid.

These real fluids for which the flow curve is not linear may be classified into three broad types:

(i) fluids for which the rate of shear at any point is some function of the shearing stress at that point and depends on nothing else;

(ii) more complex systems for which the relation between shear stress and shear rate depends on the time the fluid has been sheared or on its previous history;

(iii) systems which have characteristics of both solids and liquids and exhibit partial elastic recovery after deformation, the so-called viscoelastic fluids.

a) Time-Independent Non-Newtonian Fluids

Fluids of the first type whose properties are independent of time may be described by a rheological equation of the form

$$\dot{\gamma} = \frac{du}{dy} = f(\tau) . \qquad (2)$$

This equation implies that the rate of shear at any point in the fluid is a simple function of the shear stress at that point. Such fluids may be termed non-Newtonian viscous fluids.

These fluids may be subdivided into three distinct types depending on the nature of the function

in equation (2). These types are

(i) Bingham plastics

(ii) Dilatant fluids

(iii) Pseudoplastic fluids

Typical flow curves for these three fluids are shown in Fig.2 (Appendix 1).

Bingham plastics are fluids which exhibit a definite yield strength: below this stress no flow occurs. At stresses above the yield value the behaviour is Newtonian. The constitutive equation for a Bingham plastic is

$$\tau_{yx} - \tau_y = \mu\dot{\gamma} \quad . \qquad (3)$$

Dilalant fluids are those which show shear thickening, an increase in viscosity with increasing rate of strain. There are few data on dilatancy in the rheological literature so that constitutive equations useful for engineering design, have not been proposed. However, for most practical purposes, the power law associated with pseudoplastic fluids, is often applicable, but in this case the index n is greater than unity.

By far the most important class of time-independent non-Newtonian fluids are the pseudoplastics. These fluids do not show a yield point but exhibit shear

thinning - a decrease in viscosity with increasing shear rate. The typical flow curve for these materials indicate that the ratio of shear stress to the rate of shear, which may be termed the "apparent viscosity", μ_a , falls progressively with shear rate and the flow curve becomes linear only at very high rates of shear. This limiting slope is known as the viscosity at infinite shear and is designated μ_∞.

The logarithmic plot of shear stress and rate of shear for these materials is often found to be linear with a slope between zero and unity.

As a result, an empirical functional relation known as the POWER LAW is widely used to characterize fluids of this type. This relation, which was originated by OSWALD (140) and has since been fully described by REINER (149), may be written as

$$\tau = K_N \dot{\gamma}^n \qquad (4)$$

where K_N and n are constant ($n < 1$) for the particular fluid: K_N is a measure of the consistency of the fluid, the higher K_N the more viscous the fluid; n is a measure of the degree of non-Newtonian behaviour, and the greater the departure from unity the more pronounced are the non-Newtonian properties of the fluid.

b) Time-Dependent Non-Newtonian Fluids

The foregoing discussion has been concerned with fluid behaviour which is essentially time-independent. However, many real fluids cannot be described by a simple rheological equation such as Equation (2).

The apparent viscosity of more complex fluids depends not only on the rate of shear but also on the time the shear has been applied. These fluids may be subdivided into two classes:

(a) Thixotropic fluids

(b) Rheopectic fluids

according as the shear stress decreases or increases with time when the fluid is sheared at constant shear rates.

If the shear stress decreases with time the liquids are said to be thixotropic; where shear stress increases with time, the liquid is said to be rheopectic.

Thixotropy is a reversible process. If a thixotropic material is sheared at a constant rate after a period of rest, the structure will be progressively broken down and the apparent viscosity will decrease with time. However, after resting, the structure of the material builds up again gradually, and if the flow curve of a thixotropic material is determined immediately after

shearing and after it has rested for varying times after shearing the result is as in Fig.3 (Appendix 1).

Rheopectic fluids present an opposite picture to thixotropy. In this case, there is a gradual formation of structure by shear, whereas so far the properties of structured materials have been explained on the basis that shearing tends to destroy structure.

In practice the occurrence of rheopectic liquids is quite rare and is limited to certain solutions.

c) Visco-Elastic Fluids

In view of the increasing range of materials which exhibit other rheological behaviour this section will be concluded with a brief account of visco-elastic fluids and other even more complex liquids which are the subject of limited investigation.

Visco-elastic liquids exhibit a combination of the properties of a purely viscous liquid and an elastic solid. The magnitude of a stress applied to them is not independent of time as in the case of an elastic solid, but is slowly reduced as viscous flow proceeds. However, if the stress is removed the substance will partially recover its original state by virtue of its elastic properties.

Any rheological equations devised to describe this phenomenon must make some allowance for this "memory" effect. This is normally accounted for by using equations which include not only shear stress and shear rate but also their time derivatives as well.

An equation, first proposed by MAXWELL (110) may be used to represent such fluids. This is given as

$$\dot{\gamma} = \tau/\mu_o + \dot{\tau}/G \qquad (5)$$

or we can write

$$\tau + \lambda_1\dot{\tau} = \mu_o\dot{\gamma} \qquad (6)$$

where

$$\lambda_1 = \mu_o/G \qquad (7)$$

μ_o is a constant Newtonian viscosity coefficient; G is a rigidity modulus.

The parameter λ_1 has the dimensions of time and is known as the relaxation time.

Liquids which are described by equation (6) are usually referred to as "Maxwell Liquids".

3.2 CHARACTERIZATION OF FLUIDS

At least two measurements must be made on any time independent non-Newtonian system in order to define its rheological properties. A Newtonian fluid requires only one i.e., the viscosity. The available techniques for determining n' and K'_N (or n and K_N) can be divided into two groups namely:

(i) Direct Methods Direct determination of the shear stress - shear rate relationship is achieved by subjecting the entire sample to a uniform rate of shear and shear stress in suitably designed and specialized instruments. These are called viscometers and can be of the cup-and-bob, coaxial cylinder or cone-and-plate type.

(ii) Indirect Methods The relationship between stress and shear is inferred from observations on the pressure gradient and volumetric flow rate in a straight pipe or capillary tube viscometer. In such devices, the shear rate is not constant, but varies from zero at the centre of the tube to a maximum value at the wall. As a consequence mathematical interpretation of the results is indirect and complex.

3.2.1 CONCENTRIC CYLINDER ROTARY VISCOMETER

This instrument is designed to shear a fluid located in the annulus between two concentric cylinders, one of which (cup) is rotating while the other (bob) is held stationary. A series of measurements of the angular speed of the rotating cylinder and the torque applied to the stationary one can be interpreted to give the relationship between rate of shear and shear stress respectively. By keeping the annular gap between the two cylinders small (radius ratio < 1.050) the radial variation in shear rate is minimized. On the other hand, small gap widths give rise to viscious heating effects.

In addition, this instrument is subject to an end effect at the bottom of the cylinders where there is no free surface. This may be eliminated by repeating the experiments with another level of fluid in the gap and obtaining torque per unit height. Alternatively an 'effective length' is obtained by calibrating the instrument with a Newtonian fluid of known viscosity. For a given torque $\dot{G}$, and bob radius R_b, the shear stress at the surface of the bob is given by

$$\tau = \dot{G}/2\pi R_b^2 L_{eff} \qquad (8)$$

If the annular gap is very small, the shear rate approaches a constant value across the annulus and is given by

$$\frac{du}{dr} = \frac{2\pi R\Omega}{R_c - R_b} \qquad (9)$$

where Ω is the rotational speed of the cup. By plotting the rate of shear against the corresponding shear stress a flow curve is obtained.

A general treatment of rotational instruments is given by REINER (149) whilst modified viscometers have been described by WELTMANN (199) and McKENNEL (130). The coaxial viscometer is generally regarded as having a low order of accuracy - a point of view not shared by WELTMANN, but it is still widely used in industry.

3.2.2 CONE AND PLATE VISCOMETER

The Schematic diagram in Fig.4 (Appendix 1) shows the basic principle of this instrument. It consists essentially of a flat, horizontal plate and an inverted cone, the apex of which is in near contact with the plate. The angle between the plate and the cone surface is very

small - usually less than one degree - and the fluid sample is located in this thin gap. Temperature control is often applied to the lower plate. The sample of fluid under shear is so thin that constancy of shear rate is easily obtained. End effects are negligible because the height of the gap at the cone periphery is so small.

If the cone rotates at a constant speed Ω r.p.s., the linear velocity at r is $2\pi\Omega r$. The gap height at r is $r\tan\phi$. The magnitude of the shear rate at r is therefore

$$\frac{2\pi r\Omega}{r\ \tan\phi} = \frac{2\pi\Omega}{\tan\phi} \qquad (10)$$

The shear rate is thus constant (independent of r) in the range $0 \geqslant r \geqslant R$ and so the shear stress τ_{yx} must also be constant over this range.

Since ϕ is very small, $\tan\phi = \phi$ and equation (10) gives

$$\text{Shear rate} = \frac{2\pi\Omega}{\phi} \qquad (11)$$

The relationship between measured torque $\dot{G}$ and shear stress is given by

$$\dot{G} = 2\pi\tau_{yx}\int_0^R r^2\,dr$$

$$= \frac{2}{3}\pi R^3 \tau_{yx}$$

i.e.

$$\tau_{yx} = \frac{3\dot{G}}{2\pi R^3} \qquad (12)$$

The range of shear rates which can be explored with the cone-and-plate viscometer extends to reasonably high values, comparable to those attainable with the concentric cylinder type. Viscous heating effects have been shown to be negligible by TURIAN (195), McKENNEL(130) and SUTTERBY (183).

3.2.3 CAPILLARY TUBE VISCOMETER

A capillary viscometer was used in this investigation and has been described in detail under Section 7. The essential feature of this device is the measurement of the frictional pressure drop associated with the laminar flow of fluid at a given rate through a long, smooth, cylindrical tube of known dimensions. From a series of such measurements at various known flow rates, the values of n' and K'_N can be deduced, as discussed below.

METZNER and REED (116) have used the MOONEY (132)-RABINOWITSCH (146) equation for interpreting capillary tube data. The expression relates volumetric flow rate to the rate of shear at the wall of the pipe and is independent of fluid behaviour, provided that the fluid

is not time dependent.

$$-\left(\frac{du}{dr}\right)_w = 3\left(\frac{8Q}{\pi D^3}\right) + \frac{D\Delta P}{4L}\,\frac{d(8Q/\pi D^3)}{d(D\Delta P/4L)} \qquad (13)$$

Since $U_m = 4Q/\pi D^2$

$$-\left(\frac{du}{dr}\right)_w = \frac{3}{4}\left(\frac{8U_m}{D}\right) + \frac{1}{4}\left(\frac{8U_m}{D}\right)\frac{d/\ln(8U_m/D)}{d/\ln(D\Delta P/4L)} \qquad (14)$$

By substituting

$$n' = \frac{d/\ln(D\Delta P/4L)}{d/\ln(8U_m/D)} \qquad (15)$$

the expression becomes

$$-\left(\frac{du}{dr}\right)_w = \frac{3n' + 1}{4n'}\,\frac{8U_m}{D} \qquad (16)$$

From a force balance

$$\tau_w = D\Delta P/4L \qquad (17)$$

Combining equations (14), (15), (16) and (17) we get

$$\tau_w = K'_N\left(\frac{8U_m}{D}\right)^{n'} \qquad (18)$$

n' may be obtained from equation (15) by a log - log plot of $(D\Delta P/4L)$ against $(8U_m/D)$; $\left(\frac{du}{dr}\right)_w$ can then be evaluated.

If the slope of the graph is constant over a range of shear stress, equation (15) represents a straight line and hence n' would be a constant. A non-linear plot means that n' and K'_N must be evaluated as point values at the appropriate shear stress.

Certain corrections must always be made to the measurements obtained on a capillary tube viscometer. These take into account the following:

1. Head of fluid above tube exit
2. Kinetic energy losses
3. Tube entrance losses

RAO and KULOOR (148) have presented methods for evaluating these effects. Correction for tube wall "slip" if any, is given in text (17).

The instrument has the advantage of reaching higher rates of shear than are attainable in rotary viscometers, and also, errors resulting from temperature rise due to viscous dissipation are usually negligible. This is a consequence of the relatively short time spent by a given element of fluid in the capillary tube. It

is cheap to construct and temperature control can be achieved by enclosing the entire apparatus in a constant temperature bath.

3.2.4 TIME DEPENDENT FLUIDS

The curve of $\frac{Q}{\pi R^3}$ against $\frac{R\Delta P}{2L}$ is unique and independent of tube dimensions only if the fluid properties are independent of time. If, for instance, data for a thixotropic fluid were plotted in this way the result would be as in Fig.3 (Appendix 1) and more thixotropic breakdown would be indicated with longer pipes and smaller diameters, i.e. longer times of shear and higher rates of shear respectively. The reverse would be true of rheopectic materials. This method is unsatisfactory and the reader is referred to the method described by GREEN and WELTMANN (72) for the characterization of thixotropic materials.

3.2.5 VISCO-ELASTIC MATERIALS

Unlike an inelastic liquid a viscoelastic fluid under shear exerts stresses perpendicular to the streamlines in the plane of shear. ROBERTS (152) has developed a technique for the measurement of these normal stresses in a uniformly sheared specimen using a cone-and-plate viscometer. In another method the liquid is subjected to periodic shearing between coaxial cylinders, maintaining one in forced harmonic oscillation and measuring the

periodic torque on the other. The general theory applicable to these instruments has been given by OLDROYD (135). A summary of the methods for experimental characterization of visco-elastic fluids is given by WILKINSON (202).

3.3 RELATIONSHIP BETWEEN n, K_N and n', K'_N

The parameters n (as obtained from the cone - and - plate viscometer (equation (4)), and n' (as deduced from capillary tube measurements (equation (15)) are related as follows:

From equation (4)

$$\ell n \tau = \ell n\, K_N + n\, \ell n \left(- \frac{du}{dr}\right) \qquad (19)$$

$$\therefore \quad n = \frac{d(\ell n \tau)}{d\left[\ell n\left(- \frac{du}{dr}\right)\right]} \qquad (20)$$

From equation (15)

$$\frac{d\left[\ell n\left(- \frac{du}{dr}\right)_W\right]}{d(\ell n\, \tau_W)} = \frac{d(\ell n(3n'+1)/4n')}{d(\ell n\, \tau_W)} + \frac{d(\ell n\, 8U_m/D)}{d(\ell n\, \tau_W)} \qquad (21)$$

From (15) and (21)

$$\frac{1}{n} = \frac{1}{n'} + \frac{d\ \ell n\ (\frac{3n'+1}{4n'})}{d(\ell n\ \tau_w)} \qquad (22)$$

$$\therefore \qquad n = \frac{n'}{1 - \frac{1}{3n'+1}\ (\frac{dn'}{d\ \ell n \tau_w})} \qquad (23)$$

where n corresponds to the shear stress τ. If n does not vary with shear stress, i.e. if the logarithmic plot of $(D\Delta P/4L)$ vs $(8U_m/D)$ is linear, then

$$n = n' \qquad (24)$$

$$K'_N = K_N(\frac{3n+1}{4n})^n \qquad (25)$$

3.4 EFFECTS OF TEMPERATURE ON PSEUDOPLASTIC CHARACTERISTICS

In the case of Newtonian fluids, the viscosity may frequently be related to temperature by the empirical Arrhenius equation

$$\mu = A'\ e^{(E/R'\ T)} \qquad (26)$$

A modified empirical equation is

$$\mu = a'\ e^{(b'\ T)} \qquad (27)$$

where a' and b' are constants evaluated experimentally for

the Newtonian fluid in question.

The temperature dependence of the rheological properties of non-Newtonian fluids is unfortunately less well established. For suspensions, in which much of the viscous resistance to flow is due to mechanical interactions between particles, the dependence on temperature may be small and due only to the effect of temperature on the viscosity of the suspending medium. WELTMANN (199) has noted that temperature variation may produce anomalous changes in non-Newtonian behaviour, particularly if solids in suspension become more or less soluble or more or less completely dispersed with changes in temperature. METZNER (115) considered such anomalous behaviour relatively infrequent with non-Newtonian fluids.

For power low fluids, direct correction factors have been used by CHRISTIANSEN and CRAIG (30) and HANKS and CHRISTIANSEN (75). The expressions suggested by the former are given in equations (144) and (145). Another approach, by PHILIPPOFF and GASKINS (143) defined apparent viscosity variation with temperature, at constant shear stress or shear rate. In general

$$\left(\frac{\partial \mu_a}{\partial T}\right)_{\tau} \neq \left(\frac{\partial \mu_a}{\partial T}\right)_{\dot{\gamma}} \qquad (28)$$

and hence led to two activation energies E_{τ} and $E_{\dot{\gamma}}$. For a power law fluid

$$E_{\tau} = \frac{1}{n}(E_{\dot{\gamma}}) \qquad (29)$$

This approach has been useful for studies on molten polyethylene

METZNER (115) summarized the effects of temperature on n′ and K'_N as follows:

n′

"The flow-behaviour index n′ may be assumed independent of temperature and concentration for small changes in such conditions ....."

"The flow behaviour index ..... does not change rapidly for either temperature or concentration of dissolved material."

K'_N

"The viscosity or consistency indices K_N and K'_N frequently change as rapidly with temperature as the viscosity of the solvent or suspending

medium. For suspensions the ratio of K'_N to the viscosity of the suspending medium is frequently nearly constant for suspensions of given concentration ....."

"..... changes in K'_N with temperature are usually an order of magnitude greater than changes in n'."

SKELLAND (177) suggested that from the above considerations the quantity K'_N may be approximately related to temperature by the expression

$$K_N = 10^{A-Bt} \qquad (30)$$

as in the case of Newtonian fluids for which $K'_N = \mu$. Then n' may be represented by its average value over a moderate temperature change. The constants A and B in equation (30) would be established from the experimental data which would of course show whether a relationship of this type would be acceptable in any given case.

3.5 THERMOPHYSICAL PROPERTIES OF NON-NEWTONIAN FLUIDS

The thermophysical properties of interest in heat transfer problems are thermal conductivity, heat capacity and density.

All available data indicate that the thermal conductivity of single liquids is not influenced by rate of deformation. Even in highly viscous systems, where high shear rate may cause anisotropies in the liquid structure, this effect is unlikely to be of any real consequence in an engineering situation. Mixtures or slurries present a much more difficult problem. Except at low solids concentration (< 10%) predictions of thermal conductivities are not recommended and usually the only safe practice is to determine the parameter experimentally. For suspensions of inert solids in liquids, MAXWELL'S expression (equation 179) may be used under the assumed conditions of no relative motion of solid and fluid, symmetrical particles and concentrations sufficiently low to preclude significant interparticle contacts. Experimental confirmation have been reported in references (88), (139) and (187).

Data on specific heat (heat capacity) and density of non-Newtonian liquids cannot be obtained from usually available sources of technical information. These properties have to be determined by conventional means; hydrometric or pyconometric methods for density, and calorimetric techniques for specific heat.

For the fluids considered here, these properties may with slight error be assumed to be that of the "solvent" phase, in this case water. Experimental confirmation of

this expedient has been obtained in references (117) and (139).

CHAPTER FOUR

LITERATURE SURVEY

4. INTRODUCTION

In this Chapter, a review of the present state of knowledge on the fluid flow and heat transfer characteristics of non-Newtonian pseudoplastic liquids will be presented. The special problems confronting experimentalists will be highlighted and the most useful recommendations given by previous workers discussed. The proposed investigation will be mainly concerned with flow in circular pipes, and in consequence only those works dealing with isothermal and non-isothermal flow of pseudoplastic fluids in circular pipes will be reviewed here. It will be noted that analogous cases of Newtonian fluids are discussed whenever necessary. This is desirable, since the analytical procedures adopted for non-Newtonian heat transfer studies are usually extensions of the Newtonian formulation.

The format adopted is as follows:

In the first section of the survey (Section 4.1) the fluid flow aspect is considered. Expressions defining the steady isothermal flow of pseudoplastics are developed

and the earlier attempts to establish some criterion for laminar-turbulent transition examined. This is followed (in the same section) by a review of the limited theoretical studies in which the peculiar aspects of flow being investigated here (contracted or expanded flow) were considered. The related case of axisymmetric entrance region flow is then briefly discussed and the few analyses recognising the influence of non-isothermal fluid properties mentioned. This section is then concluded by an examination of reported experimental works on geometries similar to those used in this project. The remaining sections of the survey deal with studies on the main topic of heat transfer. In Section 4.2, the theoretical and experimental contributions reviewed refer primarily to undistrubed flow in straight tubes. The Chapter is then concluded, (Section 4.3) with comments on works of particular relevance to heat transfer investigations reported in this thesis.

4.1 NON-NEWTONIAN FLOW CHARACTERISTICS

4.1.1 Laminar Hydrodynamics in Pseudoplastic Fluids

For time-independent fluids, the rheological equation is

$$\dot{\gamma} = f(\tau) \qquad (2)$$

which, for pipe flow, reduces to

$$\dot{\gamma} = -\frac{du}{dr} = f(\tau) \tag{31}$$

where τ is now the shear stess at radius r. The negative sign indicates that the velocity decreases as the radius increases.

For steady isothermal axial flow of an incompressible fluid, the equation of motion may be integrated to give the shear stress distrubtion -

$$\frac{d}{dr}(r\tau_r) = (\frac{\Delta P}{L})\, r \tag{32}$$

Integrating

$$\tau_r = (\frac{\Delta P}{2L})\, r + \frac{C}{r} \tag{33}$$

For circular pipes

$$\tau_r\Big/_{r=0} = 0$$

$$\therefore \quad \tau_r = \frac{r\Delta P}{2L} \tag{34}$$

$$\tau_r\Big/_{r=R} = \tau_w$$

$$\tau_w = \frac{R\Delta P}{2L} \tag{35}$$

Therefore $\tau = \tau_w \cdot \frac{r}{R}$ and equation (31) becomes

$$\dot{\gamma} = -\frac{du}{dr} = f(\tau_w \cdot \frac{r}{R}) \tag{36}$$

Integrating we get

$$u(r) = \int_o^R f(\tau_w \cdot \frac{r}{R})\, dr \tag{37}$$

since $u(R) = 0$ if we assume no slip at the walls.

Further we have

$$Q = \int_o^R 2\pi r u(r)\, dr \tag{38}$$

or

$$Q = \pi \int_o^R u(r)\, d(r^2) \tag{39}$$

which on integrating by parts yields

$$Q = \pi \int_o^R r^2 f(\tau_w \cdot r/R) \quad \text{since } u(R) = 0.$$

Substituting $r = R\tau/\tau_w$ we get

$$\frac{Q}{\pi R^3} = \frac{1}{\tau_w^3} \int_o^{\tau_w} \tau^2 f(\tau)\, d\tau \tag{40}$$

For a power law fluid we have

$$\tau = K_N \left(\frac{du}{dr}\right)^n = K_N \dot{\gamma}^n \tag{4}$$

Therefore

$$\dot{\gamma} = f(\tau) = (\tau/K_N)^{1/n}$$

Hence

$$\frac{Q}{\pi R^3} = \frac{1}{K_N^{1/n}\,\tau_w^3}\int_0^{\tau_w} \tau^{2+\frac{1}{n}}\, d\tau \qquad (41)$$

and after integrating and substituting for τ_w we get

$$Q = \frac{n\pi R^3}{3n+1} \cdot \left(\frac{R\Delta P}{2LK_N}\right) \qquad (42)$$

For Newtonian fluid n = 1, $K_N = \mu$ and the equation again reduces to the Poiseuille form.

From equation (4) and (35)

$$U = \left(\frac{n}{n+1}\right)\left(\frac{\Delta P}{2LK_N}\right)^{1/n}\left(R^{\frac{1}{n}+1} - r^{\frac{1}{n}+1}\right) \qquad (43)$$

and since

$$Q = \pi R^2 (U_m) \qquad (44)$$

$$U = U_m\left(\frac{3n+1}{n+1}\right)\left[1 - (\xi)^{\frac{n+1}{n}}\right] \qquad (45)$$

where

$$\xi = \frac{r}{R} \qquad (45a)$$

Equation (45) is the equation for the velocity profile under isothermal flow in circular pipes, for any fluid obeying the power law. Typical velocity curves are shown in Fig.5 (Appendix 1). The corresponding shear rate pofiles are shown in Fig.6.

Although the above derivations for velocity profiles and pressure drop are rigorous, some criterion needs to be established for laminar-turbulent transition. Such a criterion would be of great significance in engineering design procedures if the methods developed were universally applicable to all fluids in the laminar region, whether they are Newtonian or non-Newtonian. The first attempts were made by ALVES, BOUCHER and PIGFORD (4), and METZNER(114), METZNER and REED (116) have presented an expression defining Reynolds number for all time-independent fluids (including Bingham Plastics). The friction factor f is defined in the usual manner by

$$f = \frac{D\Delta P}{4L} \Big/ \frac{1}{2}\rho U_m^2 \qquad (46)$$

and in order to be able to use the conventional chart for Newtonian and non-Newtonian fluids alike in the laminar region, the familiar relationship between friction factor and Reynolds number in the laminar region is maintained viz:

$$f = 16/Re' \tag{47}$$

The generalized Reynolds number is then found by combining Equations (17), (18) and (46) to give

$$Re' = \frac{D^{n'} U_m^{2-n'} \rho}{K'_N 8^{n'-1}} \tag{48}$$

For a power-law fluid Equation (48) can be rewritten in terms of n and K_N since

$$n' = n \tag{24}$$

and

$$K'_N = K_N \left(\frac{3n+1}{4n}\right)^n \tag{25}$$

Hence substituting we get

$$Re' = \frac{D^n U_m^{2-n} \rho}{\frac{K_N}{8}\left(\frac{6n+2}{n}\right)^n} \tag{49}$$

In this way data for all time-independent fluids should follow the conventional $f = 16/Re'$ relation rigorously in the laminar region if the fluid parameters n' and K'_N are evaluated at the actual value of $8U_m/D$ under consideration. The transition from laminar to turbulent flow when predicted by this method occurs as f falls below 0.008. WELTMANN (196) has also suggested a similar correlation for non-Newtonian fluids using an 'apparent viscosity', in the definition of

Reynolds number. The 'apparent viscosity' η is given by

$$\eta = \left(\frac{4n}{3n+1}\right)\left(\frac{\tau}{du/dr}\right) = K_N \left(\frac{3n+1}{4n}\right)^{n-1}\left(\frac{8U_m}{D}\right)^{n-1} \qquad (50)$$

DODGE and METZNER (48) have studied the flow of aqueous CMC solutions and have observed that there is distinct f.vs.Re' plot for each value of n. As a consequence, critical Re appears to increase with decreasing value of n. This work has been confirmed by SHAVER and MERRILL (172). The pseudo stable laminar or transitional flow condition has been attributed to the viscoelastic property of the higher concentrations of CMC solutions used in the reported investigations. Viscoelasticity tends to suppress the formation and propagation of turbulent eddies. An interesting consideration arises for n = 0, i.e. the case of ultimate pseudoplasticity. The laminar and turbulent velocity profiles for this situation will be identical and thus, the turbulent friction factor - Reynolds number correlation would simply be an extension of the laminar relationship. In view of the apparent increase of the critical Re' with decreasing n, a question arises as to whether or not a turbulent flow condition could ever be obtained for this case. With a perfectly flat laminar velocity profile, the flow instability frequently attributed to the influence of a velocity gradient is absent. Everywhere within the tube,

except at the wall itself, the stability parameter of ROUSE (154) would be zero, an indication of complete stability. Directly at the tube wall, the stability parameter becomes indeterminate. If turbulence were to begin just at the tube wall, it is not clear that propagation would ensue throughout the tube. Thus with such fluids it seems a turbulent condition cannot be established at all.

RYAN and JOHNSON (156) have suggested the use of a local stability parameter (Z') which is a function of the ratio of input energy to energy dissipation for an element of fluid. For a Newtonian fluid, maximum value of the parameter is given as

$$Z' = Re_{C_r} \sqrt{\frac{4}{27}} = 808 \qquad (51)$$

This criterion has been extended and experimentally verified for power law fluids

$$Z' = \frac{R}{\tau_W} \rho Uz \frac{\partial Uz}{\partial y} \quad , \quad \text{at } \frac{dZ'}{dy} = 0 \qquad (52)$$

where Uz is local axial velocity, undisturbed flow.

HANKS and CHRISTIANSEN (75) have used a modified power law equation to solve the momentum and heat equation. The Ryan and Johnson-Criterion was thus extended to the case of non-isothermal flow. KEEVIL and McADAMS (93) showed experimentally that the critical Reynolds number is essentially independent of temperature gradients.

4.1.2. Laminar Tube Flow Through an Abrupt Contraction and Divergence

As has been noted earlier, in pipeline design the pressure losses in fittings such as valves, orifices, venturi sections, abrupt changes in diameter, etc. are of prime importance and often account for considerable portion of the total pressure loss in the complete system. Also flow of fluid from a reservoir up to and through the entrance region of a tube of circular cross section is encountered in many situations, such as in fibre spinning, tubular heat exchangers, and capillary-tube viscometry. For Newtonian flow the losses due to fittings are well known, (see McADAMS (127)), and, although the theory is far from complete the well established design methods are quite satisfactory.

In a configuration where the abrupt contraction or expansion is preceded by a long tube or a large chamber, it is more realistic in view of the present knowledge to consider transport phenomena as occuring in two separate processes:

(1) flow from the upstream tube or chamber up to the tube entrance,

and

(2) flow in the tube entrance.

The need for this method of analysis is strongly emphasised by evidence that unexpected flow phenomena may occur. For

example, it has been reported by CLEGG (39) and SCHOTT et al (167) that with non-Newtonian fluids, under some laminar flow conditions, a torus vortex may develop around and upstream from the entrance to a tube or orifice. LA NIEVE (96) suggests that a vena contracta may form in the tube entrance at relatively low Re. Under certain conditions shear rupture ("melt fracture") may occur at the entrance to a tube. The circumstances under which these and other rather unexpected phenomena may occur and their roles in momentum and energy transport are neither adequately known nor defined. In this respect the numerical solutions of CHRISTIANSEN, KELSEY and CARTER (32) for isothermal Newtonian fluids; CHRISTIANSEN and KELSEY (33) for the non-isothermal case; and CHRISTIANSEN and KELSEY (34) for both isothermal and non-isothermal cases of non-Newtonian flow are of considerable significance.

CHRISTIANSEN et al (32) considered the specific case of flow through an abrupt contraction. With an identical entrance model to that developed by VRENTAS et al (197) numerical solutions were obtained for the case where the larger tube was real, with no slip at the wall, and for the siutation where it was a frictionless stream tube. The ratio of the large tube to the small tube was varied from one to eight, and the Reynolds number from 0.01 to as high as 500. In confirmation of the results

obtained by VRENTAS et al the authors noted that for the stream tube/real tube geometry at Re = 1 and β (contraction ratio) = 4, axial diffusion of vorticity causes velocity profile development to begin more than one half diameter upstream from the tube entrance. For Re > 200 profile development took place almost entirely within the tube. At high contraction ratios, the profile was shown to develop at greater distances further upstream. (See Fig. 8).

For non-Newtonian fluids CHRISTIANSEN and KELSEY (34) considered laminar inelastic flow of Powell-Eyring fluids. The general equations of motion, including inertial and axial-diffusion terms, and the equation of energy, including axial diffusion and radial convection terms, were coupled with a temperature dependent form of the Powell-Eyring flow equation and then solved simultaneously for flow from a larger tube of circular cross-section through an abrupt contractioninto a smaller tube. The small tube walls were at a temperature equal to or higher or lower than that of the entering fluid. Results were presented for the case in which the fluid does not adhere to the upstream-tube surface but does adhere to the smaller tube surface. The computations included radial and axial velocity profiles; temperature profiles; and lengths of the small tube, Leq, having a fully developed flow pressure loss equivalent to the excess pressure loss attributable to flow contraction

and development in the tube. These were presented for a large tube - small tube diameter ratio of 2 as functions of Peclet number (Pe), of 5 to 100, Re of 0.01 to 100; Z/D for the smaller tube; $\psi(H)$; a temperature factor, and the Powell-Eyring equation constants. The isothermal results indicated that as in Newtonian flow velocity profile deformation began upstream of the entrance to the smaller tube at low Re (0.01 and 50). For $\beta = 2$, the profiles were more or less concave at Re around 20 but became flatter for higher Re (> 50). They were still far from uniform. The equivalent length was shown to be somewhat smaller as the non-Newtonian characteristics increased at higher Re; but the reverse was indicated at low Re. From the non-isothermal analysis, the effect of Re on computed entrance-temperature was shown to be small. However Peclet number seemed to have a very substantial effect of Leq - this parameter increasing greatly with Re.

Flow through sudden expansions constitutes one of the few cases in which an approximate analytical solution can be obtained for the drop in static pressure and the loss in mechanical energy to overcome friction caused by the transition in the flow channel. For pseudoplastic systems SKELLAND (177) has produced such a solution and gives the expression for pressure and mechanical energy losses as:

$$\frac{p_1 - p_3}{\rho} = \frac{p_2 - p_3}{\rho} = \left(\frac{3n+1}{2n+1}\right) \frac{Q^2}{(\pi R_1^2)^2} \left[\left(\frac{R_1}{R_2}\right)^4 \left(\frac{R_1}{R_2}\right)^2 \right] \qquad (53)$$

The mechanical loss

$$\sum F \text{ expansion} = \frac{3n+1}{2n+1} \frac{Q^2}{(\pi R_1^2)^2} \left[\frac{n+3}{2(5n+3)} \left(\frac{R_1}{R_2}\right)^4 - \left(\frac{R_1}{R_2}\right)^2 \cdots \right.$$

$$\left. \cdots + \frac{3(3n+1)}{2(5n+3)} \right] \qquad (54)$$

For locations 1, 2, 3 see Fig.7 (Appendix 1).

4.1.3. Axisymmetric Laminar Entrance Flow

At high Reynolds numbers (> 500) even for contracted flow, the assumption of a uniform entrance velocity becomes a valid (although rough) approximation. This is still more so for viscous or high Prandtl number fluids. Existing entry flow predictions may therefore be used, if only as first order estimates. These will now be briefly discussed.

Theeoretical studies of non-Newtonian entrance effects have been confined to power law fluids, BOGUE (14), SCHOWALTER (168), COLLINS and SCHOWALTER (42) and TOMITA (188, 189) have all used boundary layer theory in developing expressions for entrance length; shape of velocity

profiles in the entrance region and pressure drop in entrance region of pseudoplastic fluids. In a later addition, LEMMON (98) solved the general equations of motion and like all the earlier works, the effects of viscous dissipation of energy, rotational motion and axial diffusion of momentum were assumed to be negligible. SKELLAND (177) has formulated analytical expressions for static pressure loss in the entrance of a tube by the application of total mechanical energy balance between the two sections in question. His expression is

$$\frac{p_o - p_z}{\rho} = \frac{32(L/R)}{Re'} + G_o \qquad (55)$$

where p_o and p_z refer to the upstream and downstream locations respectively (Fig.7). Re' is the generalised Reynolds number defined by equation (48). G_o is a function of n, the non-Newtonian index. Curves of G_o plotted against n have been produced by CHRISTIANSEN (29) who summarised the theoretical and experimental findings of LA NIEVE (96). It is worth pointing out that equation (55) gives the total pressure drop between two axial positions in the entrance region of the tube, as the sum of the pressure drop which would occur if the flow were fully developed for the total length plus a correction factor G_o to account for the developing flow region.

The analogous entry region problem for Newtonian fluids has been the subject of many theoretical and well

reviewed studies. The earlier and notable works in this field were those of GOLDSTEIN (70), BOUSSINESQ (19), LANGHAAR (95) and SCHILLER (161). Schiller used an integral method to predict an entry length for 95% velocity development:

$$Ze / D = 0.029\ Re \qquad (56)$$

However, experimental results of BERNHARDT (8) indicate that this value is about equal to 0.05 Re. This agrees well with the value given by KNUDSEN and KATZ (94). To the earlier works may now be added the more rigorous numerical computations of CAMPBELL and SLATTERY (25), SPARROW, LIN and LUNDGREN (179), HORNBECK (83), CHRISTIANSEN and LEMMON (35), FRIEDMANN, GILLIS and LIRON (64) and SCHMIDT and ZELDIN (163). In these later works ((64) and (163)) the complete Navier-Stokes equations were solved. The results were in agreement with the earlier works of Vrentas et al (197). The most recent contributions have been presented by FARGIE and MARTIN (59) using a combination of the integral method of Campbell and Slattery (25) and the differential momentum equation. The predicted hydrodynamic entry length is in close agreement with that of Tomita (188) but contrasts sharply with that of Bogue (14). The authors suggested that the differences were due, not so much to the different methods of solution as to the inclusion or otherwise of viscous dissipation terms in the boundary

layer equations. Smaller entry lengths have been consistently predicted by analysis neglecting the effect of viscous heat generation.

4.1.4 Effect of Viscous Heat Dissipation on Flow Development

Since non-Newtonian fluids are very viscous, frictional heat dissipation can play a significant role in the flow development. The few Newtonian studies on this aspect of otherwise "isothermal" flow therefore provide valuable information on which non-Newtonian predictions may be based. Viscous heating effects on predicted isothermal Newtonian flow development and pressure drop have been considered seriously only in a recent paper by MARTIN (104) for adiabatic wall conditions although FARGIE and MARTIN (59) noted the need for a more generalised approach which covers non-isothermal flow and the effect on flow development of temperature-dependent viscosity. POLAK (144) suggest that for any fluid with temperature dependent viscosity, there exists an unstable situation in which viscous heating and viscosity variation causes layers of warm fluid near the wall (with higher shear stress and lower through flow) to become still warmer. This leads to a "hot slip zone" occuplying only a small part of the flow passage. MARTIN (104) showed that in the entrance region, viscosity reduction due to viscous heating increased

the hydrodynamic entry length by less than 10% over the range of Prandtl and Reynolds numbers of interest in engineering design. A reduction in pressure drop compared to that of isothermal flow was also predicted. To account for possible axial conduction the authors recommended that further studies take heat transfer into consideration.

4.1.5 Experimental Studies on Entrance Flow

Experimental measurements with viscous fluids are few. For Newtonian fluids, reported works on those of EMERY and CHEN (57) and MARTIN and FARGIE (105). The former obtained data which suggest that the entry length for development of the velocity profile greatly exceeds that for the pressure gradient. MARTIN and FARGIE considered flow through an abrupt contraction. Centre-line velocities were obtained and indicated virtually uniform velocities outside the boundary layer. In an attempt to assess the influence of viscous heat generation on the predicted results, the authors made radial temperature transverses. No conclusive evidence of such effect was obtained; the measured bulk temperature rise being very small. It was however, noted that the size of the instrumentation may have precluded measurements in the region of interest very close to the pipe wall.

For non-Newtonian fluids, WELTMANN and KELLER (199) found from experiments on Bingham plastics and

pseudoplastic suspensions that the entrance losses were effectively the same as for Newtonians. This was consistent with the measurements of TOMS (190), DODGE and METZNER (48) and LA NIEVE (96). However, both McMILLEN (129) and ASTARITA and GRECO (5) have measured pressure drops much larger than predicted by published analysis. In the former case, the excessive losses were attributed (48) to possible viscoelastic effects on the CMC solutions used in the reported tests. This view has been confirmed by SYLVESTER and ROSEN (184) who used Separan solutions which were considered to have elastic characteristics. In a more recent contribution RAMA MURTHY and BOGER (147) used a technique which involved streak photography in the determination of velocity profiles for water and Methocel solutions. The results confirmed predictions of the existence of a uniform velocity profile at the entrance of a 2 to 1 contraction for $20 \leqslant Re \leqslant 1942$ and $0.585 \leqslant n \leqslant 1.0$. At low Re the presence of a stationary vortex on the upstream side of the contraction was observed. This vortex was absent at high Re - a fact already indicated by the numerical analysis reviewed earlier.

In concluding this section it is worth noting that the observations of ASTARITA and GRECO (5), SYLVESTER and ROSEN (184) and RAMA MURTHY and BOGER (147) suggest

that a contraction ratio of 2 may be the maximum that can be used without the formation of a "Vena Contracta" in laminar flow for Newtonian fluids.

4.2 HEAT TRANSFER CHARACTERISTICS OF NON-NEWTONIAN (AND NEWTONIAN) FLUIDS

Heat transfer to non-Newtonian fluids in laminar flow in tubes has been treated theoretically by a number of workers but there is a distinct lack of published experimental work which would allow these theoretical predictions to be fully tested. The problem of heat transfer to highly non-Newtonian fluids under turbulent flow has received even less attention and so far only order of magnitude predictions are possible. However, this region is not as important as the laminar region for most non-Newtonian fluid systems. The consistency of these fluids is usually high and turbulent conditions while desirable from heat transfer conditions are often difficult to achieve in practice. The difficulties occuring in obtaining efficient heat transfer with non-Newtonian liquids are largely due to the relative stability of laminar flow; in this way they are not unlike highly viscous Newtonian liquids. Data from this field is, therefore, of considerable value as a first approximation. Consequently the Newtonian studies will be treated first in the following discussions.

4.2.1 Laminar Heat Transfer to Newtonian Fluids in Circular Sections

With Newtonian high viscosity liquids heat transfer is normally controlled by molecular conductivity and large temperature gradients may result. Temperature - position relationships become especially important because of their effect on viscosity. Furthermore, since both velocity gradients (momentum transfer) and temperature gradients (heat transfer) are inter-related, it is necessary to consider the information available regarding velocity profiles. This has been done in the preceeding section. One of the 'apparent advantages' of a study of laminar flow problems is that they can be described by equations of motion, energy, and mass which can be simplified to such an extent that the determination of exact solutions should be possible. A complete solution of the combined equations gives the temperature distribution. The wall temperature profile may be used to obtain heat transfer coefficients and correlate with other parameters like flow, thermal and physical properties, pipe dimensions etc. Such correlations are especially useful in engineering design and hence all attempts in heat transfer experiments are directed towards obtaining this correlation.

In dealing with expressions for rates of heat transfer it is very important to specify the rheological

model upon which a particular relationship is based and the boundary conditions for which the equations of state have been solved. The entry boundary conditions likely to be encountered are:

(i) Velocity and temperature profiles fully developed

(ii) Velocity profile fully developed, temperature profile developing

(iii) Simultaneous developments of velocity and temperature profiles.

For each of these cases the following wall thermal boundary conditions are of engineering interest:

(a) Constant wall temperature
(b) Constant wall heat flux
} No peripheral variation of temperature

(c) Linear variation of wall temperature

(d) Arbitrary variation of axial temperature or heat flux

(e) Arbitrary variation of peripheral temperature or heat flux.

The first assumption to be made in the following discussion will be that the physical properties of the fluid, that is to say, ρ, μ, k, Cp etc. are independent of temperature. In many cases of viscous flow this is a severe restriction since any temperature gradients within a viscous liquid usually give rise to distortions of the anticipated velocity profiles due to the sensitivity of the viscosity

to even small changes in temperature. Natural convection may or may not be significant depending on the severity of the temperature gradients and its effect on the physical properties, the geometry and flow rates associated with a particular problem. In view of the foregoing considerations, suitable non-isothermal correction factors are necessary for analytical solutions of the heat transfer equations.

The equations governing the laminar flow and heat transfer in any system are:

The Continuity equation:

$$\frac{D\rho}{Dt} = -\rho \text{ div } u \tag{57}$$

The Momentum equation (Navier/Stokes equations):

$$\rho \frac{Du}{Dt} = \rho F - \text{gradp} + \mu\nabla^2 u + \tfrac{1}{3}\mu \text{ grad divu} \tag{58}$$

The Energy equation:

$$\rho Cp \frac{DT}{Dt} - \frac{Dp}{Dt} = k\nabla^2 T + \mu\Phi(u) + H \tag{59}$$

The detailed derivation of these equations can be found in a number of standard texts, for example, SCHLICHTING (162) and GOLDSTEIN (70). These equations describe behaviour under unsteady flow conditions with a Newtonian, compressible

fluid. All subsequent discussion will be limited to steady flows so that derivatives with respect to time will be zero. The second terms on the left and right hand sides of equation (59) can generally be ignored; however in the presence of large pressure gradients these terms, which account for compression or expansion work and the dissipation of energy due to friction respectively, can assume significant proportions. This is certainly true of the flow of highly viscous liquids in narrow passages. Here frictional heat generated by flow, and cooling due to expansions must be included. The present investigation will be dealing with highly viscous fluids and so these points will be taken up later. For the moment, compressibility, frictional dissipation and internal heat generation, H, will be omitted from the discussions as will natural convection effects represented by the body force term F in equation (58). With these conditions equations (57), (58) and (59) reduce to:

The Continuity equation:

$$\text{div } u = 0 \tag{60}$$

The Momentum equation:

$$\rho(u.\text{grad})u = -\text{grad}p + \mu\nabla^2 u \tag{61}$$

The Energy equation:

$$(u.\text{grad})T = \alpha\nabla^2 T \qquad (62)$$

$$\alpha = k/Cp\rho \quad \text{(thermal diffusivity)}$$

In addition to these equations a number of boundary conditions are required; these prescribe values of temperature and velocity at the boundaries of the field of flow. The particular case we are considering is that of steady state laminar flow in a circular pipe with heat transfer. In cylindrical co-ordinate system, equation (62) gives the temperature distribution as:

$$u\frac{dT}{dZ} = \alpha\left[\frac{1}{r}\frac{dT}{dr} + \frac{d^2T}{dr^2}\right] \qquad (63)$$

if we neglect longitudinal heat conduction. This is the basic equation which must be solved subject to specific boundary conditions.

In his classical work GRAETZ (71) made one of the earliest attempts to solve this equation. He based his solutions on the "isothermal" condition in which the physical properties (Cp, ρ, μ, k) are assumed to be independent of temperature. Also this condition assumes

that a fully developed velocity profile remains unaltered along the tube, despite changes in fluid temperature with distance from inlet. On this basis GRAETZ obtained two solutions to equation (63), one assuming plug flow and the other assuming a constant parabolic velocity distribution along the tube. The solutions assume constant wall temperature along the tube in each case. In plug flow the local value of velocity u at any radius r equals the mean velocity U_m. This situation in fact corresponds to the laminar flow of power law fluid with infinite pseudoplasticity, for n equals zero as shown in Fig.5 (Appendix 1). The GRAETZ expression relates to the temperature of the fluid T at any point located a distance r from the centre line and z from the mean inlet to the heated section of the tube. Details of Graetz's treatment have been given in DREW (50) and JAKOB (87). In a more convenient form it is expressed as

$$\frac{h_m D}{k} = \frac{2}{\pi} \; Gz \left[\frac{1 - 4E(\pi/Gz)}{1 + 4E(\pi/Gz)} \right] \tag{64}$$

where

$$E\left(\frac{\pi}{Gz}\right) = \sum_{j=1}^{j=\infty} \frac{1}{a_j^2} \exp\left(- a_j^2 \frac{\pi}{Gz}\right) \tag{65}$$

a series involving the Graetz number; h_m is a mean or average heat transfer coefficient defined for the fluid over the tube length $0 \leqslant z \leqslant L$, to be used with the arithmetic mean temperature difference. Equation (64) becomes unwieldy for Graetz numbers above 500. This difficulty is overcome by an asymptotic solution which is approximately valid at Graetz numbers above 100, as presented by METZNER, VAUGHN and HOUGHTON (117).

$$\frac{h_m D}{k} = \frac{8}{\pi} + \frac{4}{\pi}\left(\frac{WC_p}{RL}\right)^{\frac{1}{2}} \quad ; \quad Gz = \frac{WC_p}{kL} \tag{66}$$

The second "isothermal" solution by Graetz assumes the parabolic velocity distribution (Fig.5 n = 1) to be fully developed upon entering the heated section and to remain unchanged along the tube, where T_w = Constant. The average heat transfer coefficient in this case is expressed as

$$\frac{h_m D}{k} = \frac{2}{\pi} Gz \left(\frac{1 - 8P(\pi/2Gz)}{1 + 8P(\pi/2Gz)}\right) \tag{67}$$

where $P(\pi/2Gz)$ is a convergent infinite series of exponential functions in $\pi/2Gz$. h_m is used with the arithmetic mean temperature difference.

LEVEQUE (99) obtained an approximate "isothermal" solution to equation (63) by assuming that the temperature boundary layer is confined to a thin zone near the tube wall in cases of high mass velocities through short tubes in laminar flow. These conditions correspond to high Graetz numbers and are therefore of practical importance. Linear velocity gradients are assumed within such thin temperature boundary layers so that

$$u = \beta_v (R-r) \tag{68}$$

where $\beta_v = (du/dr)_w$, the velocity gradient in the vicinity of the wall. On this basis Leveque's final expressions (originally for flow over a flat plate) may be adapted as follows for the average Nusselt number with constant wall temperature (177)

$$NU_m = \frac{h_m D}{k} = 1.615 \left(\frac{\beta_v C_p \rho D^3}{8kL} \right)^{\frac{1}{3}} \tag{69}$$

For a Newtonian fluid β_v, the velocity gradient at the wall is $\frac{8U_m}{D}$ in laminar flow, so that

$$NU_m = \frac{h_m D}{k} = 1.615 \left(\frac{4}{\pi} Gz\right)^{\frac{1}{3}} = 1.75 (Gz)^{\frac{1}{3}} \tag{70}$$

h_m is used with the same temperature difference as before.

The Graetz solution has been extended by SELLARS, TRIBUS and KLEIN (170) to include the boundary condition of uniformly constant heat flux at the wall. Other conditions were, constant fluid properties, fully established parabolic velocity profile before heating begins. The local Nusselt number is given as

$$Nu_L = \frac{1}{\frac{11}{48} + \frac{1}{2}\sum_{m=0}^{\infty} \frac{\exp\{[-B_m^2(L/R)]/Pe}{B_m^4\,\phi'_m(-B_m^2)}} \qquad (71)$$

where B_m^4 are coefficients, B_m^2 are exponents and ϕ'_m are functions of r/R. Sellars et al reported values of these coefficients and exponents and presented equations evaluating ϕ'_m over various ranges of r/R. The Leveque solution for the local Nusselt number for the corresponding case of constant wall temperature profile is

$$Nu_L = 1.17(WCp/kL)^{\frac{1}{3}} \qquad (72)$$

For small $\frac{L/R}{Pe}$, equation (71) may be written as

$$Nu_L = 1.639\left(\frac{L/R}{Pe}\right)^{\frac{1}{3}} \qquad (73)$$

For $L/R < 0.01$, i.e. $\frac{2}{\pi} Gz > 100$

$$Nu_L = 1.413(Gz)^{\frac{1}{3}} \qquad (74)$$

For large values of $\frac{L/R}{Pe}$, i.e. $\frac{L/R}{Pe} \geq 2.5$

$$Nu = 4.364 \qquad (75)$$

Subsequent developments of the Graetz solution have been directed towards the effect of axial conduction (SINGH (176), MUNAKATA TSUYOSHI (194), SCHNEIDER (164)), internal frictional heat generation (SINGH (176)), and wall resistance (SCHENK and DUMORE (159)). BROWN (22) gives more accurate values for the eigenvalues and eigenfunctions for the evaluation of the series.

SIEGEL, SPARROW and HALLMAN (175), by using GOLDSTEIN'S (70) temperature distribution equation, for conditions of uniform wall heat flux, large L and fully developed thermal situation, have arrived at a solution for the thermal entrance region by integration of the energy equation. The variation of local Nusselt number with Graetz number was derived as a function of L/R. This solution has been extended by SPARROW et al (178) for arbitrary non-uniform wall heat flux and arbitrary internal heat source.

Solutions of the energy equation with simultaneous development of the velocity and temperature fields

for laminar flow in the inlet region of a circular tube and uniform wall heat flux have been given by a number of authors. The earlier studies are notably those of KAYS (91), ULRICHSON and SCHMITZ (96), MANOHAR (103) and HEATON et al (78). Kays has solved the Graetz problem for heat transfer involving simultaneous development of the parabolic velocity profile, by using the LANGHAAR (95) velocity model. Langhaar obtained an approximate solution for the axial velocity component in the entrance region by linearizing the boundary layer equation. The equation is of the form

$$U = \frac{I_0(Y) - I_0(YR)}{I_2(Y)} \qquad (76)$$

where I_m is the modified Bessel function of the first kind and of order m and Y is given in tabular form by Langhaar as a unique function of the dimensionless axial distance from the tube entrance. Ulrichson and Schmitz have refined Kay's work, by including the radial component of velocity in the entrance region. Their results show that, the effect of the radial velocity is to cause a significant decrease in the calculated local Nusselt number in the entrance region from that obtained by Kays.

In almost all the above studies, the Prandtl numbers were low (0.7 to 10) and the analyses usually involved some approximations in the governing equations.

The significance of the neglected terms were sometimes in doubt. The analytical approach of TEST (186) has considered in detail, the significance of various terms in the momentum, continuity and energy equations. The fluids used in the present project are very viscous and hence fall outside the range of Prandtl numbers covered by literature reviewed above. In this respect the approximate solution of ROY (155) and the recent analytical works of BUTTERWORTH and HAZELL (24), COLLINS (43), and MARTIN and FARGIE (105) represent very significant contributions to heat transfer studies for high Prandtl number fluids.

The work of MARTIN and FARGIE (105) incorporating both experimental and analytical studies relate to tube entry configurations and fluid Prandtl number of particular interest to the present investigation and will therefore be reviewed in greater detail. The authors extended an earlier investigation of isothermal flow (59) to simultaneous development of the hydrodynamic and thermal boundary layers where the extent of viscosity variation is influenced both by the applied heat flux and the viscous heat generation. Starting with the equations of conservation of mass, momentum and energy for steady axisymmetric flow and variable viscosity, to which the usual boundary layer approximations had been applied (and neglecting viscous heat generation), the authors assumed the following dimensionless velocity profiles:

(refer to Fig.9 (Appendix 1) for notations)

$$\left.\begin{aligned} u &= \phi && (0 \leqslant y \leqslant \alpha) \\ u &= \phi\left[1 - \left(\frac{y-\alpha}{1-\alpha}\right)^2\right] && (\alpha \leqslant y \leqslant 1) \end{aligned}\right\} \qquad (77)$$

where ϕ and α are functions of Z only such that when Z = 0, $\alpha = \phi = u = 1$, thus satisfying the relevant boundary conditions. The temperature profile (dimensionless) was:

$$\begin{aligned} t &= 0 && (0 \leqslant y \leqslant \beta) \\ t &= \frac{(1-\beta)}{b}\left[(8-2\beta)\left(\frac{y-\beta}{1-\beta}\right)^2 + (\beta-2)\left(\frac{y-\beta}{1-\beta}\right)^4\right] \\ & && (\beta \leqslant y \leqslant 1) \end{aligned} \qquad (78)$$

where only even polynomials in $(y-\beta)/(1-\beta)$ were retained to preserve symmetry about the pipe axis. This profile also satisfied the additional boundary conditions:

$$\begin{aligned} &y = \beta, \quad t = 0, \quad \partial t/\partial y = 0 \quad \text{for all Z} \\ &y = 1, \quad \partial t/\partial y = \text{constant}, \quad \frac{1}{y}\frac{\partial}{\partial y}\left(y\frac{\partial t}{\partial y}\right) = 0 \quad \text{for all Z} \end{aligned} \qquad (79)$$

By an integral differential method the following expression was obtained

$$\frac{Pr_w}{Pr_o}\frac{dz}{d\alpha} = -\frac{(1-\alpha)(6+\alpha)(1+4\alpha+9\alpha^2+4\alpha^3)}{5\alpha(3+2\alpha)(3+2\alpha+\alpha^2)^2} \qquad (80)$$

depicting the effect of uniform and temperature dependent Prandtl number on heat transfer. Equation(80) shows that for given α and ϕ the flow development parameter $z(=Z\nu/U_oR^2)$ becomes greater when $Pr_w < Pr_o$ due to wall temperature being higher than fluid entry temperature; and consequently increased heat transfer can be expected relative to the case of uniform Prandtl number.

The expression for local Nusselt number was given as:

$$Nu = \left[\frac{(6-\beta)(1-\beta)}{16} - \frac{z}{Pr_o}\right]^{-1} = \left[\frac{(1-\beta)}{16}\left\{(6-\beta) - \left(\frac{1-\beta}{1-\alpha}\right)^2 \times \left[\frac{490+307\beta+12\beta^2-25\beta^3-16\alpha(37+18\beta-6\beta^2)}{70(3+2\alpha+\alpha^2)}\right]\right\}\right]^{-1} \qquad (81)$$

(see Fig.10 (Appendix 1) for graphical representation of the Nu-Gz relationship)

Another significant point arising from this work is that the dimensionless heat flux can be expressed in the following functional form:

$$\frac{q''D}{kT_o} = f(\alpha, \beta, Pr_o, a) \qquad (82)$$

where a is obtained from the relationship

$$\frac{Pr_w}{Pr_o} = \left(\frac{T_o}{T_w}\right)^a \qquad (83)$$

expressing the assumed dependence of dynamic viscosity on temperature. The implication of equations (81) and (82) is that for given fluid entry temperature, pipe diameter and fluid properties Pr_o, k and ϕ the applied wall heat flux can be regarded as an alternative parameter to α and β on the field of Nu against Gz. The experimental verification of this statement as obtained by the authors will be discussed in the next subsection.

4.2.1(a) Experimental Methods

The foregoing survey has confirmed the extensive nature of the theoretical studies into the problems of laminar convective heat flow in Newtonian fluids. However, experimental studies have not kept pace with the theoretical predictions. The few experimental studies that have been made, were not always under such conditions for which analytical solutions are available. Additional

difficulties encountered in experimental studies have been the variation of fluid properties with temperature and the influence of natural convection. AKINS and DRANOFF (1) avoided these difficulties by measuring wall temperature profiles at low heat fluxes for laminar flow in vertical tubes where natural convection is negligible. Natural convection tends to increase the rate of heat transfer to a fluid in laminar flow through a horizontal tube. This effect was first examined by COLBURN (41) whose pioneer work led to the equation

$$\left(\frac{h_m D}{k}\right)_b = 1.75\left(\frac{W\ Cp}{kL}\right)_b^{\frac{1}{3}} \cdot \phi^{\frac{1}{3}} \qquad (84)$$

where

$$\phi^{\frac{1}{3}} = \left(\frac{\mu_b}{\mu_f}\right)^{\frac{1}{3}} (1+0.015\ Gr_f^{\frac{1}{3}}) \qquad (85)$$

The correction factor ϕ, allowing for radial variation of fluid properties and natural convection was evaluated from data obtained in both vertical and horizontal tubes. It has been pointed out (107) that since ϕ is a multiplier of Gz_b, the effects of free convection appear to increase in importance as the forced flow rate is increased, which is contrary to experience.

SIEDER and TATE (174) produced data which was correlated by

$$\left(\frac{h_m D}{k}\right)_b = 1.86\left(\frac{L/D}{Re\ Pr}\right)^{-\frac{1}{3}} \left(\frac{\mu_b}{\mu_w}\right)^{0.14} \qquad (86)$$

$$= 2.00(Gz)_b^{\frac{1}{3}} \left(\frac{\mu_w}{\mu_b}\right)^{-0.14} \qquad (87)$$

to give Nusselt numbers somewhat higher than the analytical Graetz solution. The bulk-wall viscosity ratio was included to correct for velocity profile distortion caused by viscosity variation with temperature. This is still the most widely used form of correction for viscosity effects.

MARTINELLI and BOELTER (107) have extended Sieder and Tate's analysis for combined forced and free convection in a tube. The analysis applied only to the cases of heating fluids flowing vertically upwards and cooling fluids flowing vertically downwards in tubes having uniform wall temperatures. Their expression is given as

$$\left(\frac{h_m D}{k}\right)_b \left(\frac{\mu_w}{\mu_b}\right)^{0.14} = 1.750\left[F_1(Gz)_b + 0.072F_2 \ \ldots\right.$$

$$\left. \ldots \left(\frac{(Gz)_b\, Pr_b}{L}\right)^{0.75}\right]^{\frac{1}{3}} \qquad (88)$$

The correction factors F_1 and F_2 were evaluated as functions of the Nu - Gz ratio. The Grashof number was

evaluated on the basis of the initial temperature difference between wall and fluid. Equation (88) differs from previous relationships in that the natural convection term is added to the Gz modulus, rather than appearing as a multiplier, the significance of the term therefore falls as the flow rate is increased.

PIGFORD (142) has made further investigations into the problem of combined free and forced convection in vertical tubes. His charts consist of a plot of Nusselt number versus Graetz number, for various values of $\frac{G_r P_r}{L/D}$. Each chart is at a constant value of (μ_w/μ_b), so that the effect of viscosity variation of the fluid is taken as considered.

For laminar flow in horizontal tubes, EUBANK and PROCTOR (58) have given the correlation

$$\left(\frac{h_m D}{k}\right)_b \left(\frac{\mu_w}{\mu_b}\right)^{0.14} = 1.750\left[Gz_b + 12.60\left(\frac{Gr_b\ Pr_b\ D}{L}\right)^{0.40}\right]^{\frac{1}{3}} \qquad (89)$$

McADAMS (127) recommends a similar equation in which the coefficients 12.60 and 0.40 are replaced by 0.04 and 0.75 respectively. With the index 0.75, the relationship should reduce to the normal free convection equation

in the absence of forced convection ($Gz_m = 0$) (157). However, the presence of the D/L term in the expression means that equation (89) cannot really reduce to that of natural convection even with $Gz_m = 0$, since, for horizontal pipes, natural convection is independent of L (137).

JACKSON, SPURLOCK and PURDY (86) have studied heat transfer to air in a constant temperature horizontal tube, their results being well represented by the semi-theoretical equation

$$Nu_m = 2.67 \left[Gz_b^2 + 0.0087^2 \ (Gr_w \ Pr_w)^{1.5} \right]^{\frac{1}{6}} \qquad (90)$$

An interesting feature of this equation is the absence of the D/L ratio from the natural convection term, this being the first suggestion that the ratio was unnecessary when dealing with flow in horizontal tubes.

OLIVER (137) investigated the effects of natural convection and radial viscosity variation in an experimental study of heat transfer to water, glycerol and ethyl alcohol in a horizontal tube with constant wall temperature. He also concluded that natural convection effects are independent of L/D. His relationship is

$$\left(\frac{h_m D}{k}\right)_b \left(\frac{\mu_w}{\mu_b}\right)^{0.75} = 1.750\left[Gz_b + 0.0083\,(Gr_b Pr_b)^{0.75}\right]^{\frac{1}{3}} \qquad (91)$$

ROSEN and HANRATTY (153) proposed that the normal laminar velocity profile will not be significantly altered by natural convection effects provided $Gr/Re < 5.0$.

SPARROW et al (179) considered the combined forced and free convection influence for laminar boundary layer flows and showed that the parameter controlling the relative importance of these effects is Gr/Re. The ratio Gr/Re may be interpreted physically as a ratio of buoyancy to inertia forces per unit volume. Criteria were given for categorizing the flow -

$0 < Gr/Re^2 < 0.30$	Forced Convection
$0.30 < Gr/Re^2 < 16.0$	Mixed Flow
$16 < Gr/Re^2$	Free Convection

(92)

The condition of constant heat flux at the tube wall for liquids flowing upward in laminar flow of vertical tubes has been investigated by GROSS and VAN NESS (74) using dimension analysis. They obtained the expression

$$h = 68 k_w (Re)_w^{0.16} (D)^{-0.36} \qquad (93)$$

Other investigators of the asymptotic Nusselt numbers for laminar flow include GLASER (68), NORRIS and STREID (134) who considered the constant longitudinal heat flux condition for circular tubes.

The recent experiments by BUTTERWORTH and HAZELL (24) and MARTIN and FARGIE (105) have extended both the range of Prandtl numbers and the stages of flow development for the constant heat flux boundary condition. Butterworth et al investigated the case where heating was started after entry sections of different lengths but of the same diameter as the heated tube. They concluded that for $Pr > 500$ the difference between measured heat transfer coefficients and values predicted with parabolic velocity profiles was negligible. Martin and Fargie obtained data from a test section, the entrance to which was an abrupt contraction. For the limiting condition of hydrodynamically fully developed flow over the range $1.7 \times 10^7 > Gz > 200$ Nusselt number was very closely approximated by

$$Nu = 1.2\ Gz^{\frac{1}{3}} \qquad (94)$$

(where Gz was defined as Re Pr D/Z).

For the other limiting case of equal thermal and hydrodynamic boundary layer, the correlation was

$$Nu = c\ Gz^{m} \qquad (95)$$

where m increased rapidly from 0.213 at Gz = 27.4 to approximately 0.5 at Gz = 10^5. This implied that the relationship between Nu and Gz was, except for regions approaching full thermal development, always of greater slope than m = $\frac{1}{3}$. Application of the correlation of SIEDER and TATE (174) led to a mean heat transfer distribution approximated by

$$Nu' = 4.01\ Gz^{0.282} \qquad (96)$$

The general trend of data presented by Martin and Fargie indicated that Nusselt number invariably increased with the heat flux parameter $q''\ D/kT_o$. However, it was not very clear from the results what percentage increase in Nusselt number can be expected for a given percentage increase in heat flux, and whether any such increase would occur at all Graetz numbers. The experiments of McINTYRE (128) suggested that heat flux dependence was of second order magnitude. Regarding the influence of inlet Prandtl number on observed Nusselt number values, McIntyre plotted $Nu/Pr^{\frac{1}{3}}$ against axial distance for various Pr values (Fig.18). He concluded that the variation of $Nu/Pr^{\frac{1}{3}}$ with Pr was also of second order magnitude but did not preclude such dependence from the

correlations since it was possible to classify his experimental results into groups having particular values of Pr.

Further experimental data is obviously needed to quantify the various trends noted in the above investigations.

4.2.2 Laminar Heat Transfer to Non-Newtonian Fluids in Circular Sections

Non-Newtonian fluids are invariably viscous, the great the deviation from Newtonian behaviour, the higher the viscosity of the fluid. It is not surprising therefore that most industrial applications involving non-Newtonian fluids are usually in the laminar region. Turbulent flow conditions, however, are very desirable from a heat transfer point of view, but the tendency for non-Newtonian fluids to supress the onset of turbulent eddies, makes attainment of this flow regime very difficult. The present investigation will be concerned with pseudoplastic, power law fluids in laminar flow and a greater part of the subsequent review will be limited to this field. However, since most of the early reported information on the physical properties of non-Newtonian suspensions were obtained from turbulent (and usually only slightly non-Newtonian) heat transfer experiments, a brief section on these studies have been included. The well established correlations for Newtonian turbulent heat

transfer are often used to check the reliability of equipment. The most notable of these have therefore also be reviewed briefly.

4.2.2(a) Analytical Methods - Power Law Model

Most theoretical analyses of laminar heat transfer in pseudoplastic fluids are performed by using the appropriate velocity profile expression in the heat conduction equation. Derivations of velocity profile expressions for the various known models have been given in the texts - SKELLAND (177) and WILKINSON (202). As in the Newtonian case, several boundary conditions are possible. Much work has been done on the constant wall temperature and constant heat flux case. The subsequent discussions will therefore be limited to these cases - which also cover the areas of interest in the present study. By substituting the velocity profile for fully developed laminar flow of power law fluids (equation (43)) in tubes, in the heat conduction equation (63) the expression

$$U_m\left(\frac{3n+1}{n+1}\right)\left[1-\left(\frac{r}{R}\right)^{\frac{n+1}{n}}\right]\frac{\partial T}{\partial Z} = \alpha\left[\frac{\partial^2 T}{\partial r^2} + \frac{1}{r}\frac{\partial T}{\partial r}\right] \qquad (97)$$

is obtained. This is the equation to which the various boundary conditions have to be applied. Using the usual

separation of variables method, equation (97) reduces to

$$\frac{d^2\psi}{dr^2} + \frac{1}{r}\frac{d\psi}{dr} + B^2\left[1 - \left(\frac{r}{R}\right)^{(n+1)/n}\right]\psi = 0 \qquad (98)$$

where $T = \psi(r)\ Z(z)$. (99)

LYCHE and BIRD (101) assuming temperature - independent physical properties, constant wall temperature, uniform inlet temperature, negligible axial conduction, and negligible frictional heat generation - obtained equation (98) and solved it for the cases n = 0, $\frac{1}{3}$, $\frac{1}{2}$ and 1 at low values of Graetz number. They calculated the eigenvalues (B_{ia}) and tabulated these together with the corresponding coefficients in the series solution for ψ, for values of i = 1, 2, and 3. Corresponding values of the eigen functions ψi are tabulated for values of r/R from 0 to 1 in intervals of 0.1. In order to indicate the variation in the heat transfer characteristics with the flow behaviour index, n, Lyche and Bird plotted the reduced temperature $\frac{T - T_o}{T_1 - T_o} = \theta$ as a function of r/R at a value of the dimensionless Graetz number WCp/kL of 5.24 for values of n = 1, $\frac{1}{2}$, $\frac{1}{3}$, and 0; n = 1 is the Newtonian case and n = 0 is the case of piston flow or infinite pseudoplasticity.

GRIGULL (73) investigating the case of constant heat flux gave equations for local values of heat transfer

coefficient beyond the point at which temperature profiles are fully developed, i.e. Nu_∞. BEEK and EGGINK (6) have dealt with cases of $n = 0$ and $0 < n < 1$ for both constant heat flux and constant wall temperature conditions. The entrance region solution is obtained by calculating the conduction of heat to a semi-infinite medium, which flows with a uniform velocity along the wall. The solution obtained is:

$$Nu_L = \frac{h_L D}{k} = C \left(\frac{U_m D^2}{(k/\rho Cp) L} \right)^{\frac{1}{2}} \qquad (100)$$

where $C = 1/\sqrt{\pi} = 0.565$ for constant wall temperature (101)

$C = \sqrt{\pi}/2 = 0.885$ for constant heat flux (102)

The corresponding asymptotic values are, for $n = 0$;

$$Nu_\infty = 5.772 \qquad (103)$$

$$Nu_\infty = 8.000 \qquad (104)$$

For $0 < n < 1$ these solutions are the same as those given by BIRD (11) for thermal entrance region. Their solutions for the constant wall temperature condition was compared with those of WHITEMAN and DRAKE (201) and LYCHE and BIRD (101). Whiteman and Drake obtained "local" Nusselt numbers, over a larger range of Graetz numbers than considered by Lyche and Bird. The latter authors however, evaluated Nusselt numbers "averaged" over the heat

transfer section. SKELLAND (177) contends that the Whiteman and Drake results are inaccurate at low values of n.

INMAN (84) has performed a mathematical analysis of thermally developed region for laminar flow of a power law fluid in a circular tube. He chose the boundary conditions of uniform axial heat input and an arbitrary peripheral wall temperature or arbitrary heat flux variation; from these, he deduced results for $T(r,z)$ for cases of uniform wall temperature or uniform wall heat flux.

PIGFORD (142) has extended the Leveque approximation for the average Nusselt number in laminar flow, to Non-Newtonian systems in pipe flow. The Leveque approximation for Newtonian systems has been given as

$$\frac{h_m D}{k} = 1.615\left(\frac{\beta_v Cp\ D^3}{8kL}\right)^{\frac{1}{3}} \qquad (69)$$

where β_v is the velocity gradient at the wall. Pigford has rewritten this in the form

$$\frac{h_m D}{k} = 1.75\,\delta^{\frac{1}{3}}\left(\frac{WCp}{kL}\right)^{\frac{1}{3}} \qquad (105)$$

where δ is the ratio of the velocity gradient at the wall

for the non-Newtonian fluid, β_v, to that for a Newtonian fluid $8U_m/D$, i.e. δ is defined as

$$\delta = \frac{\beta_v}{8U_m/D} \tag{106}$$

In equation (105) $\delta^{\frac{1}{3}}$ may be regarded as a factor which corrects the Newtonian equation (69) for changes in heat transfer rate due to the fact that the velocity gradient at the wall is different for non-Newtonian fluids i.e.

$$\delta^{\frac{1}{3}} = \frac{\text{Nusselt Number in non-Newtonian Case}}{\text{Nusselt Number in Newtonian Case}}$$

$$= \frac{Nu_{nn}}{Nu_n} \tag{107}$$

METZNER and REED (116) have shown that, for a non-Newtonian fluid

$$\beta_v = \frac{3n' + 1}{4n'} \frac{8U_m}{D} \tag{108}$$

$$\therefore \quad \delta = \frac{3n' + 1}{4n'} \tag{109}$$

They also indicated the usefulness of equations (107) within the limits:

(i) for $Gz > 20$ and $n' > 0.1$

(ii) for $n < 0.1$ and $Gz > 20$, $\delta = f(Gz)$ which is expressed graphically.

The shortcoming of equation (105) is that, as the region of ultimate pseudoplaticity ($n' = 0$) is reached, a case of infinite heat transfer arises. Thus Leveque's assumption is not valid in this region, since, as plug flow is approached, the region in which velocity distribution is linear is much smaller than the region with a temperature gradient. This implies that the velocity gradient is, in this case, not the controlling factor in heat transfer. The method used by BEEK and EGGINK (6) provide better solutions here.

Entrance region coefficients have been investigated by McKILLOP (131), GILL (66) COLLINS and SCHOWALTER (42), PAWLEK and CHI-TIEN (141), and BIRD (11). McKILLOP (131) in his theoretical analysis used the finite difference technique of KAYS (91) to compute a solution for the energy equation, involving the radial convective term (this term being neglected by KAYS). The boundary conditions were those of constant wall temperature and constant wall heat flux. The velocity profile in the entrance region was obtained from the momentum equation, in a procedure similar to that of COLLINS and SCHOWALTER (42). His data are presented in graphical form for

(i) Average Nusselt number

$$Nu_m = f(Zo, n) \text{ at } Pr = 100 \qquad (110)$$

(ii) Local Nusselt number

$$Nu_{local} = f(Zo, n) \text{ at } Pr = 0, 1 \text{ and } 100 \qquad (111)$$

where

$$Zo = \frac{2z}{D_i Re}$$

The fluid properties were not temperature dependent and the results confirm the theoretically established fact that for high Pr fluids, the local heat transfer coefficient is independent of velocity profile development. Nusselt numbers tend towards the fully developed velocity profile case with increasing Pr.

GILL (66), for the case of constant wall temperature and power law fluid, uses MERCER'S (111, 112) method involving Leveque approximation, for evaluating thermal entrance region coefficients, without going into the eigenvalue problems. The local heat transfer coefficient is given as

$$Nu_L = 1.156 \frac{Pe^{\frac{1}{3}}}{(L/D)^{\frac{1}{3}}} - 1.40 \qquad (112)$$

The result is interesting, because of the constant term involved. The constant may be made to vanish by including additional terms in the series for T(r,z). For simultaneous development of velocity and temperature, very near

the tube entrance ($z \to 0$), the Pohlhausen flat plate solution should closely approximate actual performance as long as the thickness of the boundary layer is small, relative to tube diameter. Pohlhausen's solution is

$$Nu = \frac{0.664}{Pr^{0.167}} \left(\frac{Re\ Pr}{L/D}\right)^{0.5} \qquad (113)$$

Thus Nu is seen as a function of Pr. Equation (113) is applicable to Newtonian fluids for $(RePr/L/D) > 600$. PAWLEK and CHI TIEN (141), have also analysed entrance effects for power law fluids - considering simultaneous development of velocity and temperature profile, and constant wall temperature. Since thermal boundary layer is much thinner than velocity boundary layer because of high Pr they assumed the Leveque approximation for U , in the thermal entrance region. Their data relates the average Nusselt number to Zo, n and Pr for values of $n = 0.25$, 0.5 and 0.75 and $5 < Pr < 200$.

The entrance region analysis of BIRD (11) offers expressions for temperature and Nusselt number which are easily applicable to experimental data for arbitrary non-Newtonian index n. Effects of temperature-dependent rheological properties and viscous dissipation were neglected. Nevertheless, as a first approximation approach, it is preferable to most of the earlier reviewed

(and mainly numerical) works. This contribution will therefore be discussed in some detail. Using the power law and under conditions of constant heat flux, the heat conduction equation (63) is solved. In the entrance region, the thermal boundary layer thickness is much less than the tube radius so that $\frac{1}{r}\frac{\partial}{\partial r}(r\frac{\partial T}{\partial r})$ may be written as $\frac{\partial^2 T}{\partial y^2}$ where y = R-r. Using the Leveque approximation that in the region near the tube wall the velocity is directly proportional to the distance from the tube wall, i.e.

$$u = p_o y \tag{114a}$$

where

$$p_o = \left.\frac{\partial u}{\partial r}\right|_{r=R} \tag{114b}$$

Equation (63) becomes:

$$p_o y \frac{\partial T}{\partial z} = \alpha \frac{\partial^2 T}{\partial y^2} \tag{115}$$

This equation has been solved by Bird to give

$$Nu_L = 0.650\left(\frac{p_o D}{U_m}\right)^{\frac{1}{3}}\left(\frac{RePr}{L/D}\right)^{\frac{1}{3}} \tag{116}$$

For a power law model

$$\frac{p_o D}{U_m} = \frac{6n+2}{n} \tag{117}$$

and for n = 1, equation (116) reduces to

$$Nu_L = 1.413\ Gz^{\frac{1}{3}} \tag{74}$$

which is the same as that given by Sellars et al (170).

For $0 < n \leq 1$, the most useful form of equation (116) is

$$Nu_L = 1.413 \left(\frac{3n+1}{4n}\right)^{\frac{1}{3}} \left(Gz\right)^{\frac{1}{3}} \tag{118}$$

Using the heat balance as an added boundary condition; in the thermally developed region, the asymptotic values for temperature and Nusselt number were evaluated by Bird and used in developing a complete expression in series form for the local Nusselt number.

The local Nusselt number was expressed as

$$Nu_L = \frac{2}{\left[\frac{s+3}{2(s+1)} - \frac{2}{(s+1)(s+3)} - \frac{(s+3)^3 - 8}{4(s+1)(s+3)(s+s)}\right] \cdots \cdots \cdots - \sum_{i=1}^{\infty} B_i e^{-a_i 3/Pe_i} \Xi(1)} \tag{119}$$

Equation (119) reduces to the solution given by Siegel et al (175) for $s(=\frac{1}{n}) = 1$. For cases of short tube lengths, the summation in equation (119) converges very slowly and hence equation (118) is recommended.

4.2.2(b) Analytical Methods - Additional Effects

The restrictive assumptions used in most theoretical analysis neglect such effects as frictional heat generation, axial heat conduction, natural convection, compressibility, and rates of shear. As any design engineer or experimentalist knows, the simplified conditions carefully chosen to render the heat conduction and momentum equations amenable to simpler analysis, cannot always be reproduced in practice. Nevertheless, these simplified theoretical procedures, form the basis upon which the effects of the neglected factors can be estimated. For example, when frictional heat generation $(\tau \frac{dU_z}{dr})$ is included in the heat conduction equation, the solution is obtained by adding a particular solution to the general solution for large L/D.

The analysis of heat transfer accompanied by the heat generation or absorption, (e.g. because of chemical reaction) has not received a great deal of attention. TOOR (191) has extended his earlier analytical work (192) to consider the situation in which heat generation occurs

as function of radius. FORABOSHI and DI FEDERICO (60) have considered the case of power-law fluid flowing in a tube and generating heat at a rate which is a linear function of temperature. SCHENK and VAN LAAR (160) considered the case of constant wall flux and developing velocity profile with viscous heat generation for the Prandtl-Ey ring type of fluids. GILL (67) has generalized the solutions obtained by SIEGEL, SPARROW and HALLMAN (175) for the case including viscous dissipation with arbitrary inlet temperature distribution. BEEK and EGGINK (6) worked on the same line as GILL (67) but considered heat generation through friction. GEE and LYON (65) considered a more realistic situation in which the wall temperature was constant, fluid consistency was temperature dependent, as was, specific heat, and thermal conductivity (linear functions of temperature). Density was assumed constant. The effects of viscous heat generation and expansion cooling were included. The velocity profile was developing. For the fully developed velocity profile case, CHRISTIANSEN and CRAIG (30) obtained numerical solutions, which included temperature effects on consistency but without the effects of either viscous or frictional heat generation. Compressibility effects have been studied by TOOR (192). The magnitude of compressibility effects in liquids is determined by the product of the absolute temperature

and the density change and this may be significant. Toor suggests that for liquids ranging from water to polymers there are non-axial maxima in the radial temperature profiles, resulting from the compressibility effects acting as a heat sink.

The contributions of MIZUSHINA and KURIWAKI (126), MITSUISHI and MIYATAKE (123) and FORREST and WILKINSON (61) may be added to the above. For power law fluids with temperature dependent rheological properties MIZUSHINA et al proposed the following correlation for local Nusselt number under constant wall flux conditions:

$$Nu_q = 1.41\left(\frac{3n+1}{4n}\right)^{\frac{1}{3}} Gz^{\frac{1}{3}} \left(\frac{K_{Nb}}{K_{Nw}}\right)^{C/n^{0.7}} \qquad (120)$$

where

$$C = 0.045\left[1.41\left(\frac{3n+1}{4n}\right)^{\frac{1}{3}} Gz^{\frac{1}{3}}\right]^{0.7} \qquad (121)$$

and K_{Nb} is the power law constant at the mean bulk fluid temperature, and K_{Nw} is at the mean wall temperature. At low values of the Graetz number, equation (120) was replaced by

$$Nu_q = 4.36\left(\frac{3n+1}{4n}\right)^{\frac{1}{3}} \left(\frac{K_{Nb}}{K_{Nw}}\right)^{0.14/n^{0.7}} \qquad (122)$$

MITSUISHI et al (123) considered the same problem but accounted for temperature effects by a parameter γ (= non-isothermal viscosity gradient at the wall/isothermal gradient) which was introduced in to the final expression for temperature. The profile is exactly the same as given by BIRD (11) when $\gamma = 1$, but for $\gamma \neq 1$ the Graetz number is multiplied by the factor γ. FORREST et al (61) in an extension of a previous work (60) for constant wall temperature, included viscous dissipation and uniform internal heat generation effects for the constant wall heat flux condition. Their analysis was numerical and the results were presented graphically for n = 0.5, 1.0 and 2.0.

4.2.2(c) Analytical Methods - Other Models

Although the present investigation is concerned with power law model fluids, a review of the progress being made in heat transfer studies to other non-Newtonian fluids obeying shear stress - shear rate laws different from the power law, is appropriate at this stage. This is particularly so because rheologists are becoming increasingly aware that the rigid classifications usually given to non-Newtonian fluids do not always present the true picture. Bingham Plastics, for example, behave like ordinary Newtonian fluids once the yield stress has been exceeded. This can also be said of pseudoplastic (power law) fluids at very high or infinite rates of shear. Quite a considerable

amount of work has been done on Bingham plastics, with the physical constants assumed constant. The Graetz type "isothermal" problem was extended by SCHECHTER and WISSLER (158), to the case of Bingham plastics with additional allowance for various patterns of heat generation within the fluid during flow. Such internal heat generation occurs, for example, in nuclear reactors using thorium oxide slurries in both core and blanket regions. A rigorous solution of the heat conduction equation (63) was attempted by HIRAI (79), but his treatment has been shown by SCHECHTER and WISSLER (158) to be in error. These errors, however, do not extent to Hirai's approximate expression for h_m using assumptions analogous to those of Leveque for the Newtonian case. This is given as

$$Nu_m = \frac{h_m D}{k} = 1.75 \left\{ \frac{WC_p}{kL} \left[\frac{3(1-C)}{C^4-4C+3} \right] \right\}^{\frac{1}{3}} \qquad (123)$$

where $C = \tau_y/\tau_w$. The expression applies when

$$(WC_p/kL)\left[\, 3(1-C)/(C^4-4C+3) \,\right] > 100$$

MICHIYOSHI et al (120) and FORREST and WILKINSON (62) have considered the constant heat flux as well as the constant temperature problems. In the latter case the effects of

temperature - dependent rheological properties were included.

The Prandtl-Eyring model has been treated by SCHENK and VAN LAAR (160). Based on the expression

$$-\frac{dU_z}{dr} = C_{PE} \sinh(\tau/A_{PE}) \qquad (124)$$

they calculated Nu_∞ under conditions of constant wall temperature for various value of B, where

$$B = (R/2A_{PE})\ (D\Delta P/dZ) \qquad (125)$$

In equation (125) the case of B = 0 is analogous to Poiseüille flow and B = ∞ to piston or slug flow. By assuming a developing velocity profile and a temperature profile of the form

$$T(r,z) = (\exp f(z))f(r) \qquad (126)$$

they obtain a trial and error solution for the heat conduction equation. CHRISTIANSEN and JENSEN (210) have also obtained numerical solutions of the energy equation but included non-isothermal effects due to temperature - dependent consistency. Wall temperature was assumed constant.

MATSU-HISA and BIRD (109) used the Ellis model to derive the Nusselt number, both in the entrance and fully developed regions, under conditions of constant heat flux as well as under constant wall temperature. In this later contribution MITSUISHI and MIYATAKE (124) used the same model and same wall conditions (109) to obtain eigenvalue expressions for temperature profiles and Nusselt numbers.

4.2.2(d) Semi-Theoretical and Experimental Methods

All treatments considered so far have been either purely analytical or numerical. Physical properties have been assumed independent of temperature and therefore velocity profiles remain constant thoughout the heat transfer section of the tube. Experimental investigations have been few and for most parts have neglected the non-isothermal effects, which become significant under certain conditions in practice. The experimental results, along with their semi-theoretical expressions for non-isothermal effects are discussed below. It has been shown (145) that previous experimental work in the area of heat transfer to suspensions and other non-Newtonian materials may divided into two categories.

One category consists of publications devoted to a study of suspension of relatively inert (i.e. non solvated) solids or of dilute suspensions of other solids.

The work of MILLER (121), ORR and DALLA VALLE (139) and WINDING and co-workers (203) and parts of the work of BONILLA et al (18) and of SALAMONE and NEWMAN (157) fall into this category. Such suspension are usually nearly Newtonian in behaviour; hence the peculiarities due to the non-Newtonian properties are difficult to evaluate experimentally. Most of these investigators made some attempt to consider this problem, but the purposes of their work did not include the presentation of broad defining equations which might apply to highly non-Newtonian systems as well as to the inert suspensions studied.

The second category deals with empirical correlations of experimental data on more highly non-Newtonian systems. METZNER, VAUGHAN and HOUGHTON (117) presented the first theoretical analyses combined with an experimental study of the variables controlling heat transfer rates to highly non-Newtonian fluids in laminar flow. The theoretical analyses, for the limiting types of non-Newtonian materials, were related to the intermediate case of Newtonian behaviour to form a coherent theory applicable to Newtonian and non-Newtonian fluids alike. The experimental data was obtained using three non-Newtonian fluids,

(i) a 1.75% solution of Carbopol in water (n for this fluid varying between 0.18 and

0.40, depending upon temperature and shear rate),

(ii) a 3.72% solution of sodium carboxymethyl-cellulose (CMC) in water (n' varying between 0.43 and 0.51 for this fluid)

(iii) a 1.40% CMC solution in water (n' = 0.70).

The experimental data covered Graetz numbers between 100 and 2000 and were correlated with a mean deviation of 13.5%. For Gz < 5, the theoretical curves of Nu vs Gz for piston flow (n' = 0) approach the limiting case of an outlet fluid temperature equal to the wall temperature of the tube. The Nusselt number may be obtained by a heat balance and is given by

$$\frac{h_m D}{k} = \frac{2}{\pi} \frac{WCp}{kL} \qquad (127)$$

GRAETZ (71) obtained a solution of the Fourier-Poisson heat conduction equation for n' = 0 and is given as

$$Nu = \frac{2WCp}{\pi kL}\left(\frac{1 - \psi_2(Y)}{1 + \psi_2(Y)}\right) \qquad (128)$$

where $\psi_2(Y)$ is a convergent infinite series of exponential functions in $\pi kL/WCp$. Since this solution is unwieldy for Gz > 500, METZNER et al (117) have extended the BOUSSINESQ (19) solution to produce an asymptotic solution valid for

$Gz > 100$ and $n' = 0$,

$$\frac{h_m D}{k} = \frac{8}{\pi} + \frac{4}{\pi} \left(\frac{WCp}{kL}\right)^{\frac{1}{2}} . \qquad (129)$$

For $n' = \infty$, case of infinite dilatancy, Metzner et al used the Leveque type of approximation to obtain

$$\frac{h_m D}{k} = 1.590 \left(\frac{WCp}{kL}\right)^{\frac{1}{3}} \qquad (130)$$

Equations (129) and (130) represent, theoretically, the maximum values of laminar heat transfer coefficient that could be obtained with pseudoplastic fluids and dilatants respectively. To consider the effect of non-Newtonian behaviour on heat transfer, they define interpolation factors δ and Δ . These are defined as follows:

(a) For WCp/kL $(= Gz)$ > 100 and n' between 0.10 and infinity

$$\frac{h_m D}{k} = 1.75\, \delta^{\frac{1}{3}} \left(\frac{WCp}{kL}\right)^{\frac{1}{3}} \qquad (131)$$

where

$$\delta^{\frac{1}{3}} = \frac{3n' + 1}{4n'}$$

(b) For values of n' below 0.10 at all values of $\frac{WCp}{kL}$ and for n' between 0.10 and 1.0 when WCp/kL is below 100

$$\frac{\frac{h_m D}{k}\ \text{non-Newtonian}}{\frac{h_m D}{k}\ \text{Newtonian}} = \Delta^{\frac{1}{3}} \qquad (132)$$

A plot of $\Delta^{\frac{1}{3}}$. vs. n′ is given.

(c) For $n' > 1.0$ and $\frac{WCp}{kL} < 100$,

$$\delta^{\frac{1}{3}} = \left(\frac{3n' + 1}{4n'}\right)^{\frac{1}{3}} \qquad (133)$$

To take into account the distortion in velocity profile due to temperature variation, they have used a Sieder-Tate type correction factor, by including a consistency ratio term. Equation (131) becomes

$$\frac{h_m D}{k\Delta^{\frac{1}{3}}} = 1.75\left(\frac{WCp}{kL}\right)^{\frac{1}{3}}\left(\frac{\gamma}{\gamma_w}\right)^{0.14} \qquad (134)$$

For Newtonian fluids $\Delta^{\frac{1}{3}} = 1.0$, γ reduces to μ and γ_w to μw.

One has to be very careful in the choice of apparent viscosity μa, when working with non-Newtonian fluids. Non-Newtonian fluids are generally classified in relation to the behaviour of the "effective" viscosity, μ_{eff}, under increasing or decreasing shear stress, μ_{eff} is defined as, for power law fluids

$$\mu_{eff} = K_N' \left(\frac{\partial u}{\partial r}\right)^{n-1} \tag{135}$$

$$= K_N \left(\frac{3n+1}{4n}\right)^n \left(\frac{8U_m}{D}\right)^{n-1} \tag{136}$$

The general apparent viscosity is defined as

$$\mu_a = \tau/(du/dr)$$

$$= K_N (du/dr)^{n-1}$$

$$= K_N \left(\frac{3n+1}{4n}\right)^{n-1} \left(\frac{8U_m}{D}\right)^{n-1} \tag{137}$$

so

$$\mu_{eff} = \frac{3n+1}{4n} \cdot \mu_a \tag{138}$$

METZNER et al (117) define their apparent viscosity

$$\mu'_a = \gamma (U_m/D)^{n'-1} \tag{139}$$

$$= K_N' \left(\frac{8U_m}{D}\right)^{n'-1}$$

$$= K_N \left(\frac{3n+1}{4n}\right)^n \left(\frac{8U_m}{D}\right)^{n-1} \tag{140}$$

$$\mu'_a = \mu_{eff} = \frac{3n+1}{4n} \mu_a \tag{141}$$

Thus, they used the equivalent of the general "effective"

viscosity. They have also presented their data in the transition region in the form of a j-factor plot. Since they have used only one L/D ratio, caution is advised in the application of these plots which may be used for order-of-magnitude estimates only.

METZNER and GLUCK (118), based on GLUCK's (69) data on CPM and CHARM's (26) data on ammonium aligante ($n = 0.5$), apple sauce ($n = 0.65$) and banana puree ($n = 0.46$) under conditions of constant wall temperature, use EUBANK and PROCTOR's (58) empirical correlation for natural convection effects

$$\frac{h_m D}{k\delta^{\frac{1}{3}}} \left(\frac{\mu_{eff\ w}}{\mu_{eff\ b}}\right)^{0.14} = 1.75 \left[Gz+12.6\left(Pr_w Gr_w D/L\right)^{0.4}\right]^{\frac{1}{3}} \tag{142}$$

Wall conditions have been chosen since viscosity for most non-Newtonian fluids is lowest at the wall, the resistance offered to convective motion is minimized and the overall effect is greater than elsewhere in the tube. Since viscoelastic effects tend to reduce convective motion, this equation (142) must be considered to be limited to purely viscous fluids.

The constant wall temperature laminar cooling and heating have been studied by OLIVER and JENSEN (138).

The pseudoplastic solutions used were those of SCMC, CPM 934 and Polyox in water and ethyl alcohol. By judicious choice of radial temperature gradients the effects of natural convections could be eliminated. They used two tubes of different diameters and showed that natural convection depended upon the wall conditions and independent of L/D. Their final equation is

$$Nu = 1.75\left(\frac{\mu_{eff\ b}}{\mu_{eff\ w}}\right)^{0.14}\left[Gz+0.0083\left(Gr_w Pr_w\right)^{0.75}\right]^{\frac{1}{3}} \qquad (143)$$

They suggest that the METZNER - GLUCK (118) correlation overcorrected for natural convection at large temperature differences. The concentrations of CPM 934 used in these tests exhibited the unusual phenomenon of increasing apparent viscosity and pseudoplastic character (lower n) with increasing temperature. By proposing a model for the superimposition of natural convection effects over forced convection, Oliver and Jenson have shown that, under certain extreme conditions, natural convection may decrease the extent of heat transfer, when fluid layers of high viscosity compared to that of bulk are formed.

CHRISTIANSEN and CRAIG (30) have considered the effect of radial viscosity variation analytically. Instead of using the Sieder-Tate correction factor,

μ_w/μ_b, they have used a function

$$\Psi(H) = \frac{\Delta H}{R'}\left(\frac{1}{T_i} - \frac{1}{T_w}\right) \tag{144}$$

They have redefined the power law, to include the effect of temperature on the shear stress - shear rate relationship, as

$$\tau = K_N \left(e^{\Delta H/R' T}\dot{\gamma}\right)^n \tag{145}$$

where

$$\dot{\gamma} = \frac{\partial u}{\partial r} \tag{146}$$

When $\Psi(H) = 0$, then, since T_i and T_w are finite, $\Delta H = 0$, and hence the viscosity term in equation (145) becomes temperature independent. They have obtained a numerical computer solution of the energy and momentum equations for the case of constant wall temperature, by using the redefined power law (equation (145)). The heat conduction in the final form is given as

$$\frac{\partial T}{\partial(1/GZ)} = 2\pi \frac{I_2}{I_1}\left(\frac{1}{\xi}\frac{\partial T}{\partial \xi} + \frac{\partial^2 T}{\partial \xi^2}\right) \tag{147}$$

where

$$I_1 = \int_{\xi}^{1} \xi^{1/n} \, e^{-\Delta H/R'T} \, d\xi \tag{148}$$

$$I_2 = \int_{0}^{1} I_1 \xi \, d\xi \tag{149}$$

$$\xi = \frac{r}{R_w}$$

The polymer solutions used by Christiansen and Craig were 3% CMC and 0.75% CPM in water. The results, using the $\Psi(H)$ technique, were correlated more accurately than the modified Sieder-Tate approach. Christainsen and Craig integrated equation (147) numerically and presented the results graphically in the form

$$Nu_m = \phi\left[Gz, n, (T_w - T_i)/T_i, \; (\Delta H/R')(1/T_i - 1/T_w) \right] \tag{150}$$

In general, $(T_w - T_i)/T_i$ is small and can be usually neglected, therefore equation (150) becomes:

$$Nu_m = \phi\left[Gz, n, \Psi(H) \right] \tag{151}$$

where $\Psi(H)$ is as defined in equation (144).

Computed solutions for equation (151) are shown in Figs.11 to 13.

These indicate effect of temperature-dependent consistency in fluids for which n = 1, $\frac{1}{3}$, and $\frac{1}{10}$ respectively. There are some limitations to the use of equation (151). First the correlation is poor at low Gz because no correction was made for the influence of natural convection effects. Furthermore, the foregoing analysis has been carried out for positive values of the parameter $\Psi(H)$ only. As a result it is only possible to make predictions for heating, for the usual case of fluid consistency decreasing with increasing temperature. Similar computations, for negative values of the parameter $\Psi(H)$ have been presented by CHRISTIANSEN, JENSEN and TAO (31) so that cooling rates can also be determined. However, it still remains to be proven by more experimental data whether the $\Psi(H)$ correlation is valid for other fluids which cannot be adequately described by the Ostwald-de Wael model (power law model). In more recent experiments, CMC solutions (1.1%, 2% and 3% concentrations) were used by MITSUISHI and MIYATAKE (125) to confirm the theoretical Nu-Gz predictions given in their early work (123).

4.2.3 Further Details of Procedures for Estimating Temperature Distributions in Laminar Flow through Tubes

It is intended during the course of this investigation to make radial temperature traverses at various locations along the experimental tube section. This

being the case, and before discussing turbulent heat transfer it will be useful to review in some detail the theoretical attempts that have been made to estimate the centre-line temperatures in a tube.

Thermal conditions are customarily described as being fully developed at and beyond the point at which the thermal or temperature boundary layers meet at the axis of the tube. The temperature distribution can be estimated for a pseudoplastic fluid under fully developed conditions, using a properly determined value of the mean or "mixed cup" temperature at the cross-section in question and the rheological constants. A few procedures have been developed notably that of CHARM (27) for pseudoplastic fluids, ECKERT (53) for Newtonian fluids and GEE and LYON (65) for Ellis Model non-Newtonian fluids. The procedure detailed below is essentially that given by CHARM (27) but with some modifications (177). Furthermore, the superflous restriction of constant wall temperature is eliminated. The following polynomial form is assumed for the temperature distribution at any distance z along the tube in the region of fully developed thermal conditions, where T_{wz} is the wall temperature at z:

$$T = T_{wz} - A(R-r) - B(R-r)^2 - C(R-r)^3$$

$$= T_{wz} - A\bar{y} - B y^2 - C y^3 \qquad (152)$$

in which A, B, C are functions of z. To evaluate A, B and C consider a differential length of tube dz, where the heat transfer through a layer immediately adjacent to the wall occurs by pure conduction, such that in heating the fluid

$$d\dot{Q}_w = -k2\pi(R-y)\,dz\,\frac{\partial T}{\partial y} \tag{153}$$

$$\frac{\partial T}{\partial y} = -\frac{\partial \dot{Q}_w}{k2\pi(R-y)\,dz} \tag{154}$$

$$\frac{\partial^2 T}{\partial y^2} = \frac{-\partial \dot{Q}_w}{k2\pi(R-y)^2 dz} = \frac{1}{R-y}\,\frac{\partial T}{\partial Y} \tag{155}$$

But y = 0 at the wall, so that

$$\left(\frac{\partial^2 T}{\partial y^2}\right)_{y=0} = \frac{1}{R}\left(\frac{\partial T}{\partial y}\right)_{y=0} \tag{156}$$

and from equation (152)

$$\left(\frac{\partial T}{\partial y}\right)_{y=0} = -A \tag{157}$$

$$\left(\frac{\partial^2 T}{\partial y^2}\right)_{y=0} = -2B \tag{158}$$

Substituting into equation (156) shows

$$B = \frac{A}{2R} \tag{159}$$

At the axis of the tube $\left(\frac{\partial T}{\partial y}\right)_{y=R} = 0 = -2A - 3CR^2$

$$C = -\frac{2A}{3R^2} \tag{160}$$

Substituting for B and C in equation (152) gives

$$T = T_{wz} - A(R-r)\left[1 + \frac{1}{2}\left(\frac{R-r}{R}\right) - \frac{2}{3}\left(\frac{R-r}{R}\right)^2\right] \tag{161}$$

The value of A corresponding to a given z (in the fully developed region) may be approximated via the following energy balance between the entrance point and point z

$$2\pi\rho\ C_p \int_o^R ru(T-T_i)\,dr = Q\rho\ C_p(\overline{T}_z - T_i) \tag{162}$$

where $\overline{T}_z$ is the mean or "mixing cup" temperature at z. Insertion of the equation

$$\frac{Q}{\pi R^3} = \frac{n}{3n+1}\left(\frac{\tau_w}{K_N}\right)^{1/n} \tag{42}$$

for Q (with $\tau_w = R\Delta P/2L$),

$$u = U_m\left(\frac{3n+1}{n+1}\right)\left[R^{\frac{1}{n}+1} - r^{\frac{n+1}{n}}\right] \tag{43}$$

for u,

and equation (161) for T in equation (162) gives

$$\int_0^R \left[R^{\frac{n+1}{n}} - r^{\frac{n+1}{n}}\right] r \left\{T_{wz} - T_i - A(R-r)\,1 + \tfrac{1}{2}\left(\frac{R-r}{r}\right) \ldots\right.$$

$$\left. \ldots - \frac{2}{3}\left(\frac{R-r}{r}\right)^2 \right\} dr = \frac{n+1}{2(3n+1)} \left(\overline{T}_z - T_i\right) R^{\frac{3n+1}{n}} \qquad (163)$$

Integrating and rearranging

$$AR\left[\frac{7}{40} - \frac{5n}{6(3n+1)} + \frac{3n}{2(5n+1)} - \frac{2n}{3(6n+1)}\right] = \frac{n+1}{2(3n+1)} \left(T_{wz} - \overline{T}_z\right) \qquad (164)$$

(Equation (163) is here corrected from its erroneous form in the original paper (27).)

Equation (164) applies under fully developed thermal conditions, a criterion for which will now be presented. The quantity A at a given z may be obtained from equation (164) after $\overline{T}_z$ has been estimated in the following manner with reference to Fig.14 (Appendix 1)

If as in many cases, the resistance to heat transfer offered by the pseudoplastic fluid is much greater than that of either the tube wall or the annulus fluid, then the temperature of the annulus fluid approx-

imates that of the inner surface of the tube (i.e. $t = T_w$). An energy balance between the two fluids gives

$$WC_p(\overline{T}_z - T_i) = W_{ann}\ C_{p\ ann}(t_z - t_1) \tag{165}$$

where $C_{p\ ann}$ is the specific heat of the annulus fluid and W, W_{ann}, C_p, $C_{p\ ann}$, T_i and t_1 are known from the statement of operating conditions. A value is assumed for $\overline{T}_z$, the corresponding $t_z = t_{wz}$ calculated from equation (165), and the values tested for validity by insertion in the following balance

$$WC_p(\overline{T}_z - T_i) = h_m 2\pi RZ \quad \frac{(T_{w1} - T_i) - (T_{wz} - \overline{T}_z)}{2.303 \log (T_{w1} - T_i)/T_{wz} - T_z)} \tag{166}$$

where h_m is calculated from the equation

$$\frac{h_m D}{k} = 2.0 \left(\frac{WC_p}{kL}\right)^{\frac{1}{3}} \left[\frac{K_{Nb}}{K_{Nw}} \frac{(3n+1)}{(3n-1)}\right]^{0.4} \tag{167}$$

suggested by CHARM and MERRILL (28).

$$K_{Nb} = (\Delta P/2L)_b \tag{168}$$

$$K_{Nw} = (\Delta P/2L)_w \tag{169}$$

or

$$\mu_{ab} = \left(\frac{\Delta P}{2L}\right)_b^{1-\frac{1}{n}} K_{Nb}^{\frac{1}{n}} \left(\frac{3n+1}{2(3n+1)}\right)^{1-\frac{1}{n}} R^{1-\frac{1}{n}} \qquad (170)$$

$$\mu_{aw} = \left(\frac{\Delta P}{2L}\right)_w^{1-\frac{1}{n}} K_{Nw}^{\frac{1}{n}} R^{1-\frac{1}{n}} \qquad (171)$$

μ_{ab} and μ_{aw} are "apparent viscosities" of the pseudoplastic fluid evaluated at the bulk average condition and at the tube wall respectively. This process is repeated until equation (166) is satisfied. The values of $\overline{T}_z$ and T_{wz} established in this way are inserted in equation (164) enabling calculation of A and hence of the temperature distribution at z from equation (161). The temperature at the centre line of the tube (r=0) is shown by equation (161) to be

$$T_c = T_{wz} - \frac{5}{6} AR \qquad (172)$$

If, when the pseudoplastic fluid is heated, equation (172) gives a value of T_c less than T_i, this indicates that fully developed thermal conditions have not been attained at the z value for which A was determined. The same indication prevails if, when cooling a pseudoplastic fluid, equation (172) predicts T_c greater than T_i. Fully

developed thermal conditions begin at z value for which equation (172) predicts T_c equal to T_i, and for all lesser z values T_c equals T_i. The insertion of "isothermal" equations (42) and (43) into equation (162) to obtain "non-isothermal" equation (164) must introduce error, somewhat like that in "isothermal" treatments described earlier.

4.2.4 Turbulent Heat Transfer - Newtonian Fluids

Although as has been stated, turbulent conditions are difficult to obtain with highly non-Newtonian fluids, the well established correlations for Newtonian turbulent heat transfer have been used by most investigators to check the reliability of both their equipments and data obtained from them. A review of the most significant works in this field is therefore appropriate. Heat transfer in turbulent flow occurs as a result of the combined processes of conduction and convection, and a knowledge of the turbulent velocity fluctuations is required to obtain a solution of the energy equation. These velocity fluctuations occur primarily by the movement of numerous macroscopic elements of fluid (eddies) between regions at different temperatures and it is very difficult to predict the behaviour of these eddies with time. Hence, studies on turbulent heat transfer include both theoretical and semi-empirical relationships as

well as empirical correlations (which give us insight into the mechanism). The empirical correlations of turbulent heat transfer data for closed conduits have been obtained using dimensionless groups. The two common forms are:

$$Nu = C \quad (Re)^{m_1}(Pr)^{m_2}\left(\frac{D}{L}\right)^{m_3} \tag{173}$$

$$St = C \quad (Re)^{m_4}(Pr)^{m_5}\left(\frac{D}{L}\right)^{m_6} \tag{174}$$

the term (D/L) being of importance in the case of short tubes. Although both (173) and (174) are equivalent, use of equation (174) is advantageous since

(i) the Stanton number may be determined without knowing or taking into account the physical properties of the fluid

(ii) at constant Prandtl number, St. varies as $Re^{-0.2}$ while Nu varies as $Re^{0.8}$, as shown below,

i.e. equation (173) requires a greater range of ordinates. The commonly accepted correlations are those of DITTUS and BOELTER (47), COLBURN (41) and SIEDER and TATTE (174). These are all based on constant wall temperature turbulent flow conditions. They are

DITTUS and BOELTER:

$$\left(\frac{h_L D}{k}\right)_b = 0.023 \left(\frac{DG}{\mu}\right)_b^{0.8} \left(\frac{C_p \mu}{k}\right)_b^{m_2} \qquad (173a)$$

where $m_2 = 0.4$ for heating

$m_2 = 0.3$ for cooling

COLBURN:

$$\left(\frac{h_L}{GC_p}\right)_b \left(\frac{C_p \mu}{k}\right)_b^{\frac{2}{3}} = 0.023 \left(\frac{DG}{\mu}\right)^{-0.2} \qquad (175)$$

where $t_f = (t_w + t_b)/2$

SIEDER and TATE:

$$\left(\frac{h_L}{GC_p}\right)_b \left(\frac{C_p \mu}{k}\right)_b^{\frac{2}{3}} = \left(\frac{\mu w}{\mu_b}\right)^{0.14} = 0.023 \left(\frac{DG}{\mu}\right)_b^{-0.2} \qquad (176)$$

Equations (175) and (176) hold good for

$$\begin{aligned} Re &> 10,000 \\ 0.7 < Pr &< 160 \\ L/D &> 60 \end{aligned} \qquad (177)$$

The available data are correlated within a maximum of $\pm$ 40% by the three equations (see McADAMS (127)).

L'ECUYER and WARNER (52) have demonstrated that for turbulent heat transfer in circular sections, there is no significant difference in heat transfer coefficients for constant wall temperature or constant heat flux boundary conditions. BERGLES and ROHSENOW (7) conducted a series of experiments at constant mass velocity and increasing heat flux to compare the ability of the correlations to account for variation of physical properties. It was observed that, with increasing radial temperature difference, the deviation from the correlating lines also increased. Equation (175) and (176) predicted higher coefficients than observed ones, especially at high temperature differences; equation (173a) predicted lower coefficients. ALLEN and ECKERT (3) have made a systematic study of data for flow of water at uniform heat flux for various heating rates and have extrapolated to zero heating rate or constant fluid property condition (EAGLE and FERGUSON (51) technique). This enables one to compare the effect of heating rate on thermal entrance length. Allen and Eckert, concluded, from their studies, that it is reasonable to set the standard of accuracy expected of smooth tube heat transfer measurements close to that expected of smooth tube friction measurements.

4.2.5 Turbulent Heat Transfer - Power Law Fluids

The work of MILLER (121), WINDING (203), SALAMONE (157) and BONILLA (18) have already been mentioned

in connection with heat transfer studies of suspensions of relatively inert and only slightly non-Newtonian suspensions. To these may be added the work of CHIN CHU et al (37) and MISHRA et al (122). The nature of these suspensions permitted studies in truly turbulent regions of flow. A greater concentration range of solid liquid suspensions (up to 45% by weight solid) was investigated by ORR and DALLA VALLE (139); who correlated both their own extensive slurry data and the earlier results of BONILLA et al (18) on aqueous chalk slurries by the equation

$$\frac{h_m D}{k} = 0.023\left(\frac{DU_m}{\mu_s}\right)^{0.8}\left(\frac{C_p\mu_s}{k_s}\right)^{\frac{1}{3}}\left(\frac{\mu}{\mu_w}1\right)^{0.14} \qquad (178)$$

where ρ and C_p are the density and heat capacity of the slurry taken as the weighted average values of the slurry components; k_s is evaluated from the expression for thermal conductivity given by TAREEF (185).

$$k_s = k_1\left[\frac{2k_1+k_p-2x_v(k_1-k_p)}{2k_1+k_p+x_v(k_1-k_p)}\right] \qquad (179)$$

k_s, k_1, and k_p are the thermal conductivities of the overall suspension, the suspending medium and the dispersed particles respectively; x_v is the volume fraction of the dispersed particles in suspension. The viscosities μ_1 and μ_w are the viscosities of the suspending liquid at the bulk mean temperature and the wall

temperature respectively; μ_s is obtained from the empirical relation

$$\mu_s = \frac{\mu_1}{(1 - x_v/x_{vb})} \qquad (180)$$

x_{vb} is the volume fraction of solid particles in a sedimented suspension or bed, evaluated after prolonged standing of the slurry. Equation (178) is the conventional form of the Dittus - Boelter equation for forced convection in tubes, incorporating the correction of Sieder and Tate. Orr and Dalla Valle and the other workers showed that this form of equation was applicable to slightly non-Newtonian fluids provided that sufficient care and thought is given to the measurement of the appropriate fluid properties.

For highly non-Newtonian pseudoplastic fluids, the most notable works are those of METZNER, VAUGHN and HOUGHTON (117) and METZNER and REED (116), CLAPP (38) and METZNER and FRIEND (119). Clapp correlated results obtained from tests on Carbopol solutions by the following two alternative empirical equations

$$\frac{h_m D}{k} = 0.0041 \left(\frac{D^n U_m^{2-n} \rho}{K'_N \, 8^{n-1}} \right)^{0.99} \left[\frac{K'_N C_p}{k} \left(\frac{8U_m}{D} \right)^{n-1} \right]^{0.4} \qquad (181)$$

with maximum deviation of + 1% and -4.5%;

$$\frac{h_m D}{k} = 0.023(9350)^{0.8(1-\frac{1}{n}n)} \left(\frac{D^n U_m^{2-n} \rho}{K'_N 8^{n-1}}\right)^{\frac{0.8}{n^n}} \quad \ldots$$

$$\ldots \left[\frac{K'_N C_p}{k} \left(\frac{8U_m}{D}\right)^{n-1}\right]^{0.4} \qquad (182)$$

with maximum deviations of +2% and -4.50%.

The range of n was $0.698 \leq n \leq 0.786$. METZNER et al (117) suggest that a suitable apparent viscosity for use in the generalized Prandtl number could be found by equating the Newtonian Reynolds number to the generalised one, as follows:

$$\frac{\rho U_m D}{\mu'_a} = \frac{D^{n'} U_m^{2-n'} \rho}{\gamma} \qquad (183)$$

giving

$$\mu'_a = \gamma (U_m/D)^{n'-1} \qquad (184)$$

Substituting this into the Prandtl number gives

$$\frac{\mu'_a C_p}{k} = \frac{C_p \gamma}{k} (U_m/D)^{n'-1} \qquad (185)$$

Also in place of the Sieder-Tate viscosity ratio correction they propose the generalized factor

$$(\gamma/\gamma_w)^{0.14}$$

and the final correlation suggested then becomes

$$\frac{h_m D}{k} = 0.023 \left(\frac{D^{n'} U_m^{2-n'} \rho}{\gamma} \right)^{0.8} \left(\frac{\gamma C_p}{k} \left(\frac{U_m}{D} \right)^{n'-1} \right)^{0.4}$$

$$\times (\gamma/\gamma_w)^{0.14} \qquad (186)$$

This expression reduces to the generally accepted form equation (178) when the fluid is Newtonian, i.e. when $n' = 1$ and $\gamma = \mu$.

4.3 HEAT TRANSFER TO FLUIDS FLOWING THROUGH AN ABRUPT CONVERGENCE AND DIVERGENCE

The section on heat transfer will be concluded by a review of the studies on the effect of an abrupt disturbance of the fluid flow on the local heat transfer characteristics for both Newtonian and non-Newtonian fluids. This aspect of heat transfer in pipes is the one with which the present investigation is mainly concerned. While a certain amount of information has been available for many years concerning the purely fluid

flow aspects of these phenomena, heat transfer data has been less extensive. Flow in tubes may often be considered as boundary layer flow since the axial velocity component usually predominates. If the flow is disturbed by a discontinuity in the tube geometry, a localised region of the fluid may experience an adverse pressure gradient which causes large transverse velocity components. The axial velocity may be reversed locally, and a standing eddy formed downstream of the discontinuity. This kind of flow is termed "separated", and separation can have a considerable effect on the local coefficient of heat transfer. In general, the boundary layer equations cannot be used to analyse this sort of problem, only a solution of the full equations will suffice.

4.3.1 Heat Transfer to Newtonian Fluids Flowing Through an Abrupt Convergence and Divergence

Of the earliest theoretical works on entry conditions in a normal straight pipe, that of LATZKO (97) on turbulent boundary layer flows, and SCHILLER (161) on laminar flows, have formed the basis of subsequent studies. Two works of more recent origin bearing directly upon the results presented in the paper by Latzko are those of KAYS (91) and SELLARS, TRIBUS and KLEIN (170). Sellars et al computed the effects of arbitrary wall temperature on heat flux variation with "Poiseuillean" flow. KAYS (91) presented a numerical

treatment of the problem of simultaneous development of velocity and temperature profiles and compared the results favourably with experiments in which both constant heat flux and constant wall temperature had been used as boundary conditions. The flow had been air from a large chamber to a pipe.

Experimentally the works of BOELTER et al (16), CHOLETTE (36) and ALAD'EV (2) were the first to investigate the nature of heat transfer during separation. BOELTER et al (16) worked on forced convection with air in tubes having different configurations. The local heat transfer coefficient was found to become very high, about four times greater than its non-separated value. It has been suggested (128) that the location of the maximum value is probably near to the point of boundary layer reattachment, i.e. the point downstream of the separation "bubble" at which the direction of flow reverses on the heat transfer surface, and the entire domain becomes a boundary layer. The magnitude of the local coefficient falls away sharply as the distance from the position of the maximum value increases. CHOLETTE'S (36) entry condition was that of an abrupt convergence from a header into a large number of small tubes in parallel; otherwise his technique was similar to that of BOELTER et al, except that his measured sections were about $10\frac{1}{2}$ diameters long so that his results close to the entrance are of very limited value. ALAD'EV (2)

used a single steam heated pipe with water as the fluid. The entry conditions were the same for all tests; the water appears to have entered the heated pipe through a short length of pipe about 1.75 times larger in diameter, the convergence being conical at about 45 degrees half angle.

The more recent and extensive investigations on the effect of abrupt convergences and divergences are those of EDE, HISLOP and MORRIS (54), EDE, MORRIS and BIRCH (55), EDE (56) and McINTYRE (128). Ede et al considered convergence ratios of 2 to 1 (54), 1.25 to 1 and 3.33 to 1 (55) and divergences in the same ratios. The fluid was water (except in (56) where air was used), and the Reynolds number ranged from 800 to 100000 in the smaller pipe which had a nominal diameter of 25mm. The boundary condition was that of constant wall heat flux. The authors concluded that for the abrupt convergences, the variation in local coefficient of heat transfer does not differ greatly from the variation found by earlier workers in the entry regions of pipes under more gradual entry conditions. (See Figs. 15, 16 and 17, Appendix 1). For abrupt divergences, however, in the turbulent region, the variation in local coefficient is considerable. Data for all diameter ratios (i.e. $Nu/Pr^{0.4}$ plotted against Z/D) follow the same trend. Coefficients near the change of section are very much greater than further along the pipe and, in contrast to the convergence results, exhibit a pronounced peak, the magnitude of which

increases in direct proportion to the diameter ratio . The peak to terminal Nusselt number ratio falls with increasing Reynolds number. Ede et al estimated that the effect of an abrupt divergence on local heat transfer coefficient was equivalent to the addition of from 7-14 diameters to the length of the pipe.

An extension of Ede's work has been carried out by McINTYRE (128) using highly viscous liquids (water/ propylene glycol mixtures). Tube configurations similar to those used by Ede et al were considered in addition to short tubes with different entry conditions. The Prandtl numbers ranged from 60 to 350; the Reynolds numbers from 100 to 10000. The effects of free convection, temperature dependent viscosity and viscous dissipation were assessed, with a view to prove that the effects of these were small. The effect of viscous dissipation was treated theoretically only, since dissipation was shown to be insignificant in the tests. Both theoretical and empirical analyses were given for cases of free convection and variable viscosity. For divergences McIntyre's data show that peak heat transfer coefficients (expressed as $Nu/Pr^{\frac{1}{3}}$) occur at 2.4 diameters downstream of a divergence for turbulent and transitional flows in the upstream pipe. At lower values of Re, the peak moves down to about 12 diameters and for $Re < 250$ the position of this maximum could be anywhere. Tests on convergences indicated that

with particular values of Re and Pr downstream, the Nu measured close to the change of section increased with the contraction ratio. Comparison with the short tube entry region tests confirmed earlier conclusions (55) that in general, the "developed" flow correlations could be used to give a reasonable estimate of undeveloped coefficients of heat transfer when a viscous medium was utilized (Fig.19, Appendix 1).

The first (and as yet only reported) attempt to correlate quantitatively the observed peak Nusselt number in separated flows with the flow parameters has been made by ZEMANICK and DOUGALL (204). Their experiments were performed with three expansion geometries of diameter ratios 2.3, 1.85 and 1.22 using air as the fluid. Data was presented for Reynolds numbers from 4000 to 5000 - 90000 depending on geometry. The general trend of their results was in agreement with those of EDE et al (54, 55 and 56). Peak Nusselt numbers were correlated with the upstream Reynolds numbers by the expression

$$Nu_{max} = 0.20\ Re^{0.667} \qquad (187)$$

For more viscous fluid McINTYRE (128) obtained data which was correlated by equation (187) to within $\pm$ 5%. Bearing in mind the high Reynolds numbers used in the above tests, it remains to be seen whether equation (187) is also

valid (with respect to the Re exponent) for the very low Reynolds numbers likely to be encountered in the present series of experiments.

4.3.2 Heat Transfer to Non-Newtonian Fluids Flowing Through an Abrupt Convergence and Divergence

The present investigation will be an extension of McIntryre's work, the difference being that non-Newtonian viscous fluids will be used. As far as the author can ascertain no previous experimental investigation of this kind has been carried out with non-Newtonian systems.

It has been shown from the literature reviewed in this chapter that theoretical analysis which neglects the effect of axial diffusion of vorticity on the flow upstream of an abrupt change of section, cannot, at least for low Reynolds numbers, form a rigorous basis for correlating experimental data. Most of the reviewed works come under this category. However, the overall validity of the experimental results can be tested by published correlations for fully developed Nusselt numbers. In this respect the works of BIRD (11) and McKILLOP (131) for non-Newtonian systems; and the correlation of MARTIN and FARGIE (105) for viscous Newtonian fluids, will form the basis of intepreting the author's experimental results.

CHAPTER FIVE

SCOPE OF PRESENT INVESTIGATION

In most process design the engineer is at some stage concerned with the transmission of heat to or from a fluid in either batch or continuous flow operation. This investigation is devoted to a particular aspect of this problem in an area which, although it affects practically all food, chemical, plastics, and general processing industries, has only attracted the attention of engineers in the last two decades or even less. In industry most of the stuff processed is more non-Newtonian than Newtonian. The processing of pseudoplastic fluids is usually in laminar flow in circular conduits - either under conditions of constant heat flux or constant wall temperature. Invariably such processes are controlled by valves, and the flows go through bends, and other configurations which may produce a disturbance in the flow. There is some data available on laminar flow heat transfer under constant wall temperature conditions in straight pipes. These give average heat transfer coefficients over the entire length of the heat transfer section. They do not give sufficient information about the significant dependence of pseuodoplastic characteristics on temperature. Much information on this

aspect may be obtained if local heat transfer coefficients are known rather than the average coefficients.

Local heat transfer coefficients may be determined by conducting experiments under conditions of constant heat flux or under constant temperature difference. The case of constant heat flux at wall will be considered. As already stated, much of the existing data has been obtained with straight pipes. The case of a discontinuous pipe flow will be investigated here. It has been felt by some engineers (45, 81, 193) that the work of EDE and others (54, 55 and 56) could have been more significant if:

(i) the change in coefficient occuring at a given point about the area of change in section were determined in relation to change in velocity. This would probably have indicated whether there was an optimum value for velocity for any given diameter radio.

(ii) the estimated water temperature rises were confirmed by traversing the flow at various stations.

Ede's results for laminar flow showed so much scatter on a $Nu\ Pr^{-0.4}$ .vs. Re plot that it was evident that some other influence besides inertia and viscosity had been at work. The effects of free convection, heated

length of pipe upstream, and a change of flow pattern need to be considered. In fact a more thorough investigation of the laminar regime is called for. Based on the foregoing comments the outline of the experimental and theoretical programme for this investigation is given below.

5.1 EXPERIMENTAL PROGRAMME

5.1.1 Laminar Heat Transfer in Newtonian Fluids

Data on heat transfer in Newtonian fluids will be collected to see how they can be extended to the case of non-Newtonian fluids. The fluids mainly concerned will be water and propylene glycol. Data on glycol will also provide data for comparison with viscous non-Newtonian fluids.

5.1.2 Turbulent Heat Transfer in Newtonian Fluids

The main fluid in this case will be water and data on turbulent heat transfer to water will be used to confirm the accuracy and reliability of the experimental set up and temperature measurements.

5.1.3 Temperature Traverse in the Area of Change of Section

The choice of heating to provide uniform wall heat flux, means that variations in $d\ddot{Q}/dz$, dq/dz and h, and fluid temperature axially and fluid temperature and

dq/dz circumferentially, would be most marked about the change of section. In consequence, the estimate of the inner surface temperature may not be sufficiently accurate. An attempt will be made to confirm the estimated water temperature rises by traversing the flow at various stations.

5.1.4 Rheological Measurements in Pseudoplastic Fluids

Experiments are necessary to choose suitable pseudoplastic fluids which are:

(i) time-independent

(ii) non-viscoelastic

(iii) least unstable to shear and heat

(iv) non-corrosive.

Characterization of the pseudoplastic fluids will be performed with suitable viscometers under conditions of shear rate and temperature similar to those encountered in the rig. Temperature dependent rheological equations of state have been postulated, for the pseudoplastic fluids investigated.

5.1.5 Laminar Heat Transfer in Pseudoplastic Fluids

(i) Local heat transfer coefficients will be determined for pseudoplastic fluids in laminar flow through an abrupt convergence of a 3.3 : 1 diameter ratio and through

an abrupt divergence of a 1 : 3.3 diameter ratio. The correlation of these results will provide information on

(a) pseudoplastic effects on heat transfer, and

(b) the effect of an abrupt convergence and abrupt divergence on local heat transfer coefficient.

(ii) By adjusting the heat flux on the wall and by varying the mass flow rate, it is possible either to include or exclude natural convection effects.

5.2 THEORETICAL/SEMI THEORETICAL PROGRAMME

5.2.1 Nusselt-Graetz Correlation

With the available literature on hand, and based on experimental results, a correlation will be attempted to relate Nu with Gz, n, K_N and Z/D and offer improvement factors to take into account the effect of natural convection and viscous dissipation.

5.2.2 Recommendations for Design Procedures

An attempt will be made to provide design procedures for the calculation of heat transfer rates in horizontal tubes with abrupt disturbances of the convergent or divergent type.

5.2.3 Theoretical Assessment of Viscous Dissipation Effects on Non-Newtonian Laminar Heat Transfer

Based on the works of TOOR (191) and GILL (67) an approximate analytical expression for temperature and Nusselt number will be derived for non-Newtonian inelastic fluids taking into account the effects of viscous heat generation.

CHAPTER SIX

A THEORETICAL ASSESSMENT OF VISCOUS DISSIPATION EFFECTS ON NON-NEWTONIAN HEAT TRANSFER

Although it has been recognised that viscous shear heat generation cannot be justifiably neglected for high Prandtl number (>500) heat transfer analyses, most of the existing assessments have been numerical. The results as presented in these reports do not lend themselves to general application.

The only work known to the author in which viscous dissipation was considered analytically and for arbitrary non-Newtonian index (n) is that of SESTAK and CHARLES (171). In this cae, the asymptotic Nusselt number expression was arrived at by a technique which did not involve the necessity of calculating temperature profiles in advance. However, since the scheme of experiments in this project include exploration of radial temperatures, an analytical procedure which provides an expression for temperature as an intermediate step in the determination of Nusselt number is to be desired. The analysis to be carried out in this

chapter will give theoretical expressions for both temperature and Nusselt number for arbitrary n.

The energy equation for laminar flow is given in GOLDSTEIN (70) as

$$\rho\, C_p U \frac{\partial T}{\partial z} = k \frac{1}{r} \frac{\partial}{\partial r}\left(r \frac{\partial T}{\partial r}\right) + \Phi(r) \qquad (188)$$

Considered here is a fluid at a constant bulk temperature T_{bi} entering a tube with a fully developed laminar velocity profile which is constant along the tube; that is, u is a function of r only and there are no radial components. The wall is maintained at a constant flux $\dot{Q}_W$, and heat is generated (or consumed) at a rate, Φ , depending only upon radial position. The physical properties are independent of temperature, and the flow has existed long enough for the temperature at all points to be independent of time. Axial conduction has also been neglected. To include non-Newtonian as well as Newtonian fluids, the stress - rate - of - strain curve is assumed to be given by a power law,

$$\frac{\partial u}{\partial r} = - A\tau^{N-1} \qquad (189)$$

The notations in equation (189) and in subsequent transformations are those used by TOOR (191). They have been

retained for ease of manipulation and will be used with reference to this chapter only.

Returning to equation (189), for N = 2, this is the equation for a Newtonian fluid, and for N > 2 the equation approximately describes the rheological properties of many high polymers. For a tube

$$\tau = - \frac{dp}{dz} \frac{r}{2} \tag{34}$$

and using the same approach as employed in section 4.1.1 the velocity profiles may be written as

$$U_1 = \frac{U}{U_m} = \frac{N+2}{N} \left[1 - \left(\frac{r}{R} \right)^N \right] \tag{190}$$

$$U_m = \frac{AR^N}{N+2} \left(- \frac{dv}{dz} \right)^{N-1} \tag{191}$$

and equation (188) becomes

$$\rho C_p U_m \frac{N+2}{N} \left[1 - \left(\frac{r}{R} \right)^N \right] \frac{\partial T}{\partial z} = k \frac{1}{r} \frac{\partial}{\partial r} \left(r \frac{\partial T}{\partial r} \right) + \Phi(r) \tag{192}$$

TOOR (191) gives the dissipation function Φ in terms of the average rate of energy generation per unit volume $\dot{W}$

as

$$\Phi = - \tau \frac{du}{dr} = \frac{N+2}{2} \dot{W} \left(\frac{r}{R}\right)^N \tag{193}$$

where

$$\dot{W} = \frac{2}{R^2} \int_o^R r \, \Phi \, dr \tag{194a}$$

$$= \frac{2A}{N+2} \left(- \frac{dp}{2dz}\right)^N R^N \tag{194b}$$

By a Bernoulli balance written on a time basis neglecting kinetic and gravitational energy changes he obtained the ultimate expression

$$\dot{W} = - U_m \frac{dp}{dz} = 2\tau_w \, U_m/R \tag{194c}$$

The following transformations

$$\theta = \frac{T - T_{bi}}{R\dot{Q}_w/k} \tag{195}$$

$$\xi = r/R \tag{45a}$$

$$Z^+ = \frac{N}{N+2} \frac{\alpha z}{R^2 U_m} \tag{196}$$

where

$$\alpha = k/\rho C_p)$$

make equation (192) dimensionless

$$(1-\xi^N)\ \frac{\partial\theta}{\partial Z^+} = \frac{1}{\xi}\ \frac{\partial}{\partial\xi}\left(\xi\ \frac{\partial\theta}{\partial\xi}\right) + \frac{\dot{R}W}{\dot{Q}_w}\ f(\xi) \qquad (197)$$

where

$$f(\xi) = \frac{N+2}{2}\ \xi^N$$

The boundary conditions are:

$$\theta(0,\xi) = \theta_0(\xi) \qquad (198a)$$

$$\frac{\partial\theta}{\partial\xi}(Z^+,0) = 0 \qquad (198b)$$

$$\frac{\partial\theta}{\partial\xi}(Z^+,1) = -1 \qquad (198c)$$

Before proceeding any further, it will be appropriate here to explain in some detail how equation (197) which assumes fully developed temperature and velocity profiles may be used to resolve the viscous heat generation problem for the case which is relevant to this particular project, that is, heat transfer to flow with both temperature and velocity profiles developing simultaneously. The procedure

to be adopted here is the same as used by GILL (67) to generalize the solutions obtained by SIEGEL, SPARROW and HALLMAN (175) to the case including viscous dissipation with arbitrary inlet temperature distribution for Newtonian fluids.

Consider a test section with an entrance section sufficiently long so that both velocity and temperature distributions are fully developed at the entrance of the section to be analysed. This convenient and exact initial condition has two outstanding virtues. First it may be achieved experimentally to any desired accuracy, and second (and most relevant), existing work which neglects energy sources may be extended to include them without much additional computation.

The energy source term $f(\xi)$ in the heat conduction equation (197) affects only $\theta_\infty(Z^+,\xi)$ and hence, an asymptotic solution $\theta_\infty(Z^+,\xi)$ is developed first. This may be regarded as a particular solution of equation (197), to which is then added the solution of the homogeneous form of the conduction equation to give a generalized solution, involving eigenfunctions and eigenvalues. For the non-Newtonian cases, the relevant eigenvalue solution has been provided by BIRD(11) and MITSUISHI (122). The purpose of the following analysis is therefore to find the asymptotic solutions to equation

(197) for arbitrary N.

Solving Equation (197) for large Z^+

After the fluid is far downstream from the beginning of the heated section, one expects intuitively that the constant heat flux through the wall will result in a rise in the fluid temperature that is linear in Z^+. One further expects that the shape of the radial temperature profiles will ultimately not undergo further change with increasing Z^+. Hence a solution of the following form seems reasonable for large Z^+.

$$\theta_\infty = C_o Z^+ + \psi(\xi) \tag{199}$$

in which C_o is a constant to be determined later.

The function in equation (199) is clearly not the complete solution to the problem. Although the function does allow the partial differential equation (197) and also the boundary conditions (198b) and (198c) to be satisfied, it is apparent that boundary condition (198a) cannot be satisfied. Hence the latter is replaced by the overall energy balance

$$-2\pi R Z^+ Q_w = \int_o^{2\pi} \int_o^R \rho C_p U_z (T - T_{bi})\, r\, dr\, d\theta \tag{200}$$

from which, the new boundary condition emerges as

$$-Z^{+} = \int_{0}^{1} \theta(1-\xi^{N})\,\xi d\xi \tag{198a}$$

Substituting equation (199) into (197) then gives the following ordinary differential equation for ψ

$$(1-\xi^{N})\,C_{o} = \frac{1}{\xi}\frac{d}{d\xi}\left(\xi\,\frac{d\psi}{d\xi}\right) + \frac{\dot{RW}}{\dot{Q}_{w}}\,\xi^{N}\left(\frac{N+2}{N}\right) \tag{201a}$$

Rearranging

$$\frac{1}{\xi}\frac{d}{d\xi}\left(\xi\,\frac{d\psi}{d\xi}\right) = \left(1-\xi^{N}\right)C_{o} - \left(\frac{N+2}{N}\right)\frac{\dot{RW}}{\dot{Q}_{w}}\,\xi^{N} \tag{201b}$$

Integrating once gives

$$\frac{d\psi}{d\xi} = \left(\frac{\xi}{2} - \xi\frac{N+1}{N+2}\right)C_{o} - \xi\frac{N+1}{N}\,\frac{\dot{RW}}{\dot{Q}_{w}} + \frac{C_{1}}{\xi} \tag{202}$$

where C_{1} is an integration constant.

By defining a dimensionless Brinkman number, modified for the constant wall heat flux boundary condition as:

$$Br_m = R\,\tau_w^N \,/\, \dot{Q}_w\, K_N^{N-1} \tag{203}$$

it can be shown from equation (194c) that

$$\frac{R\dot{W}}{\dot{Q}_w} = \frac{1}{1+\frac{N}{2}}\,(Br_m) = f(Br_m) \tag{204}$$

The quantity Br_m is a measure of the magnitude of the viscous dissipation effect.

Equation (202) can then be written as

$$\frac{d\psi}{d\xi} = \left(\frac{\xi}{2} - \frac{\xi^{N+1}}{N+2}\right)C_o + \frac{C_1}{\xi} - \frac{\xi^{N+1}}{N} f(Br_m) \tag{205}$$

Integrating again gives

$$\psi = \left(\frac{\xi^2}{4} - \frac{\xi^{N+2}}{(N+2)^2}\right) C_o + C_1 \ln \xi + \frac{\xi^{N+2}}{N(N+2)} f(Br_m) + C_2 \tag{206}$$

where C_2 is the second integration constant. Substitute for ψ in equation (199) to get

$$\theta_\infty = C_o Z^+ + C_o\left(\frac{\xi^2}{4} - \frac{\xi^{N+2}}{(N+2)^2}\right) - \frac{\xi^{N+2}}{N(N+2)} f(Br_m) \tag{207}$$

The constants of integration C_1 and C_2 and the constant C_o, are determined from the boundary conditions given in equations (198)

From

$$\frac{\partial\theta}{\partial\xi}(Z^*,0) = 0; \qquad C_1 = 0 \tag{208a}$$

From

$$\frac{\partial\theta}{\partial\xi}(Z^*,1) = -1; \qquad C_o = -\frac{2(N+2)}{N} + \frac{2(N+2)}{N^2} f(Br_m) \tag{208b}$$

and from

$$-Z^* = \int_0^1 \theta(1-\xi^N)\xi d\xi$$

$$C_2 = \frac{N^3 + 6N^2 + 12N}{4N(N+2)(N+4)} - \left(\frac{2(N+2)}{N^2}Z^* + \frac{1}{4N}\right) f(Br_m) \tag{208c}$$

The final expression for temperature becomes:

$$\theta_\infty = -\frac{2(N+2)}{N}Z^* - \frac{N+2}{2N}\xi^2 + \frac{2}{N(N+2)}\xi^{N+2} + \frac{N^2 + 6N + 12}{4(N+2)(N+4)}$$

$$+\frac{Br_m}{(N+2)}\left(\frac{N+2}{N^2}\xi^2 - \frac{2\xi^{N+2}}{N^2} - \frac{1}{2N}\right) \tag{209}$$

For the Newtonian case N = 2 and

$$\theta_\infty = -4Z^+ - \xi^2 + \frac{\xi^4}{4} + \frac{7}{24} + \frac{Br}{4}m\left(\xi^2 - \frac{\xi^4}{2} - \frac{1}{4}\right) \qquad (210)$$

GILL (67) gave his solution as

$$\theta_\infty = -4Z^+ - \xi^2 + \frac{\xi^4}{4} + \frac{7}{24} + \frac{R\dot{W}}{2\dot{Q}_w}\left(4Z^+ + \xi^2 - \frac{\xi^4}{2} - \frac{1}{4}\right) \qquad (211)$$

The inclusion of the $4Z^+$ term in the expression in brackets, appears to have been an error since the viscous dissipation effect $\Phi(r)$ (in equation (188)) was assumed to be a function of ξ only. The addition of this parameter does not however affect the final expression for the asymptotic Nusselt number but may lead to errors when temperature profiles are evaluated from equation (211).

SIEGEL et al (175) solved for the case where viscous dissipation was negligible and fluid properties constant with temperature. Their expression was given as:

$$\theta_\infty = -4Z^+ - \xi^2 + \frac{\xi^4}{4} + \frac{7}{24} \qquad (212)$$

Comparison with equation (210) shows clearly the manner in which viscous dissipation alters the temperature

profile if temperature independent fluid properties are assumed.

To obtain the asymptotic Nusselt number for arbitrary N

$$Nu_{\infty} = - \frac{2\dot{Q}_w R}{k(T_w - T_b)} \tag{213}$$

the fluid bulk temperature is evaluated from

$$\theta_b = 2 \int_0^1 U_1 \theta \xi d\xi \tag{214a}$$

i.e.

$$\frac{T_b - T_{bi}}{\dot{Q}_w R/k} = - \frac{2(N+2)}{N} Z^+ \tag{214b}$$

The wall temperature is given by

$$\theta_{\infty}(Z^+,1) = \theta_w \tag{215a}$$

or

$$\frac{T_w - T_{bi}}{\dot{Q}_w R/k} = - \frac{2(N+2)}{N} Z^+ - \frac{N^2+10N+20}{4(N+2)(N+4)} + \frac{Br_m}{2(N+2)N} \tag{215b}$$

From equations (213), (214) and (215)

$$Nu_{\infty} = \frac{2}{\frac{N^2+10N+20}{4(N+2)(N+4)} - \frac{Br_m}{2(N+2)N}} \qquad (216)$$

For a Newtonian fluid N = 2 and

$$Nu_{\infty} = \frac{2}{\frac{11}{24} - \frac{Br_m}{16}} \qquad (217)$$

which is the same expression obtained by GILL (67) viz:

$$Nu_{\infty} = \frac{2}{\frac{11}{24} - \frac{R\dot{W}}{8\dot{Q}_w}} \qquad (218)$$

Solving for small Z^+

The general solution to equation (197) may now be obtained by letting

$$\theta(Z^+,\xi) = \theta_{\infty}(Z^+,\xi) - \theta_1(Z^+,\xi) \qquad (219)$$

where θ_1 satisfies the homogeneous form of equation (188) and the boundary conditions which follow from equations (198). θ_1 may be expressed conventionally as

$$\theta_1 = \sum_{i=0}^{\infty} B_i \, e^{-a_i Z^+} \phi_i(\xi) \qquad (220)$$

where $\phi_i(\xi)$ are solutions to the associated Sturm-Liouville equation

$$\frac{1}{\xi} \frac{d}{d\xi} \xi \frac{d\phi_i}{d\xi} + a_i(1 - \xi^N) \phi_i = 0 \qquad (221)$$

with zero derivatives at the wall and centre of the tube. Since a_o is zero for this problem, in view of equation (219), it can be shown that B_o is zero. Hence i may be considered to take values from 1 to ∞ without changing equation (220). BIRD (11) has calculated B_i, a_i and $\phi_i(\xi)$ for N = 3 neglecting viscous dissipation.

The B_i in equation (220) are given by

$$B_i = \frac{\int_o^1 \phi_i(\xi) [\theta_\infty(0,\xi) - \theta(0,\xi)] \xi (1-\xi^N) \, d\xi}{\int_o^1 \xi (1-\xi^N) \phi_i^2(\xi) \, d\xi} \qquad (222)$$

where $\int_o^1 \xi (1-\xi^N) \phi_i^2(\xi) \, d\xi$ is conventionally taken as unity without loss of generality.

Using equation (221) and the boundary conditions for $\phi_i(\xi)$ which are determined from equations (198) it can

be shown that

$$\int_0^1 \xi(1-\xi^N)\phi_i(\xi)\,d\xi = 0 \qquad (223)$$

$$i = 1,2,....m$$

GILL (67) postulates that if $\theta(0,\xi)$ is chosen to be the asymptotic solution obtained from an inlet section of arbitrary length with a constant heat flux $\dot{Q}_w$, and if a step change in heat flux from $\dot{Q}_{w1}$ to $\dot{Q}_{w2}$ occurs at z = 0, then with equations (222) and (223) it may be shown that

$$B_i = (1 - \dot{Q}_{W1} / \dot{Q}_{W2})\, B_i' \qquad (224)$$

where B_i' are the expansion coefficients neglecting dissipation assuming a constant wall heat flux. If the inlet section is well insulated then

$$\dot{Q}_{W1} = 0$$

and

$$B_i = B_i' \qquad (225)$$

Therefore the B_i' previously calculated (11, 123) may be used directly for the more general problem involving heat generation.

The final expression for temperature becomes

$$\theta(Z^{+},\xi) = \theta_{\infty}(Z^{+},\xi) - \sum_{i=1}^{\infty} B_i' e^{-a_i Z^{+}/Pe} \phi_i(\xi) \qquad (226)$$

where θ_{∞} is given by equation (209). Nusselt number for a dissipative laminar non-Newtonian fluid becomes

$$N_u = \frac{2}{\frac{N^2+10N+20}{4(N+2)(N+4)} - \frac{Br_m}{2(N+2)N} - \sum_{i=1}^{\infty} B_i' e^{-a_i Z^{+}/Pe} \phi_i(1)} \qquad (227)$$

Reverting now to the power law index n, as defined in equation (4) and used in all other sections of this thesis, equations (209) and (227) become

$$\theta_{\infty} = -\frac{2(3n+1)}{(n+1)} Z^{+} - \frac{3n+1}{2(n+1)} \xi^2 + \left(\frac{2n^2}{(n+1)(3n+1)}\right) \xi^{\frac{3n+1}{n}}$$

$$+ \frac{19n^2+8n+1}{4(3n+1)(5n+1)} + \frac{n}{(3n+1)(n+1)} Br_m \left[\frac{n(3n+1)}{(n+1)^2} \xi^2 \cdots \right.$$

$$\left. \cdots - \frac{2n^2}{(n+1)^2} \xi^{\frac{3n+1}{n}} - \frac{n}{2(n+1)} \right] \qquad (209a)$$

$$Nu = \frac{2}{\frac{31n^2+12n+1}{4(3n+1)(5n+1)} - \frac{n}{2(3n+1)(n+1)}Br_m - \sum_{i=1}^{\infty} B_i' e^{-a_i Z^+/Pe} \phi_i(1)} \qquad (227a)$$

In equation (227a) the influence of viscous dissipation on Nu becomes very clear. Negative values of Br_m which correspond to cooling of the fluid, decrease the value of Nusselt number, with a resultant increase in the wall-bulk fluid temperature difference. On the other hand, positive values of Br_m, which correspond to heating of the fluid, decrease the temperature difference. The significance of viscous dissipation in relation to the fluids used in this project will be discussed later.

CHAPTER SEVEN

EQUIPMENT

7.1 EXPERIMENTAL FLUIDS

7.1.1 Non-Newtonian

As a logical basis for the design of apparatus, the test fluids had to be specified. For the present investigation polymeric solutions have been considered in preference to other pseudoplastic systems. Selection was based on the following criteria:

(i) pronounced non-Newtonian characteristics,

(ii) good shear stability,

(iii) availability and cost,

(iv) thermal stability,

(v) absence of visco elastic properties.

Sodium Carboxymethyl Cellulose (CMC), Methocel 60HG (MC) and Carbopol934 (CPM) satisfied the above conditions and were used in the tests. Other materials which have been used previously for a variety of studies are listed in TABLE 1, (Appendix 2).

7.1.2 Newtonian

In selecting the heat transfer medium for the

Newtonian tests, the main consideration was to obtain data against which the reliability and accuracy of the non-Newtonian systems could be assessed. Propylene-glycol mixtures which had been tested under similar conditions (128) were used.

Detailed specifications of all items of equipment described in the remaining sections of this chapter are given in Appendix 2 .

7.2 VISCOMETRIC APPARATUS

A capillary viscometer was designed and built on the lines recommended by BOWEN (20). Properties of polymer samples were determined with it to assess their suitability. However, this was a time-consuming and laborious method so when, at a later stage of the investigation a cone - and - plate viscometer (Weissenberg Rheogoniometer) became available, all subsequent characterization was done on it.

7.2.1 Capillary Viscometer

As shown in Fig.20(Appendix 2) this consisted of a cylindrical reservoir (76mm diameter x 0.61m long) fitted at both ends with standard 9 x 10^5 N/m^2 - flanges. Provision was made for screwing precision-bore stainless steel tubes in to the bottom flange. The top end

incorporated (i) a quick-coupling connection for a gas supply and (ii) a thermometer well. A three-way valve initiated and stopped the gas flow and also vented the reservoir. (Fig.21, Appendix 2). Reservoir pressure was controlled and measured by a regulator and a calibrated gauge respectively. An auxiliary gauge indicated the line pressure.

To ensure adequate temperature control the whole apparatus was inserted into a constant temperature bath equipped with a stirrer and a high sensitivity thermostat. Two mercury-thermometers (0.05°C stem-subdivisions) placed, one in the reservoir thermometer well, and the other in the bath indicated the respective temperatures. (Plate 1, Appendix 2).

7.2.2 The Weissenberg Rheogoniometer

The basis of this device is the cone-and-plate viscometer but the complete instrument can be used to perform tests under either rotary or oscillatory modes of stress (for viscoelastic materials). The detailed description and setting up procedures are given in the "Instruction Manual" supplied by the manufacturers - FAROL RESEARCH ENGINEERS LIMITED.

7.3 HEAT TRANSFER EQUIPMENT

The design and construction of the equipment was based on the objectives of obtaining accurate local heat transfer coefficients under conditions of uniform wall heat flux, for laminar flow of pseudoplastic liquids in circular tubes with abrupt changes in diameter.

The Schematic diagram in Fig.22a,(Appendix 2) shows the flow path and arrangement of the apparatus. The liquid was drawn under gravity from the storage tank (1) and pumped (2) through a cooler (3). Fluid leaving the heat exchanger could be returned to the tank through "bypass valves" (4) and (5), or diverted into one of two parallel pipelines connected to the heated test section. The primary circuit was through valve (6), the main inlet valve, which together with its bypass (7) regulated the rate of flow to the experimental tubes along pipe section (9), with valve (8) closed. After passing a packed mixing tube (10), the fluid was taken round a 180 degree bend before entering the heated tubes through the inlet box (11). This device enabled the entry temperature to be measured and also helped to baffle irregularities in the flow caused by the upstream bend. Situated at the outlet of the experimental tubes (12) was another arrangement (13) in which the bulk of the fluid was agitated and the exit temperature recorded; stirring was achieved here with perforated discs. This device also

restricted the flow, thus maintaining a system pressure higher than atmospheric throughout, and the possibility of air leakage into the test fluid was thereby minimized. The flow circuit was completed through a two-way valve (14) one leg of which led to the storage tank and the other to a 'weigh-tank' (15) where the flow rate was determined. A small centrifugal pump (16) recirculated the weighed fluid to the reservoir.

All pipe connections to the storage vessel were submerged. A motorized stirrer (17) was provided to keep the solution well agitated. An immersion heater (18) maintained the required temperature.

The alternative leg of the flow circuit was the "isothermal pressure drop" (pipe-line viscometer) section (19). This was used by closing valve (6) and opening (8). The fluid then proceeded to the heated tubes.

7.3.1 Mixing and Storage Tank

A stainless steel reservoir 760mm in diameter and 920mm high was used to prepare and store solutions. The tank was fitted with a 76mm diameter discharge line. Drainage was through a 19mm diameter gun-metal gate valve. Two motorized stirrers, one high, and the other low speed mounted in the tank ensured adequate agitation of the

mixtures while an immersion heater maintained the necessary solution temperatures. The tank was open at the top and could be covered by suitably cut hardboard to prevent evaporation.

7.3.2 Circulating Pump and Piping

In order to minimize the frictional losses lengths of 50mm internal diameter plastic ("durapipe") pipes were employed for most of the circuit. Plastic was used (in place of stainless steel) on ground of cost while safe-guarding against corrosion. Preliminary design calculations indicated that a pump discharge pressure of 9×10^5 N/m^2 gauge would be required to maintain circulation of 0.5% Carbopol Solution ($n = 0.38$, $K_N = 30 NS^n/m^2$) through a 25mm interal diameter test section.

Consequently a stainless steel, easy clean positive rotary pump was used. "Bypass control" was adopted (on the basis of cost in place of speed control) for flow regulation. Anti-vibration pads were used to reduce transmission of vibrations from the pump to the test section.

7.3.3 Heat Exchanger

Control of inlet temperature was in a water cooler. This was a "shell and tube" type with water on the shell

side. The water supply was provided by a cooling tower arrangement capable of dissipating 88KW whilst delivering 6 Kg/s of water at 24°C. In practice lower water temperatures could be obtained depending on the weather.

7.3.4 Inlet Mixing Arrangement

To ensure uniformity of the fluid temperatures before and after the heated test section, mixing arrangements were used.

For the inlet section, a combination of a packed tube and a mixing box was employed. The tube was constructed of a 50mm internal diameter, 0.61m long aluminium brass piping filled tightly with 6.35mm diameter "raschig" ceramic rings. Fig.23 (Appendix 2) shows the mixing box assembly. This was manufactured from tufnol and perspex materials, both good thermal and electrical insulators. The test-section was thus isolated so that practically no loss of heat or current could occur through the ends of the experimental tubes. Mixing was achieved by a range of venturi-type perspex tubes with throat diameters 3 to 13mm, chosen to produce a high Reynolds number at the constriction thereby causing a levelling of the temperature in the fluid whilst minimizing the pressure drop necessary for effective mixing. A transparent section was incorporated into the box to permit observation of the fluid

during experiments thus enabling incipient fouling or bubbling to be detected. Sealing was effected by the use of rubber 'O' rings between the demountable parts; 'p.t.f.e' tape was compressed between the threaded joints, and silicone rubber (which cured at room temperature) was used as a sealant around the thermocouple leads.

7.3.5 Heated Test Section

The heated section (experimental tubes with its fittings and mixing boxes) was enclosed in a rectangular wooden box lined with 40mm of polystyrene sheet. The box was then packed with spherical beads 5mm diameter and of the same material so that, at least 150mm of insulation was provided in all directions away from the test tubes. Polystyrene was considered to be a good insulator, its conductivity being only 1/600 times that of the tube materials, and 1/10 times that of the test fluid. Heat loss through the insulation was estimated at less than 5% and the condition of uniform flux at the inner tube wall was therefore well approximated. Heat rate values were derived from measurements of the electrical power dissipated in the tube.

The surface finish of the inner walls was such that they could be described as hydraulically smooth (frictional force independent of surface roughness).

When two tubes were connected in series, the wall thickness selected ensured that the heat generated per unit length was the same for both tubes. This condition gave rise to a nearly linear rise in the fluid bulk temperature, a similar surface temperature for each tube, and a practical thickness to diameter ratio in each case. By keeping the copper leads well away from the diameter discontinuity, the possibility of distorting the temperature distribution in this region was eliminated.

The tubes just described were the same as those used previously by McINTYRE (128) for Newtonian (Propylene-Glycol) experiments.

7.3.6 Tube Fitting

Fig.24(Appendix 2) shows the fittings for connecting the test sections to the mixing boxes and each other. The brass flanges used to produce a sudden change in diameter were of high electrical conductivity to minimize the volt drop from the upstream to the downstream tube. The fitting was brazed to the stainless steel ensuring an even distribution of solder in the process; thus making a good electrical contact. In between the two parts of each fitting good electrical contact and hydraulic sealing were established

by the insertion of a thin, brass shim which was compressed by eight, small securing bolts, these being evenly tensioned around the periphery of the flanges. Functional tests indicated no uneveness of heating close to a fitting which would have implied a poor electrical contact. Voltage drop measured across the fitting was entirely negligible being of the order of 5×10^{-4}V.

7.3.7 Outlet Mixing Tube

An aluminium brass tube 25mm internal diameter x 180mm long was flanged at both ends. Inside, at three 25mm axial intervals a perspex disc with three holes (each 3mm diameter) was located with araldite perpendicular to the flow. The holes were misaligned from disc to disc to induce maximum flow disturbance and mixing.(Fig.26,Appendix 2 .) Downstream of the baffles two thermocouples, protected by stainless steel sheaths were inserted through holes in the wall of the tube, one from the top to a depth of half the tube diameter, the other, from the side to one-quarter diameter. The steel sheaths were fixed to the tube with 'araldite' cement which also prevented liquid seepage from the clearances.

7.3.8 Isothermal Pressure Drop Section

This section consisted of a 4m long stainless steel pipe 17mm internal diameter, the initial 1m of which made

up the entry length. Two burr-free static pressure taps 2.5m apart were drilled through the walls of the pipe and connected to a mercury manometer. The first tapping was located 30mm downstream from the end of the entrance section so that flow at this point was undisturbed. Facilities were provided for flushing the pressure lines with mains water and suitable bleed and guard valves were installed on all manometers. For higher pressures, a calibrated 0 - 4 bar 'Bourdon' test gauge could be connected to each of the tappings.

The material and diameter chosen for this pipe-line viscometer corresponded to that of one of the heated experimental tubes. Thus fluid properties were monitored under approximately same wall stress and shear rate conditions as obtained in the heat transfer tests (especially for the low heat flux runs).

7.3.9 Power Supply

Direct current heating was preferred thereby avoiding stray e.m.f's being induced into the instrumentation. The ease with which the power requirements at the test section could be adjusted to match flow conditions also influenced the choice.

A mains 415 volts - 3 phase a/c supply was transformed, rectified and smoothed to give 0 to 30 volts d/c,

0 to 1000A at the test section. A controller stabilised the voltage to ± 1% of any specified setting. Copper leads carried the current to the experimental tubes. These were attached to straps, also of copper, which were mounted on the tubes(Fig.25, Appendix 2). The strap to tube contact area was machined to the tube outside diameter whilst the upper and lower portions were separated by 0.08mm to allow for the compression strain when tightening.

The potential difference over the test section was measured close to the points where the leads made contact with the tube, and the current was given by the volt drop across a calibrated shunt in series with the positive lead. These measurements were recorded with the same potentiometer as the thermocouple e.m.f's. A voltage divider, ratio 50 : 1 was included into the circuit to reduce the potential to a manageable level.

7.4 INSTRUMENTATION

7.4.1 Thermocouples and Voltage Measurements

For measurements of tube wall temperature, fluid inlet and outlet temperatures, and voltage drop across the heated test section, Nichrome Constantan thermocouples were used. This combination yielded high voltage-temperature gradient whilst having a low thermal

conductivity.

The thermocouples were made from wires 3m in length and 0.27mm in diameter. The cold junctions were formed by soft soldering each wire to a copper lead then setting each pair in paraffin wax, contained in a 5mm diameter glass tube. These glass tubes were immersed in Dewar flasks filled with water and ice chips. The copper leads were connected to a vernier potentiometer through a selector switch, and the thermocouple e.m.f's were measured by comparison with a standard cell, the voltage being given as the potentiometer setting corresponding to a null reading galvanometer.

The hot junctions were formed by resistance welding the two wires together either in parallel or in line (butt welding). The latter method was required for those positioned inside the inlet mixing box, and the former was used on all other applications. The mixing box junctions were bead shaped, but the test section junctions were flattened into a spade-shape for fitting to the outer surfaces.

The diagram, Fig.23 (Appendix 2) shows how a cruciform array of ten beads were positioned in the mixing box.

The thermocouples for the heated test section were affixed as follows. At a given axial location the periphery of the tube was covered with a strip of adhesive cellophane tape of thickness 0.05mm. This served to insulate the thermocouple electrically whilst presenting negligible thermal resistance, so that the temperature drop acorss the tape was immeasurably small (an estimate being 0.025% of the temperature difference used in calculating the coefficient of heat transfer).

The hot junction bead was bound firmly onto the surface of the tube with several layers of the adhesive tape, so that at a given axial position a minimum of 50mm of the lead encircled the tube. Since the peripheral region described was almost isothermal, the possibility of heat conduction in the leads affecting the readings was avoided.

7.4.2 Radial Temperature Traversing Arrangement

The set up used for the radial traversing tests is shown in Fig.27 (Appendix 2). One end of a 30mm long steel piece, same diameter as the rotating stem of a micrometer head was "sweated" onto the latter, thus effectively extending it. The other was grooved and located by a lock screw in a specially drilled slot, half-way down the vertical axis of a cylindrical bush

20 mm diameter, 26 mm high. The opposite face of the bush was also drilled to take a 4mm diameter ceramic tube. Through two separate holes running along the length of this protective tubing, the wires of a 36 - gage Nichrome-Constantan thermocouple were threaded, one in each, and the ends forming the "cold junction", brought out from the sides of the bushing to which the ceramic piece was cemented with "Araldite". Where they emerged from the unattached tip of the sheath, a "hot junction" was made by resistance-welding the two wires together, and the hole filled in with Araldite. This not only prevented fluid leakage by capillary action along the sheath, but also located the thermocouple head at a fixed position relative to it.

The micrometer head was locked upright on to a crosspiece the other end of which was keyed to a separate cylindrical bar positioned parallel with the head. This slide bar was cemented to an electrically insulating block straddling the experimental pipe. The thermocouple carrying bush was likewise rigidly attached to another piece which was free to move along the slide bar.

Vertical traversing was then achieved by rotating the "knurled" head of the micrometer in the usual manner. The method of attachment allowed thermocouple movement

only in the up or down direction without rotation of the bushing to which it was fixed.

The experimental tube wall was tapped with a hole just large enough to take the 4mm diameter ceramic sheath and sealed as shown in Fig.27(b). An "Enots" gland fitting was brazed on to the pipe over the tapped hole. Adequate sealing was provided by an "O" ring inserted between the two sections of the fitting and through which the ceramic tube entered the hole in the pipe wall. Plate 2 (Appendix 2) shows the insulated 'heat transfer' section with the micrometer traversing arrangement in position.

CHAPTER EIGHT

EXPERIMENTAL PROCEDURE

3.1 FUNCTIONAL TESTS

3.1.1 Calibration of Thermocouples

The thermocouple junctions were made locally and had to be checked against standard NPL calibrated mercury - in - glass thermometers. Six thermocouples were taken randomly from the test section and the hot junctions set in parafin wax contained in 6mm dia. glass tubes. These were immersed in a uniform temperature, circulating oil bath, with the cold junctions in a Dewar flask containing a mixture of ice and water. Setting the bath temperature to rise slowly between 10°C to 90°C, readings were taken at 4K intervals of both the standard thermometer and the thermocouple e.m.f.s. The temperature - microvolt relation for the Nichrome-Constantan junction used is shown in Fig.28 (Appendix 3). Readings were reproducible to within ± 2 microvolts or ± 0.05K and the calibration differed from literature values by 2%. This error was probably because of non-uniformities in the thermocouple wires.

To further check on the reliability of the tube thermocouple readings and to justify the method of fixing them, a series of "isothermal tests" were carried out. The thermocouples were positioned and fixed on the tube as they would be for a typical heat run. With initially water, and then a glycol solution recirculating at a high ate of flow, a small voltage was applied to the test section to bring the circulating liquid to the desired temperature. The voltage was switched off and the liquid temperature allowed to settle to a stable isothermal value. The inlet mixing box temperature, the outlet mixing tube temperature and finally the test section couple temperatures were recorded and compared. Since no heat was being put into the tube, the inlet and outlet temperatures were equal, any differences being immeasurably small. The temperature of the tube exterior was slightly less than the liquid temperature, due in part to conduction through the wall, and in part to imperfect contact of the thermocouples or conduction in the leads. Tube wall conduction was taken account of in the calculation of wall temperatures, but the latter was estimated from the difference between the tube and fluid temperatures recorded. In general the slight drop in tube couple readings increased with temperature. Recorded errors varied from -0.02K to -0.06K with fluid temperatues at 22°C and 60°C respectively, and ambient temperature at 17°C. For a typical test the maximum deviation represented an error of less

ıan 5% on the accuracy of the measured coefficient of heat ;ansfer. The method of fixing the thermocouples to the ɜst section was kept simple in view of the large number of ɔcations which were necessary.

.1.2 Calibration of Viscometers

(a) Capillary Tube Viscometer

Accuracy of this instrument was checked with a ewtonian fluid of known viscosity. In this case, an queous glycerol solution (89.5% weight by weight) was haracterised. The exact internal diameter of each :apillary tube used was determined by weighing the quantity ıf mercury necessary to fill the bore, and the length ıccurately measured with a vernier calliper. In all, ;ifteen tubes were available giving a range of lengths ınd diameters so that the effects of each of these ɗimensions on the flow characteristics could be observed.

The glycerol solution was tested at a specific temperature using two different tube diameters and three different lengths, and results compared with values determined by SEGUR et al (169) and SHEELEY (173). The pressure drop-flow rate curve is given in Fig.29 (Appendix 3).

All tables and figures referred to in the remaining sections of this chapter are placed in Appendix 3.

(b) Cone - and Plate Viscometer (Weissenberg Rheogoniometer)

This instrument had a range of torsion bars orresponding to different viscosity (and hence torque) imits. To check that a given bar was appropriate for particular fluid consistency a silicone fluid of known iscosity was characterized at a specific temperature F111 Dimethyl Series for high viscosities and MSS 550 eries for low viscosities). Accuracy with respect to emperature was assessed by determining the viscosities f glycerol solution at various temperatures and comparing ith values given in texts (169) and (173). The calib-ation data are shown in Tables 1 and 2.

1.3 Heat Loss from Experimental Section

The usual procedure of equating the heat input ıs measured by the electrical power supplied) to the ıthalpy rise in the transport medium (indicated by the .fference between the inlet and outlet temperatures) is ıly as reliable as the accuracy with which the fluid ɜmperatures can be determined. Of the two hundred and venty two tests performed only twenty-four had a bulk ɜmperature rise of up to $1^{o}K$. For a rise of $0.5^{o}K$ an ɔror of $\pm$ 0.05K in determination of the bulk temperature ifference therefore implied a 10% heat balance discrepancy.

Typical assessments are given in Table 3, for bulk temperature increases greater than 0.7°K. In these investigations, more emphasis has therefore been placed on limiting heat loss through the insulation to less than 2% of the heat input. Comparison of the estimated and measured values of the outlet temperatures provided checks on the accuracy and acceptability of individual tests.

8.2 MEASUREMENT OF FLUID PROPERTIES

8.2.1 Newtonian Fluids

Water properties were obtained from the publication "Engineering Sciences Data" Vols. 1 and 2 (208). For glycol solutions the major source of information was the text "Glycols" by CURME AND JOHNSON (209). Generally it was possible to obtain quick checks on the percentage of water in the glycol solutions by simply measuring the density with a BS 718 hydrometer. However, this practice was misleading since the density of a 70% solution was virtually the same as that of 80% in the 20 - 40°C temperature range. To obtain more reliable checks, the viscosities of the various solutions were determined over a range of temperatures with appropriate suspended level visometers and compared with the literature values to find the corresponding glycol

concentration. The properties of propylene-glycol and water are given in Tables 4 and 5 respectively.

8.2.2 Non-Newtonian Fluids

The physical properties of water based polymer solutions in small concentrations, (thermal conductivity, specific heat capacity and density) are generally regarded as being reasonably approximated by those of the dominant solvent phase. To verify this assumption a 2% (weight by weight) solutions of CMC (Cellofas B50) and Methocel (60HG) were sent to the National Engineering Laboratory (East Kilbride) for thermal conductivity determinations. The results are given in Table 6. The densities of Methocel solutions, 0.5% (w/w) and 3.0% (w/w) were measured by the author over a range of temperatures using BS 178 (high surface tension grade) hydrometers. The experimental values are shown in Table 7 (water values have also been included for comparison).

8.3 THERMOCOUPLE ARRANGEMENT

8.3.1 The Sudden Convergence

Since this investigation was a direct extension of Newtonian Studies using the same experimental tubes (128), it was decided to employ similar thermocouple dispositions as in the earlier tests. However, when during experiments a particular arrangement was found inappropriate for the prevailing conditions, the necessary alterations were made. For the convergence tests the following thermocouple arrangement was used:

Large Diameter (Upstream) Tube:

Sets of two thermocouples were fixed, one on top and the other diametrically opposite, at 0, 1, 2, 8, 18, 38 and 48 diameters upstream from the discontinuity. This rather coarse arrangement was dictated by previous experience since it was known that only slight variations in local heat transfer coefficient occurred in the region just upstream of the tube joint.

Small Diameter (Downstream) Tube:

Groups of four thermocouples were located symmetrically round the tube periphery at 0.5, 1, 2, 3, 4, 5.5, 7, 8.5, 10, 11.5, 13, 15, 20, 25, 40, 97, 98 and 100 diameters downstream of the change of section.

8.3.2 The Sudden Divergence

Small Diameter (Upstream) Tube

The thermocouples were arranged in a similar manner to those on the upstream (large) tube of the convergence configuration. Axial locations in this case were at 0, 1, 3, 4, 50, 80, 90 and 100 diameters upstream of the discontinuity.

Large Diameter (Downstream) Tube

Regions of particular interest downstream of a sudden increase in diameter have been shown by previous Newtonian tests to lie between the change of section and 3 to 5 diameters away from it. Consequently groups of eight thermocouples were taped round the tube circumference at 0, 1, 2 and 3 diameters. Sets of four couples were used at other locations namely 4, 5.5, 7, 8.5, 10, 11.5, 13, 20, 25, 46, 47 and 48 diameters.

To verify that groups of four thermocouples were adequate, eight junctions were used at 15 and 40 diameters since in the latter case flow conditions were regarded as approaching fully developed status at this location.

8.3.3 Tube Heating Arrangement

In all the tests both the upstream and downstream tubes were heated. The dimensions were as follows:

Tube Geometry	Heated Length Upstream (dia)	Heated Length Downstream (dia)
3.34:1 Convergence	48	100
1.3.34 Divergence	100	48

8.4 HEAT TRANSFER TO NEWTONIAN FLUIDS

Heat transfer runs were carried out with water (turbulent regime) and aqueous propylene glycol solutions (laminar/turbulent regime) to check

(i) the performance of new items of equipment and

(ii) assess the reliability and accuracy of the entire apparatus for collecting meaningful heat transfer data by comparing the results with available and well established correlations.

The procedure for a typical test run was as follows:

The cooling water pump, the fluid circulating pump and the power supply to the heated section were

switched on. With the flow rate set at an initially high value, a quantity of the fluid was bled off at intervals until no air bubbles (or any other fouling matter) could be seen from the transparent viewing sections. While the apparatus warmed up the cold junction-flasks were filled up with fresh ice and water mixtures and the potentiometer calibrated. The inlet mixing box thermocouples readings were then checked and as the fluid temperature began to rise, the flow rate and the voltage were reset to specific values. By continuous regulation of the amount of heat dissipated in the heat exchanger, the fluid inlet temperature was allowed to rise and gradually approach the required value.

In the case of glycol solutions viscosity measurements were made and the composition determined. After recalibrating the potentiometer the inlet and outlet fluid temperatures were recorded at five minute intervals until a steady state condition was attained. To monitor any severe time dependent fluctuations in tube temperature, continuous readings were taken at several selected locations. A steady-state was achieved when consecutive inlet temperature readings remained constant for a minimum of 30 minutes. On the average this state was reached in about 2 hours from the start of operations (less for turbulent flows).

The desired test data was obtained by recording the following after recalibrating the potentiometer:

(i) Time

(ii) Room Temperature

(iii) Voltages and current

(iv) Inlet Temperature (10 thermocouples)

(v) Outlet temperature (2 thermocouples)

(vi) Tube surface temperatures (up to 94 thermocouples)

(vii) Inlet temperature

(viii) Outlet temperature

(ix) Voltages and current

(x) Time

This completed the first pass. A second set of readings (i) to (x) was then obtained after further recalibration of the potentiometer. Finally, the flow rate was determined by diverting the fluid into the weigh-tank.

The above operation took about 25 to 30 minutes. Averaging the results of the two sets of readings obtained accounted for the small variations (not more than 0.05K) likely to occur in the inlet temperature of the fluid during data recording, provided the mixing box readings taken at the half way stage were the same as the average readings at the beginning and end.

8.5 HEAT TRANSFER TO PSEUDOPLASTIC FLUIDS

8.5.1 Pseudoplastic Solution Preparation

(a) Carbopol 934 Carbopol 934 resin is a fine white powder and is hydrophilic. The aqueous solution was prepared by heating water to 60°C, agitating it vigorously and slowly adding the resin. A thin, hazy highly acidic solution resulted. This was left to stand for a few minutes to release entrapped air bubbles.

To obtain the desired consistency, the solution was neutralised with dilute Sodium Hydroxide (10%) solution, under slow agitation. The recommended formula was 195 parts of water, to 1 part of resin to 4 parts of sodium hydroxide solution - all by weight. Care was taken to avoid the formation of gel clusters and the entrapment of air bubbles in the resultant viscous system. The agitation was continued for an hour and the solution allowed to stand overnight before being used.

Formulations of the following concentrations were prepared:

0.15%(w/w), 0.25%(w/w), 0.5%(w/w)

(b) Methocel 60 HG Methocel is a white grainy gum. This solution was prepared in a similar way to the above. One third the total water required was heated to 80-90°C

and the grains added slowly with constant agitation until fully dispersed and wetted out. The remaining water was added cold (or as ice) and the stirring continued until solution was complete. For maximum clarity the mixture was cooled to 5-10°C after complete dispersion of the resin.

Methocel solutions, depending upon the original compositions of the powder, tend to gel at different temperatures. The particular samples used here gelled at 60°C and hence temperatures exceeding 55°C were avoided both during characterization and experimentation.

The exact concentration of the solution was obtained by evaporating a known weight of liquid sample in an oven at 90°C.

The following concentrations were used:

0.5%(w/w), 1.0%(w/w), 2%(w/w)

(c) Sodium Carboxymethyl Cellulose (CMC) The particular grade employed was manufactured under the trade name Cellofas B50 by I.C.I. It is a cream/white granular resin. Preparation was best achieved by adding half the total amount of water to the tank and stirring vigorously. The granules were then dispersed as near the vortex as

possible at a fairly rapid rate making sure that all the material was added before a substantial consistency developed. The tank was then topped up with the remaining water and the temperature increased to 50 or 60°C. A clear solution resulted. Polymer concentrations of 0.5%(w/w) and 1%(w/w) were employed.

8.5.2 Characterization

The pseudoplastic fluids were characterized in a cone and plate viscometer except for the initial samples of Methocel for which the capillary viscometer was used. The effect of temperature was also studied. Special care had to be taken to avoid evaporation of solutions at higher temperatures when using the cone and plate type viscometer (a vapour hood was attached). The shear rate range used was 15 to 1200 sec^{-1} and the temperature 20 - 60°C (except for Methocel where the upper limit was 40°C). These were of the same order as conditions encountered in the rig.

In Tables 8 to 17, the shear rate, shear stress data for all solutions used are listed, while Figs. 30 and 31 show typical graphical representation of results from a capillary tube and a cone and plate viscometer respectively.

8.5.3 Heat Transfer Runs

The procedure was exactly as outlined in Section 8.3. In addition, samples were taken at the end of each run (and at the beginning for the first test of the day) and characterized to obtain n and K_N values for that particular test. This enabled any shear or biological degradation of the polymer to be monitored.

8.5.4 Isothermal Pseudoplastic Pressure Drop

It will be recalled that this section was included in the apparatus only as an alternative monitoring method in the event of the cone-and-plate viscometer being unavailable. However, the latter instrument was available all through the experimentation period and was used. No pressure drops were therefore taken. Comparison between cone-and-plate and pipe line viscometry results was adequately provided, in the latter case by the capillary viscometer used in earlier characterizations. (Fig. 29).

8.6 RADIAL TEMPERATURE TRAVERSES

Exploration of radial temperature profiles was carried out only for the divergence arrangement. The test fluids were water and 0.25%(w/w) Carbopol 934.

One traversing thermocouple was positioned 3 diameters after the change of section and another 40 diameters downstream. When a steady state was achieved as in Section 8.3, the pipe wall thermocouples at 0, 1, 2, 3, 4 and at 25, 40 and 46 diameters downstream of the change of section were recorded to ensure that the chosen flow rate and heat flux produced the desired temperature profile around the locations of the traversing gear.

In addition, for a typical test the following were recorded:

(i) Time

(ii) Ambient Temperature

(iii) Voltage and Current

(iv) Inlet and Outlet mixing box thermocouples

(v) The traversing couple readings at 10 radial positions for each axial location.

The inlet and outlet bulk temperatues were regularly checked between radial increments during traversing.

To end the tests items (i) to (iv) above were recorded again and the flow rate determined as in Section 8.3.

After the initial experiments with 0.25% Carbopol the test section was turned through ninety degrees and a few more data taken for this mixture.

8.7 CONTROL OF TEST CONDITIONS

8.7.1 Newtonian Runs

The important non-dimensional parameters necessary to identify data from Newtonian heat transfer experiments are Reynolds number (Re) and Prandtl number (Pr). While the former could be varied arbitrarily over a chosen range, the latter had to be set to specified values for any one series of tests. With aqueous glycol there were two ways of obtaining the desired Prandtl number. Either (i) the solution was diluted to reduce its viscosity and hence Pr; or (ii) the fluid inlet temperature was raised and the viscosity thus lowered. For the high Pr tests pure (100% nominal) glycol was used and the viscosity altered by the second method. However, the inlet temperature could only be preset with 2K accuracy so that Pr was liable to vary by up to 10% of the desired value (due to temperature dependence of viscosity). This did not have any significant effect on the results obtained.

The other variable set to particular values during a test, the wall heat flux, was recorded (as a

product of voltages and current) on the same potentiometer used for the thermocouples. Deviations from desired fluxes never exceeded 1%.

8.7.2 Non-Newtonian Runs

Whereas it was possible to determine the amount of polymer resin in Methocel solutions by evaporating a known weight of sample, no such rigorous procedure could be found to determine the exact concentration of Carbopol and CMC solutions (that is, apart from the initial weighings during preparation). The values quoted for these mixtures can therefore be only nominal. However, when two samples of the same nominal concentration were prepared on separate occasions the rheological constants agreed sufficiently to indicate that any slight errors in initial weight determinations were inconsequential.

The generalised parameters Re′ and Pr′ are dependent on velocity (and hence tube diameter). This means that for any given solution, both parameters will be different for the two tube sections constituting the experimental configuration. Therefore no attempt was made to preset any of these items. Also, since the polymers were degraded by shear (especially the Carbopol solutions) the fluid consistency (or "apparent viscosity") could change very substantially between the first and last runs on any given solution. To minimize this in some of the tests, the

solution was circulated continuously for two or three days and the consistency determined at hourly intervals until no appreciable change occured for consecutive readings. The first run was then made. This meant, of course, that the non-Newtonian index n which was originally desired could be drastically altered by the time the first run was carried out. Where a particular value of n was desired, the test was performed immediately after preparation of solution and the rheological properties determined before and after the test.

With Methocel solutions some difficulty was encountered in obtaining sufficiently high wall - to - bulk temperature differences to produce a rise in fluid temperature between inlet and outlet of the test section without triggering gelation at the wall surface. After a series of experiments where large voltages had been used to obtain the desired temperature differences, the tubes were dismantled and visually inspected. They were then cleaned by pulling a piece of cloth through. No significant fouling or scaling on the walls was observed.

Once prepared, Carbopol mixtures posed no special problems. However, the initial 0.5%(w/w) formulation was so viscous that it could not be pumped and more water had to be added until the solution began to flow. The final polymer concentration was therefore probably slightly less than the

0.5% quoted. This expedient did not reflect on the accuracy of data derived from the tests, since the rheological properties used in subsequent calculations were determined from samples taken during the actual runs.

8.8 SUMMARY OF TESTS CARRIED OUT

8.8.1 Newtonian Fluids

The 3.34 : 1 sudden convergence tube arrangement was first investigated. With water as the fluid, twelve tests were carried out in the turbulent regime to provide data for comparison with known correlations and hence further check the performance of the equipment. The important parameters for these and other tests to be discussed are summarised at the end of this chapter. In order to extend the Prandtl number range of previous glycol tests (128) and also assess the ability of equipment to reproduce data, a total of sixty five experiments were carried out with two concentrations of glycol namely, 100% (nominal) and 79.5%. These tests covered the laminar, transitional and turbulent flow regimes. The tube wall heat flux was chosen arbitrarily in each case, to give a moderate temperature difference between wall and fluid and hence avoid free convection effects. To determine the influence of heat flux on the results, six additional runs were made with the 79.5% solution.

For the 1 : 3.34 divergence configuration, twelve tests were performed. These were primarily designed to provide data for comparison both with McIntyre's (128) results for Pr = 55 and later tests (in the present series) using fluids which were only slightly non-Newtonian.

8.8.2 Non-Newtonian Fluids

With the same divergence arrangement employed for the Newtonian experiments the first non-Newtonian runs were made using 0.5% aqueous solution of Methocel (60 HG). The tube wall temperatures were kept low to avoid gelation of this particular grade of polymer. This solution was only slightly non-Newtonian and very low Reynolds numbers could not be obtained. Eight tests were performed at this concentration. To confirm the behaviour of data from the above series, twelve further runs were carried out with a marginally higher level of polymer (1.0%). Before these latter rests, the tubes were cleaned and the thermocouples re-calibrated. For more non-Newtonian conditions Carbopol solutions were used in 0.15%, 0.25% and 0.5% concentrations. The twelve runs with 0.15% provided results for comparison with Newtonian data in the 500 Prandtl number range while the nine each with 0.25% and 0.5% covered the very low Reynolds number conditions.

The final tests on this tube arrangement were carried out with Sodium Carboxymethyl Cellulose (CMC)

solutions; eight using 0.5% and sixteen with 1.0% mixtures. Half of the latter runs investigated the effect of heat flux. At 0.5% concentration this polymer was only marginally non-Newtonian and the results furnished further information in the light of the observed behaviour of Methocel solutions.

For the 3.34 : 1 sudden convergence geometry Carbopol in 0.5% solution (9 tests) was first investigated. This was the same preparation as used in the divergence tests, but the consistency had been substantially reduced by shear degradation. Data comparable to Newtonian results for Pr = 440 were obtained.

In the hope that more non-Newtonian data on Methocel (60 HG) could be obtained, a 2% concentrationwas prepared and tested (10 runs). However, even at this level the flow index (n) was just below 1.0 although the Prandtl number range was increased. Eight runs with a new mixture of 0.25% Carbopol provided results in the Pr = 600 bracket (same as for 100% pure glycol). Moreover the measured rheological constants, afforded a very reliable check on previous solution preparation and characterization.

Higher Reynolds numbers were obtained with CMC formulations at 0.5% and 1.0% levels. While the six and ten tests respectively, yielded results covering Prandtl

numbers 75 to 300, these samples (like the 0.25% Carbopol) confirmed the reproducibility of earlier methods of preparation and viscometry.

8.8.3 Radial Temperature Traverses

Six tests were carried out with water in the turbulent/transitional flow regime. In the last four runs, two Reynolds numbers were specified and two different wall fluxes applied for each. For all the remaining runs (twelve off) 0.25% Carbopol solution was employed. Of these, the first nine were performed with the heated section in the same position as for the water tests. As before, for any chosen Reynolds number, two different heat fluxes were used. The section was then turned through approximately ninety degrees (clockwise), and additional runs made under conditions similar to those of four of the preceding tests. All the Carbopol experiments were in the laminar regime.

8.8.4 Test Parameters

The controlling variables for all the experiments are summarised below. Details of individual runs have been listed in Table 22. Fluxes upstream were less than downstream values by a factor of $\left(\frac{\text{downstream diameter}}{\text{upstream diameter}}\right)$, while

Reynolds numbers for Newtonian fluids was in inverse proportion to the tube diameter. For non-Newtonians the relationships were

$$\frac{Re'_{(upstream)}}{Re'_{(downstream)}} = \left(\frac{\text{upstream diameter}}{\text{downstream diameter}}\right)^{3n-4}$$

$$\frac{Pr'_{(upstream)}}{Pr'_{(downstream)}} = \left(\frac{\text{upstream diameter}}{\text{downstream diameter}}\right)^{3-3n}$$

The computer program used in evaluating the non-dimensional parameters has been listed in Appendix 4. Typical "print-outs" have also been included.

NEWTONIAN TESTS

Tube Geometry --- 3.34 : 1 Convergence

Fluid	Reynolds Number Re	Prandtl Number Pr	Flux W/m^2 $\dot{Q}$
Water	28000-50000	5.7-6.9	4869-28413
100% (nominal) Glycol	300- 2400	300-600	1102- 5000
79.5% Glycol	600-13000	76-160	1500-10800

Tube Geometry --- 1 : 3.34 Divergence

79.5% Glycol	666- 3400	71- 73	172- 1864

NON-NEWTONIAN TESTS

Tube Geometry ---- 1 : 3.34 Divergence

Fluid	Flow Index n	Generalised Reynolds No Re'	Generalised Prandtl No. Pr'	Flux $\dot{Q}$ w/m^2
0.5% Methocel (60HG)	0.96	793-2000	37-45	530-1090
1.0% Methocel (60HG)	0.96	885-2009	57-59	310-585
0.15% Carbopol 934	0.63-0.70	58-143	463-785	300-1500
0.25% Carbopol 934	0.59-0.67	40-116	756-1414	480-1420
0.5% Carbopol 934	0.39-0.53	3-27	4000-10344	498-1543
0.5% CMC	0.90	180-2300	57-66	388-2688
1.0% CMC	0.82	25-350	458-522	577-2264

Tube Geometry --- 3.34 : 1 Convergence

Fluid	n	Re'	Pr'	$\dot{Q}$
0.5% Carbopol 934	0.54-0.65	223-1268	246-460	1238-5798
0.25% Carbopol 934	0.56-0.60	116-1624	250-743	2361-9631
2% Methocel(60HG)	0.91	257-2600	233-278	1854-5037
0.5% CMC	0.90	1027-4268	75-95	2385-16843
1.0% CMC	0.76-0.78	268-2258	188-287	3821-10875

CHAPTER NINE

ANALYSIS AND DISCUSSION OF RESULTS

9.0 INTRODUCTION

In this chapter the considerable amount of data obtained from the present experiments will be examined and the significant aspects discussed. As is common with such projects where the volume of data is large and varied, it has not been possible (in the interest of clarity) to include results of all the experiments in the graphs presented. However, where such omission has occurred, all the relevant information has been included either in tabular form or as samples of computer "outputs". In all cases the data included in the graphs are sufficient to highlight any particular aspect of the results being discussed. The format adopted is as follows:

In the first section (9.1) meaningful interpretation is given to the information obtained both from the main heat transfer equipment and the peripheral apparatus. The basis of presentation of data is justified where necessary. In the remaining section (9.2) the information deduced from the first part is discussed in detail. All the Tables and Figures referred to in this chapter are placed in Appendix 3 unless otherwise stated.

9.1 INTERPRETATION OF DATA

9.1.1 Calibrations

(a) Thermocouples

The temperature - e.m.f. relationship for the nichrome-constantan thermocouples is shown in Fig.28. As discussed in section 8.1.1, the deviation from literature standards was within acceptable limits and the obtained calibration chart was used.

(b) Cone - and - Plate Viscometer

Table 1 gives the measured shear rate - shear stress values of the silicone oils at 25°C and compares them with the known viscosity of these oils. The data are in excellent agreement, indicating the accuracy of the instrument over the range of shear rate encountered in the rig. In Table 2, the variation of viscosity of 89.5% (w/w) aqueous glycerol with temperature as obtained with the cone - and - plate viscometer is given. Comparison with values reported by SEGUR et al (169) and SHEELEY (173) is favourable. Thus the performance of the viscometer over the range of temperatures encountered in the heat transfer section is satisfactory.

(c) Capillary Tube Viscometer

Isothermal pressure drop and flow rate data may be

used to determine the rheological constants of any inelastic, time-independent fluid. The logarithmic plot of $\frac{D\Delta P}{4L}$ vs $\frac{8U_m}{D}$ for the Newtonian 89.5% (w/w) aqueous glycerol solution at 30°C is shown in Fig.29. The derived n' value is as expected for a Newtonian fluid while the K_N' ($=\mu$) agrees excellently with viscosity data from the cone - and - plate viscometer. The ability of this rather crude instrument to yield accurate data is thus established. Further indication of the performance is given by the coincidence, in Fig.29, of data obtained with different capillary tube lengths and diameters. This confirms the expected absence of time-dependent and shear rate effects.

9.1.2 Heat Loss From Experimental Section

Under a wall boundary condition of uniform heat flux, the local fluid temperature at a given axial location from the start of heating is estimated by equating the heat generated in that length of pipe to the fluid enthalpy rise up to the section under consideration. However, in practice, the actual heat transferred from the tube wall is modified by losses from

(i) the insulation surrounding the pipe

(ii) logitudinal conduction in the wall

(iii) circumferential conduction in the tube wall.

Insulation losses become significant when low heat fluxes are used. In the present series of tests, the lowest fluxes were applied for all tests using Methocel 60(HG) because of the low gelation temperature of this material. The resultant axial bulk temperature rise was therefore very small, - only 7 of the 26 tests with this material had bulk temperature increments of up to $0.5^{o}K$. A heat balance was carried out for all other tests where the fluid bulk temperature rise was greater than $0.5^{o}K$. Typical results have been given in Table 3. The test numbers quoted represent at least one run from each solution (polymeric and Newtonian) and each of the two geometries used. The heat balance data show that the desired objective of limiting the overall heat losses to within 5% of the total heat input was satisfactorily achieved.

The effect of heat flux variation along the length of a tube on the local heat transfer coefficient can be assessed by considering the ratio of heat conducted longitudinally ($d\dot{Q}/d(Z/D)$) to that transferred radially $\dot{Q}$. This is given by the parameter

$$\epsilon = \left| \frac{1}{\dot{Q}} \frac{d\dot{Q}}{d(Z/D)} \right|$$

If ϵ is much less than unity over the entire heat surface, with the exception of the points at the commencement and

completion of heat transfer, then the effect of variable heat flux distribution is unimportant. This parameter may be expected to be significant for tests with low wall fluxes. The lowest fluxes encountered were under the following conditions:

Newtonian Tests:

$Re_2 = 185$; $Pr_2 = 73$; flux = 172 W/m^2
(Divergent Configuration)

$Re_2 = 687$; $Pr_2 = 436$; flux = 1102 W/m^2
(Convergent Configuration)

Non-Newtonian Tests:

$Re'_2 = 259$; $Pr'_2 = 395$; flux = 1238 W/m^2
(Convergent Configuration)

$Re'_2 = 133$; $Pr'_2 = 417$; flux = 289 W/m^2
(Divergent Configuration)

For the divergence tests, ϵ valued at 1, 2 and 5.5 diameters was 0.03, 0.006, and 0 respectively, for the Newtonian case, and 0.018, 0, and 0, for the non-Newtonian fluid. At the position of observed maximum (or minimum) wall temperatures, the respective values were 0.3 and 0.0003. Axial conduction for the convergence runs was only significant at 1 diameter from the change of section, ϵ being 0.20 for the Newtonian test. The value was zero for the non-Newtonian case.

In general, to correct for axial flux variations, the calculated local heat flux was compared with the mean

value for the entire tube and the appropriate adjustment made. For the tests considered above these corrections amounted to 1.7% at 1 diameter, reducing to zero at 3 diameters downstream of the divergent section. At the position of minimum wall temperatures the correction was 3.7% for the Newtonian, and 0.4% for the non-Newtonian conditions. (Incidentally the position of temperature minima coincided at 11.5 diameters for the two cases quoted). Higher corrections were necessary with the convergent geometry. Adjustments of 17% and 1.8% were made at 1 and 3 diameters respectively, from the change of section for the Newtonian fluid. The corresponding figures were 0.3% and 0% for the non-Newtonian test.

Evidence of circumferential tube wall conduction was given by the substantial differences between temperatures measured by thermocouples situated at the top of the tube and those at the bottom. This "stratification" is usually attributed to natural convection effects and is consequently particularly severe at very low Reynolds numbers and large axial distances and for tubes having large diameters. Figs. 35 and 36 give typical wall temperature profiles for both the convergent and divergent geometries used. The degree of stratification under the particular test conditions encountered in the case shown in Fig.35 is indicated. In order to estimate the errors

likely to arise from this phenomenon, wall temperature profiles were obtained with the experimental divergent tube at two different orientations; - zero degree corresponding to the position of the tube during the main heat transfer tests, and 90° clockwise from this initial position. For the conditions shown in Fig. 36B (Re_2 = 320) the breakdown of errors is as follows: at axial distances 1, 25 and 40 diameters downstream from change of section, $\delta T/\Delta T$ have values of 0.8%, 7.7%, and 0.4% for zero degree orientation, (the low value of 40 diameters is caused by conduction at this location where the tube was drilled and a brass stub braised on to take the micrometer used in the traversing tests). With the tube turned 90°, these values became respectively 26%, 14.2% and 10.2%. For the same axial positions the differences between the measured circumferential mean tube temperatures were 0.8%, 0.2% and 0.6%. At 4 diameters downstream, corresponding to the region of observed minimum tube temperature, $\delta T/\Delta T$ was 65% and 1.9% (for 0 and 90 degrees) respectively, and the difference between mean temperature amounted to 11%.

From these observations it may be concluded that the measured local heat transfer coefficient is independent of the degree of circumferential conduction. However, values obtained at regions of flow instability may be subject to significant errors due to this effect.

9.1.3 Fluid Properties

For the Newtonian fluids (water and propylene glycol) the physical properties were obtained from well established sources (208) and (209). These are given in Tables 4 and 5. The physical properties of the non-Newtonian solutions used here (excepting "apparent viscosity") were taken to be that of water - the dominant solvent phase. Tables 6 and 7 give experimental data justifying this expedient. In Table 6, the thermal conductivities of CMC and Methocel in 2% (w/w) concentrations as determined experimentally (212) for this project are compared with water values from text (208). The values for Methocel are shown to be slightly less than that of water. In the range of temperatures encountered in the rig, i.e. 20°C to 50°C this discrepancy amounts to an average of only ± 1.4%. For CMC, conductivities are indicated which were greater than water values by an average of 6% over the same range of temperatures. The actual deviation is probably less than this figure since the accuracy of the technique used in these determinations was estimated at ± 3%.

It may therefore be concluded that at the maximum concentration levels employed in these experiments (0.5% for Carbopol 934, 1% for CMC, and 2% for Methocel 60(HG)), thermal conductivities given for water can be used with no more than a maximum of ± 3% error. Table 7, confirm that

densities of even higher concentrations of Methocel than used here are practically the same as for water over the range of temperatures encountered in the heat transfer tests.

9.1.4 Temperatures

(a) Pipe Wall Temperatures

The temperature of the outer surface of the pipe was as determined by the thermocouples positioned on the tube periphery. Since direct current was used to generate a uniform heat flux in the wall of the pipe, the inner wall temperature, was deduced by a modification of the formula originally used by EDE et al (54), to take into account possible conduction in the pipe wall. The improved expression was obtained by McINTYRE (128) and given as

$$t_i - t_o = \frac{(\phi_i - s\phi_o)}{(1 - s^2)} \left[r_i \lg(s) + s(1-s^2)\frac{r_o}{2} \right] - (1 - s^2)\ \frac{r_o}{2}\ \phi_o \qquad (228)$$

where $s = \frac{r_i}{r_o}$ and $\phi = \left(\frac{\partial t}{\partial r}\right)$

ϕ_o and ϕ_i are deduced from

$$\phi_i = \dot{Q} \ / \ (2\pi k_p r_i) \qquad (229)$$

$$\phi_o = q \ / \ (2\pi k_p r_o) \qquad (230)$$

If ϕ_i and ϕ_o are set to zero, equation (228) is similar to that obtained by EDE et al (54).

It is implied in the above expression that

(i) thermal and electrical properties vary little with temperature (for stainless steel, as used in the experiments, electrical and thermal conductivities vary by a nominal 0.02 per cent Kelvin).

(ii) the tube wall is thin compared with its radius. This is likely to be the case when the overall temperature correction is much smaller than the temperature difference used in calculating heat transfer.

(b) Fluid Bulk Temperature

As mentioned in section 9.1.2 the local bulk temperature at any axial position from the start of heating was calculated by carrying out a simple heat balance between, the net heat input to the elemental section and the enthalpy rise of the fluid between the inlet of the pipe and the location under consideration. To obtain the total rise between inlet and outlet of the composite pipe, a summation of all such short sections was made.

The mixing cup, when used for viscous liquids is highly inefficient and dependence upon the temperatures

indicated may lead to erroneous results. However, when pressure drop considerations permit an adequate design of such devices, the bulk temperatures indicated may satisfactorily be used as first order estimates of the accuracy of the tests by comparing with the values calculated from the heat balance. This was done in the experiments carried out here and the ratio $(t_{calculated} - t_{measured}) / t_{calculated}$ was never greater than $\pm$ 0.5% except in three cases, two with $Pr_2 = 75$ and one with $Pr_2' = 5174$ where the above ratio was 1% and 2% respectively. When this ratio exceeded 5% the data from that particular test was discarded. More rigorous justification of the estimating procedure was provided by results of the radial temperature traversing experiments. These are discussed in later sections. Typical fluid bulk temperature variation with axial distance is shown in Fig. 35. A linear relationship, as expected, is indicated.

9.1.5 Local Film Heat Transfer Coefficients

The heat flux to the heated section was calculated from the product of the voltage and current measurements. After allowing for the insulation losses, the net heat transferred to the fluid was obtained. Since the inside wall temperature at any axial position and the corresponding bulk temperature were known, the radial temperature gradient (Δt_r) was known and hence, the local film heat

transfer coefficient was evaluated as

$$h_z = \frac{\dot{Q}}{\Delta t_r}$$

With this value of h_z, the local Nusselt number corresponding to the bulk condition was calculated from

$$Nu_{zb} = \frac{h_z D}{k_b}$$

The corresponding Graetz number was evaluated for laminar flow condition as

$$Gz_b = \frac{W\ Cp_b}{k_b L} = \left(\frac{\pi}{4}\ \frac{Re\ Pr}{Z/D}\right)$$

For turbulent flow, the Stanton number corresponding to the bulk temperature is given as

$$St_b = \frac{h}{Cp_b G} = \frac{Nu}{Pr_b Re_b}$$

The non-dimensional parameters determined as above were in the following ranges for the equipment used here:

Laminar Flow:	h_z ($W/m^2\,^oK$)	Nu_z	Gz_b
Convergence Tests:			
Newtonian	257-1544	14-84	$(1.01-286)10^3$
Non-Newtonian	317-2170	9-70	$(1.41-318)10^3$
Divergence Tests:			
Newtonian	77-2066	14-376	$(0.27-121)10^3$
Non-Newtonian	36-1200	3-1113	$(0.9 -225)10^3$

Transitional/Turbulent Flow:			St_b
Convergence Tests:			
Newtonian (water)	6892-13713	195-388	$(0.8 -1.1)10^{-3}$
Newtonian (Glycol)	477-10023	26-546	
Non-Newtonian	638-5810	26-164	

9.1.6 Turbulent Heat Transfer in Newtonian Fluids

As stated earlier the tests with water and 79.5% (w/w) aqueous propylene glycol were conducted primarily to provide data for comparison with previous works and established correlations, thus proving the adequacy of the equipment. Only the sudden convergence geometry was investigated in these experiments. The results have been presented and discussed under "Comparison of Results" in Chapter 10.

9.1.7 Laminar Heat Transfer in Newtonian Fluids

(a) Sudden Convergence

Experiments with 100% (w/w nominal) propylene glycol were undertaken in order to extend the range of Prandtl numbers covered by previous studies (128) on the same tube geometry. Laminar Newtonian heat transfer is usually correlated by an expression of the form

$$Nu = f(Gz)^{\frac{1}{3}} = f(Re\ Pr/Z/D)^{\frac{1}{3}} \qquad (231)$$

With this in mind, results for Pr 400 and 600 have been presented in Figs. 37 and 38 respectively as plots of $Nu/Pr^{\frac{1}{3}}$ vs Z_2/D_2 for various Re_2. More data was obtained for lower Pr. They have not however been presented individually but used, where appropriate, to compare both with previous Newtonian results and present non-Newtonian studies (at low Pr'). The lower Prandtl number convergence heat transfer has in any case been previously covered in greater detail in reference (128).

(b) Sudden Divergence

As with the earlier turbulent tests (Section 9.1.6(a)), divergence tests were undertaken primarily to investigate the reproducibility of data from the present equipment. The results have therefore been presented and discussed

under "Comparison of Results" in Chapter 10.

9.1.8 Characterization of Pseudoplastic Fluids

Tables 8 - 17 give the shear rate - shear stress values for each polymer concentration for temperatures between 20°C and 60°C. A typical plot of the shear rate vs. shear stress is given in Fig.31. These log-log plots yielded straight lines over the range of shear rates encountered in the rig and hence the power law was assumed valid. From these plots, n and K_N were evaluated and given also in the above tables. At the concentrations used, 'n' was found to be invariant with temperature.

In all cases, K_N varied with temperature and could be represented by the relationship

$$K_N = Ae^{B/T} \qquad (232)$$

The variation of K_N with inverse absolute temperature has been given in Figs. 32, 33 and 34. The values of 'A' and 'B' are listed in Table 21. In the characterization of run samples, there was observed to be little variation in the values between those of a run sample and those of a fresh solution sample, especially for the case of Methocel and CMC. For Carbopol there was a slight change after each set of runs and hence it was necessary to obtain the 'n' and 'K_N' values for each run sample at various

temperatures. To circumvent this, the K_N and n values of the reference sample were defined as K_N^* and n* and those for the run samples as 'K_{NR}' and 'n_R'. $(K_{NR})_t$ and $(n_R)_t$ could then be evaluated as

$$\left(K_{NR}\right)_t = \left(\frac{K_{NR}}{K_N^*}\right)_{25^oC} \left(K_N^*\right)_t \qquad (233)$$

$$\left(n_R\right)_t = \left(n_R\right)_{25^oC} + (t-25)\Delta n^* \qquad (234)$$

Δ n* in equation (234) represents the observed change in n* per unit temperature rise for the reference sample. Equation (232) and (233) have been verified by HOBSON (80) and used successfully by MAHALIGHAM (102). Tables 18 and 19 show the effect of circulating 0.15% and 0.25% Carbopol in the rig. It is seen that K_N decreases very rapidly in the first 1 to 2 hours and undergoes more gradual degradation thereafter.

9.1.9 Laminar Heat Transfer to Pseudoplastic Fluids

(a) General Aspects of Undisturbed Flow-Heat Transfer

Although it was not the main objective of this project to investigate fully-developed heat transfer, in

the absence of any previous correlations for non-Newtonian heat transfer coefficients downstream of an abrupt convergence or divergence, it was felt that examination of the behaviour in regions where known and adequate correlations exist would give some idea of how to present the disturbed flow heat transfer data meaningfully. For the purposes of the analysis which now follows, conditions 50 diameters upstream of the expansion (preceded by 100 diameters of heated tubing) is considered fully developed. As stated in Section (9.1.7), laminar Newtonian heat transfer is well correlated by an expression of the form shown in equation (231). This equation neglects such secondary effects as axial heat conduction, free convection, viscous dissipation, and property variation with temperature. It was shown in Section (9.1.2) that at axial locations greater than 10 diameters corrections for axial conduction become negligible. This effect can therefore be discounted in the following analysis. Although the experimental conditions were carefully chosen to minimize the effects of free convection, such effects cannot be entirely precluded. Regarding viscous dissipation, it is to be expected that for the high consistencies usually associated with non-Newtonian fluids such effects would be very significant. In Chapter 6 an analytical expression was derived for the asymptotic Nusselt number which takes into account viscous dissipation. Equation (227) may be rewritten as

$$Nu_{\infty}^{-1} = Nu_{o}^{-1} - \frac{\chi}{16} \qquad (227a)$$

where Nu_o is the Nusselt number for non-dissipative flow; χ is a function of the modified Brinkman number Br_m and given as

$$\chi = \frac{2n}{3n+1} Br_m \qquad (235)$$

From equation (227a) it is seen that $Nu = Nu_o$ when χ, and hence Br_m is zero. For every value of the flow behaviour index n, there exists a corresponding value of the Br_m group (or χ). Of all the polymer used here 0.5% Carbopol exhibited the highest consistency and lowest n. The effect of viscous dissipation may therefore be expected to be most severe with these solutions and at large axial distances. The parameter Br_m, observed for the 0.5% Carbopol solutions ranged from 0.004 to 0.050 with the corresponding ratio $\frac{Nu_{\infty}}{Nu_o}$ of 1.002 to 1.024. The maximum value was obtained with the very first batch of solution and in the first run. This therefore represents the absolute maximum since the consistency of these materials are known to decrease with circulation. Viscous dissipation will therefore be neglected in this analysis. The criterion for significant dissipation (i.e., when $Nu_{\infty}/Nu_o > 1.05$) may be expressed for this investigation as

$$\chi > 2.2\, Nu_o^{-1}$$

where Nu_o is obtained from equation (118). Viscosity variation with temperature is not excluded.

Fig.39 shows the Nu - Gz plot for all the polymer solutions (except Methocel the results of which will be treated separately in later sections). This is compared with the equation

$$Nu_z = 1.413\, Gz^{\frac{1}{3}} \qquad (74)$$

which is the equation for the Newtonian case. It is seen that although the deviations from this line are not very dramatic, this equation generally underpredicts Nu_z. Non-Newtonian behaviour has to be taken into account. The correction factor as discussed in section (4.2.2a) is $\Delta^{\frac{1}{3}} = (3n+1/4n)^{\frac{1}{3}}$. The Nusselt numbers combined with this parameter are plotted against Gz. Fig.40 shows that equation (118)

$$Nu_z = 1.413\, \Delta^{\frac{1}{3}} (Gz)^{\frac{1}{3}} \qquad (118)$$

gives a better fit. However, there is some scatter especially from the 1.0% CMC data. Temperature effects on viscosity have to be considered. It was shown in the preceding

section how K_N values for the polymers varied with temperature. Hence one can assume that distortion of the parabolic velocity profile with respect to temperature would be significant. This distortion is usually corrected for by the use of a Sieder-Tate type correction parameter $(\mu_{\text{apparent}_w} / \mu_{\text{apparent}_b})^{0.14}$. This reduces here to $(K_{Nw}/K_{Nb})^{0.14}$ since n was shown to be temperature independent. The choice of the index 0.14 is justified only by the knowledge that it has been used very often to correlate data satisfactorily for Newtonian fluids. This factor is denoted by $M^{0.14}$ in this, and subsequent chapters. The use of the index 0.14 assumes that the non-Newtonian fluid properties are as temperature dependent as Newtonian fluids of the same consistency. This was shown not to be the case in section (9.1.8). With the exception of 1% CMC, the consistency parameter K_N was remarkably insensitive to temperature increments of less than 10K. In Fig.41(a) the Sieder-Tate type (index = 0.14) is used to improve the correlation. Fig. 41(b) shows the same data corrected by an alternative factor suggested by MIZUSHINA (126). This takes into account possible variation of the rheological properties with temperature. The comparison indicated here can only be tentative since the radial temperature differences employed in this investigation were relatively small. As expected, for data obtained from CMC (which showed greatest K_N - temperature dependence) the MIZUSHINA (126) correction given as

$$Nu_z = 1.41\ Gz^{\frac{1}{3}} \Delta^{\frac{1}{3}} \left(\frac{K_{Nb}}{K_{Nw}} \right)^{C/n^{0.7}} \qquad (120)$$

where

$$C = 0.045\ (1.41\ Gz^{\frac{1}{3}} \Delta^{\frac{1}{3}})^{0.7} \qquad (121)$$

provides a marginally better correlation. For the rest of the data, there is no discernible advantage in using either form of correction. The Sieder-Tate type will therefore be retained throughout, but it is appreciated that at higher polymer concentrations and greater tube to wall temperature differences than used here, equation (120) will give a more realistic correlation. Retaining $M^{0.14}$ ensures that direct comparisons can be made between the present and previous studies using the same type of correction. It is of interest to note that for 1% CMC (n = 0.82), $M^{C/n^{0.7}}$ equals 1.09 compared to $M^{0.14}$ of 1.03 under the same test conditions. This means that using $M^{0.14}$ "under corrects" for viscosity variation by about 5.5%. This error is less than 2% for all the other polymer concentrations used here. Returning to the correlation, it is seen from Figs. 41(a) and (b) that equation (118) still predicts slightly lower Nu. An improved correlation is attempted by including the effects of natural convection although, as already stated the effect was expected to be only slightly significant.

The dimensionless group reflecting natural convection is the Grashof number (Gr). This parameter has been

evaluated for each run and presented in Table 22. The estimations were done both at the wall and bulk conditions. The former, Gr_w has been used in accordance with equations

$$Nu_b/\Delta^{\frac{1}{3}}{}_M{}^{0.14} = 1.41\ [Gz_b + 12.6(Gr_w Pr_w\ D/L)^{0.4}\ ]^{\frac{1}{3}} \qquad (89a)$$

$$Nu_b/\Delta^{\frac{1}{3}}{}_M{}^{0.14} = 1.41\ [Gz_b + 0.0083(Gr_w Pr_w)^{0.75}\ ]^{\frac{1}{3}} \qquad (91a)$$

to correct for free convection. Wall conditions were chosen for Pr_w and Gr_w since any property variations would be most severe at this position. The above equations are compared with present data in Figs. 42 and 43. It is seen that equation (91a) gives a better correlation. This confirms the reservations noted in section (4.2.1a) about the inclusion of the D/L term in equation (89a). The criteria for significant natural convection effects in the present investigation may be expressed (empirically) as

$$Gr_w/Re_w > 1.0$$

$$Gr_w/Re_w^2 > 30 \times 10^{-4}$$

The final correlation for heat transfer in non-Newtonian fluids, under conditions of uniform heat flux and laminar fully developed flow in circular tubes is then

$$\frac{Nu_b}{M^{0.14}} \frac{1}{\Delta^{\frac{1}{3}}} = 1.413 \left[Gz_b + .0083 (Gr_w Pr_w)^{0.75} \right]^{\frac{1}{3}} \qquad (91a)$$

At lower values of Gz ($< 10^3$) the factor 1.413 will be modified. This will be taken up in later sections.

It will be recalled that the purpose of the above correlation has been to obtain a suitable grouping of the parameters influencing heat transfer in non-Newtonian fluids. From equation (91a) it is reasonable to assume that the $Nu - f(Gz)^{\frac{1}{3}}$ will yield unique relationships provided the non-Newtonian data is corrected for pseudo-plastic behaviour by the factor $\Delta^{\frac{1}{3}}$. $Nu/Pr'^{\frac{1}{3}} \Delta^{\frac{1}{3}}$ may then be plotted against Z/D for specific generalised Reynolds numbers. The strict applicability of the $Gz^{\frac{1}{3}}$ correlation at all axial positions will be discussed later in connection with the sudden convergence tests.

(b) Sudden Convergence

The axial variation of heat transfer coefficient is shown in Figs. 44 to 48 as plots of $Nu/Pr'^{\frac{1}{3}} \Delta^{\frac{1}{3}}$ vs Z_2/D_2

for specific generalized Reynolds numbers (Re_2'), downstream of the change of section. Other aspects of the convergence data are shown in Figs. 49 to 65.

(c) Sudden Divergence

As for the convergence tests, heat transfer coefficients downstream of the change of section have been shown in the first instance as graphs of $Nu/Pr^{\frac{1}{3}} \Delta^{\frac{1}{3}}$ vs Z_2/D_2 in Figs. 66 - 72 for specific upstream (Re_1') and downstream (Re_2') generalized Reynolds numbers. Other details of the experiments are shown in Figs. 73 - 87.

9.1.10 Fluid Radial Temperature Profiles

The radial variation of the fluid temperatures obtained with water and 0.25%(w/w) Carbopol for the divergent geometry is presented in Figs. 88 - 96. The ratio $(T - T_i) / (T_w - T_i)$ has been plotted as a function of reduced radius $\xi (= r/R)$ with Reynolds number, (Re_1',Re_2') axial distance (Z_2/D_2), Prandtl number (Pr'), and heat flux ($\dot{Q}R/k$) as parameters. The inlet condition has been used (instead of centre-line temperature) since in this form the data can be used directly for practical purposes. In any case, the centre-line temperature was in all the tests well approximated by the inlet temperature.

In concluding this section, it is worth explaining at this stage the disposition of the figures referred

to in the following sections. So far, the illustrations have been numbered as they are referred to in the text. This arrangement will be retained. It is hoped this will minimize cross referencing, although this cannot entirely be avoided.

9.2.0 DISCUSSION OF RESULTS

9.2.1 Accuracy of Data

(a) Heat Input

The electrical power supplied to the heated section was selected through a stabilised voltage controller whose sensitivity was of the order of ± 1%. This would be the tolerance on each of the measured items - voltage and current.

(b) Heat Loss

The heat loss from the heating section was discussed in section 9.1.2. For most tests this was limited to 2% ± 0.5%.

(c) Temperature Measurements

The calibration of thermocouples and measurements of the tube wall and bulk fluid temperatures have been each discussed in the last section. The overall errors arising from these and other variations in tube geometry may be

summarised as:

Source	Error
Tube Temperature	± 0.05K
Fluid Temperature	± 0.02K
Circumferential wall thickness deviations in tubes	± 2.5%
Axial wall thickness variations in tubes	± 1%
Variation in radius of tube	0.2%

(d) Flow Measurement

The error in flow measurement based on the sensitivity of the weigh-scale was 0.3%.

(e) Overall Error in Heat Transfer Coefficients

The maximum accumulative error in the heat transfer coefficient, h, is given by the formula:

Let

$$X = X(a_1, a_2, a_3, \ldots, a_n)$$

then

$$dX = \frac{\partial X}{\partial a_1} da_1 + \frac{\partial X}{\partial a_2} da_2 + \ldots + \frac{\partial X}{\partial a_n} da_n$$

Hence relative error is given by

$$E_r = \frac{dX}{X} = \sum_{n=1}^{N} \frac{\partial X}{\partial a_n} \frac{da_n}{X}$$

Since

$$h = \dot{Q}/\Delta T$$

$$E_r = \Delta h/h = \left| \frac{\Delta \dot{Q}}{\dot{Q}} \right| + \left| \frac{\Delta T}{T} \right|$$

Based on a tube - to - fluid temperature difference of $3^{\circ}K$ (lower average used here), the error in the axial distribution is 5.5%; rising to 7% for the circumferential distribution. At higher differences, say $8^{\circ}K$ (higher average used) the corresponding errors reduce to 4% and 5.6%. For most of the tests conducted here the probable error in measuring local h was no more than $\pm$ 3%.

9.2.2. Reproducibility of Data

Experimental data intended for practical use should not only be accurate but also reproducible under identical conditions. In the present project, reproducibility has been viewed from two standpoints. One is obtaining of same rheological constants for reference samples of the same concentration. The other is the reproduction of heat transfer characteristics under similar experimental conditions.

The shear stress - shear rate data for 0.25% CPM reference samples 1 and 2 (Tables 11 and 15 respectively), and 1.0%(w/w) CMC reference samples 1 and 2 (Tables 14 and 17 respectively) are in good agreement. Although not as dependable as comparison of data obtained with same equipment, Table 20 gives further evidence of reproducibility of the present rheological results. The index 'n' as obtained by various other workers for similar polymers as employed here are listed. Reproducibility with respect to heat transfer characteristics is discussed under the appropriate headings (Sections 10.1.1 and 10.1.2).

9.2.3 Temperature Profiles

In general the tube and bulk temperature profiles obtained with Newtonian and non-Newtonian fluids were similar differing only according to the geometry employed. The temperature distribution will therefore be discussed together under the convergent and divergent test conditions. The only exception to the above observations (and only for the divergent case) are tests with Methocel solutions. These will be treated separately.

In Fig.35 the tube wall and fluid bulk profiles are shown for a typical convergent test. The tube temperature rises with increasing distance from the start of heating. The top of the tube becomes progressively hotter than the

bottom as the distance increases indicating the influence of natural convection effects. The most severe cases of stratification encountered were with 1.0% CMC solutions where relatively high fluxes were used (to study the influence of heat flux on heat transfer). At $Re_2' = 353$, $Pr_2' = 203$ and with a flux of 4983 W/m^2 the ratio $\delta T/\Delta T$ was 23% at 20 and 25 diameters downstream of the change of section. When the flux was reduced by 50% the ratio dropped to 10%. For the more viscous solutions natural convection was insignificant and the stratification ratio was around 4% except very near the change of section where a value of 12% was recorded for one test with 0.25% Carbopol. The influence of Reynolds number could be expressed as follows: under the same wall flux conditions, an increase in Reynolds number from 329 to 1300 reduced $\delta T/\Delta T$ (at 25 diameters) from 8.8% to 4.7%.

For the divergence tests (Figs. 36(A), (B) and (C)), a minimum occured in the tube wall temperature at 2 to 5 diameters from the change of section. Thereafter, the temperature rises gradually (except for Methocel tests) and becomes practically constant at 20 to 25 diameters from the change of section. The stratification noted in the convergent tests was more severe under the divergent conditions since with a larger tube diameter the effect of natural convection becomes more pronounced. This was particularly so at the point of minimum tube wall temperature ,

ranging from $\delta T / \Delta T$ of 22% to 54% corresponding to fluxes of 862 W/m² and 1543 W/m² respectively. These figures were obtained with 0.5% Carbopol at Re_2' of 18, and Pr_2' of 3724. For these viscous materials, increasing the Reynolds number did not seem to have any significant effect on either the degree of stratification or the position of the noted axial minimum. This is not so surprising when it is realised that for the 0.5% Carbopol, available pressure drop could only increase Re_2' from 3.1 (minimum) to 35 (maximum).

The abnormal behaviour of Methocel solutions under the divergent flow conditions is seen from Fig. 36(C). The profile for 0.5% Methocel is compared with that of CMC of the same concentration. After the already noted minimum at 2 diameters from the section change, the Methocel profile rises very sharply to reach a well defined peak, usually at 10 diameters downstream. The wall temperature in effect increases by about 43% in 8 tube diameters from the minimum position compared to a 10% rise for the CMC profile. Thereafter there is a more gradual drop but the temperature never approaches a constant value even after 40 diameters, it tends rather to increase again after this position right up to the tube exit. For $Re_2' > 1000$ no significant effect of Reynolds number on the position of the maximum temperature was noticed. For $Re_2' < 1000$ (only in one case could such a low value be maintained with this solution), the peak was shifted upstream to 7 diameters. However, there

was evidence that both Reynolds number and heat flux influenced the rate of increment from the minimum to the maximum value. This behaviour must be attributed to natural convection having the reverse effect, i.e. reducing rather than increasing the heat transfer coefficient Nu. Such free convection effects have been established experimentally (138) where it was shown to be the result of stratification of the fluid in the tube into layers which differ in temperature and therefore viscosity. Similar tube wall profiles have been reported in previous studies using a different grade of Methocel; HOBSON (80), for an annulus and MAHALINGHAM (102) for a circular tube. In the latter case, Carbopol 934 was also reported to exhibit, only to a small extent, the same type of behaviour. These findings suggest that free convection apart, the phenomenon may be one of flow instability dependent upon the flow parameters, the heat flux, and the molecular structure of these non-Newtonian materials. Further work is required to correlate all these factors.

So far only the wall temperature has been mentioned. The fluid bulk temperature profile is also shown in Figs.35 and 36(C). A linear but gradual increment is observed from the inlet to the outlet of the tube in all cases. The minimum rise obtained here was $0.13^{o}K$ and the maximum $1.96^{o}K$.

9.2.4 Laminar Heat Transfer in Newtonian Fluids - Sudden Convergence

The heat transfer coefficient expressed as $Nu/Pr^{\frac{1}{3}}$ and shown in Figs. 37 and 38 follows the usual distribution downstream of a sudden change of section. A high coefficient obtained very close to the entry region rapidly decreases with increasing distance to attain 70% of its terminal value in about 6 or 7 diameters downstream. Both the Nusselt number and the rate of flow development increases with Reynolds number. For the same Reynolds number, lower Prandtl numbers yield higher coefficients for a given wall heat flux and inlet conditions. It is also noticeable that at one diameter from the change of section, a small peak occurs in the heat transfer coefficient profile. This corresponds to a lowering of the tube wall temperature due to a possible separated flow effect, since the plotted Nusselt numbers had already been corrected for axial heat conduction. The absolute values of Nu was generally about 10% less than predicted by gradual entry theoretical predictions of SELLARS et al (170). The later correlations of MARTIN (105) seem to reflect the downstream characteristics better. This point is taken up later in Chapter 10. Other aspects of contracted Newtonian flow heat transfer have been extensively treated by McINTRYRE (128) and will therefore not be discussed any further. However, in as much as the above results were similar in certain respects to the non-Newtonian data, any further elaboration has been

done under the latter heading.

9.2.5 Characterization of Pseudoplastic Fluids

The pseudoplastic fluids used for the heat transfer runs were: -

(i) Carbopol 934 (CPM):

0.15%, 0.25% and 0.5%

(ii) Methocel 60HG (MC):

0.5%, 1.0% and 2.0%

(iii) Sodium Carboxymethyl Cellulose (CMC):

0.5% and 1.0%

The K_N and n values for the reference samples listed in Tables 8 to 17 show that n decreases with increasing concentration. However for Methocel 60HG no appreciable decrease in n was obtained by increasing from 0.5% to 1%. Other grades of Methocel (e.g. Methocel 90HG) have been shown to become more non-Newtonian as concentration increased even slightly. The index 'n' is practically temperature independent for all but one solution - 1% MC. The variation amounted to only 3% and was not sufficient to alter the pseudoplastic characteristics. Thus the assumption of constant 'n' with respect to temperature is valid for any theoretical analysis. As is expected of high viscosity fluids K_N is temperature dependent. The

relationship has already been stated as

$$K_N = Ae^{B/T} \qquad (232)$$

where B is positive with units of ^oK. It is observed from Table 21 that at the levels employed here, B is practically independent of polymer concentration for Methocel and CMC and increases only marginally with solution strength for Carbopol. This aspect of pseudoplastic behaviour is in agreement with the observations of other workers (102, 123), with respect to CMC and Carbopol. MAHALINGHAM (102) has noted an increase in B with increasing Methocel concentrations. He used Methocel 90(HG) of heavier molecular weight than that employed here. It is therefore more than likely that the discrepancies arise from this difference in the properties of the polymers.

Since B is independent of concentration for the solutions used here, the effect of temperature on K_N is also practically independent of this parameter. This is in surprising contrast with some viscous Newtonian aqueous solutions. For example, it was observed in the present and previous (128) studies on propylene glycol that by changing the composition of the water-glycol mixture both the viscosity and the temperature dependence of this property could be altered significantly. A possible (but only intuititive at this stage) explanation of the

behaviour of the non-Newtonian solutions is that, as with the other physical properties (density and specific heat), the effect of temperature on a water based polymeric mixture at low polymer concentrations is dominated by this effect on the dominant solvent phase, in this case water. This will be particularly true over the temperature range 20°C to 50°C encountered here. A more detailed study of the molecular structure of these polymers in solution will be necessary to shed more light on this matter.

It was noted in earlier sections of this thesis that more realistic analysis of pseudoplastic velocity profiles can only be obtained if temperature effects are also considered. The constancy of B in equation (232) greatly simplifies any such mathematical analysis.

The stability of the above polymeric solutions has been mentioned already in connection with the control of experimental conditions. Shear degradation was most marked with the Carbopol mixtures. While with CMC and Methocel the consequent reduction in consistency was only significant in the first two or three hours after preparation, a gradual but noticeable degradation persisted throughout the runs on any batch of Carbopol solution. This behaviour has also been observed in previous studies using this material (102). The implication is that the values of n and K_N obtained would depend on the period of

circulation before the characterization was done. As a result, comparison of K_N values with those of other workers becomes difficult. Nevertheless, reasonable agreement is shown in Table 20 between present 'n' values and those of others.

9.2.6 Laminar Heat Transfer in Pseudoplastic Fluids

(a) Sudden Convergence

The data presented in Figs. 44 to 48 show that $Nu/Pr^{\frac{1}{3}} \Delta^{\frac{1}{3}}$ is a valid function of (Z/D) for specific Reynolds numbers downstream of a sudden convergence. The uniqueness of this form of presentation will be discussed presently. General observations based on these data may be summarised as follows:

(i) Nusselt number decreases as the axial distance increases downstream of the change of section,

(ii) the value of Nu increases with Reynolds number,

(iii) the rate of decrement of Nu with distance increases with Reynolds number,

(iv) the rate of decrement of Nu with distance is accelerated as non-Newtonian index n increases,

(v) heat transfer is enchanced or suppressed by increased pseudoplasticity (lower n) depending on Reynolds number,

(vi) there is a well defined peak in the Nu profile for $Re_2' > 700$ and occurs at 1 diameter downstream of the section change.

The above points will now be discussed in detail. In Figs. 44 to 48, the parameters chosen to present the sudden convergence data were based partly on the existing and proven laminar flow theory, and partly on experimental verification (Section 9.1.9) that conditions just upstream of the change of section were well correlated by the selected dimensionless groups. It therefore remains to be established how the presence of the discontinuity modifies the exact nature of the function which represents data in its absence. Starting with the premise

$$Nu^* = \frac{Nu\ (\text{gradual entry theory})}{Nu\ (\text{contracted flow experiment})}$$

$$= f(M,\ Re_2',Pr_2',\ n,\ Z_2/D_2) \qquad (236)$$

where M has already been defined as the parameter correcting for temperature - dependent viscosity. The effects of viscous dissipation and free convection have also been shown to be insignificant (Section 9.1.9), and therefore are not included in equation (236). Considering first the Reynolds number function, the experimental parameter

$Nu/Pr^{\frac{1}{3}} \Delta^{\frac{1}{3}} M^{0.14}$ has been plotted against Reynolds number at two selected axial locations 1 and 40 diameters, and for each polymer and concentration tested. (In all cases the dimensionless groups in equation (236) refer to the downstream section and the subscript 2 will be dropped in this discussion). Despite the scarcity of points when plotted for individual solutions, Figs. 49 to 52 indicate clearly how best to approach the attempted correlation with respect to Reynolds number. For reasons to be discussed later, the data falls into two distinct Reynolds number ranges, Re less than and greater than 1000 respectively. This is shown more clearly in Fig. 53 where all the data corresponding to the selected axial locations are plotted together.

The effect of non-Newtonian index n (or Pr′) is shown in Figs. 54 and 55 where the Nu* vs Z/D distribution has been given for Re′ > 1000 and Re′ < 1000 respectively. The experimental Nu was first corrected for variable viscosity (with $M^{0.14}$) before the ratio Nu* was evaluated. It is seen from Fig. 54 that when Re′ > 1000, n(or Pr′) has practically no effect on the ratio. However for Re′ < 1000, a relatively higher ratio is obtained with the lowest n while a smaller value is given as n tends to unity. This reflects the combined effect of the sudden contraction and pseudoplasticity on heat transfer for low Reynolds numbers and will be discussed later in this

section. It is also noticeable that the maximum deviation from a mean of the curves occurs for n = 0.9 which may be regarded as a Newtonian situation. An error analysis indicated that the ratio Nu* was internally consistent for all the runs using a particular polymer concentration as follows:

$\pm$ 4% for 0.5%(w/w) Carbopol;

$\pm$ 5% for 0.25%(w/w) Carbopol;

$\pm$ 8% for 2%(w/w) Methocel;

$\pm$ 5% for 1%(w/w) CMC.

The relative agreement between the various solutions (excepting 2% Methocel) expressed as maximum deviations from a mean value was within $\pm$ 6% at all diameters. As already stated greater deviations were recorded for the Methocel runs, ranging from $\pm$ 19% at 1 diameter to $\pm$ 9% at 40 diameters when Re′ was less than 1000.

Based on the above observations, a correlation of the type

$$Nu^* = \frac{Nu\ (\text{gradual entry theory})}{Nu\ (\text{contracted flow expt})} = f(Re', Z/D)$$

was sought. This is in fact fitting an expression to the mean of the curves given for each Reynolds number range. The correlations are given as

$$Nu^* = 1 + \frac{3}{(Z/D)^{0.50}}, \qquad 1000 < Re' < 2100 \tag{237}$$

$$Nu^* = 1 + \frac{3.85}{(Z/D)^{0.50}}; \qquad Re' < 1000 \tag{238}$$

The smoothed curves are given in Fig.56. The constant coefficient 1 in equation (237) and (238) was assumed at the start of the curve fitting procedure. This is merely stating the fact that when Z/D tends to infinity the Nusselt number assumes a constant value. That this value will be the same as predicted by existing 'continuous' tube theory is supported by data in Fig.64. Here at the higher Reynolds number (corresponding to large axial distances) the contracted flow effect disappears and the experimental Nu is as predicted. To verify that the correct parameters were chosen for the above correlations, the equations may be rewritten

$$\begin{aligned} Nu\ expt &= Nu(theory) \times (1+A/(Z/D)^C)^{-1} \\ &= 1.413\ (Re'\ Pr'/(Z/D))^{\frac{1}{3}} \Delta\ ^{\frac{1}{3}}{}_M{}^{0.14} \ \ldots\ldots \\ &\quad \ldots\ldots\ (1 + A/(Z/D)^C)^{-1} \end{aligned} \tag{239}$$

where A and C take the values given in equations (237) and (238) depending on the Re' range. If the parameter

$$\frac{Nu_{expt}\left(1 + \frac{A}{(Z/D)}C\right)(Z/D)^{\frac{1}{3}}}{Pr^{\frac{1}{3}} \Delta^{\frac{1}{3}} M^{0.14}}$$

is plotted against Re', the slope is expected to be $\frac{1}{3}$ when flow is laminar. This is confirmed by Fig.57. A few data obtained in the transitional region of flow has been included in this plot. The critical Re when the above expressions become invalid is clearly indicated.

Regarding the generality of the above expressions it is appreciated that since no tests were performed with other contraction ratios, the equations can only be regarded as particular solutions to a more general problem of heat transfer to non-Newtonian fluids at low Reynolds numbers, and in contracted flow situations. It must be pointed out that because of the marked differences in behaviour between Newtonian and non-Newtonian fluids at low Re downstream of a sudden contraction, previous laminar flow data (128) on other contraction ratios could not be used to indicate the modifications necessary to the given expressions to take into account the contraction ratio parameter. The errors involved in using equations (237) and (238) are as follows: in the higher Re' range, the maximum deviation is $\pm$ 6% and over 95% of the data is correlated by equation (237). Greater deviations occur with equation (238), mostly with data from 2% Methocel ,

these range from 10 to 22% for this material while for all the other polymers equation (238) gives results accurate to within ± 7%.

Other aspects of the sudden convergence data will now be considered. The observed progressive reduction in Nusselt number with increasing axial distance is in agreement with entry region heat transfer. In the areas near the change of section the flow is still developing and heat transfer is enhanced. However, for $Re' < 500$ the velocity development seems to have been nearly completed prior to entry to the contracted section. The Nu decreases to within 90% of its terminal value in the first 2 to 3 diameters for all the polymers tested. The accelerated flow development is illustrated in Fig.58 where a typical Newtonian flow development under similar conditions have been included for comparison. This behaviour suggests the existence of a stationary vortex upstream of the contraction. Because of the presence of this vortex, the area available for flow upstream of the contraction is reduced. For continuity to be maintained, the fluid must start to accelerate further upstream of the contraction with a partially developed velocity profile resulting at the entrance. As the Reynolds number increases, the size of the vortex decreases with the entrance profile undergoing a transition for a partially developed to a uniform

profile as the vortex disappears. The fact that this partial development persists at the relatively high Re of 500 (compared to a value of 50 numerically computed in ref. (32) for a contraction ratio of 2) would indicate that the larger contraction used in this investigation, and the pseudoplastic nature of the experimental fluids combine to extend both the critical Reynolds number and the distance upstream of the convergence at which velocity deformation begins. The influence of Re' and 'n' on the flow development is illustrated in Figs 59 and 60 respectively. These plots confirm observations made above.

The effect of non-Newtonian index on heat transfer is shown in Figs. 61 and 62. It is seen that for Re' < 500 there is no improvement as pseudoplasticity increases, rather, there is a reduction in Nu. This contradicts the analytical predictions as expressed in equation (118). In these the 'stubbier' velocity profiles associated with non-Newtonian fluids are expected to delay flow development and hence enhance heat transfer in the entrance region. But as has been shown above, under contracted flow conditions and at low Reynolds numbers, the reverse is the case. Fig.63 shows the overprediction inherent in assuming "uniform" velocity profiles at the entrance of a sudden convergence section at small Reynolds numbers. For $1000 < Re' < 2500$ heat transfer is marginally improved as n decreases (pseudoplasticity increases). This is

illustrated in Fig.61. However, the non-Newtonian Nusselt number is still less than for a Newtonian fluid under the same conditions. The suppression of heat transfer as n decreases at low Re is also the result of the same vortex effect discussed above. In Fig.64, the experimental Nu for Re' = 2146 and 2780 are compared with values from theoretical analysis assuming uniform entrance velocity profile. The polymeric solutions here are 0.5% and 1% CMC. For Re' = 2146 the experimental Nu is still 73% less than the "theoretical" near the entrance region. The percentage difference diminishes with distance to 7% at 25 diameters downstream. On the other hand, at Re' = 2780 the experimental Nu is underpredicted by 9% near the entry indicating that the transitional regime is just being approached. This infact occurs as from Re' = 2500 in the present tests. The extension of the laminar - transitional range of Re' for non-Newtonian fluids has been observed in previous studies by METZNER et al (117).

A well defined peak was noticed at about 1 diameter downstream, in most cases for Re' > 1000, but in some, for as low as 700. The same observation has already been noted with respect to the Newtonian tests (Section 9.2.4). Also previous studies (54, 55, 128) noticed this behaviour but in these, substantially higher Reynolds numbers were used (2500 to 10000). ASTARITA and GRECO (5) have reported pressure drop data which suggest that a "vena contracta"

(to which the peaks are often attributed) can occur for Re as low as 186 for 41.7% glycerol flowing through a 2.5 contraction. However for water, RAMA MURTHY et al (147) observed no such effect for Re < 2100 and for a contraction of 2. These contrasting reports confirm the observations made earlier (Section 4.1.5), namely, that a contraction ratio of 2 may be the maximum that can be used without the formation of a "vena contracta" in laminar flow, for both Newtonian and non-Newtonian fluids. It must be noted however, that data obtained from measurements taken a 1 diameter from change of section are liable to significant effects of tube wall conduction. The results observed at this location may therefore not be so reliable.

In concluding this discussion on the convergence data, the effect of heat flux will be examined bearing in mind earlier remarks about the insignificance of variable viscosity and free convection effects. Fig.65 shows the results of tests carried out with both Newtonian and non-Newtonian solutions. The trends are similar and will therefore be discussed here together. In general under laminar conditions, increase in heat flux enhances heat transfer to a degree depending on the Reynolds number. For the Newtonian tests (in which considerably high fluxes could be applied) a 700% increase in flux at $Re' = 700$, improves heat transfer by 47% at 1 diameter and by 28% at

25 diameters. The non-Newtonian tests show that at $Re' = 2200$, a 46% increase in flux, enhances heat transfer by 24% at 1 diameter and by 7% at 25 diameters. The Nusselt numbers Nu' plotted here have been corrected for variable viscosity and free convection and by using $Nu'/Pr'^{\frac{1}{3}}$ instead of Nu', the slight variations in Prandtl number due to any changes in viscosity are accounted for. Although the dependence of the Nu - Gz correlation on heat flux cannot be altogether discounted in laminar flow, especially when the heat transfer medium exhibits high temperature dependent viscosity, the order of magnitude indicated in Fig.65 suggests that the correlation can only be a weak function of the flux parameter. In the present investigations, the heat flux effect is considered minimal since as has been mentioned, the polymeric solutions used have relatively low temperature dependence. The 24% enhancement noted is within the range of errors that can result from even slight inaccuracies in fluid property determination. The influence of heat flux parameter $(\dot{Q}D/k)$ on laminar flow correlations has been treated in some detail by MARTIN (105) and will be referred to again in discussion on the divergence tests (Section 9.2.6b) and radial temperature profiles (Section 9.2.7).

(b) Sudden Divergence

The data obtained at low Reynolds numbers downstream of a sudden divergence exhibited some complex characteristics. It will therefore be appropriate (and helpful in understanding the results) to describe briefly the manner in which flow development is likely to take place after the change of section. The model shown below is, in all probability, an oversimplification but will suffice for the purposes of the discussion to follow. It is similar to that used (with slight modifications) by McINTYRE (128) in a theoretical analysis for Newtonian fluids.

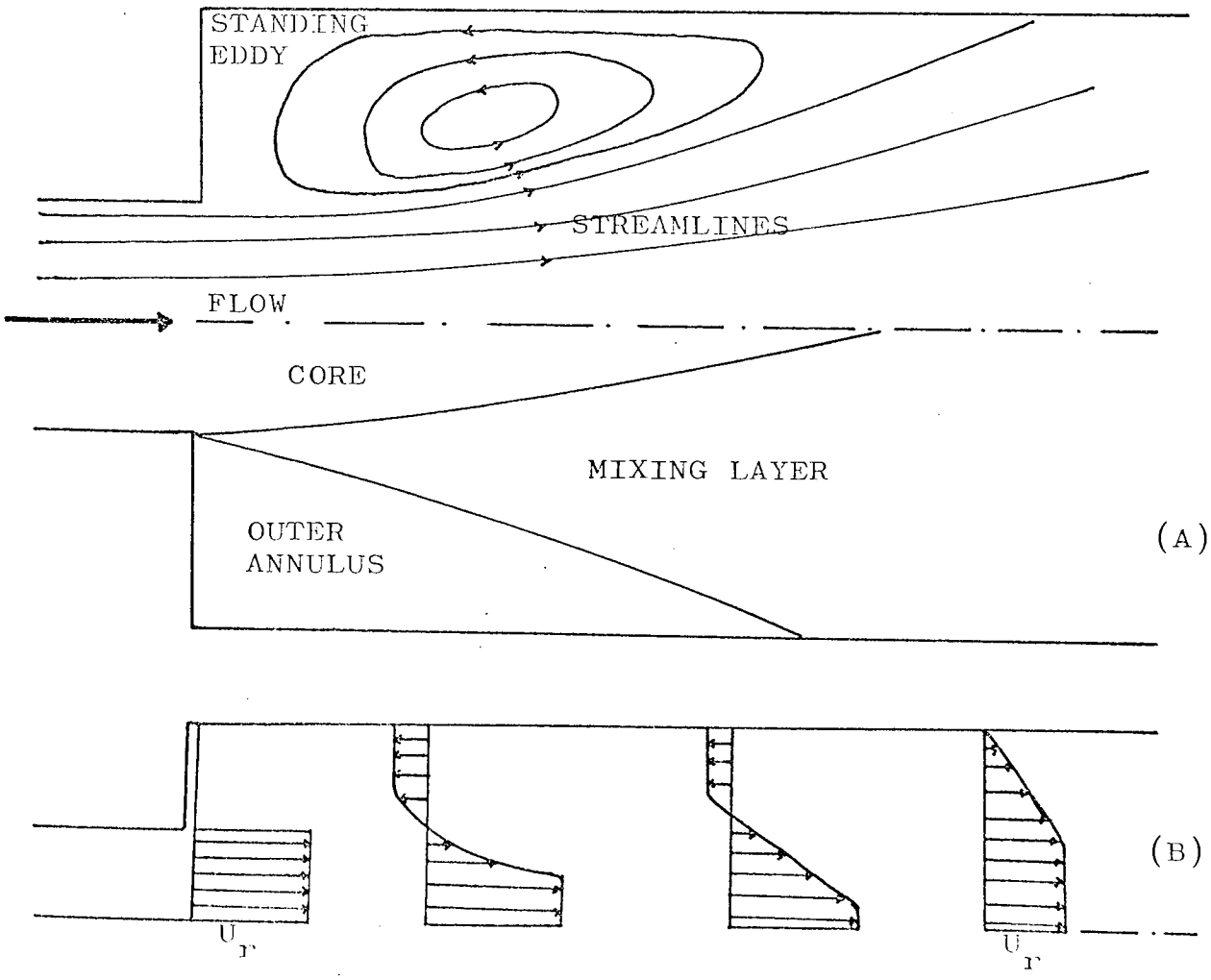

RADIAL VELOCITY PROFILE

The model (shown in sketches A and B) consists, at the entrance, of a fast moving inner core with a uniform velocity, separated by a mixing layer from an outer annulus of a slow recirculating fluid. The velocity profile of this annulus is also presumed uniform. Further downstream the velocity profiles "straighten out" as the momentum of the core fluid is dissipated in the mixing layer which becomes thicker. A standing eddy is seen to be present just downstream of a sudden divergence. When heat is applied to the situation described, the slow moving layer near the walls gets warmer than the fast central core. The consequent difference in fluid properties gives rise to buoyancy effects and the heavier core tends to fall to the bottom of the tube. Increasing the heat flux enhances this phenomenon and the flow instability due to this "bottoming" starts nearer to the change of section. With the flux constant, an increase in Reynolds number may trigger a localised turbulence in the core fluid. An increased heat transfer is obtained. The onset of this instability moves farther upstream with higher flow rates, until the condition in the leg preceding the divergence becomes turbulent and the violent mixing associated with such flow occurs at the entrance of the divergence.

Bearing the above simple but representative picture

in mind, the results of the divergence experiments will now be discussed. In Figs. 66 to 72, the axial distribution of the heat transfer coefficient is shown as plots of $Nu/Pr'^{\frac{1}{3}}\Delta^{\frac{1}{3}}$ vs Z_2/D_2 for different Reynolds numbers. The trend is, in general, similar to that obtained in previous Newtonian studies (55, 128). The significant features may be summarised as follows:

(i) A peak occurs in the Nu profile.

(ii) The position of this peak depends on the range of the upstream Reynolds number and to a lesser extent on the non-Newtonian nature of the flow.

(iii) Flow exhibits 'turbulent' characteristics near the area of maximum heat transfer.

(iv) Away from the position of the observed maximum, the heat transfer coefficient attains a value associated with a pipe with no discontinuity.

(v) Increase in pseudoplasticity (lower n) delays flow development and hence, enhances heat transfer near the change of section.

A detailed discussion of these and other aspects will now be given.

A common feature of the data obtained in the present investigations (both for the convergence and divergence configurations) is the tendency for the results to fall

into groups associated with three identifiable flow regimes: a laminar, a "pseudo transition", and a "pseudo turbulent" regime. The possible causes of this behaviour have already been discussed for the convergence geometry. For the divergence configuration, the state of flow in the downstream tube depends on conditions in the upstream leg. When flow is laminar upstream, a stable laminar regime can be maintained after the change of section ($Re_2' < 500$). As the flow rate is increased and a transitional condition obtained upstream, an unstable situation exists after the divergence. Flow may be laminar or "turbulent" in character ($500 < Re_2' < 1000$). When the flow upstream is turbulent, laminar conditions cannot be maintained in the downstream tube ($1000 < Re_2' < 2100$). Data from all the Carbopol concentrations fall into the laminar grouping while the 0.5% CMC and the Methocel results represent the "turbulent" flow regime. The 1% CMC data covers the "transitional" and "turbulent" regions of flow. As will be shown later, the above subdivisions are in no way rigid or precise but intended to give a general classification for the purposes of interpretation.

At very low Reynolds numbers downstream ($Re_2' < 50$), there may be more than one of the observed peak in the Nusselt number profile. This is the case in Fig. 68 where such low flow rates were obtained with 0.5%(w/w) Carbopol.

The first occurs at 2 diameters and the second anywhere between 5.5 to 13 diameters downstream. These locations depend on both the Reynolds number and wall heat flux. As mentioned at the beginning of the discussion, the buoyancy effect on the core of the fluid entering the divergent section is enchanced by heat flux while the onset of core instability is influenced by the upstream Reynolds number. The first small peak may therefore be associated with the position where the central layer touches the bottom wall of the tube due to buoyancy effects while the more prominent second peak reflects the onset of local turbulence. The maximum Nu is never greater than 4 times the terminal value at these low Reynolds numbers.

As the Reynolds number increases (> 50) but still less than 500, a turbulent-type peak is obtained at 3 or 4 diameters with a more rapid diminution as the distance downstream increases. The maximum Nu is 8 to 12 times the value far downstream (say 40 diameters). When the upstream flow is transitional or turbulent very high heat transfer rates are given just after the divergence downstream. The peak Nusselt number occuring at 2 or 3 diameters is on the average 15 times the limiting value. This falls very rapidly to only 5 times the terminal figure at 7 diameters.

In addition to the peak common to all the data discussed so far, Nu profiles obtained with Methocel (0.5% and 1.0% w/w) exhibited a definite but less well defined minimum usually at 10 diameters, but in a few cases anywhere between $11\frac{1}{2}$ to 15 diameters downstream. Only in one case was this minimum observed at 7 diameters. The downstream Reynolds number in this latter run was the lowest of the series, and would indicate that the location of minimum Nu moves further downstream as Reynolds number increases. However a comparison of Reynolds numbers corresponding to each of the minimum positions showed such dependence to be very weak, the position remained at 10 diameters at all $Re_{2'}$ between 1130 to 2900. It was observed on the other hand that reducing the heat flux tended to move the onset of this minimum Nu further downstream. The influence of heat flux was much stronger than that of Reynolds number, an increase of flux from 315 to 354 W/m^2 moved the position from 15 to 10 diameters upstream for the same downstream Reynolds number. In confirmation of the effect of heat flux, the free convection parameters (Gr_w/Re_w^2) and (Gr_w/Re_w) were found to be up to 20 to 25 times the maximum criterion stated in Section (9.1.9) at these locations. This was the same trend shown at the position of the peak Nusselt number, where (Gr_w/Re_w) and (Gr_w/Re_w^2) were about 2 and 10 times the critical values respectively in the extreme cases. Based on this information, an attempt was made to correlate the positions of

the maximum and minimum Nu with Gr_w/Re_w^2. As shown in Fig.73 no conclusive correlation between these parameters could be obtained. While excessive free convection is usually associated with increased heat transfer, the reverse seems to be the case at the minimum Nu position. This abnormal effect is illustrated in Fig.74. It was noted in Section (9.2.3) that other investigators have observed similar behaviour in straight pipe studies with non-Newtonian fluids. OLIVER and JENSON (138) also carried out a theoretical analysis of the effects of natural convection by proposing a "double layer" viscosity model. The assumption was made that the flow in each layer takes place as though the liquid of that layer filled the whole tube, thus a hypothetical "slip velocity" is always present between the layers. The authors predicted that when the flow rate in the viscous layer is one tenth of the total flow rate (for the case of a parallel plate), a reduction of heat transfer coefficient compared with a single fluid flow of 20% occured in the presence of slip. This reduced to 14% in the absence of slip. This model infact envisages a condition of increased apparent viscosity under wall conditions. While the present characterization (with respect to temperature) of Methocel showed that consistency variation with temperature was very small, this parameter nevertheless decreased rather than increased with temperature. However, it has been mentioned that the particular Methocel grade used here has a very low gelation temperature. It is therefore more than

likely that away from the tube entrance, as the tube wall gets hotter, the Methocel solution tends to gel in a thin layer very close to the wall of the tube. This layer will then have an "apparent viscosity" higher than the bulk and the condition proposed by the "two layer" theory for a reduction in heat transfer is satisfied. The radial temperature differences between tube wall and fluid bulk was estimated in some cases to be up to $14^{o}K$ at these positions of minimum Nu. This would support the above explanation and also the existence of pronounced natural convection. Another significant aspect of this phenomenon is that the data exhibiting it were all obtained under relatively high flow rates (transitional/turbulent flow upstream). This ties in with the results presented by OLIVER and JENSON. The "two-layer" effect on heat transfer was particularly noticeable as the flow rate was increased. This was so because the predicted reduction in heat transfer was shown to depend both on the viscosity ratio and the angular extent of the high viscosity layer. The latter parameter is a function of flow rate. Since the reversed influence of free convection just described was only noticed for one polymer and only in the divergence tests, it is reasonable to assume that the molecular structure of this particular material and to a lesser extent the tube configuration accentuates this phenomenon. Present data is not sufficient to warrant any further correlation.

The position of the peak Nusselt number has been shown to depend on the Reynolds number. This is illustrated graphically in Fig.75 where the possible influence of pseudoplasticity is also indicated. Increasing the Reynolds number tends to shift the peak location upstream. There is however, considerable scatter below $Re_2' \leq 50$ indicating the significant effect of heat flux. At $Re_2' > 1000$, the maximum position remains unchanged at 2 to 3 diameters irrespective of further increases in Reynolds number and heat flux. The influence of 'n' is seen to be only significant at $Re_2' < 100$. Increasing pseudoplasticity would seem to move the maximum position farther upstream. It is not possible, from the present data, to separate the effects of 'n' and heat flux. It is more than likely that since a lower n corresponds to a higher viscosity (and hence Pr_2') the influence of heat flux is more pronounced in these cases. The comparative Prandtl numbers for the indices shown in Fig.75 are approximately as follows:

n	0.46	0.63	0.7	0.82	0.9
Pr_2'	3000	1000	500	400	55

As with the location, the value of the maximum heat transfer coefficient was dependent on the upstream Reynolds number (Re_1'). In order to obtain a quantitative relationship, $Nu_{max}/Pr'^{\frac{1}{3}} \Delta^{\frac{1}{3}} M^{0.4}$ was plotted against Re_1' for each of the polymer solutions tested. This is given

in Figs. 76 to 81. In each case the "best line" was drawn by a"least squares regression". The functional relationship may be expressed for each polymer concentration as follows:

Fluid	n Average	$f(Re_1')$
0.15% CPM	0.67	$0.00009\ Re_1'^{1.67}$
0.25% CPM	0.63	$0.0004\ Re_1'^{1.50}$
0.5% CPM	0.46	$0.035\ Re_1'^{0.69}$
0.5% and 1% MC	0.93	$0.00005\ Re_1'^{1.65}$
0.5% CMC	0.9	$0.0177\ Re_1'^{0.96}$
1.0% CMC	0.82	$0.109\ Re_1'^{0.72}$

The Methocel data were correlated together since the 1% tests were undertaken just to check the peculiar behaviour noted in earlier tests with 0.5% MC. The best correlation was given by 0.5% CMC where over 96% of all the data was represented by the given function to within $\pm$ 8%. The worst was with 1.0% CMC where some points deviated from the given line by up to 400%. In all other cases 80 to 90% of the data were fitted by the given expressions with maximum deviations ranging from $\pm$ 5% to $\pm$ 20%. A closer examination of the 1% CMC and 0.15% CPM data showed why the deviations were so large with these two solutions. It also indicated why the Reynolds number - function varied so much between the polymers and concentrations.

In Figs. 76 and 81, the disposition of the points suggests that two separate "best lines" may be drawn, one for $Re_1' > 1000$ and the other for $Re_1' < 1000$. To get a more precise range of the critical Reynolds number, all the data were plotted on one graph in Fig. 82. Three distinct flow regimes, as proposed earlier were conclusively indicated. A transitional range is seen to exist between Re_1 500 and 2000. A final correlation was obtained as follows:

$Re_1' > 1000$

$$Nu_{max}/Pr'^{\frac{1}{3}} \triangle^{\frac{1}{3}}M^{0.14} = 0.028\ Re_1'^{0.9} \qquad (240)$$

$Re_1' < 1000$

$$Nu_{max}/Pr'^{\frac{1}{3}} \triangle^{\frac{1}{3}}M^{0.14} = 0.046\ Re_1'^{0.64} \qquad (241)$$

For $Re_1' > 1000$, 94% of the data was correlated by equation (240). The maximum deviations were obtained in the range $700 < Re_1' < 2000$ as expected. This amounted in one case to -77%. In the range $Re_1' > 2000$ the maximum deviations are of the order of $\pm$ 29%. At the lower Re_1 range (< 700), over 95% of the data is well fitted by equation (241). The maximum deviation is $\pm$ 23% except for some data in the transitional band which are underpredicted by about -35% to 65%.

The effect of the pseudoplastic index 'n' on flow development is shown in Fig. 83. Increasing pseudoplasticity delays flow development. This is to be expected in view of the stubbier velocity profiles associated with non-Newtonian fluids.

The influence of the index 'n' on heat transfer rates is illustrated in Figs 84 to 86. It is seen in Fig. 84, that despite the very high Prandtl number of the most non-Newtonian fluid tested (average n = 0.48), increased heat to transfer is obtained relative to the less non-Newtonian (and hence less viscous) fluids. The delayed flow development shown in Fig. 83 is obviously the dominant factor enhancing heat transport at these low Reynolds numbers. In Figs. 85 and 86 Newtonian and non-Newtonian heat transfer rates are compared. The same trend as seen in Fig. 84 is confirmed. However, for $Re_2' > 500$, when the upstream flow is transitional, the bi-stable situation downstream can cause higher or lower heat transfer near the entrance of the divergent section. The non-Newtonian peaks may therefore be higher or lower than the Newtonian ones as the case may be. Further downstream, slight improvement as a result of pseudoplasticity is indicated.

The effect of heat flux isshown in Fig. 87. These data were obtained with 1% CMC. As with the convergence tests, increase in heat flux is seen to improve the heat

transfer rate at low Reynolds numbers. However, the observed increase is only a small fraction of the ratio of the fluxes used - a 400% increase in flux results in a 50% increase in heat rate. At higher Reynolds numbers (> 1000), raising the heat flux tends to reduce the heat transfer coefficient away from the entrance. This effect is only marginal and it may be concluded that at high flow rates, heat flux has no significant influence on the absolute value of the heat transfer coefficient.

9.2.7 Radial Temperature Profiles

In Fig. 88 the reliability of the traversing equipment is reflected in the good agreement between turbulent flow (water) data and the profile valuated by the "Martinelli Analogy" for uniform heat flux given in most standard texts (92, 127). Fig . 89 compares experimental profiles obtained at 3 and 40 diameters downstream with water. At 3 diameters the profile is seen to be almost flat except very near the wall where all the heat transfer takes place. This location was chosen for investigation because the main heat transfer tests reported in Section (9.2.6) showed the maximum heat transfer coefficient to occur at or near this region. However, because of the fittings used to mount the traversing gear, it was difficult to ascertain whether the marginal reduction in tube wall temperature noted at this position (for the conditions shown in Fig.89) was due to axial

conduction or the expected separated flow reattachment. At 40 diameters the profile is shown to be approaching a fully developed shape as the thermal boundary layer thickens, but is still substantially far from parabolic. In Fig. 90 (A and B) the effect of heat flux is indicated. No significant change in profile shape is noted at 3 diameters. At 40 diameters, increase in flux tends to thicken the thermal boundary layer. At a low heat flux, even for such considerable distances away from the entrance, the fluid core temperature is still flat and extends up to 70% of the tube radius.

Regarding the symmetry of the observed temperature distribution, it was not possible with the present instrumentation to explore the full tube bore - especially since the tube used in these tests was of a relatively large diameter. However, the tube wall temperature at 40 diameters showed no significant stratification between the top and the bottom of the tube. It is therefore reasonable to assume vertical symmetry at this position and under turbulent conditions. No such symmetrical re-attachment of separated flow can be expected at positions near the change of section for low Reynolds numbers. This is confirmed by data from the non-Newtonian tests now to be discussed.

Data from tests with 0.25%(w/w) Carbopol are given in Figs. 91 to 96. In general, at 40 diameters the profiles are similar to those observed with water except that the "plug" radius extends over a wider portion of the tube. This is not surprising since the latter tests were conducted at much smaller Reynolds numbers and for very high fluid consistencies. As with the main heat transfer data, the non-Newtonian radial traversing results show strong dependence on upstream conditions especially near the discontinuity. Also the effect of heat flux is quite marked in this region. In Figs. 91 and 92 the radial profiles at 3 and 40 diameters have been shown for $\dot{Q}R/k$ of 102 and 46 respectively. The upstream Reynolds number is in each case, the same and transitional. At 40 diameters, the influence of heat flux is only slight. On the other hand at 3 diameters, the effect of flux is substantial. A flat profile extending up to 90% of the tube radius is obtained with low heat flux. At the higher heat flux the data confirm the existence of layers of fluid having different viscosities. This substantiates the flow pattern postulated in Section (9.2.6b) in which a faster but colder central core fluid is separated by a mixing layer from an annulus of recirculating standing eddy. Figs. 93 and 94 show this behaviour to be much pronounced at still lower Reynolds numbers ($Re_2' < 50$). The wall - to - centre line temperature differences under the conditions shown in Figs. 93 and 94 were 3.2°K and 2.8°K

respectively at 3 diameters, and 5.15°K and 4.88°K respectively at 40 diameters. The differences between the fluid layers at say $\xi = 0.2$ and $\xi = 0.7$ were 2.1°K at $Re_2' = 30$ and 2.7°K at $Re_2' = 18$ respectively, at Z/D = 3. It is considered that measurement errors of this magnitude could easily have been detected. To ensure that the observed profiles were not the result of fluctuations in inlet fluid temperature, the tube was traversed both in the downward (wall - to - centre) and the upward (centre - to - wall) directions for a given flow condition. Reproducible results were obtained.

In one of the earlier experimental studies mentioned HOBSON (180) measured temperature profiles in the core of an annulus with 1% Carbopol solutions. He noted that while normal stable laminar profiles were obtained at low wall heat fluxes, definite signs of instability were exhibited quite close to the core wall as the wall temperature increased. This was reflected in temperature fluctuations the amplitude and band width of which increased with the wall heat flux (or temperature). These temperature fluctuations were attributed to transient bulk eddy motion. For the flow situation encountered in the present tests, Newtonian analysis of heat transfer in separated flow (53) indicates that, between the core of the fluid and the recirculating zone energy is transferred through the separating "free-shear" layer not only by

conduction but also as mechanical work produced by the shear stresses acting at the dividing streamline. This energy flux is usually small compared to the heat transfer by conduction as long as the velocity outside the shear layer is small. For high velocity flow, a situation may arise where the temperature in the separated region is larger than the temperature in the mainstream provided no heat is removed from the solid walls. The case of a viscous Newtonian fluid with uniform wall flux has been computed numerically by McINTYRE (128). The divergence ratio was 1 : 2 and the temperature distribution is shown as closed isotherms of the different values in the circulating zone just after the divergence. The Prandtl number of the non-Newtonian solution (0.25% CPM) tested here ranged from 1372 to 1848. It is therefore reasonable to surmise that considerable viscous energy is generated in the shear layer with a consequent increase in local fluid temperature. It was not possible to distinguish the 'viscous heat' contribution to the large heat transfer rates observed at positions near the abrupt expansion from the predominant buoyancy effects. This was because in terms of the wall - to - bulk temperature differences, this shear contribution is, as noted above, usually very small. It can therefore be concluded from the above observations that while the temperature profiles for $Z_2/D_2 = 3$ shown in Figs. 93 and 94 may not occur with the less viscous Newtonian fluids (water) even at the high flow rates

indicated (Fig.89), the combination of heat flux effect and the shear - strain relationships of viscous non-Newtonian fluids promote the observed radial temperature distribution at relatively low flow rates.

Another significant aspect of the small Reynolds number data is that while at low $\dot{Q}R/k$ the flat profile extends to about $\xi = 0.9$ for $Re_2' = 62$ ($Re_1' = 1000$), it only extends to $\xi = 0.2$ for $Re_2' = 30$ ($Re_1' = 497$). The inference is that the size of the standing eddy is reduced by increasing Reynolds number as expected.

In Figs. 95 and 96, the effect of tube orientation is indicated. The data confirm that in the absence of severe free convection and far away from the change of section ($Z_2/D_2 \geq 40$) the radial temperature profile is symmetrical. This appears also to be the case at $Z_2/D_2 = 3$ when the upstream Reynolds number is transitional and the effect of heat flux is only small. However for laminar stable conditions upstream and downstream, asymmetrical reattachment is indicated in the region near the sudden expansion. This is to be expected since the 'buoyancy' effect noted in Section (9.2.6b) is the predominating factor under these conditions.

9.3 POSSIBLE METHODS OF APPLICATION OF RESULTS

9.3.1 Sudden Convergence

The flow of non-Newtonian fluids including slurries, from a larger tube or chamber up to and through the entrance-flow region of a smaller tube of circular crosssection with energy transfer to or from the walls of the smaller tube, is of importance in the design of such equipment as heat exchangers, chemical reactors, and nuclear reactors.

For a 3 to 1 contraction local values of heat transfer coefficient, h, can be derived from Figs. 44 - 48 for non-Newtonian indices ranging from 0.54 to 0.91. It will be necessary to interpolate the data so that plots of $(Nu/Pr'^{\frac{1}{3}} \triangle^{\frac{1}{3}})$ vs. (axial distance) can be determined for other 'n'. However for this configuration it is recommended that equations (237) and (238) be used to avoid laborious interpolation, since for any particular 'n' and axial location, values of Nu (or h) can easily be evaluated from existing theories for straight pipes (equation (118)).

It is often more convenient for designers to think in terms of an "effective increase in tube length", which is defined as

$$L_{eff} = \int_0^L \left(\frac{Nu_z}{Nu_\infty} - 1\right) dz$$

where Nu_∞ is the value of Nu at large axial distances and L is the tube length. The integral is easily evaluated numerically. For example, at $Re_2' = 300$, the additional length required is 1 diameter for n = 0.60 and 3.5 diameters for n = 0.91. These data indicate that where it is desired to avoid large local increases in heat transfer rates, a more non-Newtonian fluid may be used with a contraction in the tube geometry and at very low flow rates. At the higher Reynolds numbers on the other hand, the enhanced heat transfer obtained with non-Newtonian fluids amounts to an extra 4.6 diameters at $Re_2' = 1160$ for n = 0.55 and 2.9 diameters for n = 0.91 at the same Re_2'. In some applications, average heat transfer coefficientsare more instructive. In such cases, the mean values may be evaluated from

$$h_m = \frac{1}{L} \int_0^L h_z \, dz.$$

The integration can be done numerically with present experimental data or analytically using equations (237) and (238).

In all the above applications, the influence of heat flux has been neglected. This may be justified at Reynolds numbers greater than 1000, but for lower flow rates, the heat flux effect must be borne in mind.

9.3.2 Sudden Divergence

Although designs employing specifically sudden divergences in channel section may be of less frequent occurence, such configurations are likely to be used in conjunction with other geometries for cooling passages in machinery and extrusion of polymers.

In the higher Reynolds number range $1000 < Re_2' < 2100$ flow downstream of a 1 : 3 divergence has been shown to exhibit turbulent characteristics. Plots of $Nu/Pr'^{\frac{1}{3}} \Delta^{\frac{1}{3}}$ against axial distance given in Figs. 66 - 72 represent unique functions. Local values of h can be derived from these graphs. It will, of course, be necessary to interpolate present data to get axial distib-ution of h for other n between 0.5 and 0.9 not specifically presented. If on the other hand mean values (h_m) or effective increase in lengths are required, the procedures suggested in Section (9.3.1) can be used.

For lower Reynolds numbers, the h versus axial distance relationship becomes a complex function of upstream conditions and wall heat flux. In the range $500 < Re_2' < 1000$ the flow can be turbulent or laminar downstream and both the magnitude and position of the peak heat transfer coefficient may be difficult to predict or

reproduce. For $Re_2' < 500$, heat flux may substantially influence the value and disposition of the peak Nu. It is therefore necessary to specify in detail the design criteria for any equipment handling non-Newtonian fluids at very low Reynolds numbers. Present data can then be interpolated to satisfy the particular conditions required.

CHAPTER TEN

COMPARISON OF RESULTS WITH PREVIOUS WORKS AND THEORY

10.1 NEWTONIAN DATA

10.1.1 Sudden Convergence

Turbulent tests were conducted with water primarily to provide data for comparison with established works, thus proving the adequacy of the equipment. The results have been presented in Fig.97 for three Reynolds numbers and compared with data interpolated from graphical correlations published by the Engineering Sciences Data Unit (208) (for $Re = 30 \times 10^3$ and 50×10^3). There was good agreement. The Reynolds numbers of rest of the water tests were very nearly the same as those shown and the results have been omitted for the sake of clarity.

The work of McINTYRE (128) provided data which were directly comparable to the present glycol results since the former investigation was carried out on the same "heat transfer section" as used here. In the first instance, flow development downstream of a 3.3 : 1 sudden convergence

has been compared in Fig.98. The local to fully developed Nusselt number ratios were evaluated after both sets of data had been corrected for variable viscosity and free convection effects. No interpolation of either data was necessary since the slight differences in the Reynolds and Prandtl numbers were not considered to have any significant effect on the nature of the flow development. Agreement at all Reynolds numbers, ranging from laminar to turbulent was good. Discrepancies near the change of section amounted to $\pm$ 5%. In Fig.99 the heat transfer rates are compared for a wide range of Reynolds numbers. Interpolation of present data was necessary for the transitional-flow data comparison. Away from the entrance, excellent agreement was obtained in all cases. Near the change of diameter, slight discrepancies ($\pm$ 2%) occur. As already observed, measurements obtained at locations very close to the contraction were unreliable due to axial heat conduction and possible separated flow effects.

The recent correlations of MARTIN (105) offer the only other source of comparable work on viscous fluids. The correlations were obtained with data from tests conducted on a pipe following a 6 : 1 contraction. In this case, however, the contraction was from a large reservoir to a smaller diameter pipe. The correlation for $Gz > 27$ is given in equation (94). In Fig.100, the present experimental Nusselt number ratio ($Nu_z/Nu_{f.d}$)

has been compared with values calculated from equation (94) at various axial locations. Good agreement is obtained away from the change of tube diameter. In the region near the contraction, Martin's correlation overpredicts present data by about 13.5%. This reflects the differences in the upstream configuration used in these two tests. With Martin's set up, flow development most probably began just inside the smaller tube whereas for the present geometry, flow development has been shown (32) to begin at 1 or 2 diameters upstream at low Reynolds numbers. Present data confirm this pattern of flow development.

10.1.2 Sudden Divergence

As with the convergence geometry, McINTYRE'S (128) investigations provided the major source of comparable data. In Fig.101, the axial distribution of the local to fully developed Nusselt number ratios are compared. The respective Prandtl numbers were 55 for McIntryre's and 72 for the present data. Here again no interpolation with respect to Prandtl number was considered necessary. When the flow in upstream tube was purely laminar or fully turbulent, good agreement was obtained between the data. However, for transitional upstream flow, large differences in the value and position of the peak Nu may occur due to the bi-stable flow situation which obtains downstream. This behaviour has already been discussed and the observed discrepancy is attributed to this

effect. At large distances away from the entrance, the agreement becomes very good as expected.

10.2 NON-NEWTONIAN DATA

10.2.1 Laminar Fully Developed Heat Transfer

In Section (9.1.9) a Nu - Gz correlation of fully developed laminar flow data was given in justification of the parameters used in presenting the results of the present investigation. In Fig.102 data from other published works (theoretical, numerical and experimental) have been included for comparison. By plotting $Nu/\Delta\ ^{\frac{1}{3}}M^{0.14}$ as the ordinate, present Newtonian data has been compared directly as well. Excellent agreement is obtained in all cases.

10.2.2 Sudden Convergence and Divergence

No previous theoretical or experimental works which could definitively be compared with present disturbed flow data are known to this author. The inadequacy of existing "gradual entrance" laminar heat transfer theory in predicting contracted flow data has already been discussed. The point is emphasized in Fig.100 where data from 1% CMC is compared with theory given by BIRD (11).

For the divergence configuration, the maximum Nusselt numbers have been correlated against upstream Reynolds

numbers for Newtonian fluids; air (204) and propylene glycol (128). Although no rigorous comparison is intended since as indicated in Figs. 76 to 82, different correlations are obtainable depending on the Reynolds number range and to a lesser extent on the flow behaviour index 'n', as a matter of interest the various expressions are shown graphically in Fig. 103. The present correlation is as obtained for $Re_1 > 1000$. ZEMANICK et al (204) operated at very high Re_1 (4000 to 90000) while McINTYRE'S data (128) covered the range $2500 < Re_1 < 20000$. The deviation of present non-Newtonian correlation from the Newtonian lines amount to $\pm$ 40% at $Re_1 = 1000$. For $Re_1 = 4500$ the present expression yields the same Nu value as Zemanick's but still deviates from McIntyre's by - 40%.

10.3 RADIAL TEMPERATURE PROFILES

The turbulent flow Newtonian data has already been compared with the "Martinelli Analogy" in Fig.88. For the non-Newtonian tests, the experimental data for Gz = 2245 and n = 0.56 is given in Fig.104 and compared with present theoretical evaluations given by equation (209a). The eigenvalues and functions used were the same as published by BIRD (11) for n = 0.5. These have been listed in Table 23 (Appendix 3). It is seen that the theory grossly over-predicts present experimental results. This is not really surprising since the theory was derived on the assumption of a fully developed parabolic velocity at the start of

heating and is therefore strictly valid for small Gz, in other words, larger distances (>> 40 diameters) away from the divergent section.

In Chapter 4, Section (4.2.3) expressions for radial temperature profiles originally given by CHARM (27) and modified by SKELLAND (177) were reviewed in some detail. These specifically referred to fully developed conditions both "thermal" and "hydrodynamic". Since the present experimental data at Z /D = 40 are far from parabolic (symbolising full thermal development) no meaningful comparison between equation (161) and current results can be made. The results of the present tests indicate that expressions of the type given for Newtonian fluids by MARTIN (105) in equation (78) will be needed to give realistic non-Newtonian radial temperature profiles. This is because equation (78) considers the temperature distribution in two sections, one within the plug radius, $0 \leq \beta \leq y$, and the other outside the plug region, $\beta \leq y \leq 1$.

The general agreement between the experimental data and expected flow behaviour after a sudden expansion validate the procedures used to estimate temperatures throughout this investigation.

CHAPTER ELEVEN

CONCLUSIONS AND FUTURE WORK

11.1 CONCLUSIONS

11.1.1 Non-Newtonian Fluid Properties

(a) The pseudoplastic rheological properties of Carbopol 934 (up to 0.5% w/w), Methocel 60HG (up to 2% w/w) and Sodium Carboxymethyl cellulose (up to 1% w/w) have been shown to obey the power law

$$\tau = K_N(\dot{\gamma})^n \qquad (4)$$

within the shear rate 15 to 1200 second^{-1}. Over this range, the index 'n' remains constant for a particular concentration. Values of n and K_N considered varied between 0.39 to 0.96 and 0.0041 to 12.0 NS^n/m^2 respectively.

(b) The temperature dependence of consistency index K_N in the range 20°C to 60°C may reasonably be expressed as

$$K_N = Ae^{B/T} \qquad (232)$$

where T is in absolute units and B is positive. For the concentrations used here, B is practically independent of concentrations, especially for Methocel and CMC. There is a marginal increment in B with Carbopol solution strength. The effect of temperature on K_N is consequently not greatly influenced by concentration.

(c) The assumption of constant 'n' with respect to temperature is valid for any theoretical analysis. Such studies are also simplified by the independence of B on polymer concentration, when non-isothermal effects are considered.

11.1.2 Sudden Convergence

(a) Local heat transfer coefficients beyond a sudden contraction in tube diameter are generally higher than the fully developed values.

(b) The coefficient decreases as the axial distance increases downstream of the convergence.

(c) The rate of decrement of h (or Nu) with distance increases with Reynolds number.

(d) The rate of decrement of h (or Nu) with distance is accelerated as non-Newtonian index 'n' increases.

(e) Heat transfer is enhanced or suppressed by increased pseudoplasticity depending on Reynolds number.

For Re_2' < 500 a partially developed velocity profile tends to yield lower heat transfer coefficients as the non-Newtonian index 'n' decreases. For Re_2' > 500, the entrance vortex effect is overcome and marginal improvement due to increased pseudoplasticity is obtained.

(f) Laminar flow theory assuming a uniform velocity profile at the entrance of a tube grossly overpredicts contracted flow non-Newtonian heat transfer for Reynolds numbers less than 2000.

(g) The degree of overprediction noted in (f) is only weakly dependent on the flow behaviour index 'n' when this parameter is less than 0.9.

(h) Correlation of the data in the form of $\frac{Nu(\text{gradual entry theory})}{Nu(\text{contracted flow expt.})}$ versus axial distance from the contraction gives a reasonably close clustering of the data for the 3.3 : 1 geometry tested and for Re_2' > 1000. For lower Reynolds numbers similar clustering is observed except when n is greater than 0.9 (which is nearly the Newtonian case). Greater dependence on the value of n is also indicated at lower Re_2' (< 1000).

(i) Non-Newtonian heat transfer coefficient downstream of a 3.3 : 1 sudden contraction may, with reasonable accuracy be predicted by the expression

$$Nu_Z = 1.413(Re' Pr'/(Z/D))^{\frac{1}{3}} \Delta^{\frac{1}{3}} M^{0.14}\left(1 + \frac{A}{(Z/D)}C\right)^{-1} \qquad (239)$$

where all parameters refer to the downstream tube section. 'C' equals, 0.5 and 'A' is 3.0 or 3.85 for Re' greater than, and less than, 1000 respectively.

(j) Secondary effects such as free convection, and viscous heat generation have little significance with respect to the heat transfer rates obtained with the polymer concentrations tested here. The experimental conditions were chosen to minimize free convection, while the frictional heat appears to have been mostly dissipated between the mixing (and storage) tank and the heated test section.

(k) The effect of heat flux on present convergence data is considered only marginal. However, the dependence of the Nu - Gz correlation on this parameter ($\dot{Q}R/k$) cannot be altogether discounted in laminar flow, especially when the heat transfer medium exhibits high temperature dependent viscosity.

11.1.3 Sudden Divergence

(a) Fully developed laminar heat transfer away from the abrupt expansion is well correlated by existing theory given for straight pipes as

$$Nu = 1.413\ Gz^{\frac{1}{3}}\ \Delta^{\frac{1}{3}} \qquad (118)$$

in the absence of natural convection effects, and by

$$Nu = 1.413 Gz^{\frac{1}{3}} \Delta^{\frac{1}{3}} \left[Gz_b + 0.0083 (Gr_w Pr_w)^{0.75} \right]^{\frac{1}{3}} \tag{91a}$$

in the presence of natural convection. For more temperature dependent rheological properties than employed here, a more realistic correction for viscosity variation with temperature will be given by the MIZUSHINA (126) expression

$$Nu = 1.413 Gz^{\frac{1}{3}} \Delta^{\frac{1}{3}} \left(\frac{K_{Nb}}{K_{Nw}} \right)^{C/n^{0.7}} \tag{120}$$

where

$$C = 0.045 (1.413 Gz^{\frac{1}{3}} \Delta^{\frac{1}{3}})^{0.7} \tag{121}$$

(b) The flow beyond the change of section shows a considerable enhancement (over the fully developed value) of the local heat transfer coefficient in the separated flow region.

(c) The degree of heat transfer coefficient enhancement, both maximum and average, increases strongly as the pseudoplasticity of the fluid increases. This is usually attributed to delayed flow development due to "stubbier" velocity profiles obtained with the non-Newtonian fluids.

(d) The location of maximum heat transfer, usually associated with the end of the separated flow region, is

a function of Reynolds number and to a lesser extent heat flux. The function (w.r.t. Re') is strong when $Re_2' < 1000$, increase in Re_2', moves the position upstream. For $Re_2' > 1000$ the maximum Nu position is independent of this parameter. Heat flux becomes significant at $Re_2' < 500$ when due to buoyancy effects, increasing the flux moves the position further upstream.

(e) At higher Reynolds numbers ($Re_2' > 500$) heat transfer coefficients downstream of a sudden divergence can be uniquely represented by plots of $Nu/Pr^{\frac{1}{3}} \Delta^{\frac{1}{3}}$ versus axial distance for specific Re'. For $Re_2' < 500$ the profile is a complex function of upstream Reynolds number and heat flux. This complexity arises as a result of the bi-stable flow condition downstream when the upstream Reynolds number is neither truly laminar nor turbulent.

(f) The peak Nusselt number exhibits a definite dependence on both the upstream Reynolds number and non-Newtonian index 'n'. The equations that reasonably represent the maximum Nusselt number data of all the polymers and concentrations tested are

$$Nu_{max}/Pr'^{\frac{1}{3}} \Delta^{\frac{1}{3}} = 0.028 Re_1'^{0.9} \qquad (240)$$

for $Re_1' > 1000$

$$Nu_{max}/Pr'^{\frac{1}{3}} \Delta^{\frac{1}{3}} = 0.046\ Re_1'^{0.64} \qquad (241)$$

for $Re_1' < 1000$

(g) With Methocel solutions, and in the transitional flow regime ($Re_{2}' > 1000$) a definite but less sharply defined minimum occurs in the heat transfer coefficient versus axial distance profile. The location is usually at 10 diameters downstream of the change of section although increasing the heat flux appears to move it further upstream at a lower Reynolds number. This behaviour is attributable to the presence of layers of different viscosity fluid in the pipe, with the higher viscosity layer nearer the hot tube wall. In this case, the tendency for methocel to 'gel' at low temperatures produces a film near the wall with an "apparent viscosity" greater than the bulk of the fluid. Reduced heat transfer results from this abnormal condition.

(h) At high flow rates wall heat flux has no significant influence on the absolute values of the heat transfer coefficient. Improved heat transfer rates are obtained at low Reynolds numbers with higher fluxes. However, the increases are usually only a small fraction of the ratio of the fluxes used to obtain them.

11.1.4 Radial Temperature Profiles

(a) Under laminar and even turbulent flow conditions, the centre-line fluid temperature is well approximated by the inlet bulk value at axial distances $\leqslant$ 40 diameters from the start of heating.

(b) For water, under turbulent conditions a flat profile extends up to 90% of the tube radius at distances near the change of section. Further away from the start of heating ($Z_2/D_2 \geq 40$) the profile approaches a parabolic shape. The rate of thermal development is increased by increasing wall flux.

(c) For non-Newtonian viscous fluids, there is conclusive evidence of layers of fluid of different viscosities at sections following a tube expansion. This is enhanced by the shear action in the stagnant, recirculating zone separating the main bulk of the fluid and the wall. Temperatures in the eddy layer become warmer than the centre-line bulk. The extent of this effect is influenced both by Reynolds number and heat flux. A higher flow rate suppresses the effect by reducing the size of the standing eddy while increasing the wall temperature enhances the recirculatory effect thus creating a suitable condition for the occurrence of the observed phenomenon.

(d) In the region of separated flow, boundary layer reattachment is generally asymmetrical particularly at low Reynolds numbers when the free convection or buoyancy effects are most significant. Away from the entrance, in the absence of severe free convection,

symmetrical temperature profiles are obtained.

11.2 RECOMMENDATIONS FOR FUTURE WORK

The results of the convergence tests strongly suggest that future efforts should be directed towards a better understanding of the flow mechanism just before and just after a sudden contraction at very low flow rates. Initially detailed velocity profile studies should be undertaken for various contraction ratios using transparent tube sections on both sides of the contraction. No heating is of course possible with this arrangement. The next step will be to use a combination of say, a transparent (acrylic) tube upstream and a stainless steel tube downstream. The downstream tube can then be heated. Such studies should employ photographic or interferometric ("Laser Dopler") techniques to avoid the inevitable disturbance of vital flow pattern encountered with pitot tubes and static wall taps. The investigation may then be extended to temperature traversing at similar locations used for the velocity profile measurements.

In the present studies, the non-Newtonian solutions were seriously degraded by the circulating pump despite considerable design modifications directed at minimizing this effect. It is suggested that in future, methods avoiding the use of conventional pumps be strongly

considered. Examples are blow cases and compressed air pumps.

With present and previous knowledge of the behaviour of water-based polymeric pseudoplastic fluids with respect to temperature, and the results of the velocity and temperature profile studies herein suggested, it may be possible to formulate theoretical expressions for contracted flow heat transfer. Such analysis may be meaningfully directed, in the manner indicated by present correlation of convergence test data, to using upstream conditions to predict downstream heat transfer for arbitrary contraction ratios and non-Newtonian indices.

The observed "reversed" free convection effects of Methocel divergence tests should be investigated in greater detail. The location of this maximum wall temperature can then be correlated with the flow parameters, the rheological constants and heat flux. It will also be instructive to correlate the radial temperature difference estimated at these locations with the above parameters. It is suggested that other molecular grades of Methocel, and higher concentrations of Carbopol and CMC be used to give some insight into the nature of the dependence of this instability phenomenon on non-Newtonian molecular properties.

REFERENCES

1. AKINS,R.G., DRANOFF,J.S., A.I.Ch.E.J., 9 625, 1963
2. ALAD'EV,I.T., Bull.Acad.Sc. U.R.S.S., 11, 1669, 1951
3. ALLEN,R.W., ECKERT,E.R.G., Trans. A.S.M.E. Paper No.63 - HT - 37, 1963.
4. ALVES, G., BOUCHER, D.F., PICFORD,R.G., C.E.P. 48 (No.8), 385, 1952.
5. ASTARITA, G., GRECO, G., Ind.Eng.Chem.Fundamentals. 7, 27, 1968.
6. BEEK, W.J., EGGINK, R., De.Ing., 7, 81, 1962.
7. BERGLES, A.E., ROHSENOW, W.M., Trans. A.S.M.E., C84, 268, 1962.
8. BERNHARDT, E.C., "Processing of Thermoplastic Materials" Chapter by Metzner A.B., "Flow Behaviour of Thermoplastics" pp48, 62, Reinhold, (New York), 1959.
9. BINGHAM, F., GREEN, G., Proc. A.S.T.M., 21, 1154, 1921.
10. BIRD, R.B., Soc.Plastic Engrs.J., 35, 1955.
11. BIRD, R.B., Chem-Ing.Tech., 31, 569, 1959.
12. BIRD, R.B., TURIAN, R., Ch.E.Sci. 17, 331, 1962.
13. BOGGS, J.H., SIBBIT, kl.L., Ind.Eng.Chem. 47 (No.2) 289, 1955.
14. BOGUE, D.C., Ind.Eng.Chem., 51, 874, 1959.
15. BOGUE, D.C., METZNER, A.B., Ind.Eng.Chem. (Fundamental) 2, 143, 1963.
16. BOELTER, L.M.K., YOUNG, G., IVERSEN, H.W., National Advistory Committee for Aeronautics T.N. 1451, 1948.

17. BOELTER, L.M.K., MARTINELLI, R.C., JONASSEN, F., Trans.A.S.M.E. 63, 447, 1941.

18. BONILLA, C.F., CERVI, A., COLVEN, T.J., WANG, S.J., Chem.Eng.Progr.Sympossium Ser. No.5, 49, 127, 1953.

19. BOUSSINESQ, J., Theorie Mathematique de la Chafeur, Bachelier (Paris) 1835.

20. BOWEN, R.L., Chem. Eng. 68, 119, 1961.

21. BRINKMAN, H.G., Appl.Sci.Res. A2, 120, 1951.

22. BROWN, G.M., A.I.Ch.E.J., 6 179, 1960.

23. BURROWS, S., PETERLIN, A., TURNER, D.T., Polymer Letters 2, 67, 1964.

24. BUTTERWORTH, D., HAZELL, T.D., "Fourth International Heat Transfer Conference", Paris FC 3.1, 1970.

25. CAMPBELL, W.D., SLATTERY, J.C., Trans.A.S.M.E. (J.Basic Eng.), 85, 41, 1963.

26. CHARM, S.E., Sc.D. Thesis, M.I.T.(U.S.A.), 1957.

27. CHARM, S.E., Ind.Eng.Chem.Fund, 1, 79, 1962.

28. CHARM, S.E., MERRILL, E.W., Food Research 24, 319, 1959.

29. CHRISTIANSEN, E.B., Chem.Eng.Progress 60 (No.8), 49, 1964.

30. CHRISTIANSEN, E.B., CRAIG, Jr., S.E., A.I.Ch.E.J., 8 (No.2), 155, 1962.

31. CHRISTIANSEN, E.B., JENSEN, G.E., FAN-SHENG TAO, A.I.Ch.E.J. 12 (No.6), 1196, 1966

32. CHRISTIANSEN, E.B., KELSEY, S.J., and CARTER, T.R., A.I.Ch.E.J. 18 (No.2), 372, 1972.

33. CHRISTIANSEN, E.B, KELSEY, S.J., A.I.Ch.E.J. 18, (No.4), 713, 1972.

34. CHRISTIANSEN, E.B., KELSEY, S.J. Chem.Eng.Sci. 28, 1099, 1973.

35. CHRISTIANSEN, E.B., LEMMON, H.E., A.I.Ch.E.J. 11 995, 1963.

36. CHOLETTE, A, Chem.Eng.Progress. 44, 81, 1948.

37. CHU CHIN JU, BROWN, F, BURRIDGE, K.G., Ind.Eng.Chem. 45, (No.8), 1686, 1953.

38. CLAPP, R.M., Intnl.Heat Conference, Boulder, (U.S.A.) 1961.

39. CLEGG, P.L., "Rheology of Elastomers". P. Mason and N. Wookey, ed.p. 174-89. Pergamon Press, New York (1958).

40 CLOUGH, S.B., READ, H.E., METZNER, A.B., BEHN, V.C. A.I.Ch.E.J. 8, 346, 1962.

41. COLBURN, A.P. Trans.Am.Inst.Chem.Eng. 29, 174, 1933.

42. COLLINS, M., SCHOWALTER, W.R., A.I.Ch.E.J., 9, 804, 1963.

43. COLLINS, M.W., Symposium on Internal Flows, 1971. Paper 10. University of Salford, England.

44. DAVIES, C.H., Comm.Proc.Instn.Mech.Engrs. 170, (38), 1127, 1956.

45. DAVIES, E.J., GILL, W.N., Int.J.Heat and Mass Transfer 13, 459, 1970.

46. De HAVEN, E.S., Ind.Eng.Chem. 51, 63A-66A, (No.7), 1959.

47. DITTUS, F.W., BOELTER, L.M.K., Univ. of California Pubs. in Engg 2, 1930.

48. DODGE, D., METZNER, A.B., A.I.Ch.E.J., 5, 189, 1959.

49. DRANOFF, J.S., Math. of Computation 15, 403, 1961.

50. DREW, T.B., Trans. A.I.Ch.E.J., 26, 26, 1931.

51. EAGLE, A., FERGUSON, R.M., Proc.Inst.Mech.Eng. (London) 2, 985, 1930, also Proc.Roy.Soc. A. 127, 540, 1930.

52. L'ECUYER, WARNER, C.F., Trans. A.S.M.E.J. Heat Transfer 91, 1962.

53. ECKERT, E.R.G., "Introduction to the Transfer of Heat and Mass", 1st ed. pp98-101, McGraw-Hill Book Co., New York, 1950.

54. EDE, A.J., HISLOP, C.J., MORRIS, R., Proc.Inst. Mech.Engrs. 170, (No. 38), 1113, 1956.

55. EDE, A.J., MORRIS, R., BIRCH, E.S., N.E.L. Report No. 73, December 1962.

56. EDE, A.J., Heat 1964, N.E.L. Report, January 1959.

57. EMERY, A.F., CHEN, C.S., Trans.A.S.M.E. (J.Basic Eng.) 90, 134, 1968.

58. EUBANK, C.C., PROCTOR, W.S., S.M. Thesis, M.I.T. 1951.

59. FARGIE, D., MARTIN, B.W., Proc.Roy.Soc.London A. 321 461, 1971.

60. FORABOSCHI, F.P., DI FEDERICO, I., Int.J.Heat and Mass Transfer, 7, 315, 1964.

61. FORREST, G., WILKINSON, W.L., Trans.Instn.Chem.Engrs. 51, 331, 1973.

62. FORREST, G., WILKINSON, W.L. Trans.Instn.Chem.Engrs. 52, 10, 1974.

63. FORREST, G., WILKINSON, W.L., Int.J.Heat and Mass Transfer 16, 2377, 1973.

64. FRIEDMANN, M., GILLIS, J., LIRON, N., Appl.Scient. Res. 19, (6), 426, 1968.

65. GEE, R.E., LYON, J.B., Ind.Eng.Chem.Ind.(Int)Edn. 49, 959, 1957.

66. GILL, W.N., Appl.Sci.Res., A11, 10, 1962.

67. GILL, W.N., A.I.Ch.E.J., 8, 137, 1962.

68. GLASER, H., MAP Voelkenrode, Ref. MAP-VG-36-818T, 1947.

69. GLUCK, D.F., M.Ch.E. Thesis Univ.of Delaware (U.S.A.) 1959.

70. GOLDSTEIN, S., "Modern Developments in Fluid Dynamics" Clarendon (Oxford), 1938.

71. GRAETZ, L., Ann.Phys.Chem., 25, 337, 1885.

72. GREEN, H., WELTMANN, R.N., Ind.Eng.Chem.(Anal), 15, 201, 1943.

73. GRIGULL, U., Chem-Ing.Tech. 8/9, 553, 1956.

74. GROSS, J.F., VAN NESS H.C., A.I.Ch.E.J. 3, 172, 1957.

75. HANKS, R.W., CHRISTIANSEN, E.B., A.I.Ch.E.J. 7, 519, 1961.

76. HARRIS, J., MAGNALL., Trans.Instn.Chem.Engrs. 50, 61, 1972.

77. HEAD, V. P., TAPPI, 35, 260, 1952.

78. HEATON, H.S., REYNOLDS, W.C., KAYS, W.M., Int.J. Heat and Mass Transfer 7, 763, 1964.

79. HIRAI, E., Chem.Eng. (Japan) 21, 1726, 1957.

80. HOBSON, R.J., Ph.D. Thesis, Univ. of Durham, England 1964.

81. HODGE, R.I., Comm.Proc.Instn.Mech.Engrs. 170 (No. 38) 1129, 1956.

82. HOPPER, J.R., M.Ch.E. Thesis, Univ. of Delaware, Newark, Delaware, 1964.

83. HORNBECK, R.W., Appl.Sci.Res. A 13, 224, 1964.

84. INMAN, R.M., N.A.S.A., TN D-2674

85. INMAN, R.M., Int.J. Heat and Mass Transfer, 5, 1053, 1962.

86. JACKSON, T.W., SPURLOCK, J.M. PURDY, K.R. A.I.Ch.E.J. 7, 38, 1961.

87. JAKOB, M., "Heat Transfer" Vol.1. John Wiley & Sons, (New York), 1949.

88. JEFFERSEN, T.B., WITZELL, O.W. and SIBBITT, W.L., Ind.Eng.Chem. 50, 1589, 1958.

89. KATZ, S. Ch.E.Sci., 10, 202, 1959.

90. KAYS, J.M., "An Introduction to Fluid Mechanics and Heat Transfer" 2ndEd. Cambridge Univ.Press (London) 1963.

91. KAYS, W.M., Trans.A.S.M.E., 77, 1265, 1955.

92. KAYS, W.M., "Convective Heat and Mass Transfer" McGraw-Hill (New York) 1966.

93. KEEVIL, C.S., McADAMS, W.H., Chem. and Met.Eng. 36, 464, 1929.

94. KNUDSEN, J.G., KATZ, D.L., "Fluid Dynamics and Heat Transfer" McGraw-Hill (New York) 1958.

95. LANGHAAR, H.L., J.Appl.Mech., 9, A55, 1942.

96. LA NIEVE, H.L., III, MSc. Thesis, Univ of Tennessee, Knoxville, Tenn. 1963.

97. LATZKO, H., Zeitschrift Angewandte Mathematik Mechanik 1, 268, 1921.

98. LEMMON, H.E., Ph.D. Thesis, Univ. of Utah, Salt Lake City, Utah, 1963.

99. LEVEQUE, M.A., Ann.Mines, 13, 201, 1928.

100. LINFORD, A., "Flow Measurement and Meters", 2nd Ed. (revised and expanded) E.& F.N.Spon Ltd. (London) 1961.

101. LYCHE, B.C., BIRD, R.B., Ch.E.Sci., 6, 35, 1957.

102. MAHALINGHAM, R., Ph.D. Thesis, Univ. of Newcastle-Upon-Tyne, Englnad, 1966.

103. MANOHAR, R., Int.J. Heat and Mass Transfer 12, 15, 1969.

104. MARTIN, B.W., Proc.Instn.Mech.Engrs. 187, (36), 435, 1973.

105. MARTIN, B.W., FARGIE, D. Proc.Instn.Mech.Engrs. 186, (24), 307, 1972.

106. MARTINELLI, R.C., Trans. A.I.Ch.E., 38, 493, 1942.

107. MARTINELLI, R.C., BOELTER, L.M.K., Univ. of California, Pubs. in Eng. 5, 23, 1942.

108. MARTINELLI, R.C., SOUTHWELL, C.J., ALVES, G., CRAIG, H.L., WEINBERG, E.B., LANSING, N.F., BOELTER, L. M.K., Trans.Am.Inst.Chem.Engrs. 38, 493, 1942.

109. MATSUHISA, S., BIRD, R.B., A.I.Ch.E.J. 11, 588, 1965.

110. MAXWELL, J.C., "Electricity and Magnetism" Vol.1, Oxford Univ.Press (London) 1873 (also Dover Books, New York 1954)

111. MERCER, A., McD., Appl.Sci.Res. A8, 357, 1959.

112. MERCER, A. McD., Appl.Sci.Res. A9, 450, 1960.

113. METZNER, A.B., I.E.C., 50, 1577, 1950.

114. METZNER, A.B., C.E.P. 50, 27, 1954.

115. METZNER, A.B., "Advances in Chemical Engineering", Vol.1, Acad.Press Ind. (New York) 1956.

116. METZNER, A.B., REED, J.C., A.I.Ch.E.J. 1, 434, 1955

117. METZNER, A.B., VAUGHN, R.D., HOUGHTON, G.L., A.I.Ch.E.J., 3, 93, 1957.

118. METZNER, A.B., GLUCK, D.F., Ch.E.Sci., 12, 185, 1960

119. METZNER, A.B., FRIEND, W.L., Can.J.Chem.Eng. 36, 235, 1958.

120. MICHIYOSHI, I., Bull.J.S.M.E., 5, 315, 1962 (Also 28, 1533, 1962).

121. MILLER, A.P., Jr., Ph.D. Thesis in Chemical Engineering, University of Washington, Seattle, 1953.

122. MISHRA, P., TRIPATHI, G., Trans.Instn.Chem.Engrs. 51, 141, 1973.

123. MITSUISHI, N., MIYATAKE, O., Memoirs of the Faculty of Engineering Kyushu University 28, (No. 2), 91, 1968.

124. MITSUISHI, N. MIYATAKE, O., Kagaku, Kogaku (Chem. Eng. Japan) 30, 813, 1966.

125. MITSUISHI, N., MIYATAKE, O., International Chemical Eng. 9, (No. 2), 352, 1969.

126. MIZUSHINA, T., KURIWAKI, Y., Mem.Fac.Eng., Kyoto Univ. 30, (No.4), 511, 1968.

127. McADAMS, W.H., "Heat Transmission", 3rd Ed. McGraw-Hill (New York) 1954.

128. McINTYRE, M., Ph.D. Thesis, Univ. of Aston in Birmingham, England, 1974.

129. McMILLEN, E.L., Chem.Eng.Progress, 44, 537, 1948.

130. McKENNELL, R., Analytical Chemstry, 28, 1710, 1956.

131. McKILLOP, A. A., Int.J. Heat and Mass Transfer, 7, 853, 1964 (Also Ph.D. Thesis Univ.of California, Berkeley, 1962).

132. MOONEY, M., J.Rheology, 2, 210, 1931.

133. NIKURADSE, J., "Applied Hydro and Aerodynamics" McGraw-Hill (New York), 1950.

134. NORRIS, R. H., STREID, D.D., Trans.Am.Soc.Mech.Eng. 36, 525, 1940.

135. OLDROYD, J. G., Proc.Roy.Soc. A.218, 122, 1953.

136. OLDROYD, J. G., Quat.Jour.Mech.Appl.Maths, 4, 271, 1951.

137. OLIVER, D.R., Chem.Eng.Sci. 17, 335, 1962.

138. OLIVER, D.R., JENSON, V.G., Chem.Eng.Sci., 19, 115, 1964.

139. ORR, C., DALLA VALLE, J.M., CEP.Symp.Series, 50, 29, 1954.

140. OSTWALD, F., Koll - Zeits., 36, 99, 1925.

141. PAWLEK, R.A., CHI TIEN, Can.J.Ch.E., 42, 222, 1964.

142. PIGFORD, R.L., C.E.P.Symp.Ser. 51, 79, 1955.

143. PHILLIPPOFF, W., GASKINS, F.H., J.Poly.Sci. 21, 205, 1956.

144. POLAK, P., J.Mech.Eng.Sci. 13(No.4), 293, 1971.

145. PORTER, J., Trans.Instn.Chem.Engrs. 49, 1971.

146. RABINOWITSCH, B., Z., Physik.Chem., 145A, 1, 1929.

147. RAMA MURTHY, A.V., BOGER, D.V., Trans.Soc.Rheol. 15, 709, 1971.

148. RAO, M.S., KULOOR, N.R., Chem. Age of India, 14, 673, 1963.

149. REINER, M., "Deformation and Flow" Lewis (London)

150. REYNOLDS, O., Trans.Roy.Soc.(London) 174A, 935, 1883.

151. REYNOLDS, W.C., Trans.A.S.M.E. Heat Transfer 108, 1960.

152. ROBERTS, J.E., Proc. 2nd. Int.Rheol.Cong. 91, Butterworth (London) 1954.

153. ROSEN, E.M., HANRATTY, T.J., A.I.Ch.E.J., 7, 112, 1961.

154. ROUSE, H., "Elementary Mechanics of Fluids", Wiley, (New York), 1946.

155. ROY, D.N., Comm.Trans.A.S.M.E., J.Heat Mass Transfer 425, 1965.

156. RYAN, N.W. JOHNSON, M. M., A.I.Ch.E.J., 5, 433, 1959.

157. SALAMONE, J.J., NEWMAN, M., Ind.Eng.Chem. 47, 283, 1955.

158. SCHECHTER, R.S., WISSLER, E.H. Nucl.Sci.Eng. 6, 371, 1959.

159. SCHENK, J., DUMORE, J.M., Appl.Sci.Res. A4, 39, 1953.

160. SCHENK, J., VAN LAAR, J., Appl.Sci.Res., A7, 96, 1922.

161. SCHILLER, L.Z., Angew, Math.Mech. 2, 96, 1922.

162. SCHLICHTING, H. "Boundary Layer Theory", 4th ed. McGraw-Hill (New York) 1960.

163. SCHMIDT, F.W., ZELDIN, B., Comm.A.I.Ch.E.J., 15, (No. 4), 612, 1969.

164. SCHNEIDER, P.J., Trans.A.S.M.E., 765, 1957.

165. SCHOFIELD, R.K., SCOTT-BLAIR, G.W., Proc.Roy.Soc. A138, 707, 1932.

166. SCHOFIELD, R.K., SCOTT-BLAIR, G.W., J.Phys.Chem., 34, 248, 1930.

167. SCHOTT, H., KAGHAN, W.S., Ind.Eng.Chem., 51, No.7), 844, 1959.

168. SCHOWALTER, W.R., A.I.Ch.E.J., 6, 24, 1960.

169. SEGUR, J.B., OBERSTAR, H.E., Ind.Eng.Chem. 43, (No.9), 2117, 1951.

170. SELLARS, J., TRIBUS, M., KLEIN, J., Trans.A.S.M.E., 78, 441, 1956.

171. SESTAK, J., CHARLES, M.E., Chem.Eng.Progr.Symp.Ser. 64, (No. 82), 212.

172. SHAVER, R., MERRILL, E., A.I.Ch.E.J., 5, 181, 1959.

173. SHEELEY, M.L., Ind.Eng.Chem. 24, 1060, 1932.

174. SIEDER, E.N., TATE, G.E., I.E.C., 28, 1429, 1936.

175. SIEGEL, R., SPARROW, E.M., HALLMAN, T.M., Appl.Sci. Res. A7, 386, 1958.

176. SINGH, S.N., Appl.Sci.Res., A7, 325, 1958.

177. SKELLAND, A.H.P., "Non-Newtonian Flow and Heat Transfer", J. Wiley & Sons., Inc.(New York) 1967.

178. SPARROW, E.M., SIEGEL, R. Nucl.Sc.Eng., 4, 239, 1958.

179. SPARROW, E.M., EICHORN, R., GREGG, J.L., Physics of Fluids, 2, 319, 1959.

180. SPARROW, E.M., LIN, S.J. LUNDGREN, T.S., Phys.Fluids 7, (No.3), 338, 1964.

181. STEPANOFF, A.J., "Centrifugal and Axial Flow Pumps" 2nd ed., J.Wiley & Sons Ind. (New York) 1957.

182. STREETER, V.L., "Hand Book of Fluid Dynamics" McGraw-Hill Book Co. (New York) 1961.

183. SUTTERBY, J.L., A.I.Ch.E.J., 12 63, 1966.

184. SYLVESTER, N.D., ROSEN, S.L., A.I.Ch.E.J., 16, (No.6), 965, 1970.

185. TAREEF, B.M., Colloid.J. (USSR) 6, 545, 1940.

186. TEST, F.L., Jl. Heat Transfer, 90, 385, 1968.

187. THOMAS, D.G., Ph.D. Thesis. Univ.of Swansea, Wales, England, 1961.

188. TOMITA, Y., Soc.Chem.Engrs.(Japan), 23, 525, 1959.

189. TOMITA, Y., Soc.Mech.Engrs. (Japan) 4, 13, 77, 1961.

190. TOMS, B.A., Proc.Ist.Int.Rheolog.Con.,Holland, II, 135, 1948.

191. TOOR, H.L., A.I.Ch.E.J., 4, 319, 1958.

192. TOOR, H.L. Ind.Eng.Chem. 48 (No.5), 922, 1956.

193. TRIBUS, M., Comm.Proc.Instn.Mech.Eng. 170,(No.38), 1129, 1956.

194. TSUYOSHI, M., Mem.Fac.Eng.,Kyushu Univ.(Japan) 26, 1085, 1962.

195. TURIAN, R.M. Ch.E.Sci., 20, 771, 1965.

196. ULRICHSON, D.L, SCHMITZ, R.A., Int.J. Heat and Mass Transfer, 8, 253, 1965.

197. VRENTAS, J.S., DUDA, J.L., BARGERON, K.G., A.I.Ch.E.J. 12 (No. 5), 837, 1966.

198. WASSERMAN, M.L., SLATTERY, J.C., A.I.Ch.E.J. 10, 383, 1964.

199. WELTMANN, R.N., N.A.C.A.Tech.Note 3397, 1955.

200. WELTMANN, R.N., KELLER, T.A., N.A.C.A. Tech.Note 3889, 1957.

201. WHITEMAN, I.R., DRAKE, W.B., Trans.A.S.M.E., 80, 728, 1958.

202. WILKINSON, W.L., 'Non-Newtonian Fluids', Pergamon (London) 1960.

203. WINDING, C.C., BAUMANN, G.P., KRANICH, W.L., Chem.Eng.Prog., 43, 527, 613, 1947.

204. ZEMANICK, P.P., DOUGALL, R.S., Trans.A.S.M.E.J. Heat Transfer, 92, 53, 1970.

GENERAL TEXTS

205. "Advances in Heat Transfer", Vols. 3 & 4, Ed. J. P. Hartnett, and T. F. Irvine Jr.

206. American Institute of Physics - "Temperature - Its Measurements and Control in Science and Industry", Reinhold Pub.Corp.(New York) 1947.

207. 'British Standards Specifications'
BS 733 : 1965
BS 1042 : Part 4, 1964
BS 718 : 1960

208. Engineering Sciences Data Unit (London), Forced Convection Heat Transfer in Circular Tubes : Parts I, II and III, item nos. 67016, 68006, 68007.

209. 'Glycols', Ed. G. P. Curme, Reinhold Pub.Corp. (New York) 1953.

210. "Progress in International Research on Thermodynamic and Transport Properties", pp. 738. Academic Press, New York (1962), Chapter by Christiansen B, and Jensen, G.

211. "Transport Phenomena", Ed. R. B. Bird, W. E. Stewart, E. N. Lightfoot. J. Wiley & Sons Inc. (New York) 1964.

212. National Engineering Laboratory Report - Y1/ASY/1, December 1972.

APPENDIX ONE

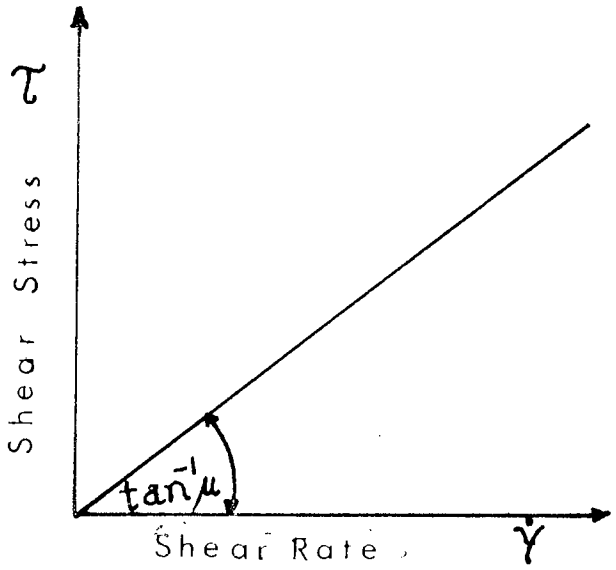

FIG 1 . Flow Curve of a Newtonian Fluid

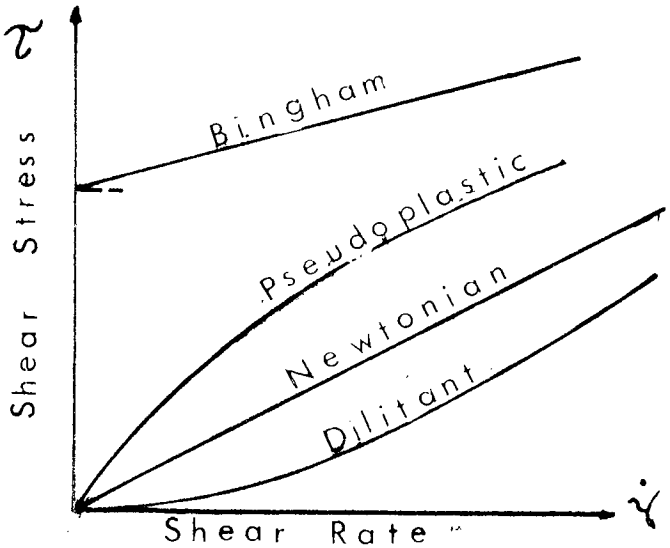

FIG 2 Flow Curves for various types of time-independent Non-Newtonian Fluids

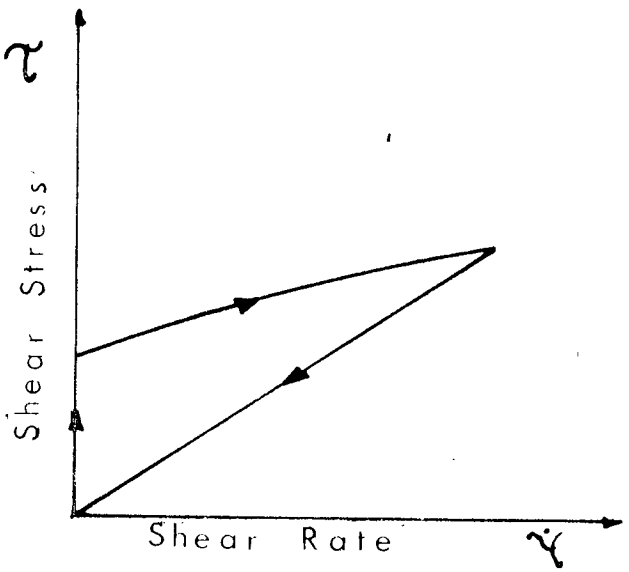

FIG 3 Hysteresis Loop for a Thixotropic Fluid

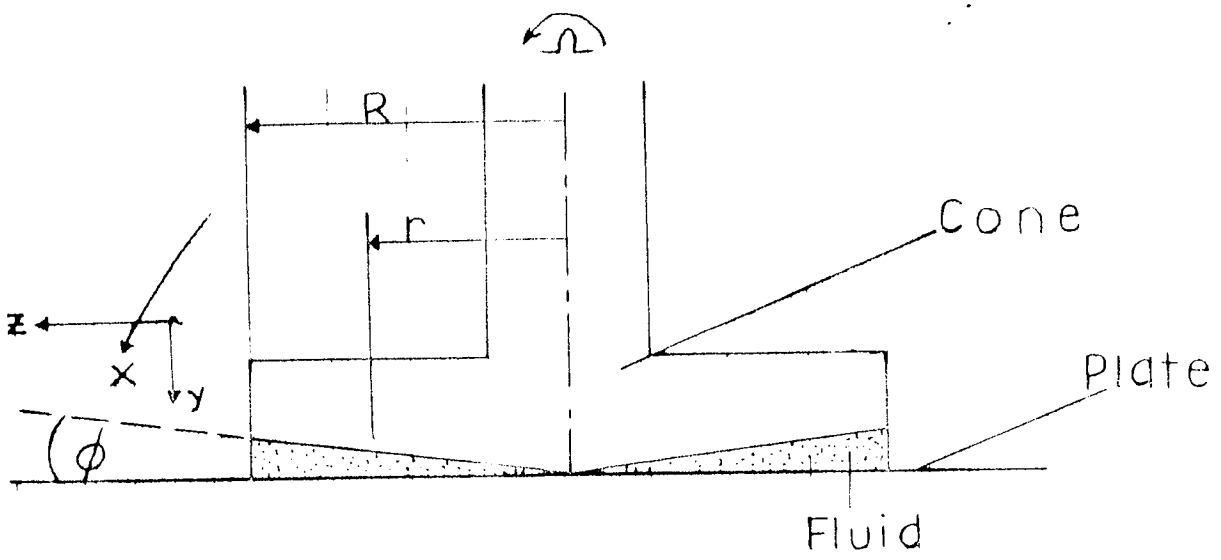

Fig. 4 Schematic diagram of the cone-and-plate viscometer

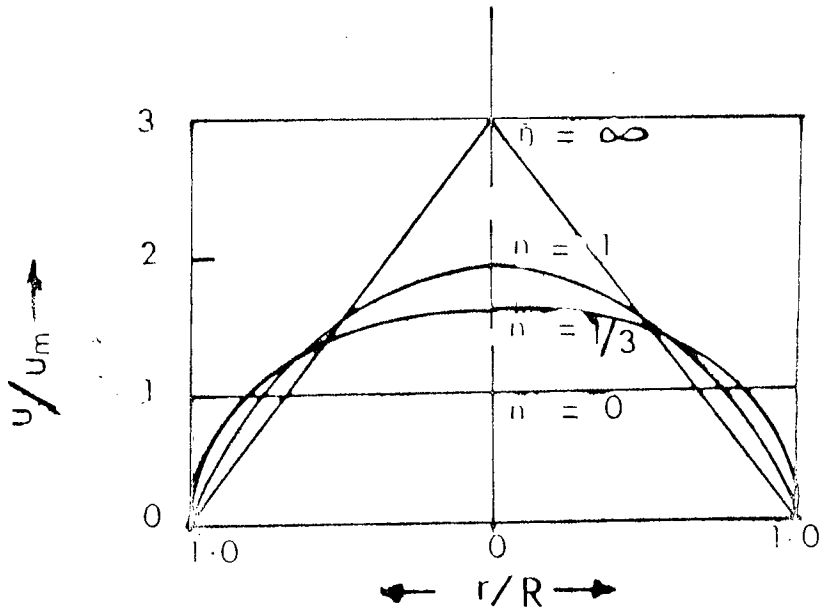

FIG 5 Velocity Profiles

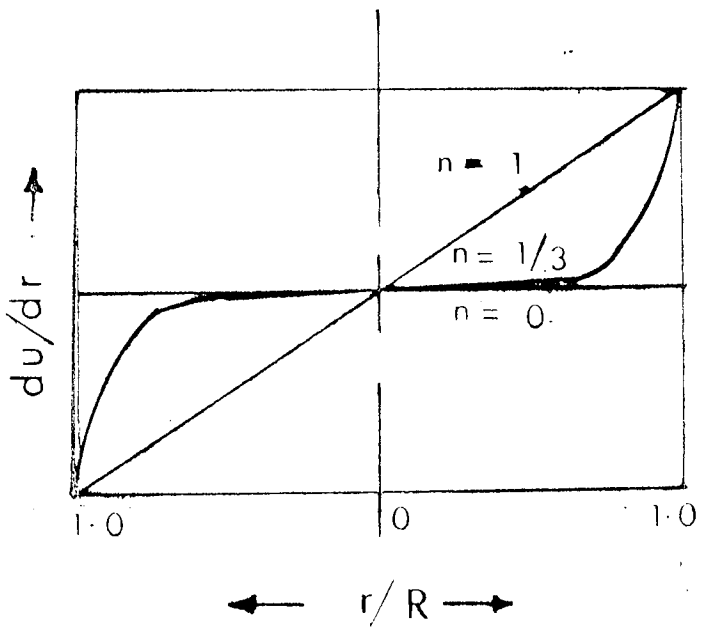

FIG 6 Shear Rate Profiles

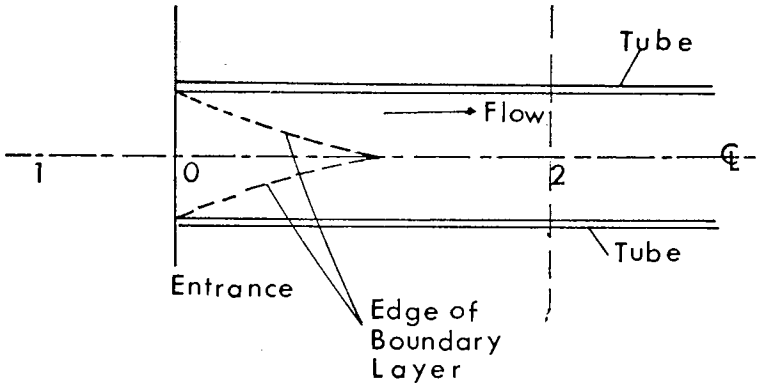

(i) Notation for application of Equation (55)

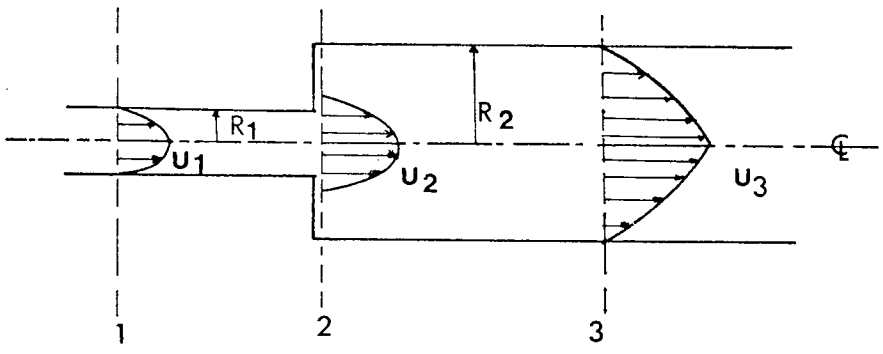

(ii) Notation for application of Equation (53)

FIG 7

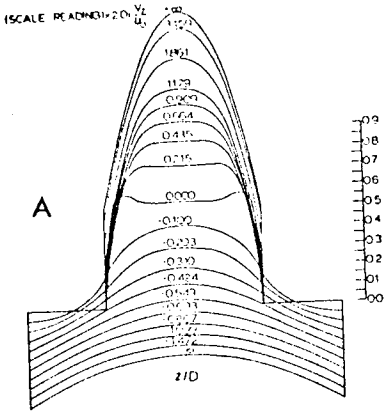

Axial-velocity profile for RT-RT contracted flow, from QL-ML 10 × 20-grid computation, for $N_{Re} = 100$ and $\beta = 2$.

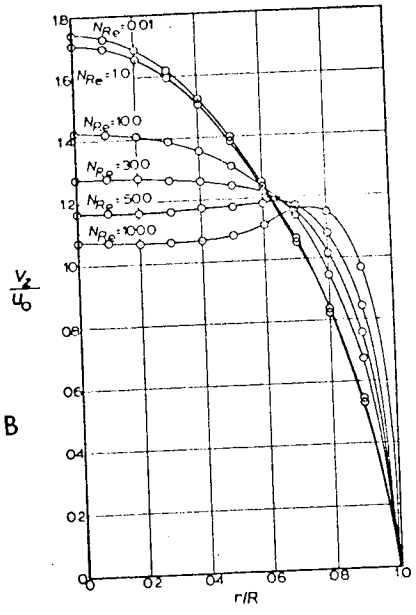

The dependence of axial velocities at the tube entrance on N_{Re} for RT-RT flow, as determined by 10 × 20-grid QL-ML computations.

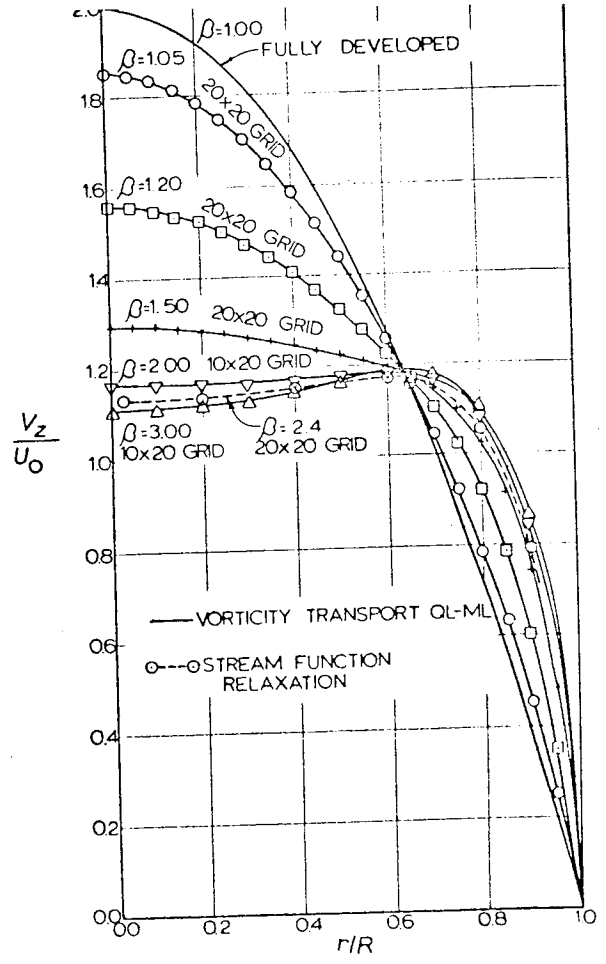

The dependence of axial velocities at the tube entrance on β at $N_{Re} = 50$.

FIG. 8 VELOCITY PROFILES COMPUTED BY CHRISTIANSEN et al (32)

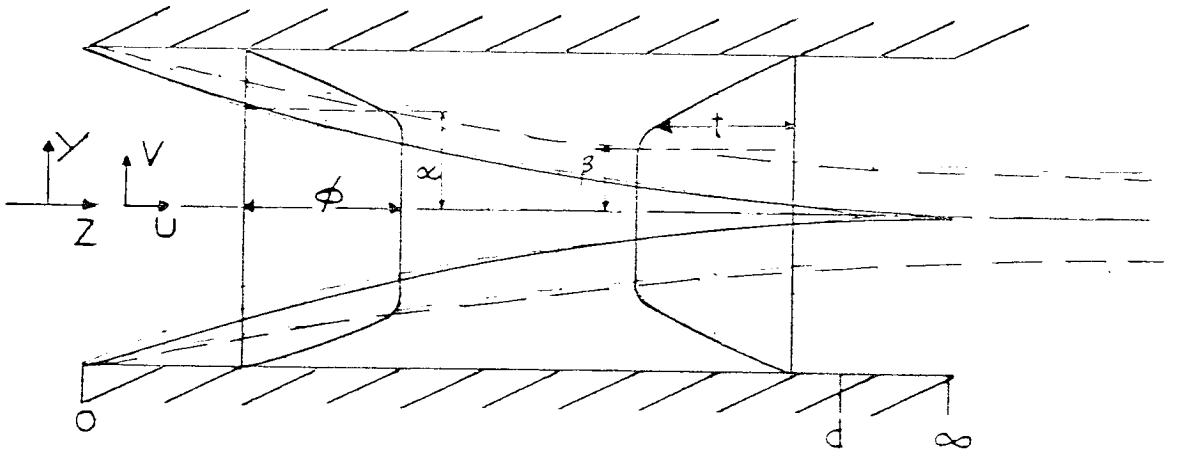

——— Edge of hydrodynamic boundary layer

– – – – Edge of thermal boundary layer

Fig. 9 Notation for Developing Flow Equations (77) and (78) Ref (105)

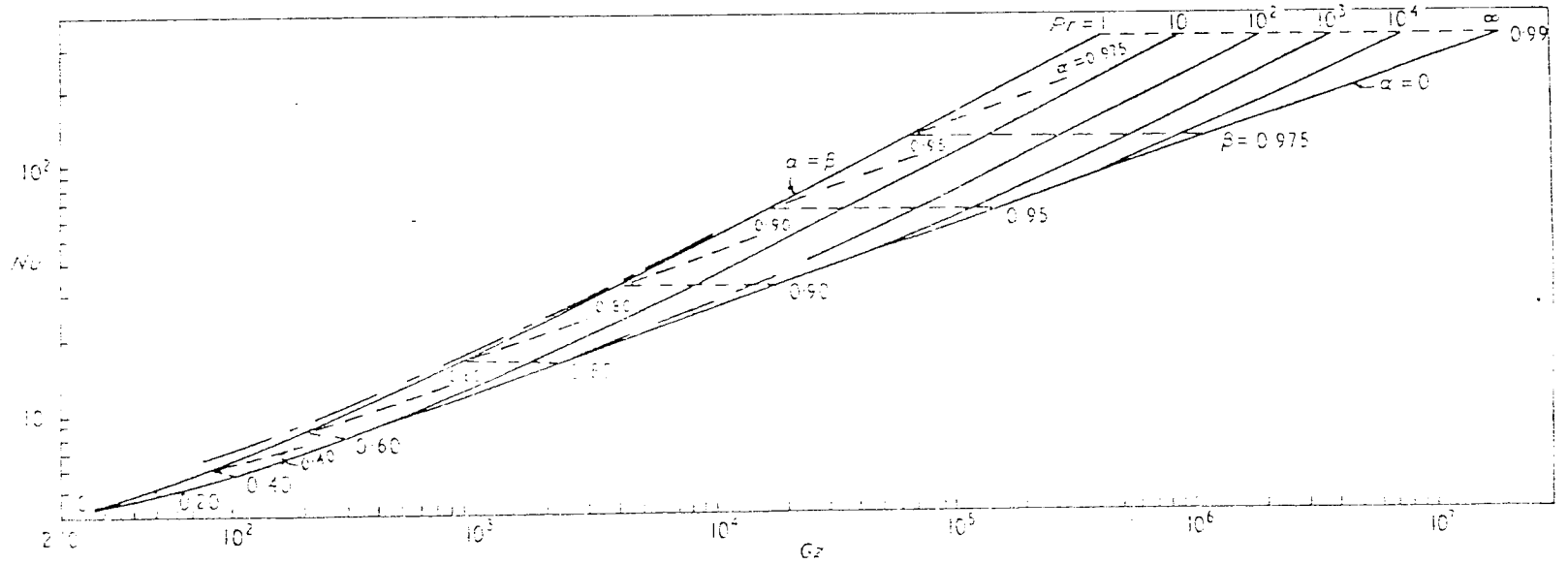

—— —— Predictions of Siegel *et al.* and Butterworth and Hewitt for hydrodynamically fully-developed flow.

— - — - Predictions of Heaton *et al.* and Manohar for $Pr = 0.7$.

Heat transfer predictions in terms of hydrodynamic and thermal boundary-layer thicknesses and Prandtl number

FIG 10 Nusselt Number Predictions --- Martin (105)

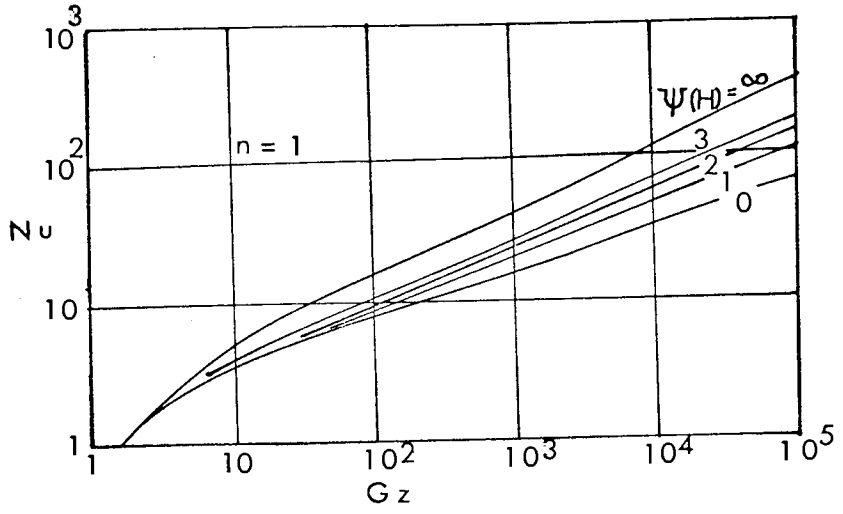

FIG 11

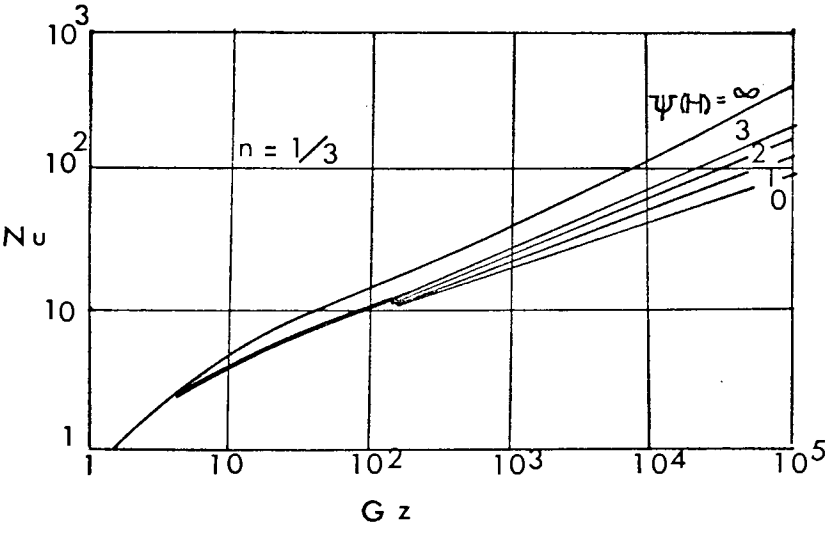

FIG 12

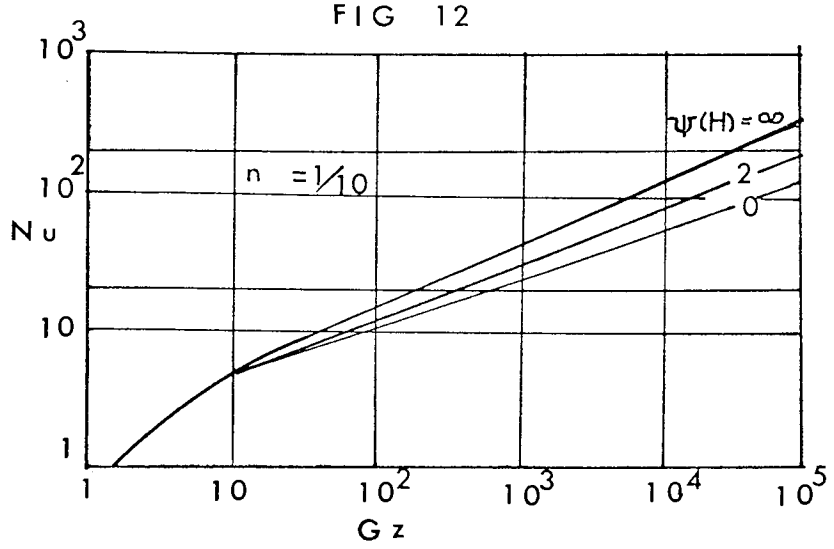

FIG 13

Nusselt number - Graetz number relationships for fluids having temperature dependent properties ----- Ref (30)

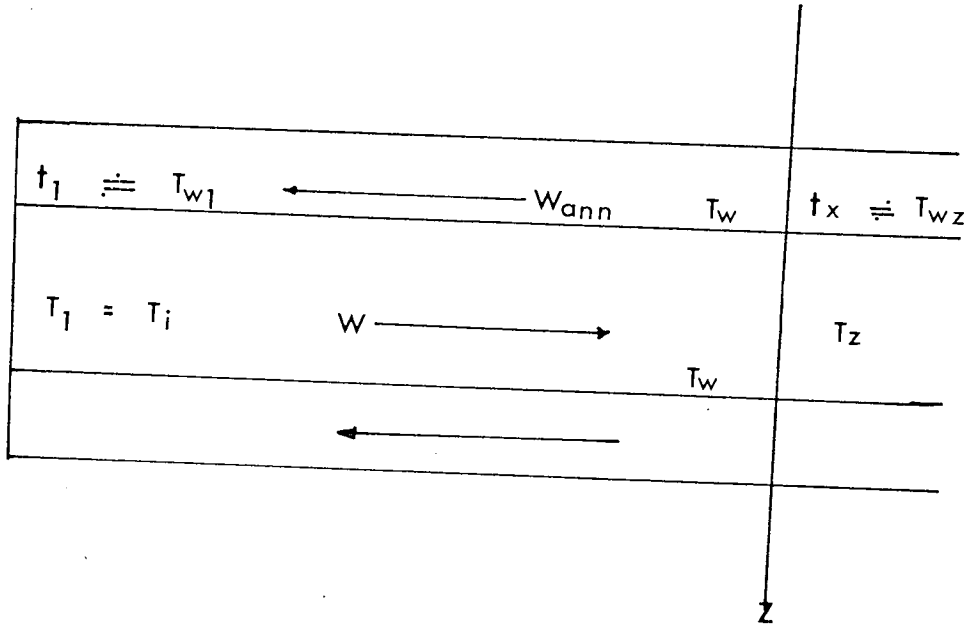

FIG 14 Notation for Equations (168) and (169).

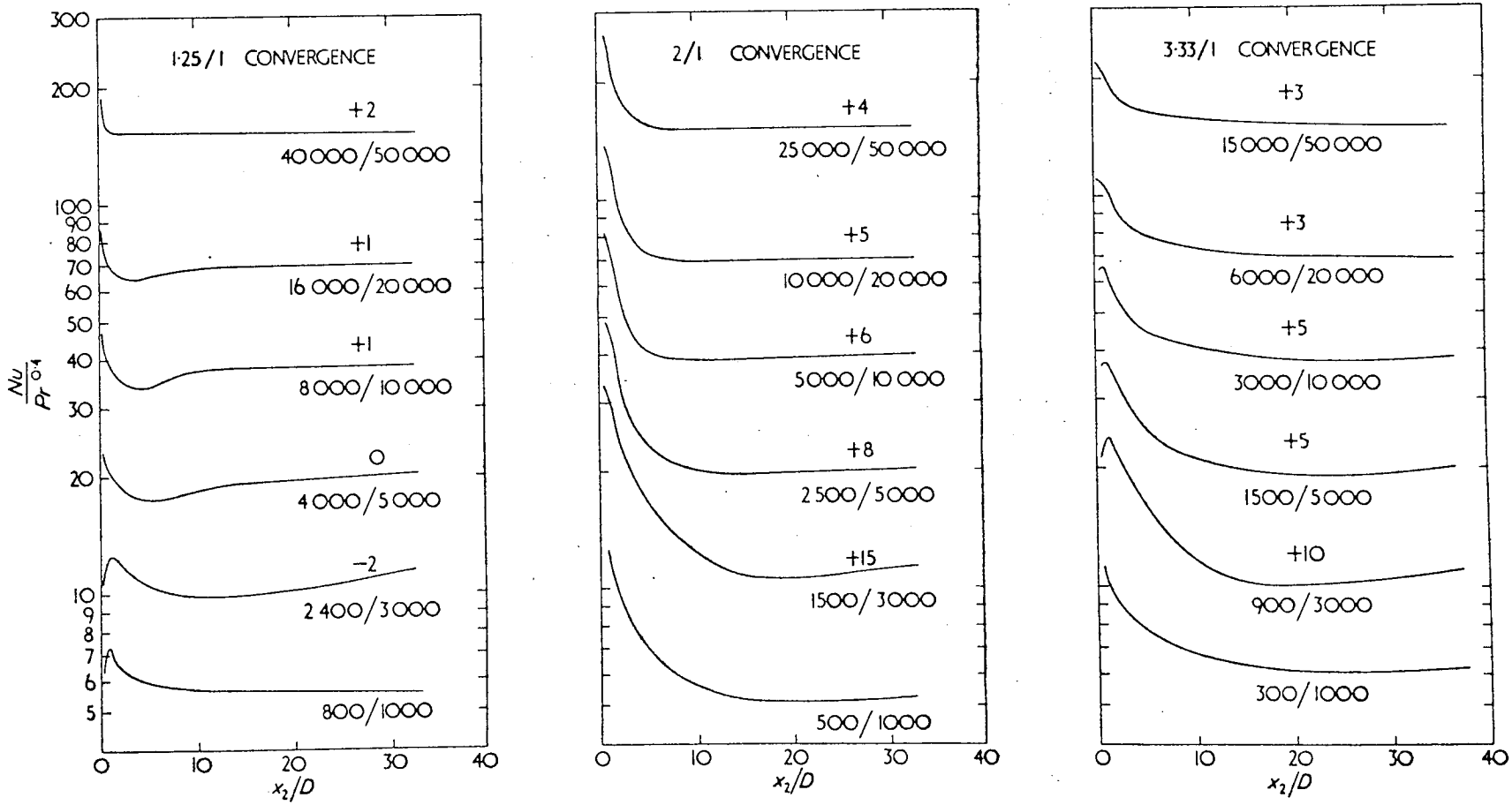

FIG 15 EFFECT OF AN ABRUPT CONVERGENCE INTERPOLATED FROM CROSS-PLOTS OF EXPERIMENTAL DATA BY E D E et al --- (54, 55)

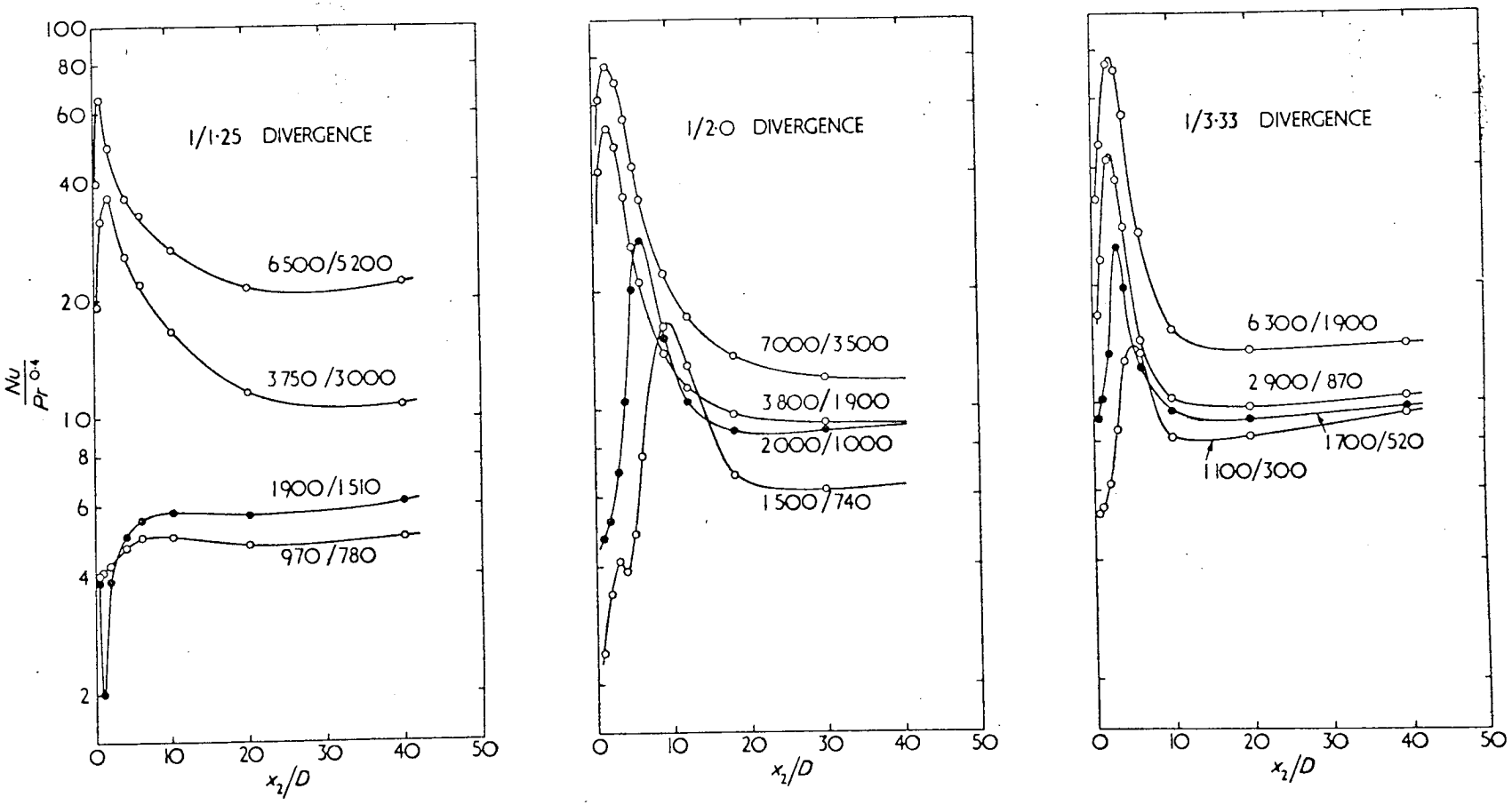

REYNOLDS NUMBER BEFORE AND AFTER CHANGE OF SECTION SHOWN BESIDE EACH CURVE

FIG 16 EFFECT OF AN ABRUPT DIVERGENCE AT LOW REYNOLDS NUMBER, EXPERIMENTAL DATA BY EDE et al. --(54, 55)

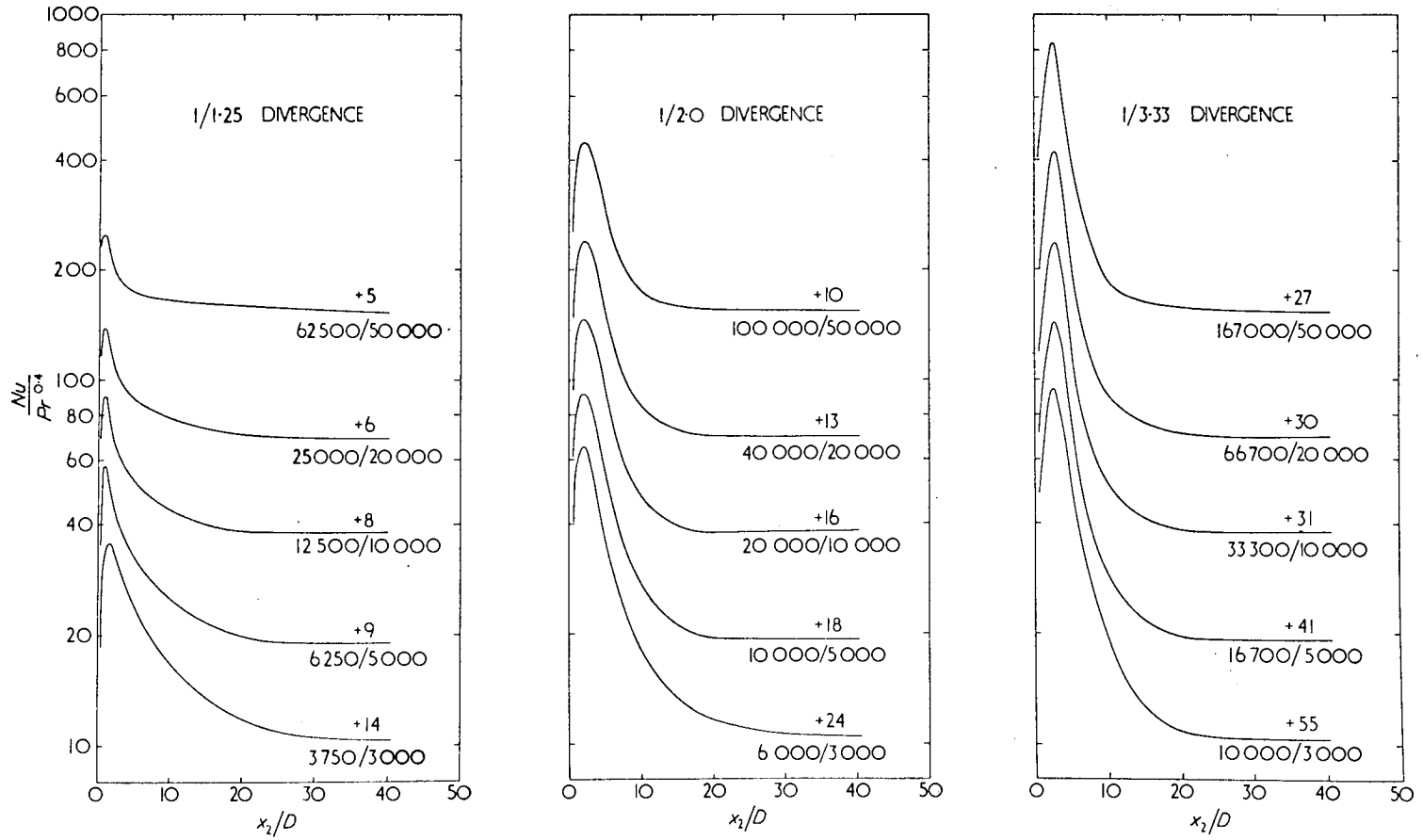

EXTRA DIAMETERS EQUIVALENT TO EXTRA HEAT TRANSFER PRODUCED BY CHANGE OF SECTION SHOWN ABOVE CURVE
REYNOLDS NUMBER BEFORE AND AFTER CHANGE OF SECTION SHOWN BELOW CURVE

FIG 17 EFFECT OF AN ABRUPT DIVERGENCE INTERPOLATED FROM CROSS-PLOTS OF EXPERIMENTAL DATA BY EDE et al ..... (54, 55)

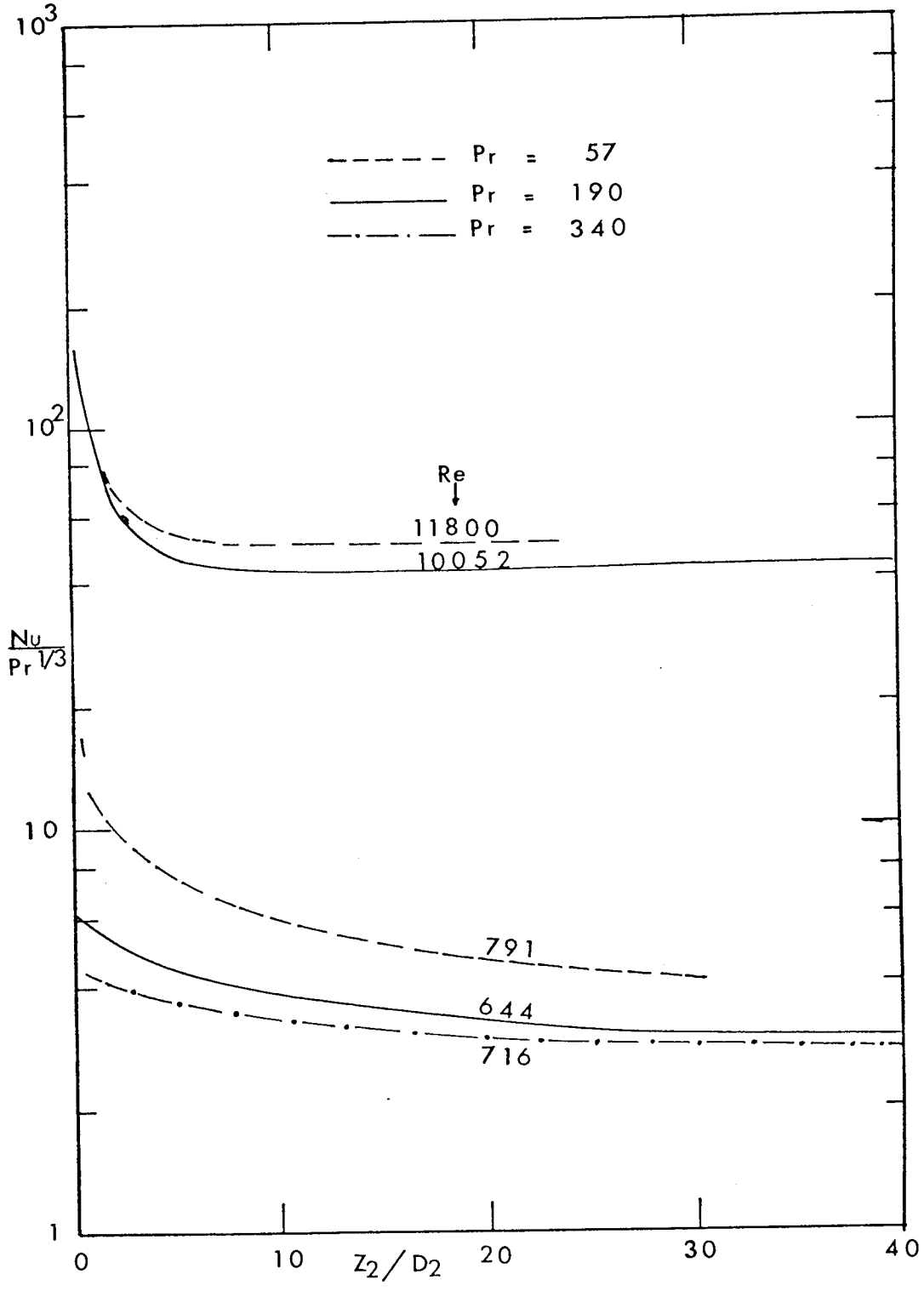

FIG 18 EFFECT OF PRANDTL NUMBER ON NUSSELT NUMBER DOWNSTREAM OF A 3.3:1 CONVERGENCE .... MCINTYRE'S (128) DATA

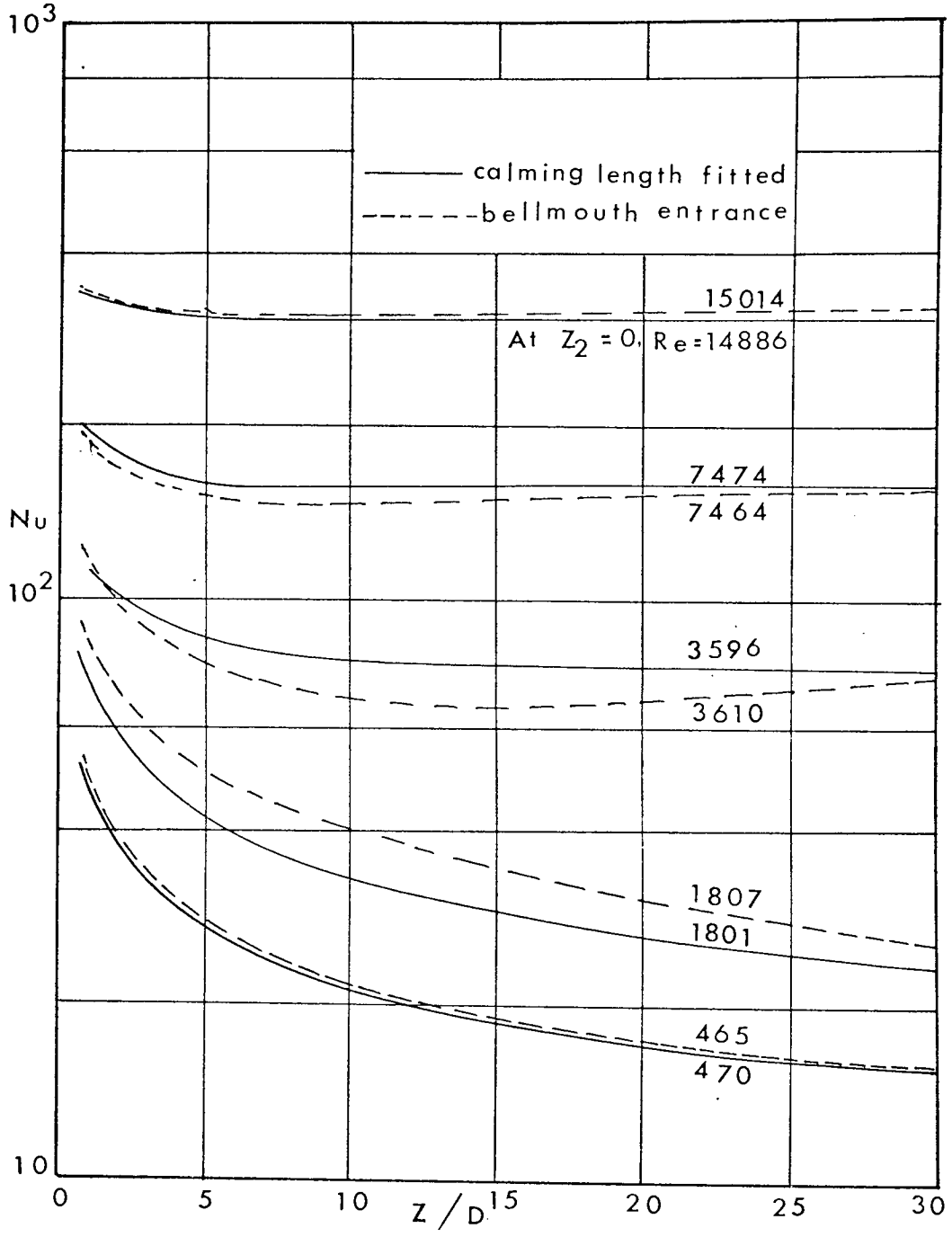

FIG. 19 NUSSELT NUMBER DISTRIBUTION IN THE ENTRANCE REGION OF A SHORT TUBE. A COMPARISON BETWEEN DEVELOPED AND UNDEVELOPED FLOW CONDITIONS --- MCINTYRE'S(128) DATA

APPENDIX TWO

TABLE 1

NON-NEWTONIAN MATERIALS USED IN PREVIOUS STUDIES

	Commercial Name	Chemical Composition	Manufacturer Supplier
(1)	CMC	Sodium Carboxymethyl-Cellulose	Imperial Chemical Industries
(2)	Methocel 90HG 15000 cps	Methyl ether of Cellulose	Dow Chemicals
(3)	Polyox	High molecular weight polymer of Ethylene Oxide	Union Carbide
(4)	Cyanamer P250	Polyacrylamide	Cyanamid
(5)	Gantrez An	Poly (methyl vinyl ether maleic anhydride)	General Aniline & Film Corp.
(6)	Jaguar	Guar Gum	Stein Hall & Co. Inc.
(7)	Courlose	Sodium Carboxymethyl-Cellulose F100	Courtauld's Limited
(8)	"Cellosize"		Union Carbide
(9)	Majol M.V.P.	Carboxymethyl-Cellulose	F.W.Berk & Co. Limited
(10)	Ammo Alg.	Ammonium Alignate	Hopkins & Williams Ltd.
(11)	PVA	Polyvinyl alcohol	Hopkins & Williams Ltd.
(12)	SPM	Sodium polymethacrylate	Hopkins & Williams Ltd.
(13)	Carbopol	Carboxypolyethylene	B.F. Goodrich Chemical Co.

TABLE 2

DIMENSIONS OF STAINLESS STEEL CAPILLARY TUBES USED IN THE CAPILLARY VISCOMETER

Tube Number	Nominal Bore (mm)	Actual Bore (mm)	Length (m)	Length/ diameter Ratio
1	2.500	2.543	0.3011	118.4
2	2.500	2.542	0.3011	118.5
3	1.500	1.508	0.2998	198.8
4	0.750	0.676	0.2999	443.6
5	0.750	0.685	0.2992	436.8
6	1.500	1.508	0.2998	198.8
7	3.000	3.193	0.3046	95.2
8	3.000	3.198	0.3046	95.2
9	3.000	3.195	0.3044	95.3
10	3.000	3.194	0.4563	142.86
11	3.00	3.196	0.4564	142.8
12	3.00	3.199	0.4563	142.6
13	3.00	2.996	0.4333	144.6
14	3.00	3.198	0.3805	118.98
15	3.00	3.197	0.3806	119.0

WEISSENBERG RHEOGONIOMETER

Specifications:

Serial Number	2046
Viscosity range	10^{-6} to 10^{8} poise
Shear rate range	7×10^{-4} to 9×10^{3} sec^{-1}
Temperature range	$-50^{o}C$ to $+40^{o}C$
(i) Drive Unit	
a) Motor	1 hp/3 phase/50cs/415V
b) Gear Box	60 Speed Unit
(ii) Plattens	
Cone - diameter	75mm
Angle	$1^{o}35'$ (0.02763 radians)
(iii) Flat Piece - Diameter	75mm
(iv) Torsion bar - Diameter	3.125mm
Total torque k_T	(N/m)/0.001 deflection 33.72

MIXING TANK ACCESSORIES

Specifications:

(i) High Speed Mixer	
Drive	1 hp direct a.c. motor 380 - 440V/3ph/50cs
Speed	1420 r.p.m.
Stirer	Dual 150mm propellers
(ii) Low Speed Mixer	
Drive	$\frac{1}{2}$ hp direct a.c. motor 240/3ph/50cs. Heidograph Varispeed gear drive

MIXING TANK ACCESSORIES (continued)

Speed Range	60 - 200 r.p.m.
Stirrer	100mm dia propeller
(iii) Heater	3kw immersion type

CIRCULATION PUMP

Model	300 ND Stainless Steel (Type 316 18/8/3 quality)
Size	760mm discharge
Capacity	4.419m^3/s against 9 x 10^5 N/m^2 discharge
Speed	700 r.p.m.
Drive	11hp 1440 r.p.m. V belt drive 415V/3ph/50cs.

COOLER

Serck Radiator Limited	Type TJ0365 No: 9047510
Materials	
Tubes	"Serck Albra" (Aluminium Brass)
Cylinder	Cast iron
Box	Cast iron

POWER SUPPLY COMPONENTS

(i) Calibrated Shunt

The Cambridge Instrument Co. Ltd.

N.P.L. Calibrated

Resistance 50 $\mu\Omega \pm$ 0.025 at 20°C with 200 - 2000 A.

(ii) Voltage Controller

Midland Transformer Co. Ltd.

On load power regulator : type RDOAM 50/250

Input 415V 0 - 50 A

Output 0 - 415V 50A

(iii) Rectifier and Smoothing Unit

Hackbridge and Hewittic Electrical Co. Ltd.

Rectifier transformer : type 106029A

Primary 415V 103 A

Secondary 26V 1640 A

(iv) Metal rectifier : type 11L2

Output 30V 2000 A

VERNIER POTENTIOMETER

H. Tinsley and Co. Limited

Type : 4025A

TABLE 3

HEAT EXCHANGER DUTY

Flow Rate kg/s	Pressure Drop N/m^2	Temperature ^oC		
		IN	OUT	DIFF
OIL SIDE (VISCOSITY 72cp)				
4	0.4828×10^5	29.2	27.0	2.2
RAW WATER SIDE				
0.38	0.2069×10^5	24	-	-
HEAT DISSIPATED = 36.755 KW				

TABLE 4

HEAT TRANSFER TUBE SPECIFICATIONS

Experiment Configuration	Inner Diameter (mm)	Wall thickness/ Variation (mm)	Length (m)	Roundness (mm)
Divergence and Convergence Ratio 3.34:1	1.709	2.65/0.10	1.8	0.020
	5.715	0.952/0.05	2.8	0.300

All tube material	AI SI type 321 Stainless Steel
Straightness	1 in 600
Surface finish of bore	3 μm
Method of manufacture	Cold drawn and seamless

The above measurements were taken on samples cut from both ends of each tube because in the manufacture of cold drawn seamless tubing the dimensional variations normally increase with the distance between the sampling points.

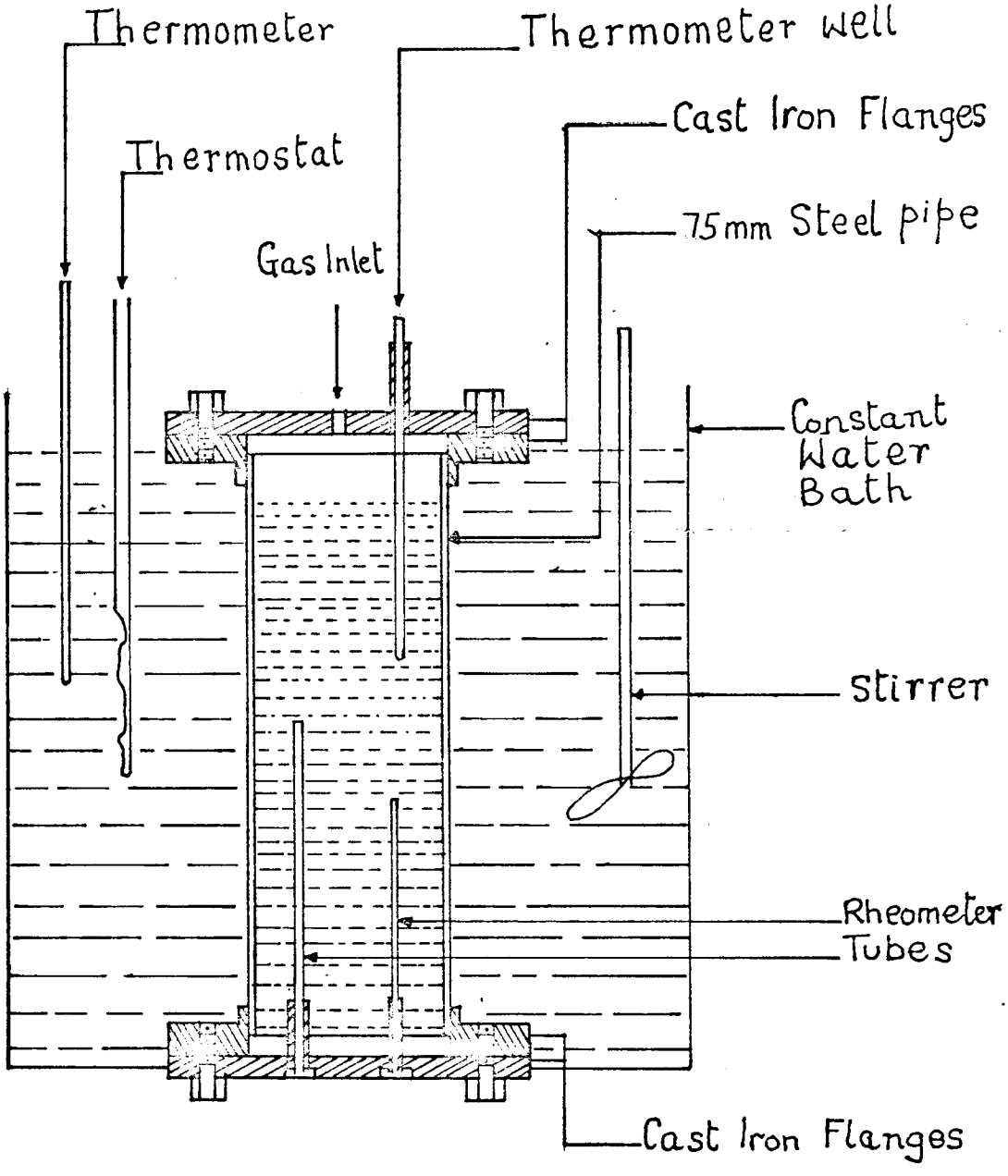

FIG 20 DETAILS OF CAPILLARY TUBE VISCOMETER

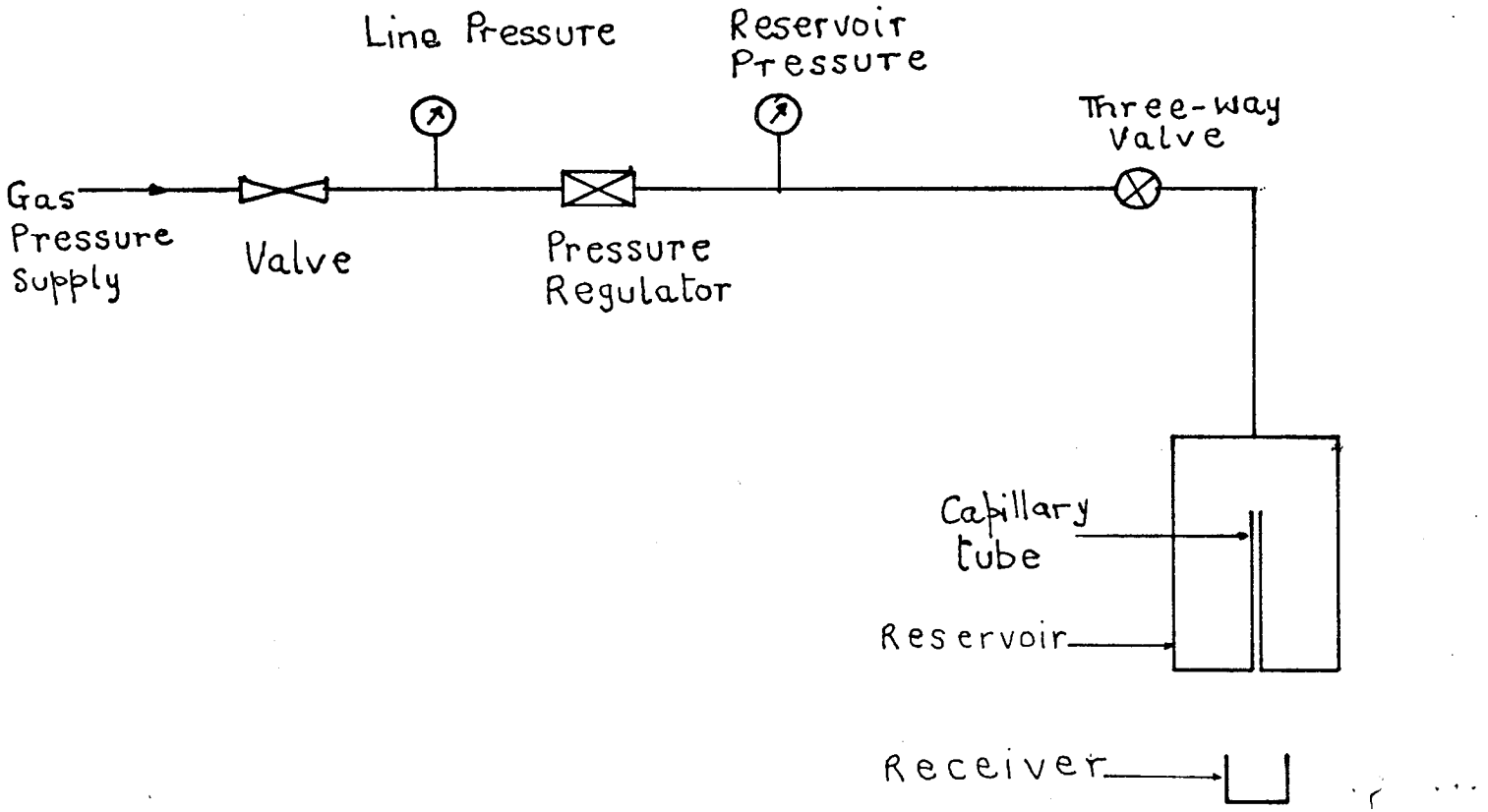

FIG 21 SCHEMATIC DIAGRAM OF A CAPILLARY TUBE VISCOMETER

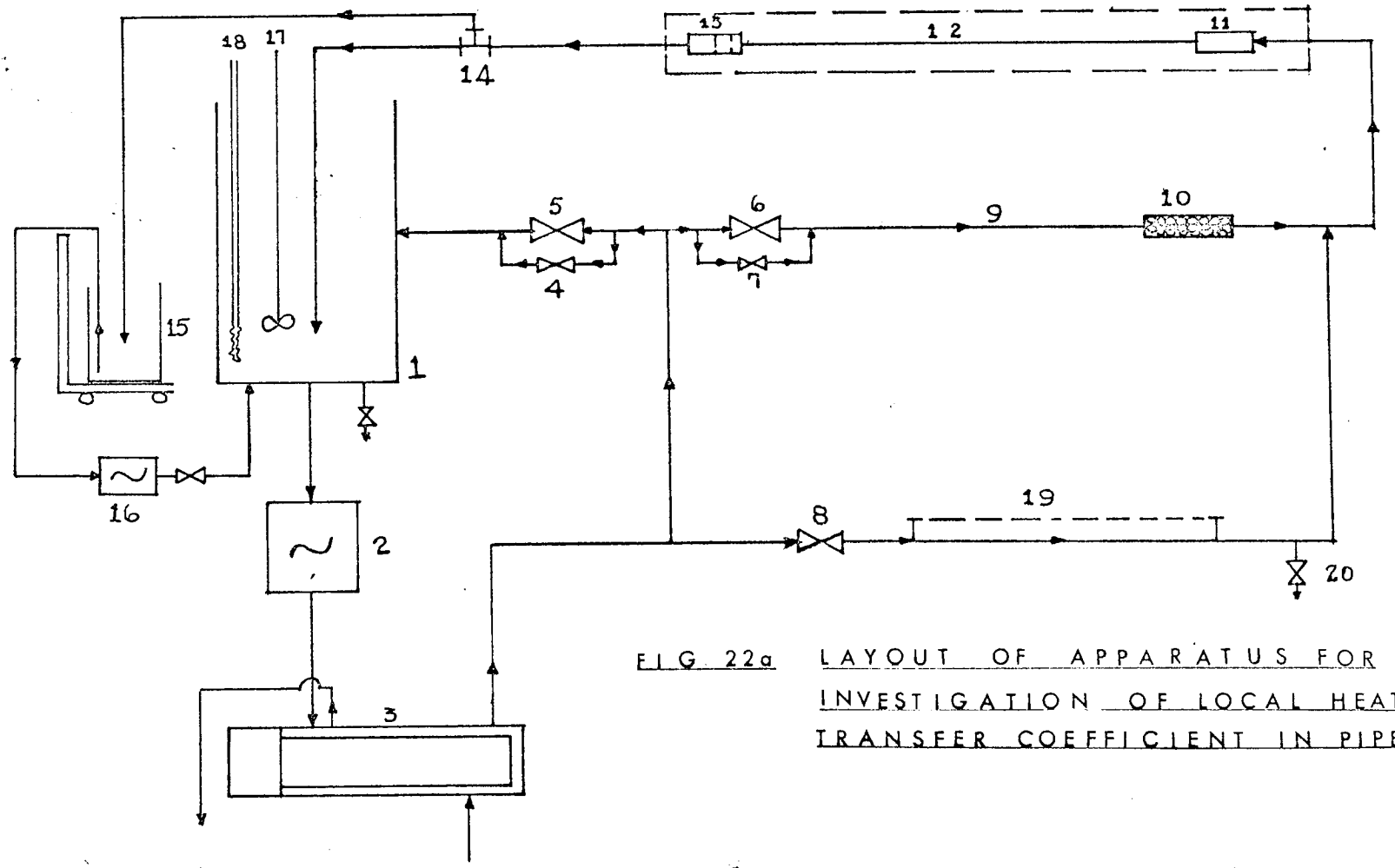

FIG 22a LAYOUT OF APPARATUS FOR INVESTIGATION OF LOCAL HEAT TRANSFER COEFFICIENT IN PIPES

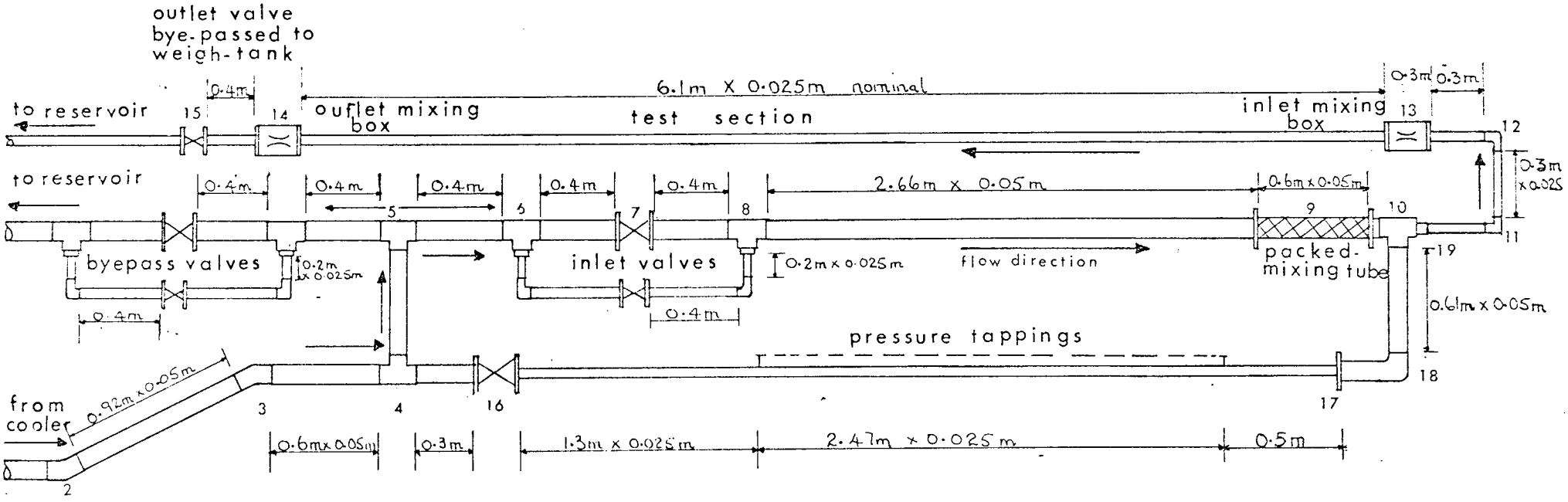

FIG 22b DIMENSIONS AND SIZES OF CONNECTING PIPEWORK FOR EXPERIMENTAL RIG

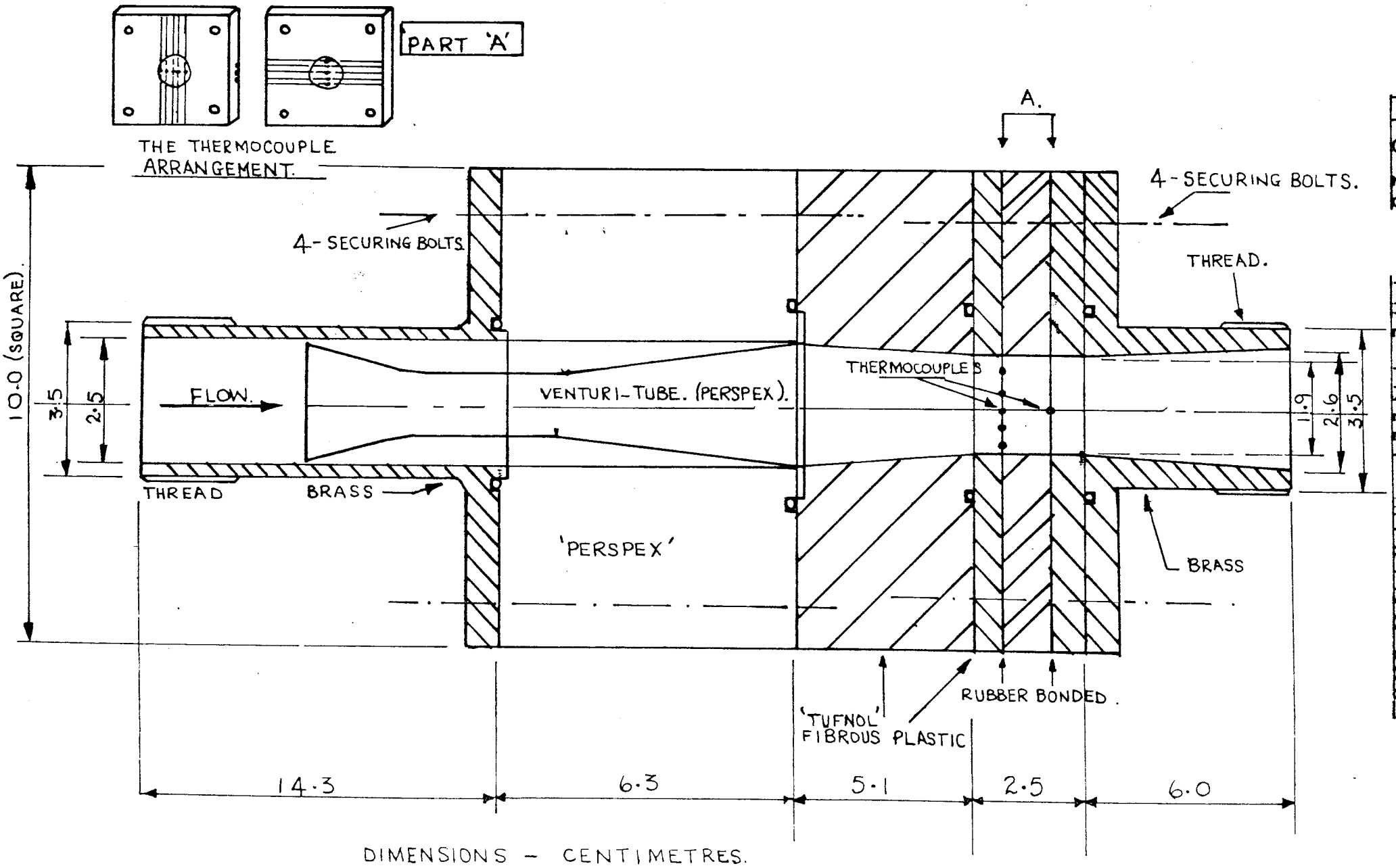

FIG 23 THE INLET MIXING BOX

FIG. 24.

(A) FITTINGS FOR JOINING TUBES

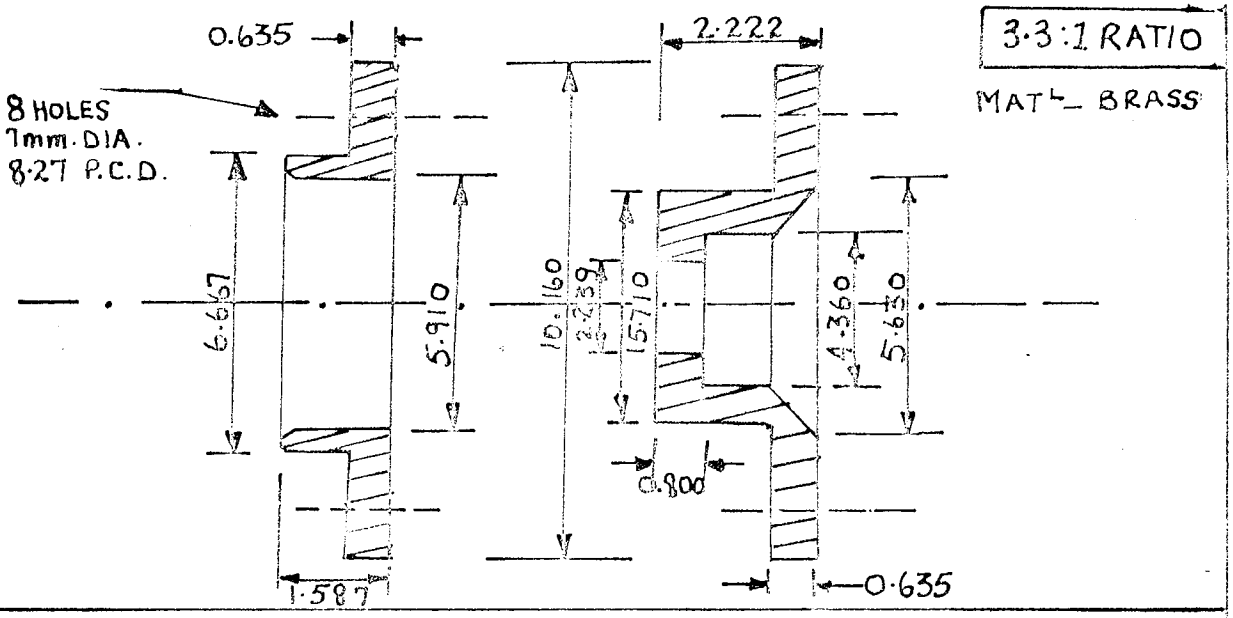

(B) METHOD OF COUPLING TUBES

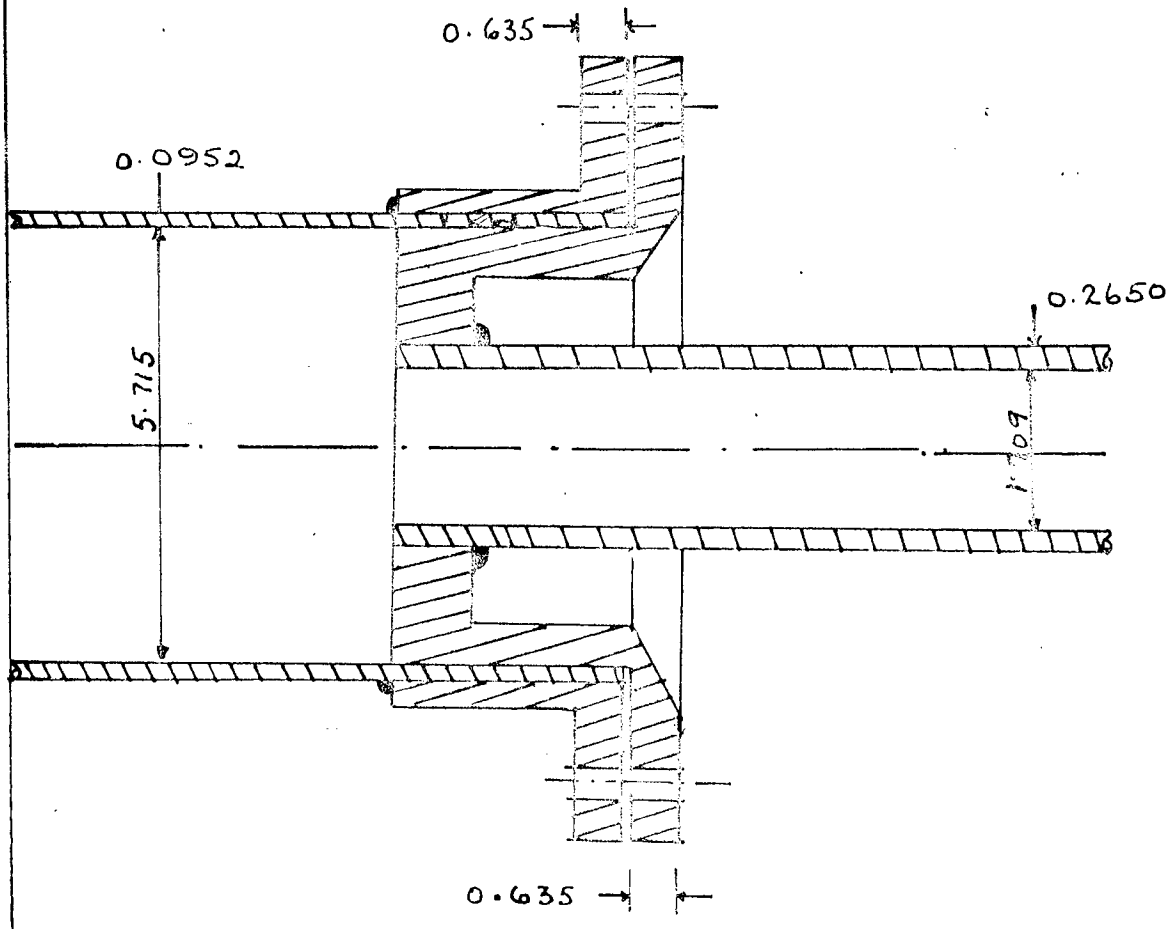

ALL DIMENSIONS — CENTIMETRES

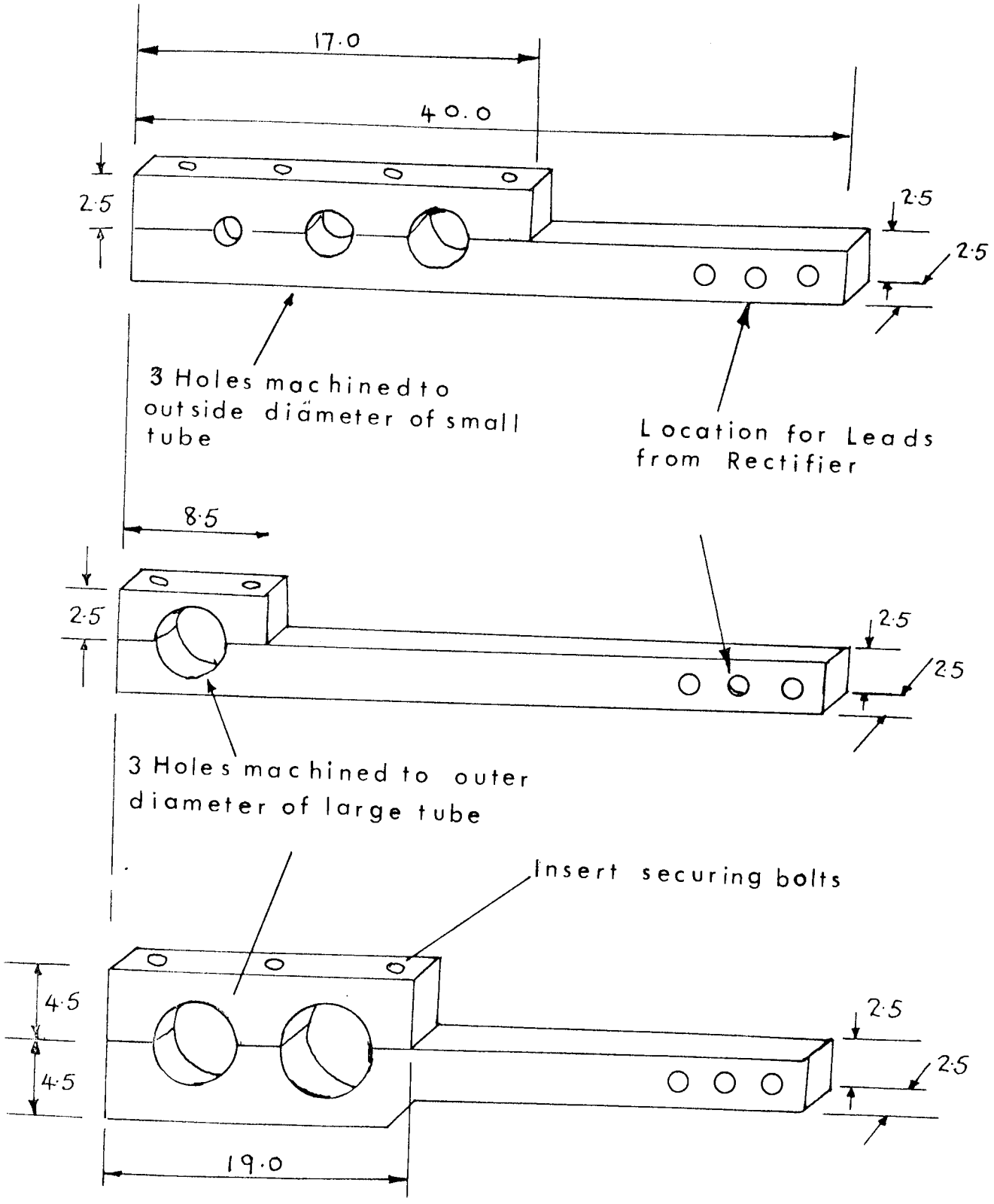

Material– Copper Dimensions– Centimetres

FIG 25 FITTINGS FOR POWER SUPPLY TO TEST SECTION

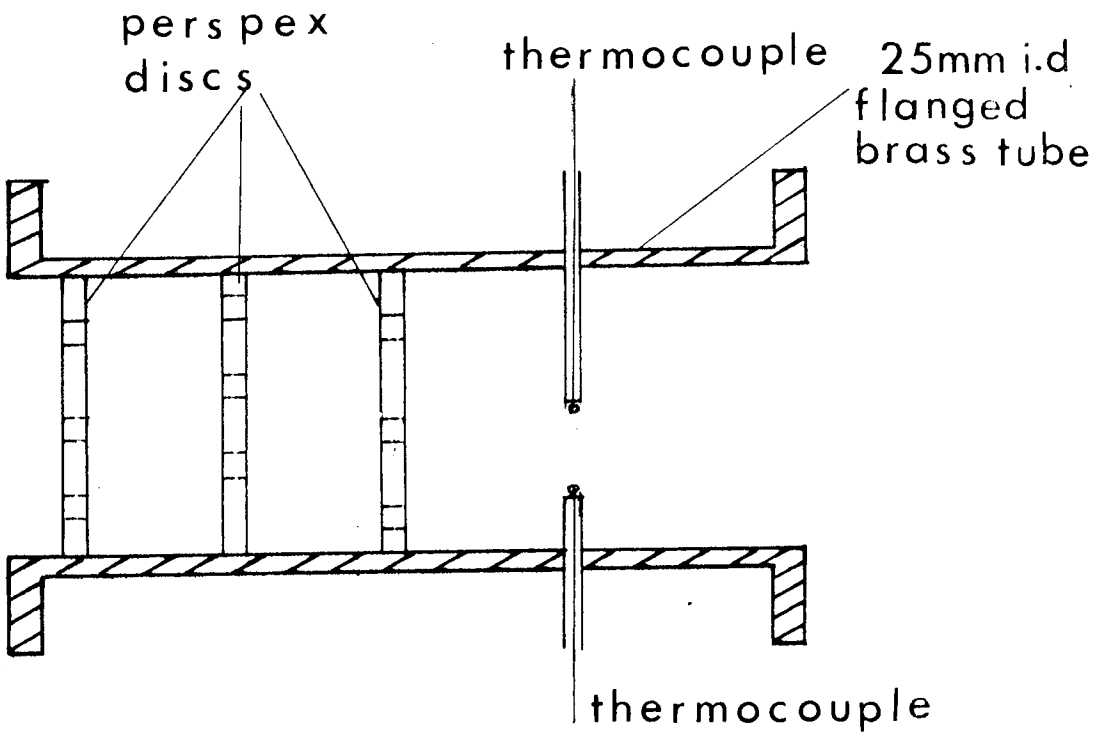

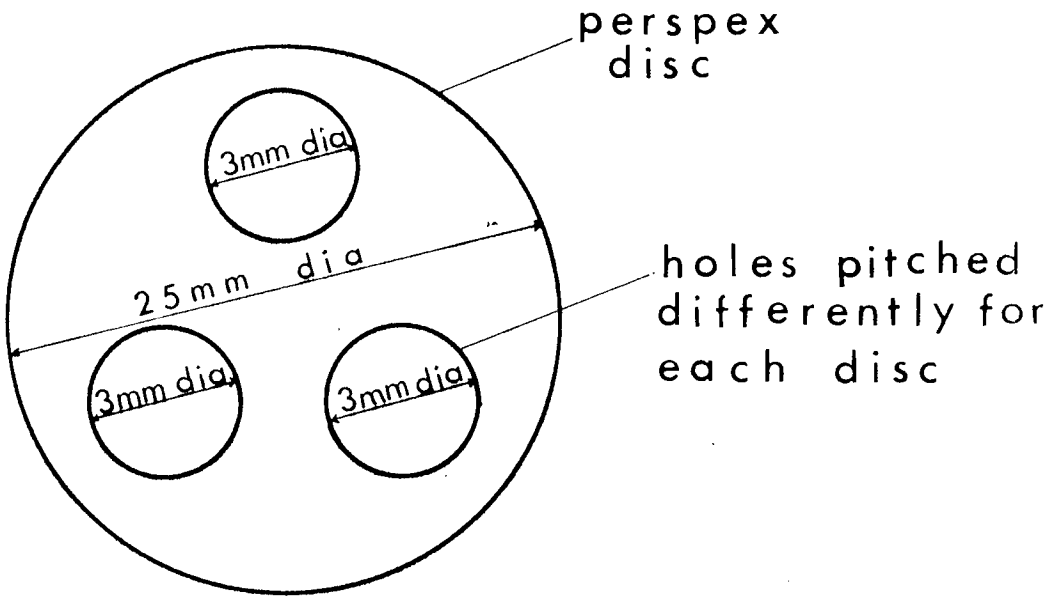

FIG 26 THE OUTLET MIXING TUBE

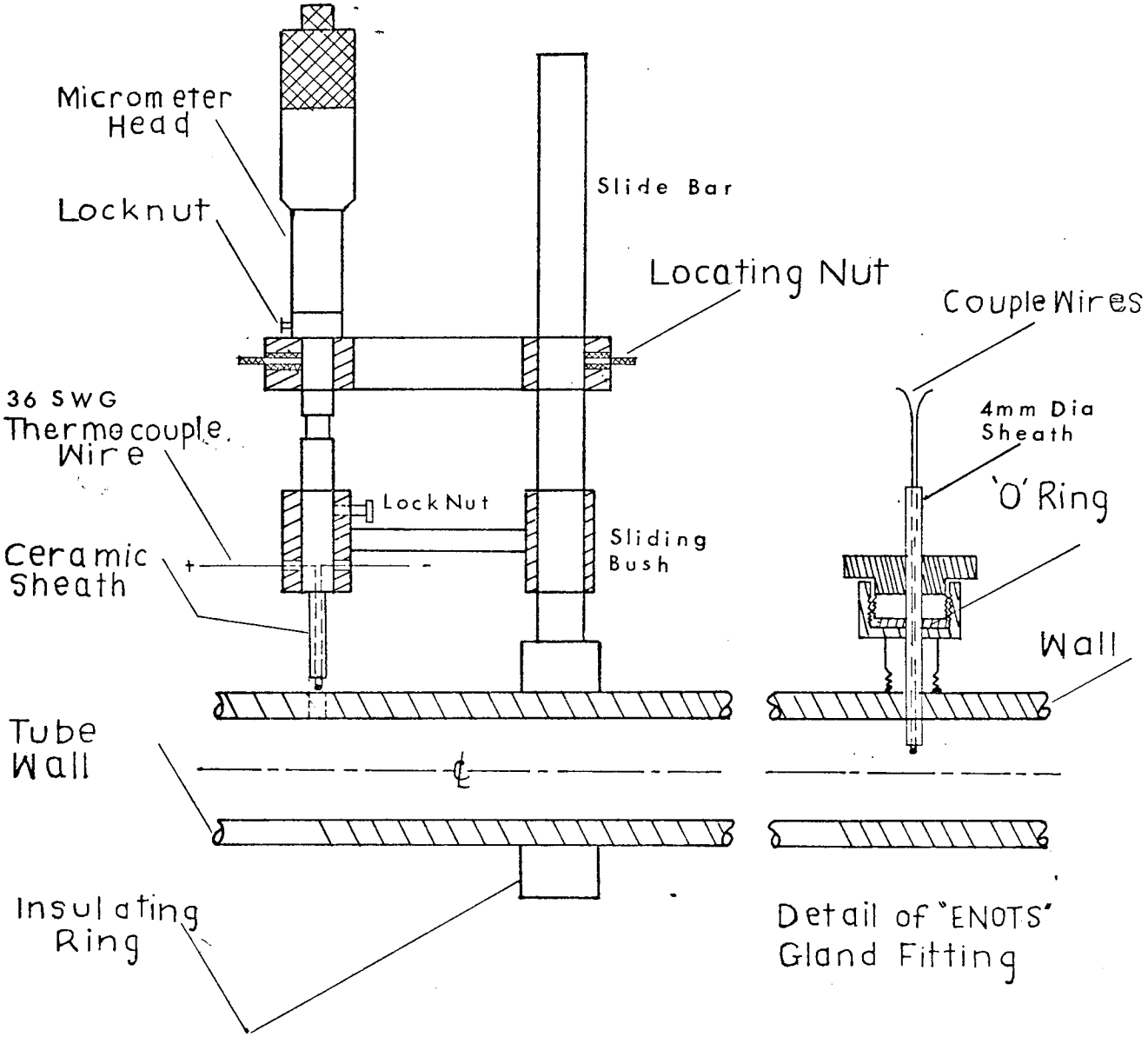

Fig.27 TEMPERATURE TRAVERSING ARRANGEMENT

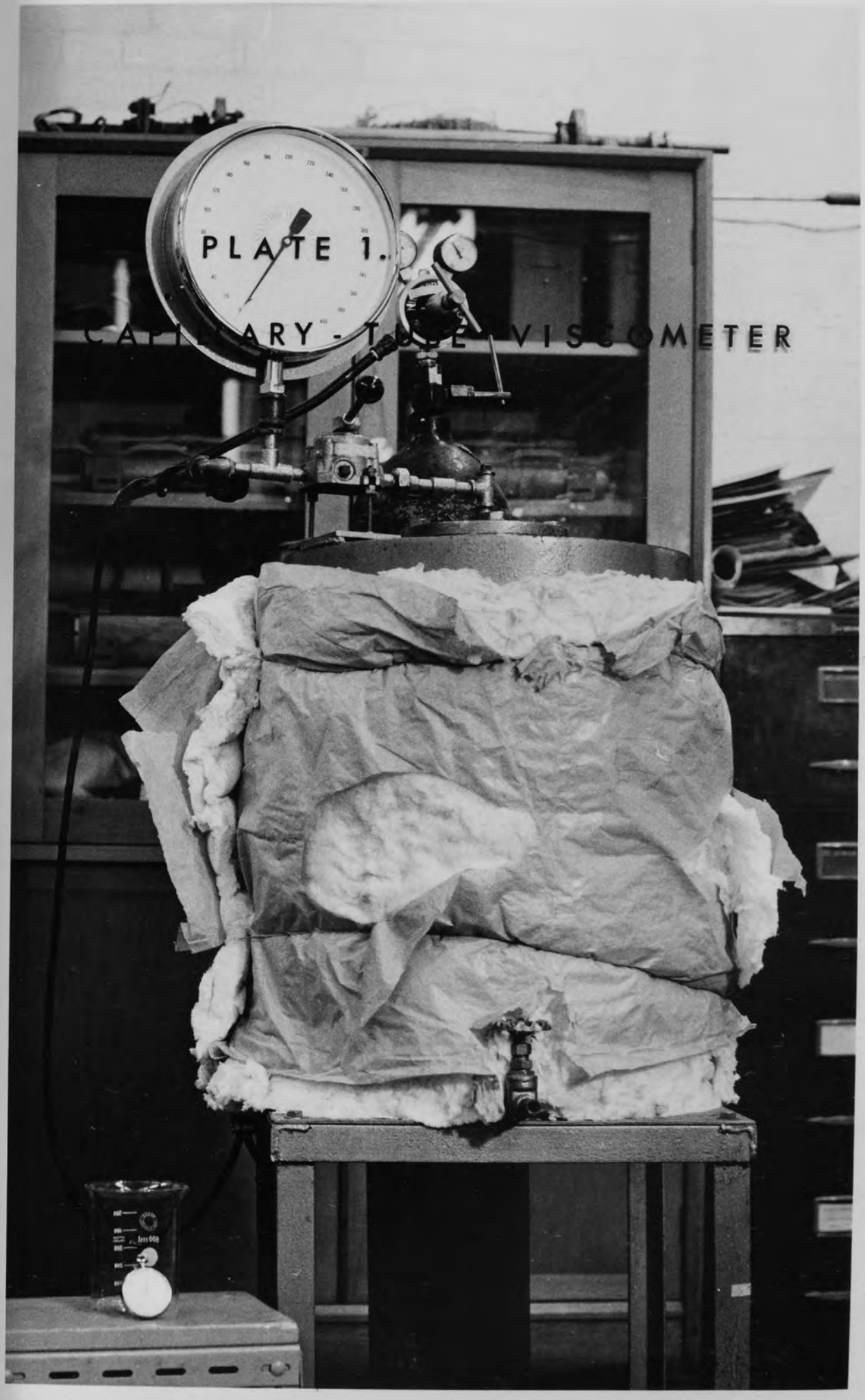

PLATE 1.

CAPILLARY-TUBE VISCOMETER

PIPE FLOW

being measured close to
uch as changes in diameter
he pipe is heated by direct
lectricity, and surface
measured by thermocouple.

APPENDIX THREE

TABLE 1

SHEAR STRESS - SHEAR RATE DATA

SILICONE OILS @ 25°C

F111/20CS		MSS550/125CS		F111/1000CS		F111/10000CS	
Shear Rate (sec^{-1})	Shear Stress (N/m^2)	Shear Rate (sec^{-1})	Shear Stress (N/m^2)	Shear Rate (sec^{-1})	Shear Stress (N/m^2)	Shear Rate (sec^{-1})	Shear Stress (N/m^2)
117		117	15.3	46.5	44.3	46.5	458.0
147	2.9	147	18.9	117	109.9	58.7	580.1
233	4.61	233	29.9	147	111.4	73.8	726.6
370	7.30	370	47.9	233	222.9	93.0	916.0
587	11.60	587	76.3	370	351.1	117	1129.7
930	18.17	930	121.5	587	555.7	147	1435.0
1171	22.90	1171	151.7	1171	1099.2	233	2198.4

TABLE 2

VISCOSITY VARIATION WITH TEMPERATURE

FOR 89.5% (W/W) AQUEOUS GLYCEROL

Temp ^{o}C	Viscometer Data (Cp)	Data from Ref (169) (Cp)	Data from Ref (173) (Cp)
20	-	205	215
25	-	143	150
30	106.4	105	107
35	80.2	79	80
40	62.0	57	-
45	46.9	47	-
50	-	34	-
60	-	21.7	-

TABLE 3

HEAT BALANCE

	Test No.	87	102	199	208	220	231	252	257	272	277	289	293	302
INPUT	Electrical (W)	6753	458	263	741	698	281	214	217	457	1255	285	393	675
	%	100	100	100	100	100	100	100	100	100	100	100	100	100
	Frictional (W) %	VISCOUS HEATING WAS FOUND TO BE NEGLIGIBLE IN ALL CASES												
	TOTAL (W)	6753	453	263	741	698	281	214	217	457	1255	285	393	675
OUTPUT	Copper Leads	2.76	2.76	2.76	2.76	2.76	2.76	2.76	2.76	2.76	2.76	2.76	2.76	2.76
	%	0.04	0.60	1.02	0.38	0.40	0.96	1.28	1.27	0.60	0.02	0.96	0.70	0.41
	Tube Ends %	THE HEAT LOSS FROM THE TUBE ENDS IS ASSUMED TO BE SMALL												
	Insulation	1.58	3.74	1.58	2.18	2.36	2.53	1.85	2.18	2.5	1.59	2.8	2.13	4.4
	%	0.03	0.80	0.6	0.30	0.35	0.88	0.86	1.0	0.54	0.01	0.97	0.54	0.66
	Fluid	6730	457	267	727	677	281	210	212	456	1240	384	386	660
	%	99.93	98.5	98.52	99.32	99.27	97.9	97.67	98.15	98.7	99.6	99.27	98.76	98.95
	TOTAL (W)	6735	464	271	732	682	287	215	217	462	1245	289	391	667
	BALANCE (W)	-18.0	+6.0	+8	-9.0	-16.0	+6.0	+1.0	0.0	+5.0	-10	+4.0	-2.0	-8.0
	%	-0.3	+1.2	+3.0	-1.2	-2.2	+2.0	+0.47	0.0	+1.09	-0.7	+1.4	-0.5	-1.1

TABLE 4

PHYSICAL PROPERTIES OF WATER AND STEAM

t ^{o}C	k $W/m^{o}C$	Cp KJ/kgK	ρ kg/m^{2}	β $(10^{-3})1/^{o}K$	$\mu \times 10^{6}$ NS/m
0	0.569	4.218	999.839	0.00	1786
10	0.587	4.192	999.700	0.01	1303
20	0.604	4.182	998.205	0.08	1002
30	0.619	4.178	995.651	0.14	798.4
40	0.632	4.179	992.219	0.19	653.9
50	0.644	4.181	998.037	0.24	547.8
60	0.654	4.184	993.037	0.28	468.3
70	0.663	4.189	977.765	0.33	404.7
80	0.670	4.196	971.793	0.36	353.3

TABLE 5

(a) Thermal Conductivity of Propylene Glycol and its Aqueous Solutions.

Temp °C	Propylene Glycol, % by wt.					
	0	20	40	60	80	100
	Thermal Conductivity, (cal)/(cm.s.°C)					
0	0.00139	0.00117	0.00100	0.00083	0.00068	0.00054
10	142	119	100	82	67	53
20	145	121	100	82	66	52
30	148	123	101	81	65	51
40	0.00151	0.00125	0.00101	0.00080	0.00064	0.00050
50	154	127	101	80	63	49
60	157	129	102	79	62	48
70	160	131	102	78	61	47

Figure:

(b) Viscosity of Aqueous Solutions of Propylene Glycol.

Temp °C	Propylene Glycol, % by wt.										
	0	10	20	30	40	50	60	70	80	90	100
	Absolute Viscosity, centipoises										
0	1.79	2.6	4.2	7.1	12.5	18.0	29.0	47.0	72.0	135.0	243.0
10	1.31	1.8	2.9	4.0	7.2	9.3	16.0	22.0	34.0	59.0	111.0
20	1.01	1.35	2.1	3.0	4.4	6.4	9.3	14.0	20.0	33.0	56.0
30	0.80	1.10	1.6	2.0	2.9	4.0	5.6	7.8	12.5	19.0	30.3
40	0.65	0.88	1.2	1.6	2.2	2.9	3.9	5.4	7.4	12.0	18.0
50	0.55	0.73	0.98	1.3	1.7	2.5	2.9	3.9	5.3	7.9	11.3
60	0.47	0.61	0.79	1.0	1.3	1.7	2.2	2.8	3.9	5.4	7.7
70	0.41	0.53	0.68	0.84	1.1	1.3	1.7	2.2	2.9	3.9	5.5

Figure:

Footnote: Tables a, b and d are as given by reference (209)
The units therefore do not conform to the S.I. system.

(c) Density of Aqueous Solutions of Propylene Glycol

Propylene Glycol, % by wt.	Temperature °C							
	0	10	20	30	40	50	60	70
	Density, (10^3 kG/m^3)							
0	0.9999	0.9997	0.9982	0.9957	0.9923	0.9881	0.9832	0.9778
10	1.0092	1.0082	1.0061	1.0030	0.9993	0.9946	0.9895	0.9837
20	1.0196	1.0178	1.0152	1.0111	1.0069	1.0015	0.9960	0.9898
30	1.0327	1.0282	1.0238	1.0187	1.0134	1.0076	1.0015	0.9950
40	1.0442	1.0376	1.0314	1.0256	1.0199	1.0133	1.0066	0.9997
50	1.0520	1.0445	1.0380	1.0316	1.0250	1.0178	1.0104	1.0033
60	1.0559	1.0490	1.0426	1.0353	1.0279	1.0208	1.0128	1.0046
70	1.0593	1.0517	1.0440	1.0364	1.0290	1.0216	1.0136	1.0055
80	1.0585	1.0510	1.0435	1.0360	1.0284	1.0208	1.0127	1.0045
90	1.0563	1.0488	1.0412	1.0337	1.0258	1.0183	1.0104	1.0024
100	1.0508	1.0435	1.0363	1.0288	1.0213	1.0137	1.0056	0.9977

(d) Specific Heat of Aqueous Propylene Glycol

Propylene Glycol, % by wt.	Temperature °C						
	0	10	20	30	40	50	60
	Specific Heat, (cal)/(g°C)						
0	1.009	1.002	0.999	0.997	0.998	0.998	0.999
10	0.994	0.990	0.989	0.989	0.989	0.990	0.992
20	0.968	0.965	0.963	0.963	0.965	0.968	0.973
30	0.934	0.934	0.935	0.937	0.940	0.944	0.949
40	0.890	0.893	0.897	0.902	0.907	0.912	0.918
50	0.838	0.845	0.852	0.860	0.868	0.877	0.885
60	0.792	0.799	0.807	0.817	0.827	0.837	0.847
70	0.735	0.745	0.754	0.765	0.777	0.788	0.801
80	0.680	0.692	0.703	0.716	0.728	0.741	0.753
90	0.623	0.636	0.648	0.662	0.675	0.688	0.702
100	0.565	0.579	0.593	0.607	0.622	0.635	0.649

TABLE 6

THERMAL CONDUCTIVITIES OF

POLYMER SOLUTIONS

W/mK

Temperature	25°C	50°C	75°C
*CMC (2%)	.627	0.604	0.605
*Methocel 60HG 2%	.604	0.634	-
Water	0.611	0.644	0.666

* Values determined at the National Engineering Laboratory, East Kilbride.

TABLE 7

COMPARISON OF DENSITIES OF POLYMER SOLUTIONS AND DISTILLED WATER

Temperature °C	Density kg/m ^{3}(10^{-1})		
	0.5% Methocel (60HG)	3.0% Methocel (60HG)	Distilled Water
12	-	1.007.0	0.99530
20	-	1.00624	0.99913
23	0.9987	1.00552	0.99760
25	0.9981	1.00504	0.99700
30	0.9969	1.00364	0.99592
35	-	1.00204	0.99406

TABLE 8

SHEAR STRESS - SHEAR RATE DATA

0.5%(w/w) METHOCEL (60HG)

(Reference Sample)

Temperature ^{o}C	20	22	25	28	30	33	37	40
Shear Rate Sec^{-1}	Shear Stress N/m^2							
318	1.83	1.77	1.68	1.50	1.49	1.36	1.23	1.10
475	2.66	2.54	2.36	2.18	2.18	1.85	1.70	1.65
628	3.44	3.27	2.99	2.81	2.81	2.45	2.24	2.18
791	4.32	4.08	3.74	3.48	3.48	3.03	2.78	2.72
950	51.5	4.88	4.46	4.13	4.13	3.62	3.32	3.18
n	0.955	0.957	0.957	0.957	0.957	0.957	0.957	0.957
K_N NS^n/m^2	.0070	.0065	.0059	.0055	.0055	.0049	.0045	.0041

TABLE 9

SHEAR STRESS - SHEAR RATE DATA

1%(w/w) METHOCEL (60HG)

(Reference Sample)

Temperature ^{o}C	20	25	28	32	36	40
Shear Rate Sec^{-1}	Shear Stress N/m^2					
318	3.41	2.91	2.69	2.36	2.11	1.92
475	4.97	4.22	3.89	3.43	3.06	2.75
628	6.53	5.59	5.07	4.47	3.98	3.57
790	8.25	7.01	6.42	5.65	5.01	4.50
950	9.97	8.50	7.69	6.74	6.00	5.40
n	0.980	0.977	0.960	0.960	0.954	0.944
K_N NS^n/m^2	.0119	.0104	.0105	.00925	.00086	.0083

TABLE 10

SHEAR STRESS - SHEAR RATE DATA

0.15%(w/w) CARBOPOL 934
(Reference Sample)

Temperature ^{o}C	25	30	40	50	55	60
Shear Rate Sec^{-1}	Shear Stress N/m^2					
147	8.8	7.5	7.19	6.47	5.17	5.04
233	11.7	10.17	9.57	8.62	6.878	6.70
370	15.9	13.69	13.00	11.71	9.35	9.11
465	18.5	15.93	15.14	13.62	10.88	10.9
587	21.5	18.51	17.61	15.83	12.70	12.35
930	29.0	25.00	23.75	21.35	17.05	16.80
1171	37.5	32.29	30.68	27.62	22.05	21.47
n	0.63	0.63	0.63	0.63	0.63	0.63
K_N NS^n/m^2	0.33	0.31	0.27	0.243	0.194	0.189

TABLE 11

SHEAR STRESS - SHEAR RATE DATA

0.25%(w/w) CARBOPOL 934
(Reference Sample 1)

Temperature ^{o}C	25	30	35	40	45	50	55	60
Shear Rate Sec^{-1}	Shear Stress N/m^2							
46.5	7.2	6.9	6.9	6.9	6.2	6.1	5.5	4.7
147	14.5	14.0	13.7	13.7	12.8	12.2	10.4	9.2
233	18.9	18.6	17.7	17.7	16.8	16.2	14.0	12.2
370	25.0	23.8	23.8	23.8	21.4	21.1	18.0	15.7
465	28.4	27.5	26.9	26.9	24.7	24.1	20.8	17.9
587	32.4	31.1	30.5	30.5	28.1	27.5	23.8	20.5
930	42.7	40.9	40.0	39.7	36.0	35.4	30.5	26.6
1171	48.9	46.4	46.2	45.8	41.2	40.6	34.8	30.5
n	0.586	0.588	0.588	0.586	0.586	0.586	0.588	0.584
K_N NS^n/m^2	0.77	0.75	0.73	0.70	0.69	0.65	0.61	0.52

TABLE 12

SHEAR STRESS - SHEAR RATE DATA

0.5%(w/w) CARBOPOL 934
(Reference Sample)

Temperature ^{o}C	25	30	35	40	45	50	55	60
Shear Rate Sec^{-1}	Shear Stress N/m^2							
46.5	30.5	29.0	29.0	26.6	25.0	24.4	24.4	24.4
147	44.3	43.7	42.7	38.2	38.2	38.2	38.2	36.3
233	53.4	53.4	50.7	46.7	46.7	45.8	45.8	41.2
370	64.1	63.2	61.0	56.5	56.5	55.0	55.0	48.2
465	70.2	69.6	68.1	62.3	62.3	59.5	59.5	52.8
587	76.3	76.3	75.1	68.7	68.7	67.2	67.2	58.0
930	94.7	94.7	90.1	80.9	80.9	79.4	77.9	71.8
1171	103.8	100.8	97.7	88.5	88.5	85.5	85.5	76.3
n	0.374	0.374	0.374	0.374	0.374	0.374	0.374	0.374
K_N NS^n/m^2	7.02	6.75	6.51	6.28	6.07	5.87	5.68	5.20

TABLE 13

SHEAR STRESS - SHEAR RATE DATA

0.5%(w/w) SODIUM CARBOXYMETHYL CELLULOSE (CMC)
(Reference Sample)

Temperature ^{o}C	20	25	30	35	40	45
Shear Rate Sec^{-1}	Shear Stress N/m^2					
147	2.60	2.44	1.98	1.80	1.68	1.62
233	4.12	3.70	3.14	2.75	2.63	2.53
370	6.30	5.62	4.76	4.15	3.85	3.79
465	7.80	6.90	5.89	5.19	4.89	4.67
587	9.62	8.24	7.15	6.41	5.98	5.86
738	11.60	10.23	8.55	7.94	7.42	7.18
930	14.05	12.52	10.53	9.77	9.16	8.85
1171	16.95	15.11	12.82	11.91	11.30	10.69
n	0.88	0.88	0.88	0.89	0.89	0.90
K_N NS^n/m^2	0.031	0.028	0.025	0.022	0.020	0.019

TABLE 14

SHEAR STRESS - SHEAR RATE DATA

1.0%(w/w) SODIUM CARBOXYMETHYL CELLULOSE (CMC)

(Reference Sample 1)

Temperature ^{o}C	20	25	30	35	40
Shear Rate Sec^{-1}	Shear Stress N/m^2				
147	0.885	0.794	0.733	0.641	0.64
233	1.33	1.191	1.053	0.931	0.92
370	1.893	1.710	1.527	1.343	1.211
465	2.259	2.015	1.801	1.664	1.551
587	2.717	2.443	2.137	1.893	1.862
930	3.786	3.389	3.053	2.687	2.691
1171	4.427	3.969	3.603	3.206	3.141
n	0.755	0.755	0.755	0.755	0.755
K_N NS^n/m^2	0.220	0.190	0.173	0.155	0.140

TABLE 15

SHEAR STRESS - SHEAR RATE DATA

0.25%(w/w) CARBOPOL 934
(Reference Sample 2)

Temperature ^{o}C	20	25	30	35	40
Shear Rate Sec^{-1}	Shear Stress N/m^2				
147	1.65	1.60	1.54	1.37	1.16
233	2.14	2.09	2.02	1.80	1.53
370	2.84	2.75	2.63	2.38	2.02
465	3.24	3.14	2.99	2.72	2.32
587	3.66	3.57	3.42	3.05	2.63
930	4.82	4.67	4.43	3.97	3.48
1171	5.50	5.34	5.07	4.58	3.97
n	0.582	0.579	0.579	0.575	0.576
K_N NS^n/m^2	0.91	0.88	0.85	0.82	0.80

TABLE 16

SHEAR STRESS - SHEAR RATE DATA

2.0%(w/w) METHOCEL (60 HG)
(Reference Sample)

Temperature ^{o}C	20	25	30	35	40
Shear Rate Sec^{-1}	Shear Stress N/m^2				
46.5	2.14	1.83	1.53	1.53	1.22
147	6.11	5.50	4.58	4.27	3.66
233	9.77	8.55	7.79	6.72	5.80
370	15.27	13.43	12.21	9.47	9.10
465	18.93	16.49	15.27	11.60	11.30
587	23.20	20.46	18.93	14.35	14.05
930	35.42	31.45	28.70	22.56	21.98
1171	43.97	38.17	34.81	27.78	26.56
n	0.913	0.913	0.913	0.913	0.913
K_N NS^n/m^2	0.069	0.059	0.053	0.047	0.041

TABLE 17

SHEAR STRESS - SHEAR RATE DATA

1.0%(w/w) SODIUM CARBOXYMETHYL CELLULOSE (CMC)
(Reference Sample 2)

Temperature ^{o}C	20	25	30	35	40
Shear Rate Sec^{-1}	Shear Stress N/m^2				
147	0.90	0.84	0.73	0.68	0.67
233	1.31	1.22	1.07	0.99	0.98
370	1.89	1.74	1.53	1.41	1.28
465	2.27	2.02	1.77	1.65	1.56
587	2.70	2.44	2.08	1.89	1.86
734	3.21	2.87	2.50	2.26	2.26
930	3.76	3.36	2.93	2.75	2.69
1171	4.36	3.97	3.51	3.24	3.14
n	0.76	0.76	0.76	0.76	0.76
K_N NS^n/m^2	0.220	0.190	0.173	0.155	0.138

TABLE 18

SHEAR DEGRADATION OF 0.15%(w/w) CARBOPOL 934

(All measurements taken at 25°C)

Circulation Period (Hours)	0	1	6	27	85
Shear Rate Sec^{-1}	Shear Stress N/m^2				
46.5	8.6	4.7	4.6	-	-
147	14.27	9.2	9.2	5.10	4.4
233	17.70	11.6	11.6	7.0	6.0
370	22.23	15.3	15.0	9.8	8.5
587	28.22	19.7	18.0	13.4	11.6
930	35.94	26.1	23.0	18.3	16.0
1171	41.12	29.8	26.0	21.5	18.9
n	0.51	0.57	0.61	0.68	0.70
K_N NS^n/m^2	1.14	0.52	0.46	0.18	0.13

TABLE 19

SHEAR DEGRADATION OF 0.25%(w/w) CARBOPOL 934

(All measurements taken at 20°C)

Circulation Period (Hours)	0	5	8	16	40
Shear Rate Sec^{-1}	Shear Stress N/m^2				
14.7	35.1	11.0	-	-	-
46.5	48.2	25.6	7.20	6.9	3.3
147	70.8	41.2	14.50	13.4	7.9
233	84.0	50.4	18.90	17.7	11.0
370	97.7	61.4	25.04	23.7	15.27
465	106.9	68.4	28.40	27.2	18.00
587	119.1	76.0	32.36	31.1	20.46
930	143.5	93.1	42.75	40.6	28.40
1171	158.8	103.8	48.85	47.0	32.67
n	0.382	0.433	0.57	0.59	0.67
K_N NS^n/m^2	10.5	4.85	0.83	0.72	0.30

TABLE 20

COMPARISON OF VALUES OF FLOW INDEX (n)

Material	Author	n	Equipment (Viscometer)
0.5% CMC (Cellofas B50)	Present	0.90	Cone and Plate
0.42% CMC (F700)	Thomas (187)	0.80	Pipeline - 25mm dia.
*0.6% CMC (High)	Wasserman (198)	0.70	Not stated
*1.5% CMC (Medium)	Wasserman (198))	0.89	Not stated
0.67% CMC	Metzner/Reed (116)	0.72	Capillary - 22mm dia.
1.0% CMC	Mitshaishi/ Miyatake (123)	0.76	Cone and Plate
1.0% CMC	Present	0.76	Cone and Plate
**0.5% Carbopol 934(I)	Present	0.40-0.53	Cone and Plate
**0.5% Carbopol 934(II)	Present	0.54-0.65	Cone and Plate
0.6% Carbopol 934	Metzner/Friend (119)	0.6 -0.65	Capillary
0.5% Carbopol 934	Mahalingham (102)	0.44	Cone and Plate
0.25% Carbopol 934	Present	0.6 -0.67	Cone and Plate
0.25% Carbopol 934	Mahalingham (102)	0.61	Cone and Plate
0.25% Carbopol 934	Bogue/Metzner (15)	0.8	Capillary
0.15% Carbopol 934	Mahalingham (102)	0.70	Cone and Plate
0.15% Carbopol 934	Present	0.63-0.70	Cone and Plate

* Wasserman's CMC data were for the high and medium molecular weight grades.

**In the present experiments label (I) indicate solution used for divergence tests while label (II) refer to same solution but slightly degraded used for convergence tests.

TABLE 21

TABLE OF CONSTANTS A AND B
IN THE EQUATION $K_N = Ae^{B/T}$

MATERIAL	A	B
0.5% MC	0.2297×10^{-5}	0.3063×10^{4}
1.0% MC	0.5508×10^{-4}	0.2245×10^{4}
2.0% MC	0.2986×10^{-3}	0.2269×10^{4}
0.5% CMC	0.4300×10^{-3}	0.1931×10^{4}
1.0% CMC	0.1630×10^{-2}	0.21107×10^{4}
0.15% CPM	0.4506	0.6029×10^{3}
0.25% CPM	0.9865	0.6154×10^{3}
0.50% CPM	6.9472	0.6897×10^{3}

TABLE 22

DETAILS OF HEAT TRANSFER TESTS

Configuration: 3.34 : 1 Convergence

Test No.	Material	Flow Index n	Flow Rate $\dot{m}$ kg/sec	Flux, x_2 W/m² Nominal Downstrm	Generalised Reynolds Number Re'		Generalised Prandtl Number Pr'		Grashof Number Gr_b
					Upstream $Z/D_1 = 48$	Downstream $Z/D_2 = 0.5$	Upstream $Z/D_1 = 48$	Downstream $Z/D_2 = 0.5$	Downstream $Z/D_2 = 40$
81	WATER	1.0	.4601	12735	10483	35047	6.7	6.7	7559
82	WATER	1.0	.50292	18661	11199	37441	6.2	6.2	14202
83	WATER	1.0	.4601	4806	10310	34468	6.9	6.9	2741
84	WATER	1.0	.4601	9594	10928	36535	6.4	6.4	7624
85	WATER	1.0	.5516	19435	13771	46040	6.0	6.0	14138
87	WATER	1.0	.5516	28413	14534	48592	5.7	5.7	23693
88	WATER	1.0	.3760	4869	8439	28214	6.8	6.8	3090
89	WATER	1.0	.3760	9497	8700	29085	6.6	6.6	7373
90	WATER	1.0	.3760	16143	8904	29768	6.4	6.4	13582
91	WATER	1.0	.361	9352	8340	27884	6.6	6.6	7219
92	WATER	1.0	.361	15867	8469	28315	6.5	6.5	13705
93	WATER	1.0	.361	20676	8613	28799	6.3	6.3	17760
101	100%	1.0	.5114	3698	209	700	622	622	161
102	GLYCOL	1.0	.5114	4956	211	702	612	612	208
103	"	1.0	.5114	709	205	682	634	634	33
104	"	1.0	.357	4668	150	502	607	607	223
105	"	1.0	.4453	3340	182	608	621	621	134
106	"	1.0	.4432	3391	180	601	626	626	141

TABLE 22 continued

DETAILS OF HEAT TRANSFER TESTS

Configuration: 3.34 : 1 Convergence

Test No.	Material	Flow Index n	Flow Rate $\dot{m}$ kg/sec	Flux x_2 W/m² Nominal Downstrm	Generalised Reynolds Number Re'		Generalised Prandtl Number Pr'		Grashof Number Gr_b
					Upstream $Z/D_1 = 48$	Downstream $Z/D_2 = 0.5$	Upstream $Z/D_1 = 48$	Downstream $Z/D_2 = 0.5$	Downstream $Z/D_2 = 40$
107	100%	1.0	.3452	2590	141	472	619	619	132
108	GLYCOL	1.0	.3229	2200	132	443	619	619	126
109	"	1.0	.3082	2209	127	423	620	620	126
110	"	1.0	.3067	2329	126	421	620	620	135
111	"	1.0	.2431	2180	101	337	614	614	143
112	"	1.0	.6396	3135	292	975	565	565	163
113	"	1.0	.3338	2524	155	518	554	554	164
114	"	1.0	.7227	4601	427	1429	440	440	311
115	"	1.0	.7727	4066	460	1538	440	440	279
116	"	1.0	.3823	2967	230	968	436	436	255
117	"	1.0	.4886	2730	292	977	437	437	258
119	"	1.0	.6510	3955	389	1300	439	439	300
120	"	1.0	.3423	2789	206	687	436	436	278
121	"	1.0	.3410	1102	203	677	441	441	121
123	"	1.0	.8620	3715	786	2627	297	297	599
125	"	1.0	.3189	2348	131	437	622	622	132
126	"	1.0	.3507	2839	214	714	431	431	281
127	"	1.0	.6428	3729	387	1293	435	435	296
128	"	1.0	.3555	3261	216	721	432	432	266

TABLE 22 continued

DETAILS OF HEAT TRANSFER TESTS

Configuration: 3.34 : 1 Convergence

Test No.	Material	Flow Index n	Flow Rate $\dot{m}$ kg/sec	Flux x_2 W/m² Nominal Downstrm	Generalised Reynolds Number Re' Upstream $Z/D_1 = 48$	Generalised Reynolds Number Re' Downstream $Z/D_2 = 0.5$	Generalised Prandtl Number Pr' Upstream $Z/D_1 = 48$	Generalised Prandtl Number Pr' Downstream $Z/D_2 = 0.5$	Grashof Number Gr_b Downstream $Z/D_2 = 40$
129A	100%	1.0	.3799	2852	232	776	429	429	275
129B	GLYCOL	1.0	.3799	2894	235	786	424	424	302
129M	"	1.0	.3799	2894	234	782	426	426	289
131	"	1.0	.7614	4609	696	2329	296	296	588
134	"	1.0	.4026	3003	370	1237	295	295	627
137	"	1.0	.3847	3006	352	1177	294	294	622
138	"	1.0	.3799	2075	347	1160	295	295	420
139	79.5%	1.0	.5754	6236	1250	4179	114	114	1602
140	GLYCOL	1.0	.5600	5528	969	3238	141	141	1112
141	"	1.0	.5633	5261	850	2842	160	160	1370
142	"	1.0	.4513	2662	676	2259	161	161	1053
143	"	1.0	.4286	2707	645	2156	161	161	1071
144	"	1.0	.4334	2734	651	2176	161	161	1074
145	"	1.0	.4253	2800	640	2141	160	160	1097
146	"	1.0	.1916	1547	290	969	160	160	1037
147	"	1.0	.5828	5425	880	2944	160	160	1088
148	"	1.0	.4274	2600	640	2140	161	161	1065
149	"	1.0	.1332	1506	202	675	159	159	1207

TABLE 22 continued

DETAILS OF HEAT TRANSFER TESTS

Configuration: 3.34 : 1 Convergence

Test No.	Material	Flow Index n	Flow Rate $\dot{m}$ kg/sec	Flux x_2 W/m² Nominal Downstrm	Generalised Reynolds Number Re'		Generalised Prandtl Number Pr'		Grashof Number Gr_b
					Upstream $Z/D_1 = 48$	Downstream $Z/D_2 = 0.5$	Upstream $Z/D_1 = 48$	Downstream $Z/D_2 = 0.5$	Downstream $Z/D_2 = 40$
150	79.5%	1.0	.4318	2573	646	2161	161	161	983
151	GLYCOL	1.0	.6699	7098	1014	3393	160	160	977
152	"	1.0	.4302	2330	645	2157	161	161	996
153	"	1.0	.4286	2492	642	2149	161	161	1104
154	"	1.0	1.1753	14413	3940	13179	76	76	3939
155	"	1.0	.6007	10776	3024	6767	76	76	4814
156	"	1.0	.4854	7875	1634	5475	76	76	4498
157	"	1.0	.4821	7703	1630	5450	76	76	4566
158	"	1.0	.4653	7859	1564	5230	76	76	4709
159	"	1.0	.1802	1818	602	2012	76	76	5209
160	"	1.0	.4432	7492	1489	4978	76	76	4461
161	"	1.0	.4790	8170	1614	5396	76	76	4951
162A	"	1.0	.4627	7364	1558	5208	76	76	4513
162M	"	1.0	.4627	7147	1559	5211	76	76	4461
163	"	1.0	.8880	9000	1346	4499	160	160	925
164	"	1.0	.2711	2036	407	1362	161	161	1162
165	"	1.0	.8701	4511	1805	6035	120	120	742
166	"	1.0	.8701	4511	1805	6035	120	120	742
167	"	1.0	.8701	1468	1789	5981	120	120	204

TABLE 22 continued

DETAILS OF HEAT TRANSFER TESTS

Configuration: 3.34 : 1 Convergence

Test No.	Material	Flow Index n	Flow Rate $\dot{m}$ kg/sec	Flux x_2 W/m² Nominal Downstrm	Generalised Reynolds Number Re'		Generalised Prandtl Number Pr'		Grashof Number Gr_b
					Upstream $Z/D_1 = 48$	Downstream $Z/D_2 = 0.5$	Upstream $Z/D_1 = 48$	Downstream $Z/D_2 = 0.5$	Downstream $Z/D_2 = 40$
168	79.5%	1.0	.4921	12345	1069	3575	114	114	3983
169A		1.0	.4921	2996	1024	3424	119	119	1004
169B	"	1.0	.4921	3136	1002	3348	119	119	1036
170	"	1.0	.4805	1575	994	3322	119	119	497
171	"	1.0	.1786	3136	382	1276	116	116	4025
172	"	1.0	.1786	1135	371	1241	119	119	1394
178	"	1.0	.9286	1368	11150	3335	71.5	71.5	28803
179	"	1.0	.9201	1864	11101	3320	71.2	71.2	332668
180	"	1.0	.6357	833	7646	2287	71.4	71.4	24408
181	"	1.0	.6039	922	7288	2180	71.2	71.2	27815
182	"	1.0	.5227	819	6252	1870	71.8	71.8	23984
183	"	1.0	.5227	855	6262	1873	71.7	71.7	24599
184	"	1.0	.4854	818	5857	1752	71.2	71.2	21479
185	"	1.0	.4546	772	5573	1667	71.8	71.8	21217
186	"	1.0	.4773	800	5723	1712	71.6	71.6	25367
187	"	1.0	.1834	557	2213	662	71.2	71.2	188775
188	"	1.0	.0522	172	617	185	72.7	72.7	68243
189	"	1.0	.1263	173	1490	446	72.7	72.7	58483
190	"	1.0	.3036	678	3609	1080	72.2	72.2	407493

TABLE 22 continued

DETAILS OF HEAT TRANSFER TESTS

Configuration: 1 : 3.34 Divergence

Test No.	Material	Flow Index n	Flow Rate $\dot{m}$ kg/sec	Flux x_2 W/m² Nominal Downstrm	Generalised Reynolds Number Re'		Generalised Prandtl Number Pr'		Grashof Number Gr_b
					Upstream $Z/D_1 = 100$	Downstream $Z/D_2 = 0.0$	Upstream $Z/D_1 = 100$	Downstream $Z/D_2 = 0.0$	Downstream $Z/D_2 = 40$
192					NON-NEWTONIAN TESTS				
192	0.5%	.96	.5812	1061	7795	2017	38.2	44.2	15054
193	METHO-	.96	.4562	1091	5790	1498	40.5	46.9	21850
194	CEL	.96	.5077	593	6445	1668	40.6	46.9	12157
195	"	.96	.4729	1062	5990	1550	40.6	47.0	17771
196	"	.96	.4441	631	5605	1451	40.8	47.1	10939
197	"	.96	.4497	616	5819	1506	39.8	46.0	16659
198	"	.96	.2371	704	5804	1502	39.2	45.3	14811
199	"	.96	.2371	532	3081	797	39.6	45.8	14604
200	1.0%	.96	.7608	585	7799	2018	49.2	56.9	8215
201	METHO-	.96	.4545	506	4585	1187	50.1	57.9	10229
202	CEL	.96	.4412	504	4446	1151	50.2	58.0	10470
203	"	.96	.4327	312	4352	1126	50.3	58.1	15243
204	"	.96	.4346	311	4378	1133	50.2	58.0	14117
205	"	.96	.3515	320	5321	912	50.4	58.3	13721
206	"	.96	.4821	595	4886	1264	49.9	57.7	18483
207	"	.96	.3368	361	3359	869	50.6	58.4	12041

TABLE 22 continued

DETAILS OF HEAT TRANSFER TESTS

Configuration: 1 : 3.34 Divergence

Test No.	Material	Flow Index n	Flow Rate $\dot{m}$ kg/sec	Flux x_2 W/m² Nominal Downstrm	Generalised Reynolds Number Re'		Generalised Prandtl Number Pr'		Grashof Number Gr_b
					Upstream $Z/D_1 = 100$	Downstream $Z/D_2 = 0.0$	Upstream $Z/D_1 = 100$	Downstream $Z/D_2 = 0.0$	Downstream $Z/D_2 = 40$
208	0.15%	.63	.5290	1498	1500	118	179	684	259
209	CARBO-	.64	.5290	502	1610	131	167	615	100
210	POL	.64	.4621	882	1458	118	161	593	210
211	"	.66	.4441	888	1278	112	177	605	206
212	"	.68	.4545	504	1320	124	174	555	109
213	"	.67	.4529	697	1474	133	156	514	242
214	"	.68	.3864	713	1284	121	153	487	243
215	"	.69	.3880	795	1244	121	158	487	265
216	"	.69	.2286	890	657	64	176	543	317
217	"	.69	.2286	332	657	64	177	543	103
218	"	.70	.3880	781	1427	144	138	409	359
219	"	.70	.3896	1271	1710	172	115.7	344.4	733
220	0.25%	.59	.4643	1410	723	49	326	1441	586
221	CARBO-	.59	.4643	481	722	49	327	1443	17
222	POL	.60	.2386	493	282	19	429	1893	17
223	"	.61	.2906	912	387	27	382	1650	35
224	"	.64	.3247	1153	531	39	310	1273	63
225	"	.64	.3166	653	529	43	304	1119	44
226	"	.64	.3231	891	544	44	302	1113	65

TABLE 22 continued

DETAILS OF HEAT TRANSFER TESTS

Configuration: 1 : 3.34 Divergence

Test No.	Material	Flow Index n	Flow Rate $\dot{m}$ kg/sec	Flux x_2 W/m² Nominal Downstream	Generalised Reynolds Number Re′		Generalised Prandtl Number Pr′		Grashof Number Gr_b
					Upstream $Z/D_1 = 100$	Downstream $Z/D_2 = 0$	Upstream $Z/D_1 = 100$	Downstream $Z/D_2 = 0$	Downstream $Z/D_2 = 40$
226	0.25%	.64	.3231	891	544	44	302	1113	65
227	CARBO-	.67	.7337	1420	2249	204	166	548	300
228	POL	.67	.5828	1116	1456	132	203	672	175
229	0.50%	.39	.6090	1543	506	17	612	5576	5
230	CARBO-	.42	.280	659	151	6.0	943	7705	2
231	POL	.45	.1570	568	74	3	1083	7933	2
232	"	.47	.7088	953	783	34	459	3130	7
233	"	.48	.5034	862	513	23	497	3269	9
234	"	.50	.2020	512	134	7	767	4688	3
235	"	.53	.1173	498	61	3	978	5366	3

TABLE 22 continued

DETAILS OF HEAT TRANSFER TESTS

Configuration: 3.34 : 1 Convergence

Test No.	Material	Flow Index n	Flow Rate $\dot{m}$ kg/sec	Flux x_2 W/m² Nominal Downstrm	Generalised Reynolds Number Re'		Generalised Prandtl Number Pr'		Grashof Number Gr_b
					Upstream $Z/D_1 = 48$	Downstream $Z/D_2 = 0.5$	Upstream $Z/D_1 = 48$	Downstream $Z/D_2 = 0.5$	Downstream $Z/D_2 = 40$
236	0.5%	.54	.7390	5798	66	1159	1714	324	32
238	CARBO-	.55	.7401	3220	73	1239	1549	304	17
239	POL	.56	.4708	3356	46	754	1561	317	26
240	"	.58	.3052	2210	28	431	1648	360	15
241	"	.60	.2012	1238	18	259	1680	395	8
242	"	.60	.2524	2405	26	373	1460	343	18
243	"	.64	.5875	3917	111	1364	804	218	45
244	"	.64	.6123	4228	117	1442	792	215	46
245	"	.65	.3517	2904	58	691	916	258	32
246	2.0%	.91	1.217	5037	595	2726	314	229	36
247	METH-	.91	0.185	1854	77	354	367	368	18
248	OCEL	.91	0.344	3667	152	696	347	253	32
249	"	.91	0.548	4601	252	1155	333	243	42
250	"	.91	0.627	4624	290	1329	331	242	42
251	"	.91	0.348	3308	153	703	347	253	29
252	"	.91	.1396	2336	57	262	373	272	25
253	"	.91	.344	4346	153	700	344	251	42
254	"	.91	.688	5586	327	1497	322	235	55

TABLE 22 continued

DETAILS OF HEAT TRANSFER TESTS

Configuration: 3.34 : 1 Convergence

Test No.	Material	Flow Index n	Flow Rate $\dot{m}$ kg/sec	Flux x_2 W/m² Nominal Downstrm	Generalised Reynolds Number Re′		Generalised Prandtl Number Pr′		Grashof Number Gr_b
					Upstream $Z/D_1 = 48$	Downstream $Z/D_2 = 0.5$	Upstream $Z/D_1 = 48$	Downstream $Z/D_2 = 0.5$	Downstream $Z/D_2 = 40$
255	2.0%	.91	.847	7344	408	1867	318	232	53
	METHOCEL								
256	0.25%	.56	.809	1553	76	1242	1650	335	22
257	CARBO-	.58	.169	169	9	138	2884	630	5
258	POL	.58	.561	970	51	780	1692	370	20
259	"	.58	.284	389	20	313	2138	467	13
260	"	.59	.500	895	49	720	1576	357	24
261	"	.60	.282	400	23	326	1894	445	13
262	"	.60	.627	1357	77	1098	1251	294	35
263	"	.60	.787	2297	133	1893	911	214	74
264	1.0%	.76	.811	7449	269	2146	465	195	65
265	CMC	.76	.295	3160	77	614	592	248	34
266	"	.76	.356	3942	97	774	566	237	45
267	"	.76	.595	5768	184	1469	497	209	68
268	"	.76	.648	5785	204	1625	490	206	59
269	"	.76	.354	3821	97	770	565	237	45
270	"	.76	.552	5837	167	1332	509	214	65

TABLE 22 continued

DETAILS OF HEAT TRANSFER TESTS

Configuration: 3.34 : 1 Convergence

Test No.	Material	Flow Index n	Flow Rate $\dot{m}$ kg/sec	Flux x_2 W/m² Nominal Downstrm	Generalised Reynolds Number Re'		Generalised Prandtl Number Pr'		Grashof Number Gr_b
					Upstream $Z/D_1 = 48$	Downstream $Z/D_2 = 0.5$	Upstream $Z/D_1 = 48$	Downstream $Z/D_2 = 0.5$	Downstream $Z/D_2 = 40$
271	1.0%	.76	.826	10875	277	2205	460	193	100
272	CMC	.78	.150	4983	39	287	595	268	69
273	"	.78	.828	8221	308	2280	415	187	77
274	0.5%	.90	.900	6631	1204	5780	115	80	196
275	CMC	.90	.190	1168	219	1050	133	93	153
276	"	.90	.446	2985	579	2779	118	82	249
277	"	.90	.676	4776	915	4392	113	79	191
278	"	.90	.425	3040	588	2825	111	77	289
279	"	.90	.628	4777	913	4384	105	73	254

TABLE 22 continued

DETAILS OF HEAT TRANSFER TESTS

Configuration: 1 : 3.34 Divergence

Test No.	Material	Flow Index n	Flow Rate $\dot{m}$ kg/sec	Flux, x_2 W/m² Nominal Downstrm	Generalised Reynolds Number Re′		Generalised Prandtl Number Pr′		Grashof Number Gr_b
					Upstream $Z/D_1 = 100$	Downstream $Z/D_2 = 0$	Upstream $Z/D_1 = 100$	Downstream $Z/D_2 = 0$	Downstream $Z/D_2 = 40$
280	0.5%	.90	.9300	1629	7536	1569	64	91	7188
281	CMC	.90	.1335	388	891	185	77	111	2081
282	"	.90	.6527	1306	6463	1556	52	65	13526
283	"	.90	.4345	1096	4202	1012	53	66	12710
284	"	.90	.6242	1566	6169	1485	52	65	17165
285	"	.90	.8864	2688	1022	2462	45	55	32723
286	"	.90	.8581	1866	9827	2366	45	56	21019
287	"	.90	.5123	1097	5714	1375	46	57	16270
288	1.0%	.82	.7610	2264	1726	269	227	435	718
289	CMC	.82	.1063	577	170	27	321	616	140
290	"	.82	.7281	2025	1635	255	229	439	630
291	"	.82	.4933	1626	1034	161	245	471	493
292	"	.82	.5787	1395	1247	194	239	458	395
293	"	.82	.3087	794	618	96	258	494	206
294	"	.82	.3087	513	617	96	258	495	130
295	"	.82	.600	1641	1353	211	228	438	509
296	"	.82	.642	1992	1467	229	226	433	704
297	"	.82	.3511	1340	718	112	252	483	397

TABLE 22 continued

DETAILS OF HEAT TRANSFER TESTS

Configuration: 1 : 3.34 Divergence

Test No.	Material	Flow Index n	Flow Rate $\dot{m}$ kg/sec	Flux x_2 W/m² Nominal Downstrm	Generalised Reynolds Number Re'		Generalised Prandtl Number Pr'		Grashof Number Gr_b
					Upstream $Z/D_1 = 100$	Downstream $Z/D_2 = 0$	Upstream $Z/D_1 = 100$	Downstream $Z/D_2 = 0$	Downstream $Z/D_2 = 40$
298	1.0%	.82	.8087	2697	2242	350	186	357	1372
299	CMC	.82	.8087	539	2231	348	187	359	195
300	"	.82	.3579	289	850	133	217	417	85
301	"	.82	.6231	458	1639	256	196	376	142
302	"	.82	.2140	1363	470	73	234	449	531
303	"	.82	.2140	299	466	73	237	454	114
					RADIAL TRAVERSING TESTS				
304	WATER	1.0	.634	3833	47199	14120	6.9	6.9	846761
305	"	1.0	.845	5204	62907	18822	6.9	6.9	896800
306	"	1.0	.854	5179	63585	19025	6.9	6.9	836065
307	"	1.0	.854	2181	63585	19025	6.9	6.9	358313
308	"	1.0	.521	2453	38744	11600	6.8	6.8	654234
309	"	1.0	.521	1004	38744	11600	6.8	6.8	281659
311	0.25%	.56	.750	2176	1010	62	376	1847	949
312	CARBO-	.56	.750	988	1010	62	376	1847	542
313	POL	.56	.795	1623	2145	131	188	922	762
314	"	.56	.795	410	2145	131	188	922	196

TABLE 22 continued

DETAILS OF HEAT TRANSFER TESTS

Configuration: 1 : 3.3 Divergence

Test No.	Material	Flow Index n	Flow Rate $\dot{m}$ kg/sec	Flux x_2 W/m² Nominal Downstrm	Generalised Reynolds Number Re'		Generalised Prandtl Number Pr'		Grashof Number Gr_b
					Upstream $Z/D_1 = 0$	Downstream $Z/D_2 = 0$	Upstream $Z/D_1 = 0$	Downstream $Z/D_2 = 0$	Downstream $Z/D_2 = 40$
315	0.25%	.56	.288	553	497	30	293	1441	456
316	CARBO-	.56	.203	408	300	18	342	1682	411
317	POL	.56	.322	1198	584	36	279	1372	794
318	"	.56	.322	314	583	36	279	1372	243
319	"	.56	.736	2188	1919	117	194	954	953
320	"	.56	.736	1015	1919	117	194	954	467
321	"	.56	.277	566	469	29	299	1467	388
322	"	.56	.340	1131	629	38	273	1341	748

TABLE 23

a_i and ϕ_i given by BIRD (11) for s = 2

i	a_i
1	0
2	22.43
3	73.10
4	151.90

ξ	ϕ_1	ϕ_2	ϕ_3
0.0	1.000	1.000	1.000
0.1	1.000	0.945	0.825
0.2	1.000	0.789	0.393
0.3	1.000	0.550	-0.079
0.4	1.000	0.290	-0.369
0.5	1.000	0.020	-0.385
0.6	1.000	-0.187	-0.181
0.7	1.000	-0.340	0.082
0.8	1.000	-0.469	0.375
0.9	1.000	-0.470	0.390

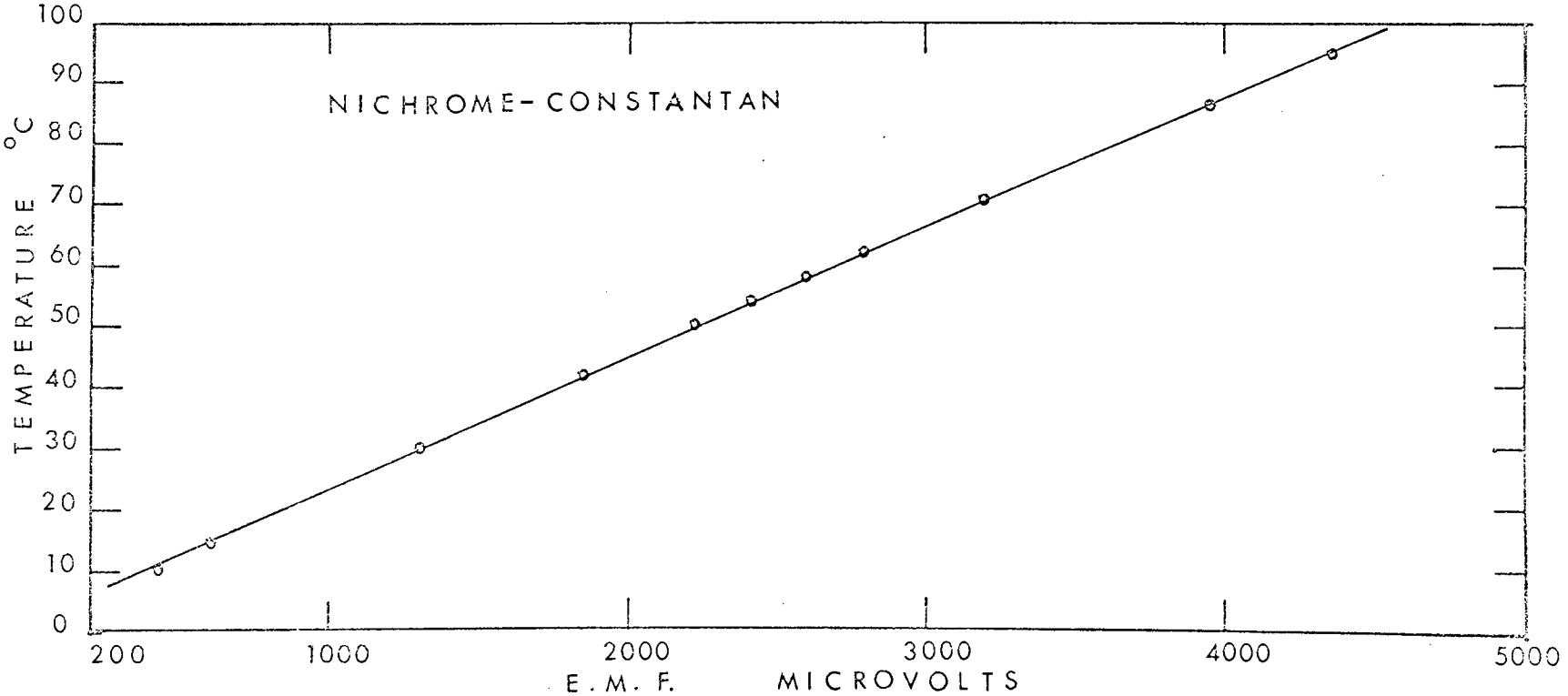

FIG 28 THERMOCOUPLE CALIBRATION

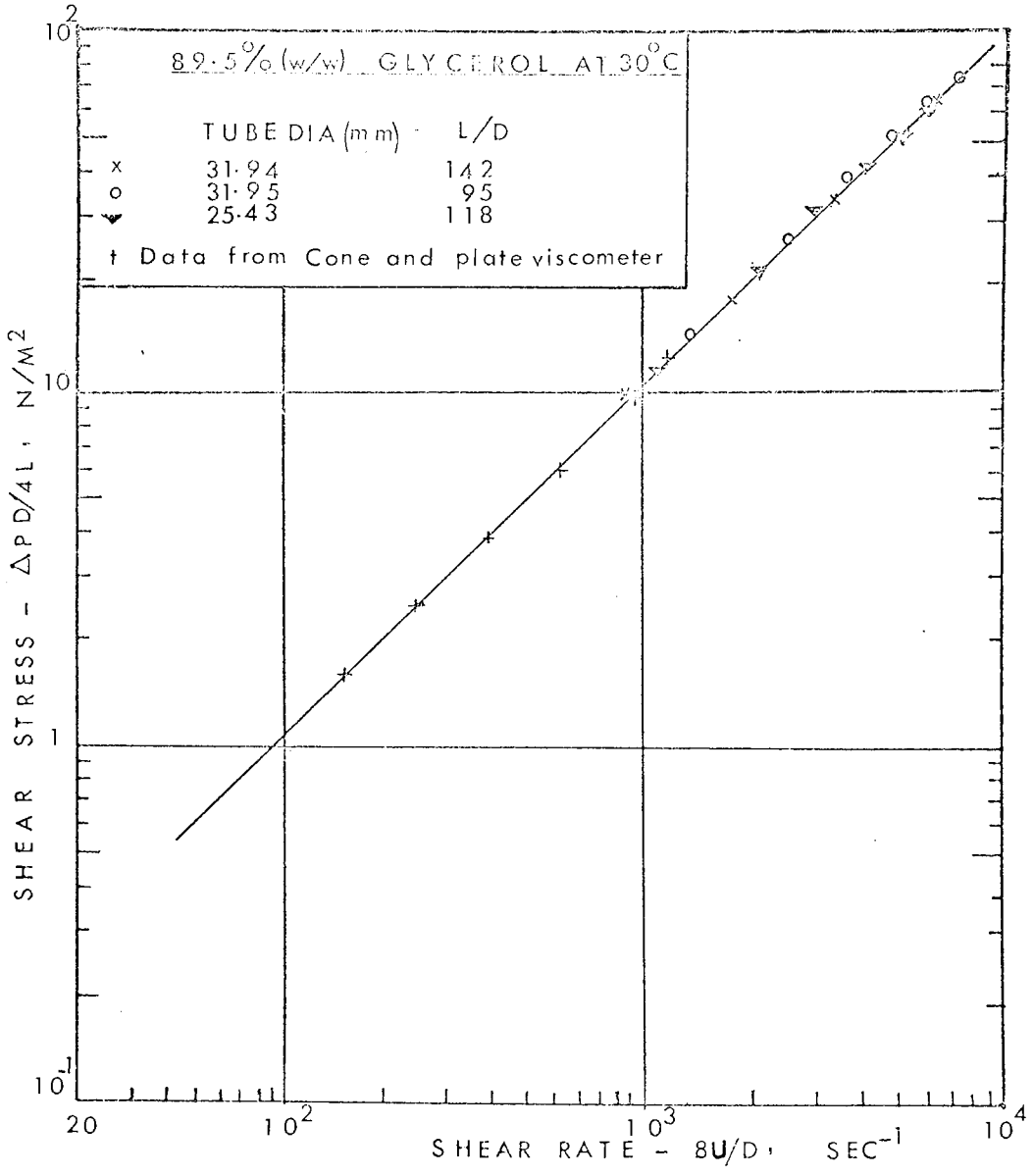

FIG 2.9 CALIBRATION DATA FOR CAPILLARY VISCOMETER

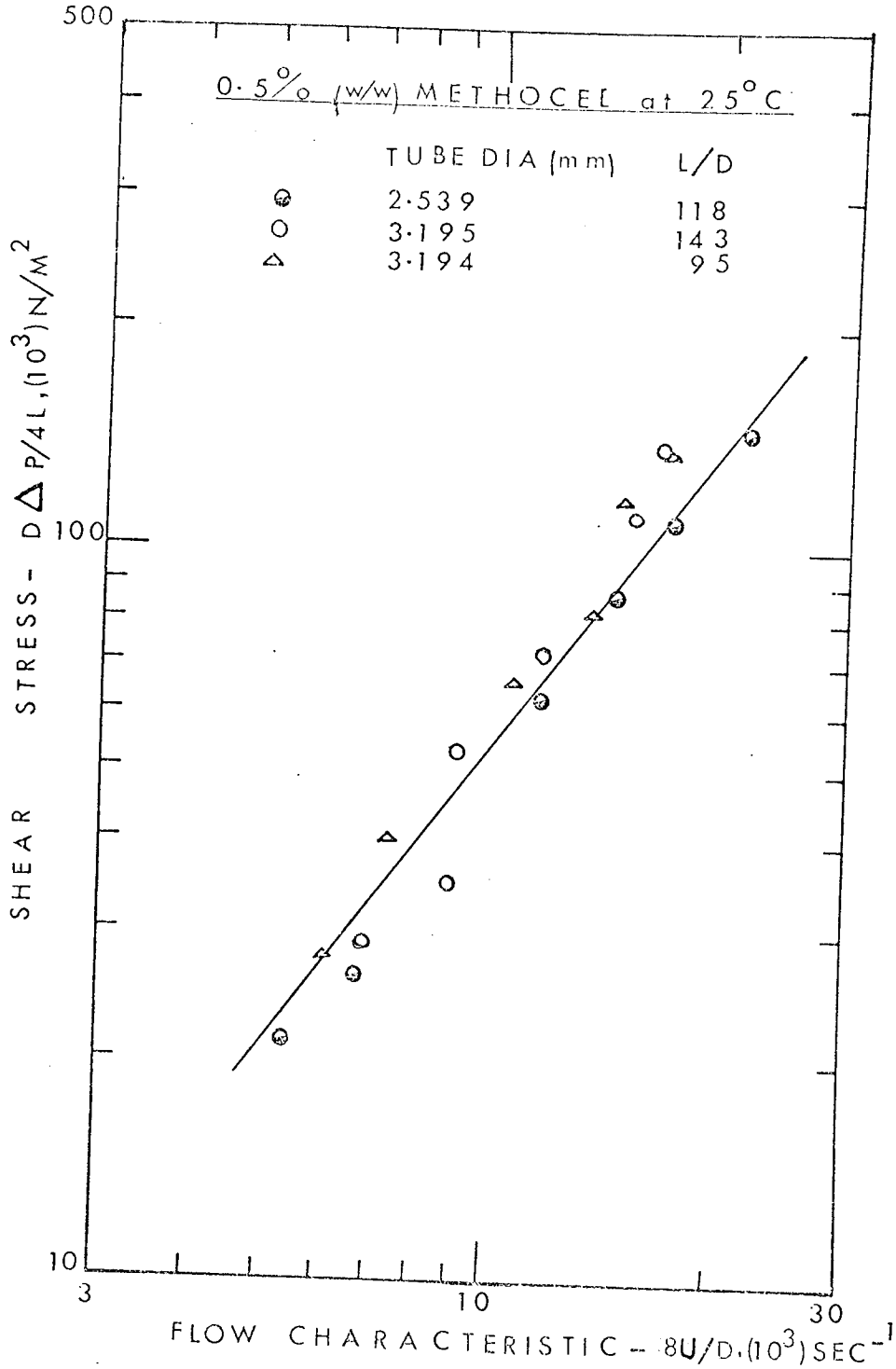

FIG 30 CAPILLARY VISCOMETRIC DATA

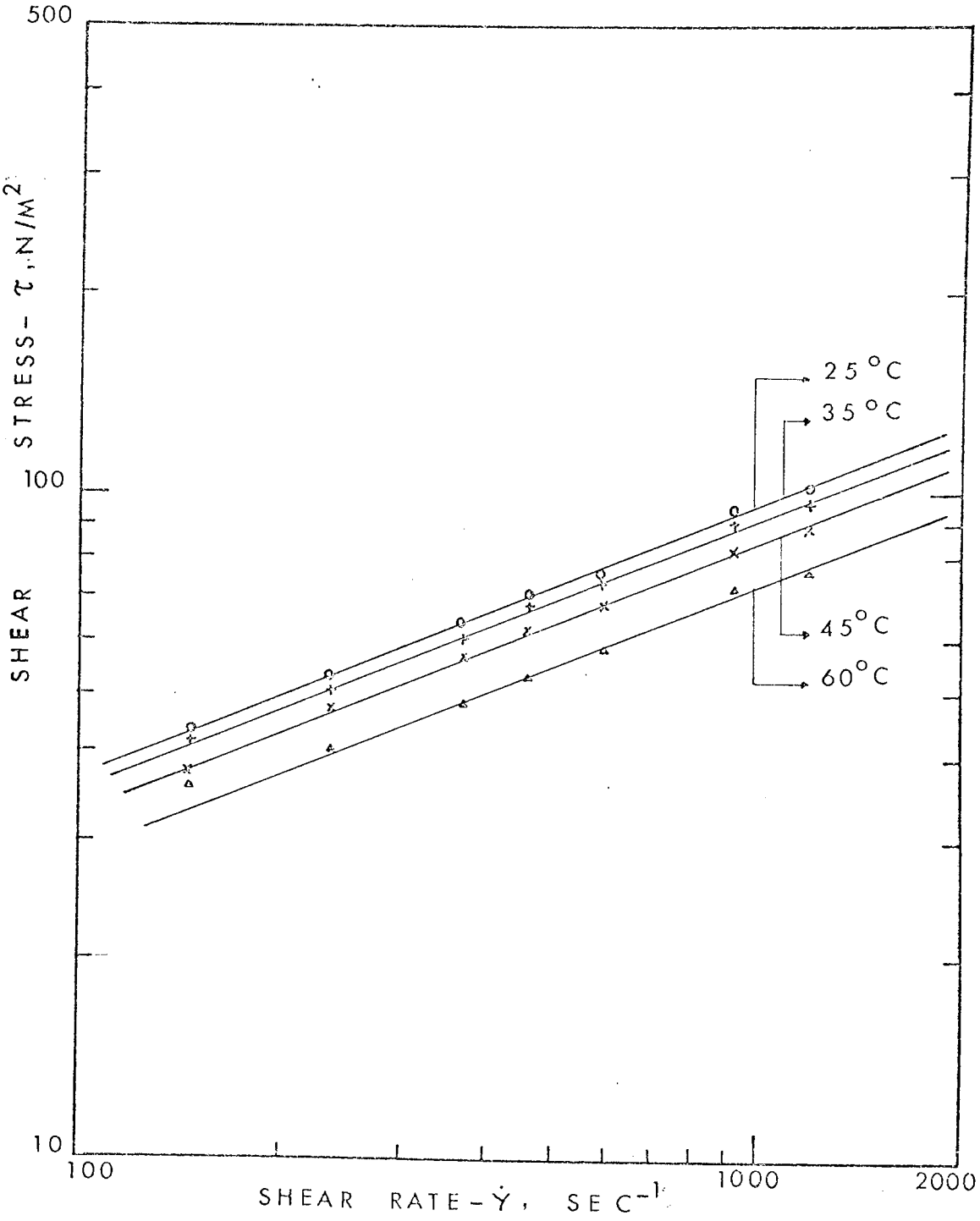

FIG 3.1 SHEAR STRESS vs SHEAR RATE FOR 5% CPM REF. SOLUTION

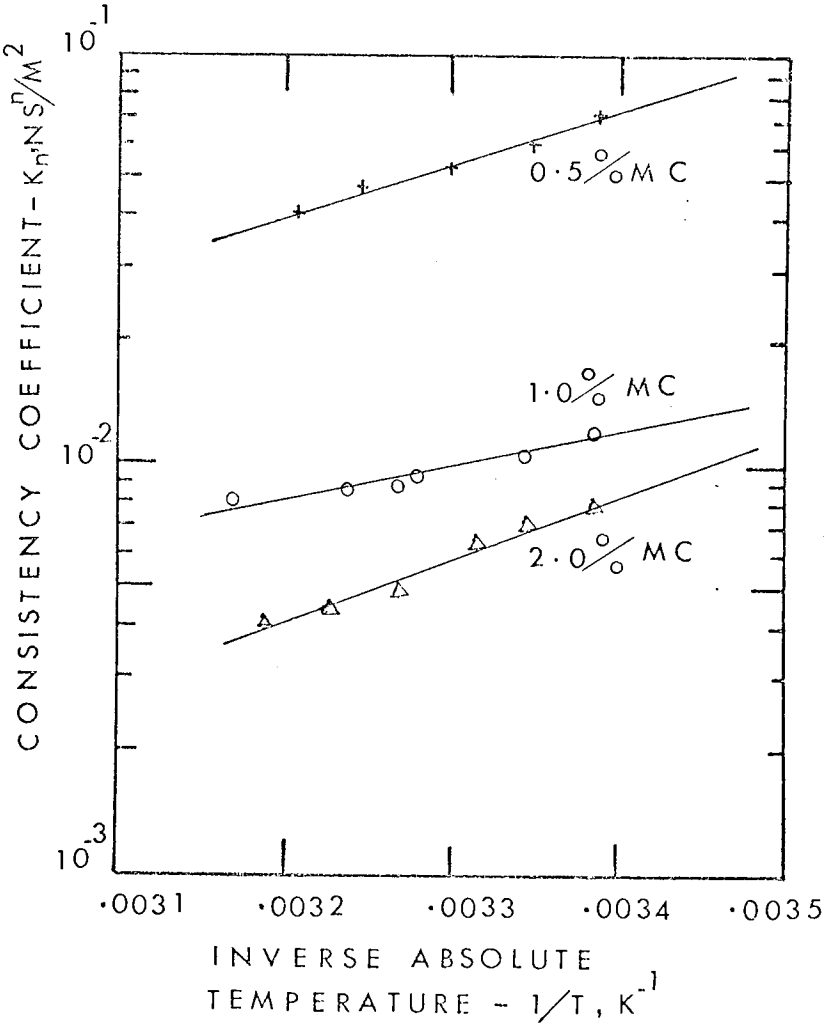

FIG 32 CONSISTENCY vs TEMPERATURE FOR METHOCEL REF. SOLUTIONS

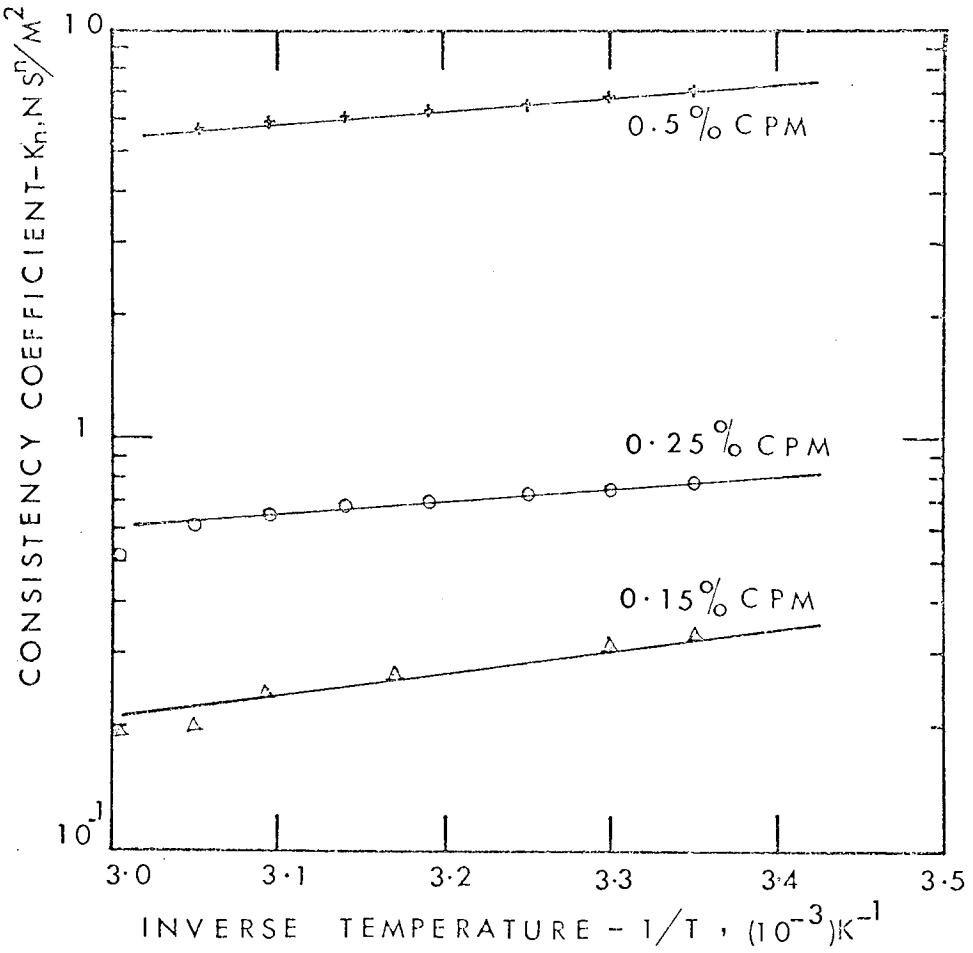

FIG. 33 CONSISTENCY vs TEMPERATURE FOR CARBOPOL REF. SOLUTIONS

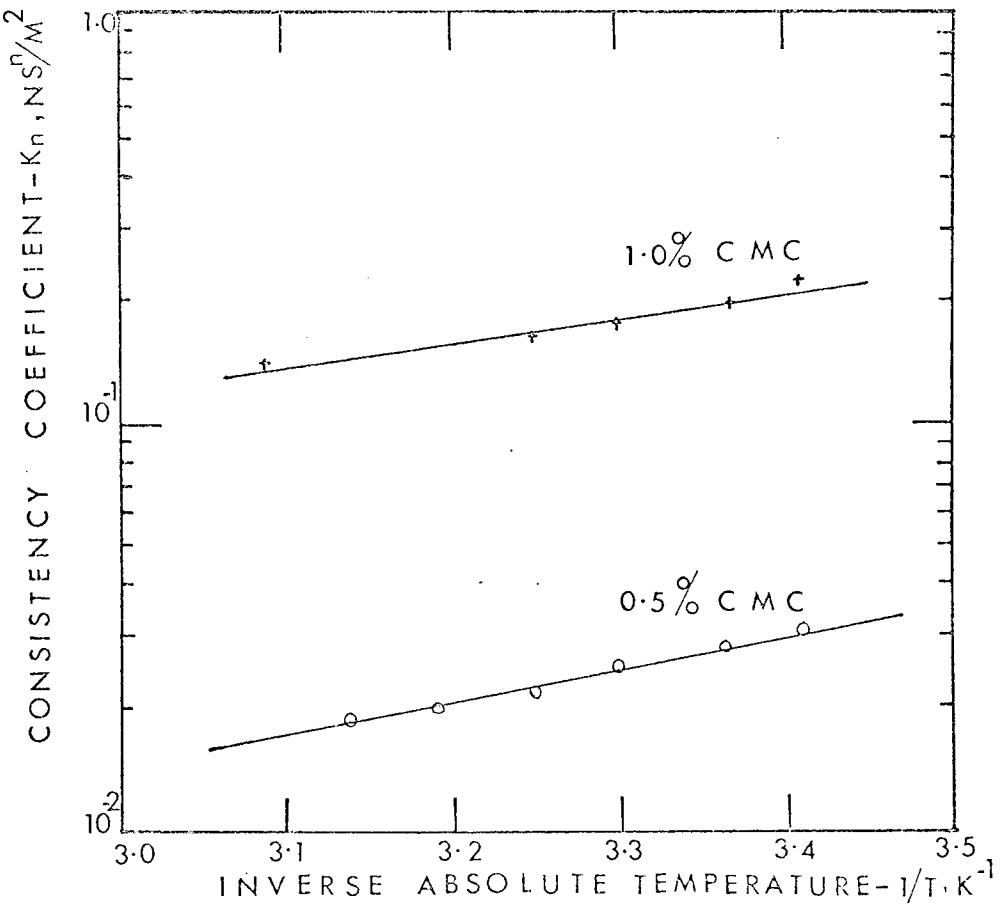

FIG. 34. CONSISTENCY vs TEMPERATURE FOR C M C REF. SOLUTIONS

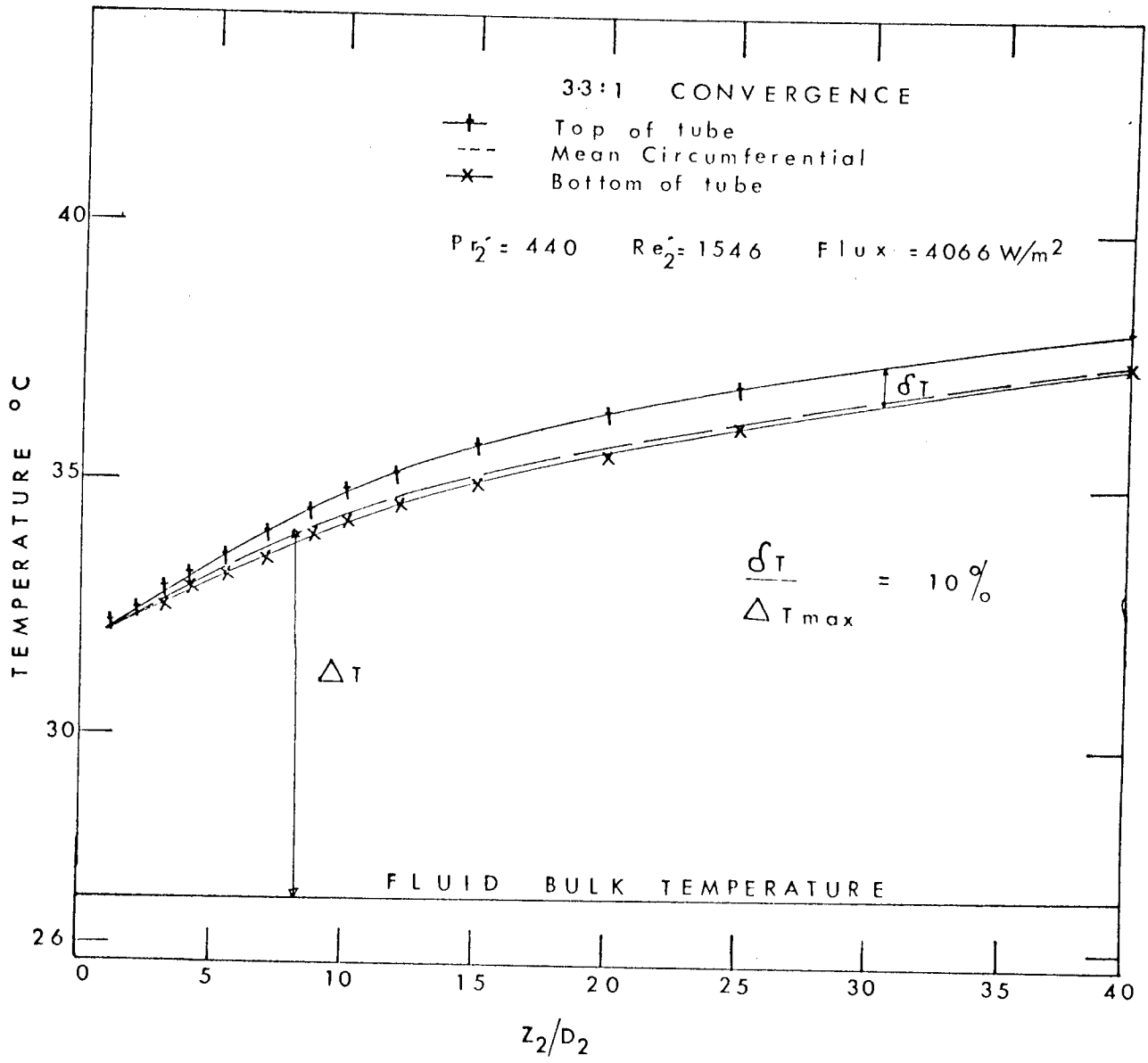

FIG.35 AXIAL TEMPERATURE PROFILE

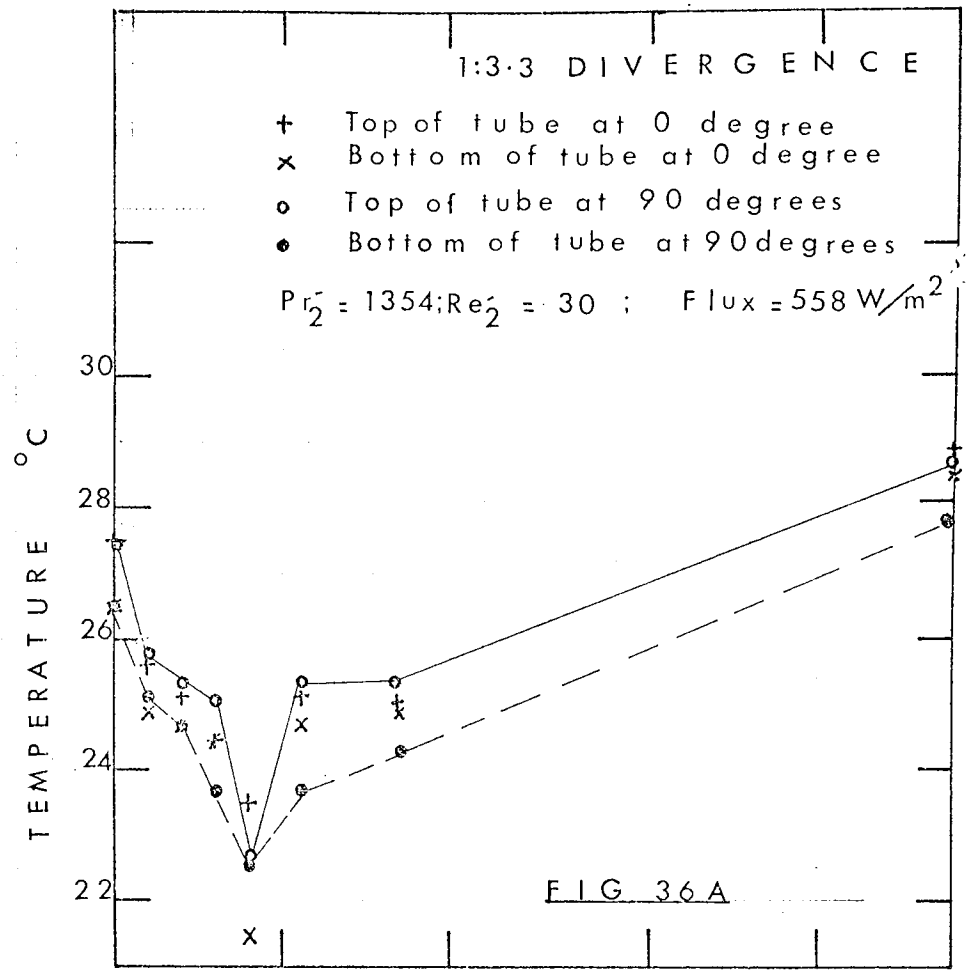

FIG 36A

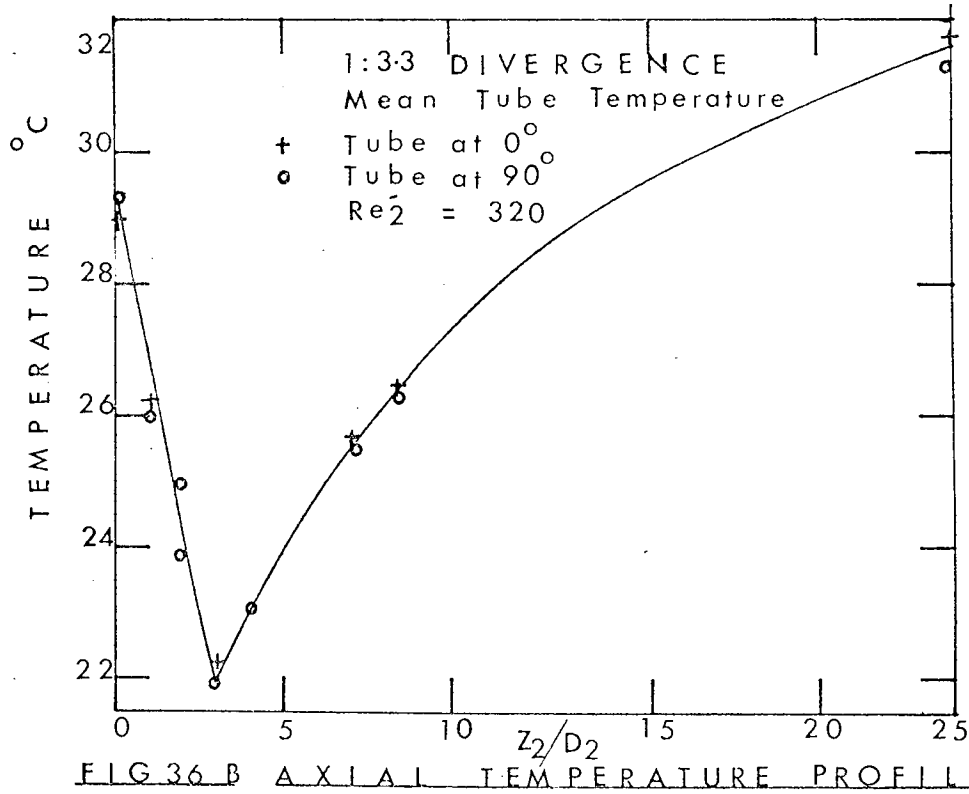

FIG 36B AXIAL TEMPERATURE PROFILE

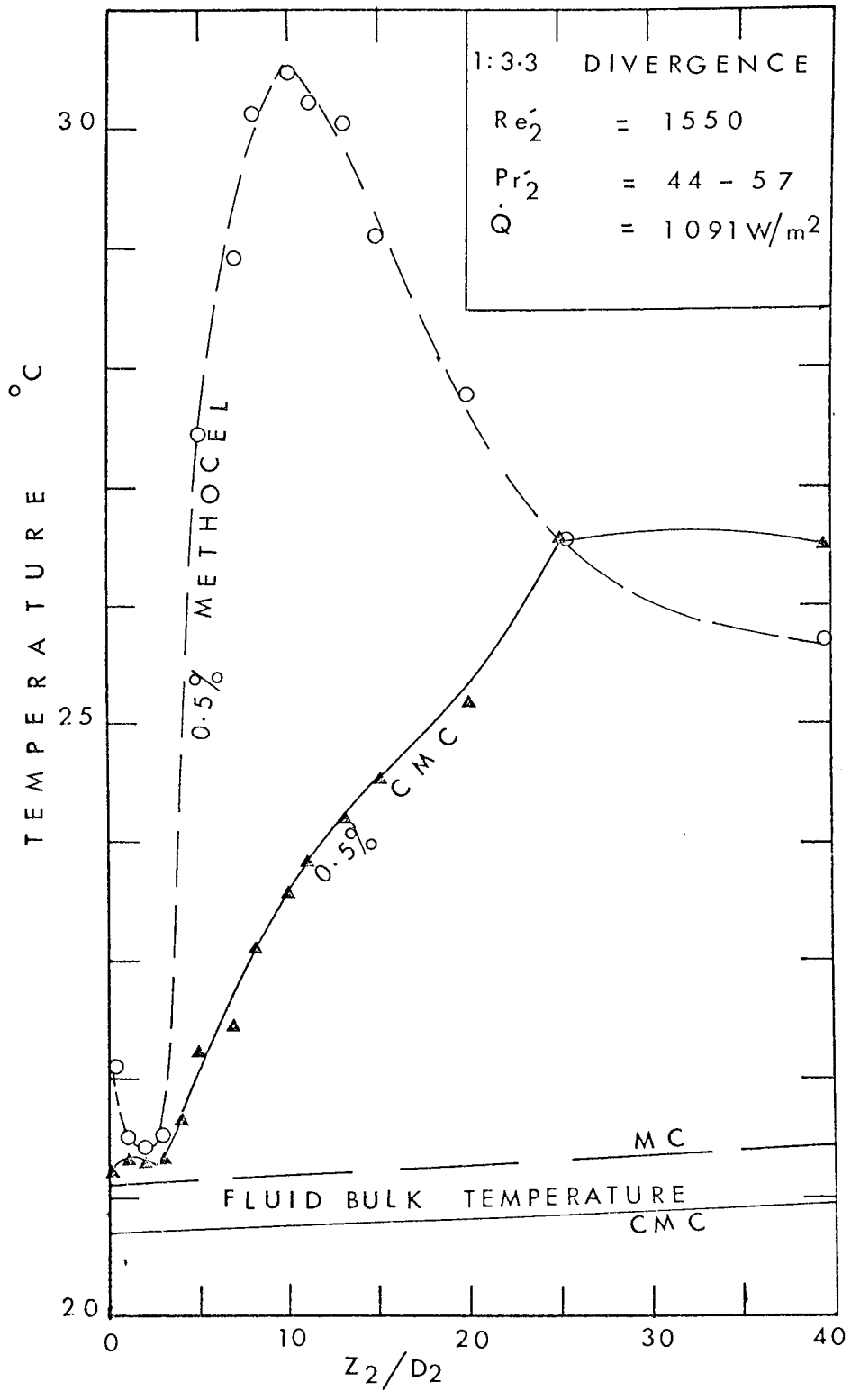

FIG 36(C) AXIAL TEMPERATURE PROFILE

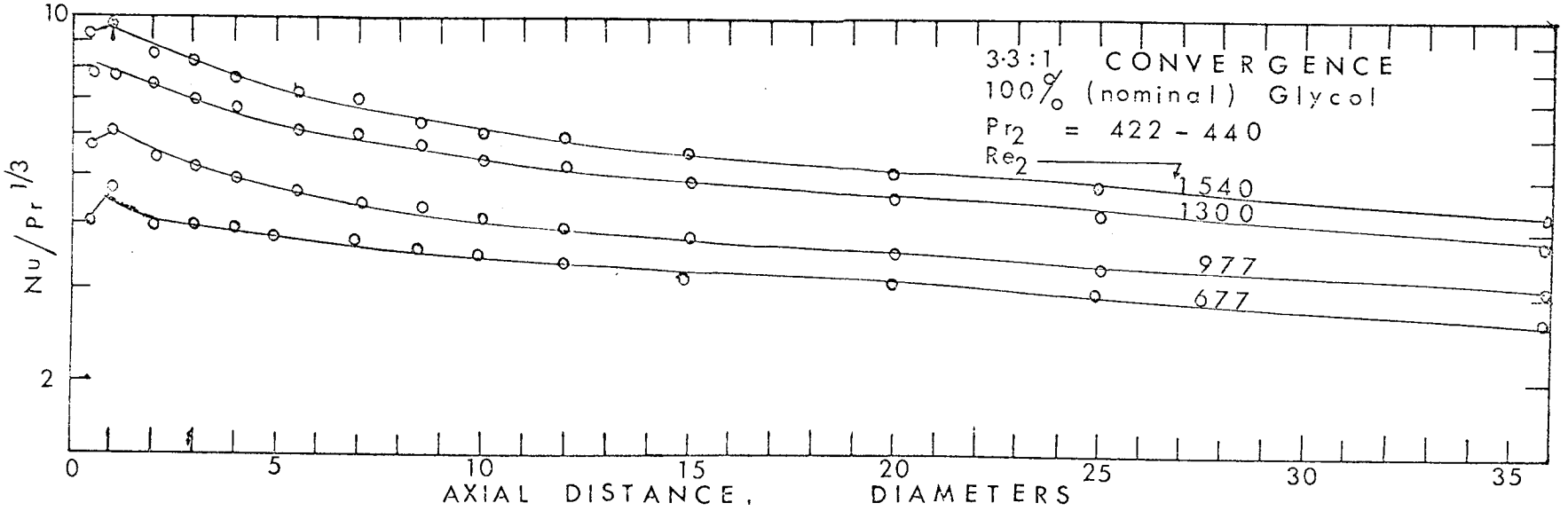

FIG. 37 AXIAL VARIATION OF HEAT TRANSFER COEFFICIENT

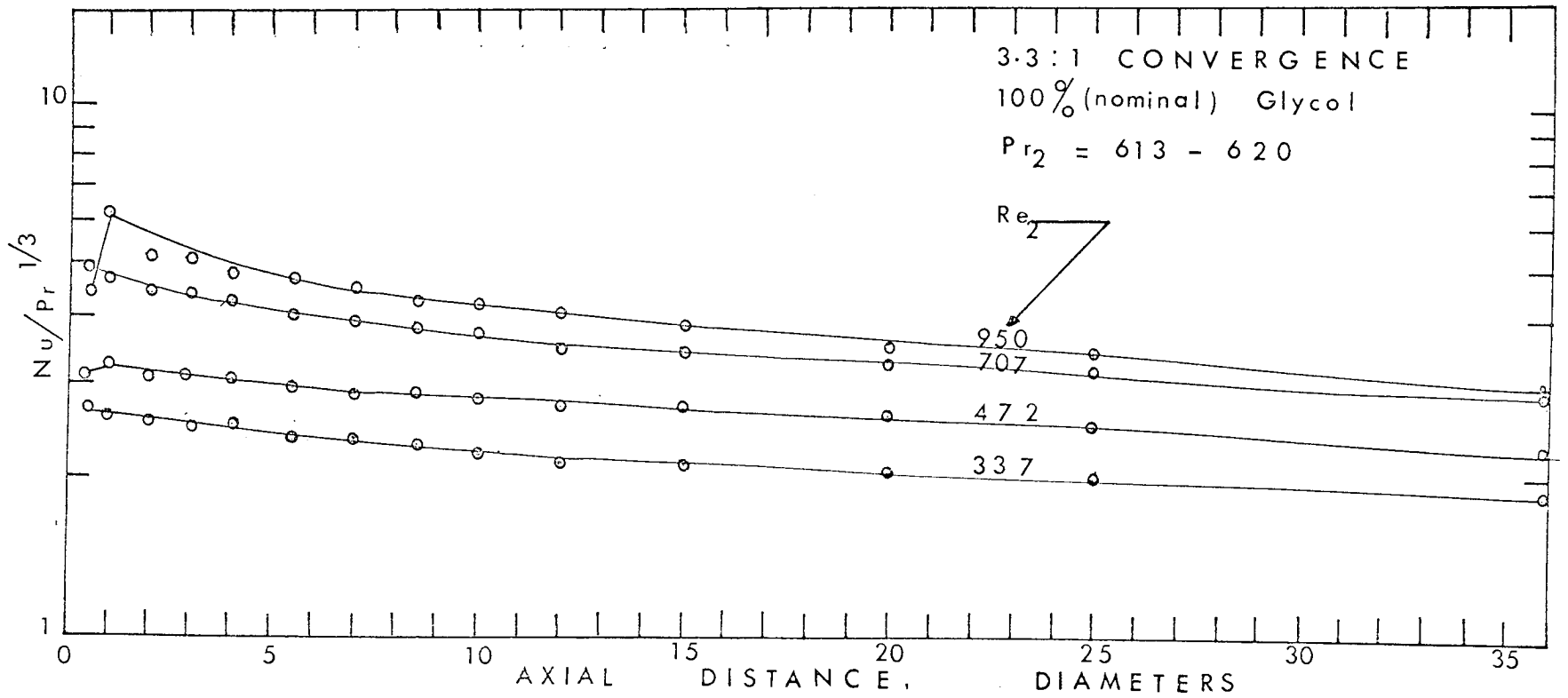

FIG. 38 AXIAL VARIATION OF HEAT TRANSFER COEFFICIENT

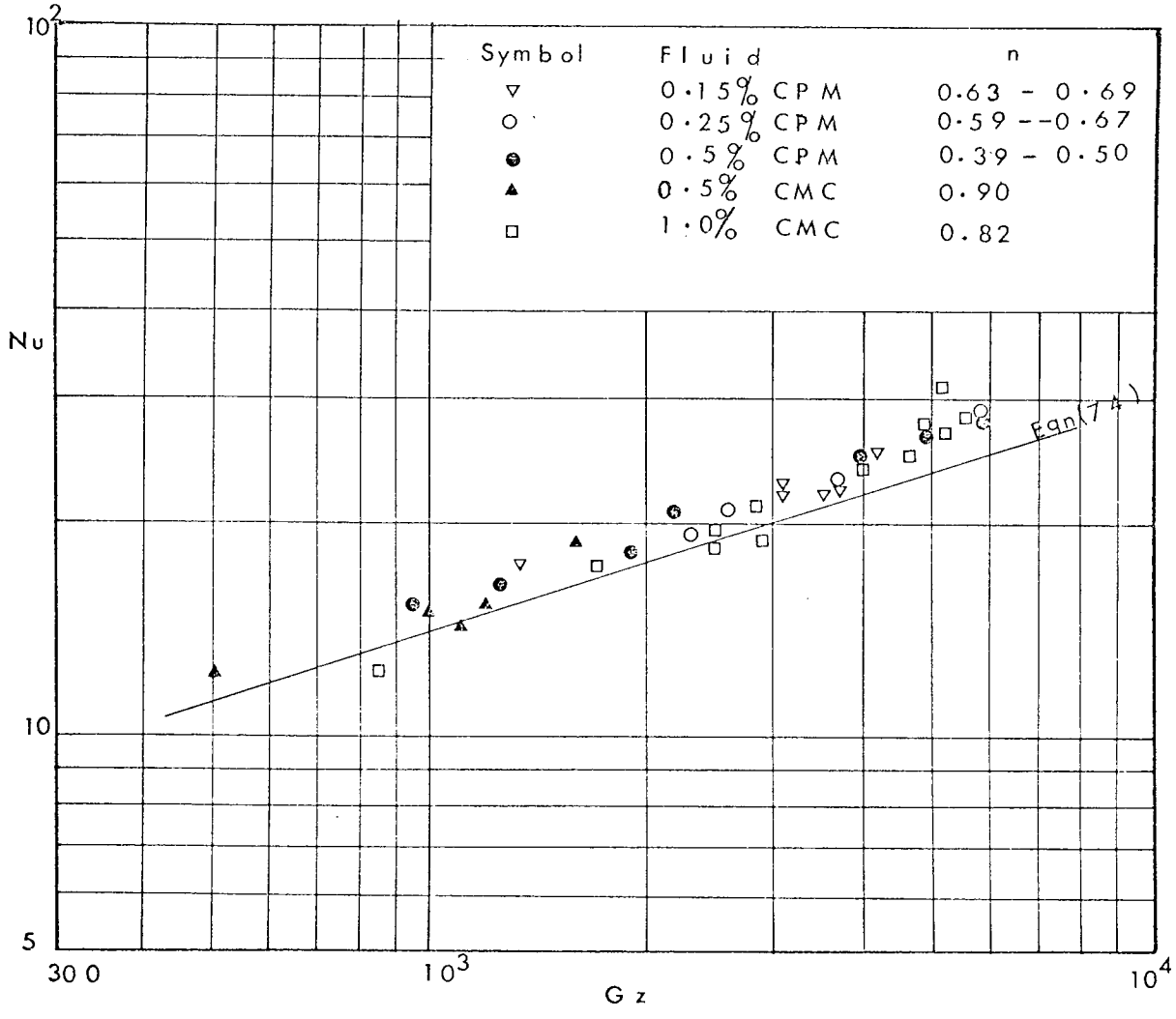

FIG. 39 Nu - Gz CORRELATION OF FULLY-DEVELOPED DATA

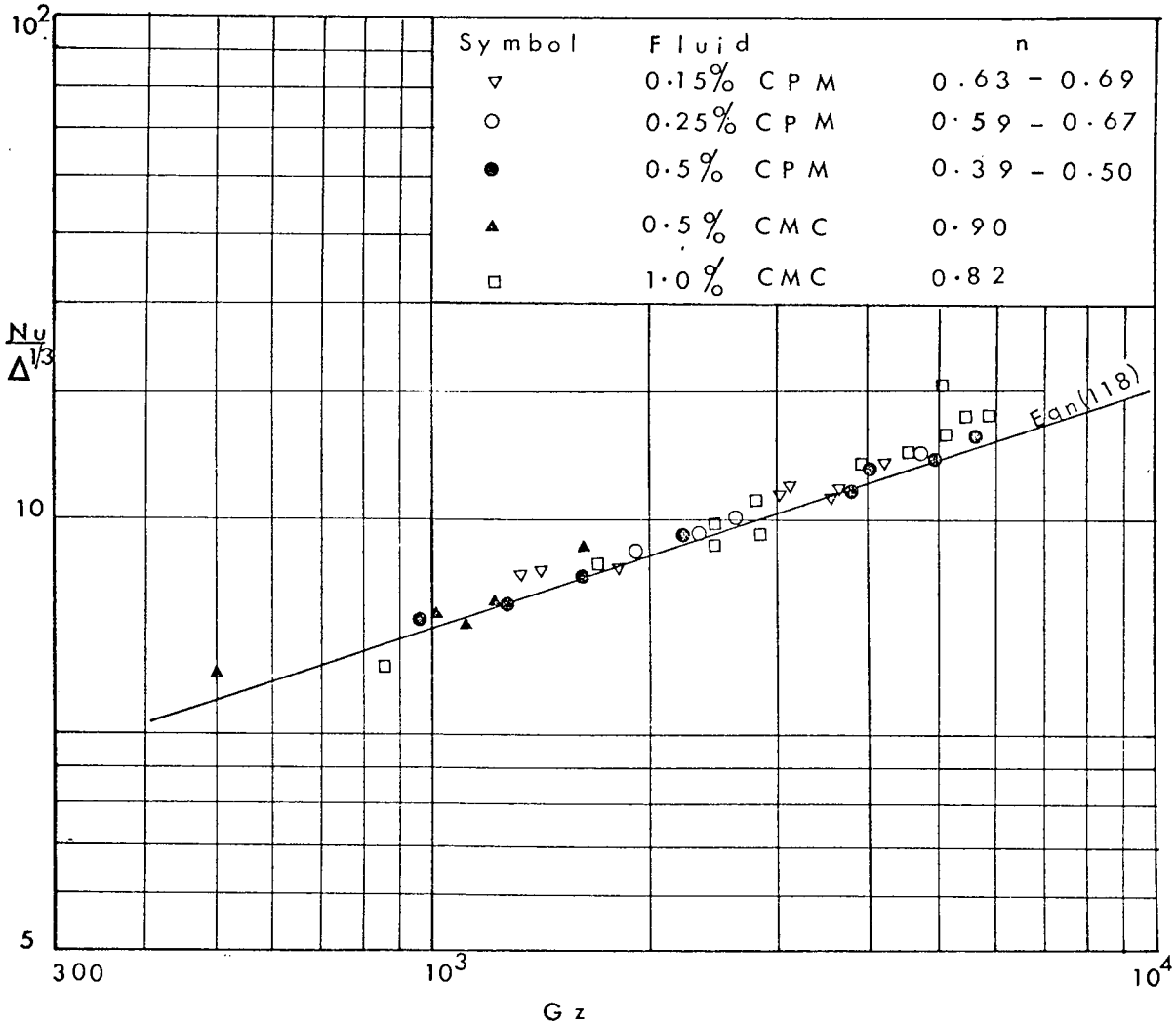

FIG. 40 Nu - Gz CORRELATION OF FULLY-DEVELOPED DATA --- CORRECTION FOR NON-NEWTONIAN BEHAVIOR

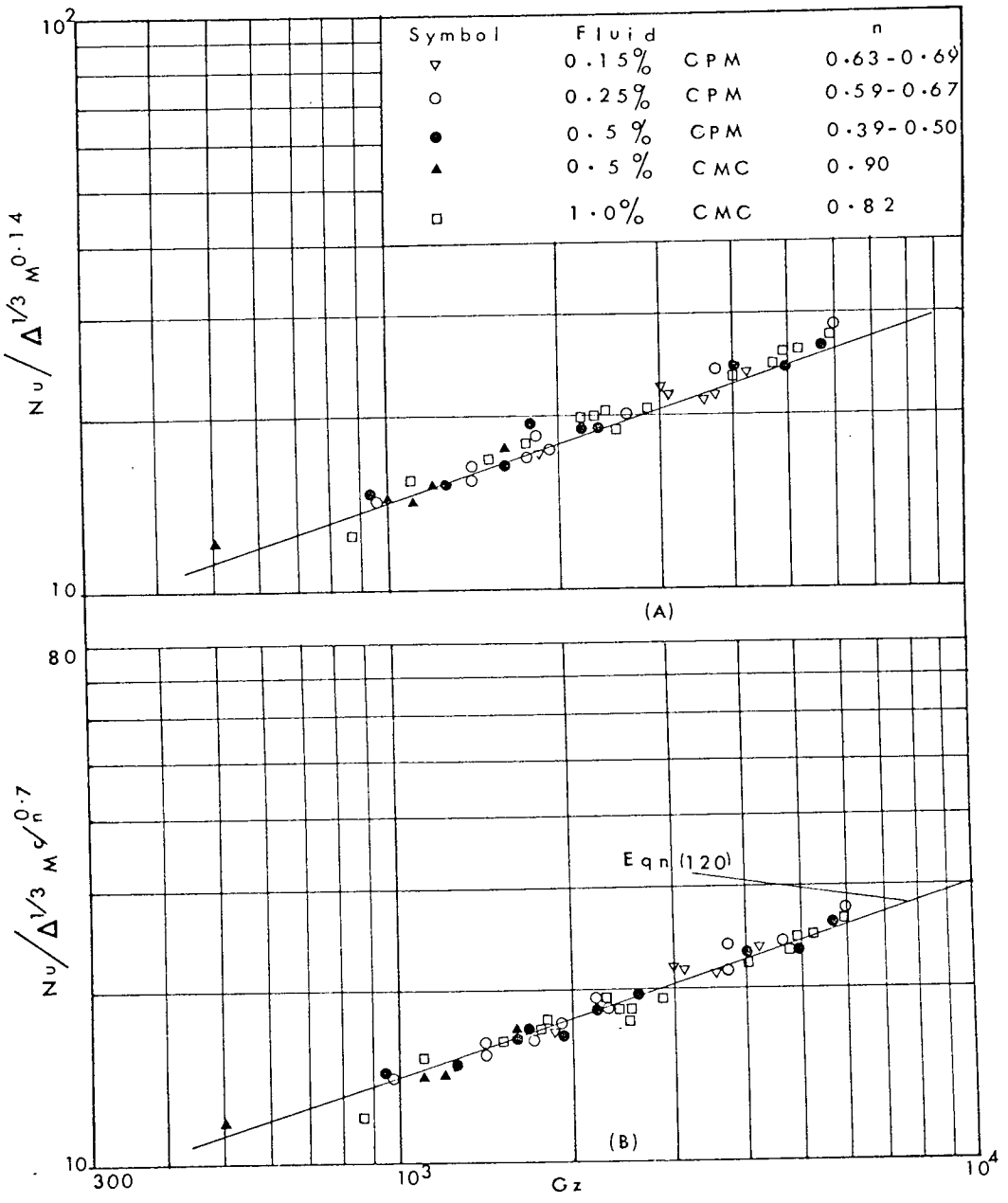

FIG. 41 Nu - Gz CORRELATION ... COMPARISON BETWEEN THE SIEDER-TATE AND MIZUSHINA TYPE CORRECTION FOR VARIABLE VISCOSITY

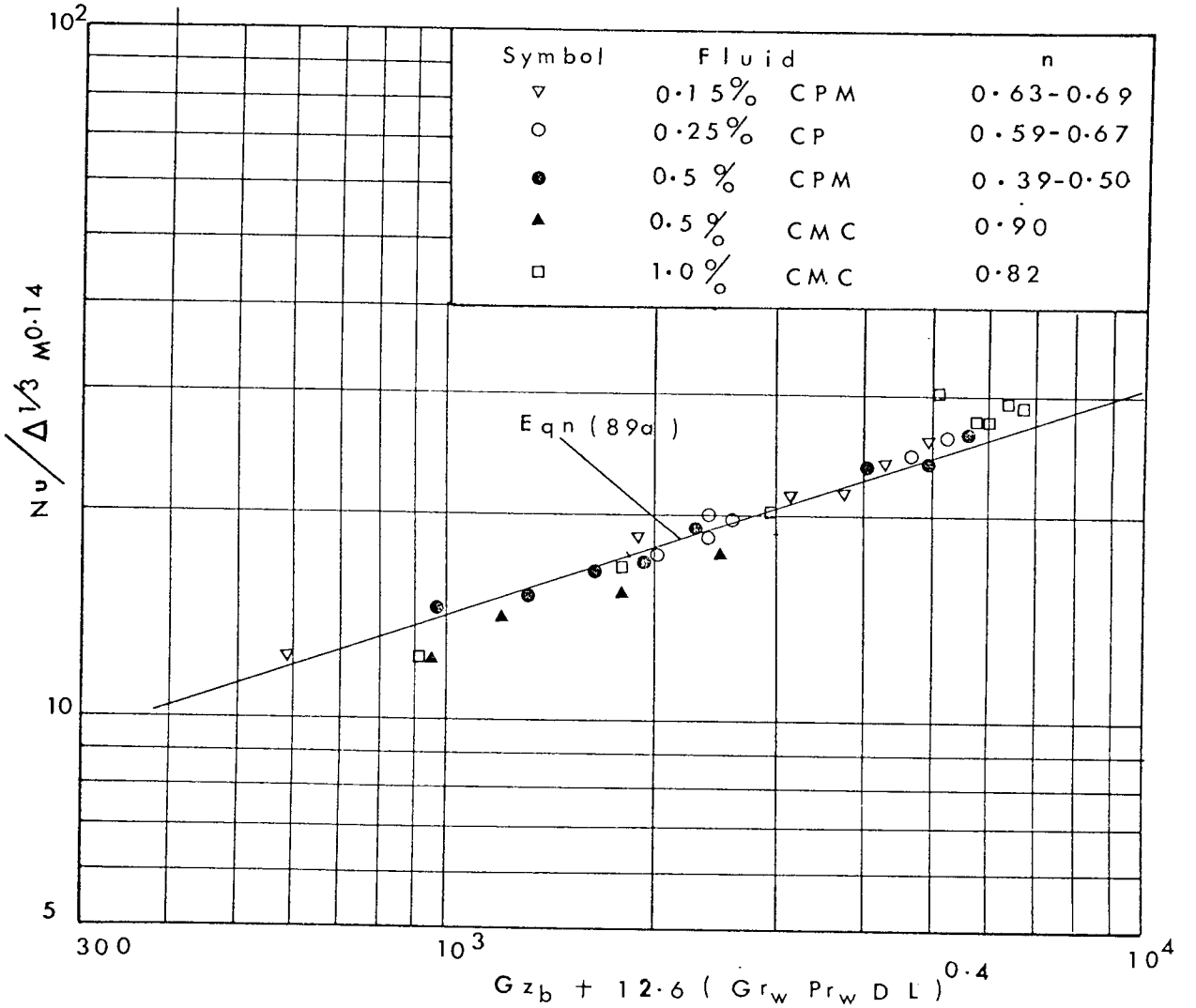

FIG. 42 Nu - Gz CORRELATION ---- NATURAL CONVECTION CORRECTION

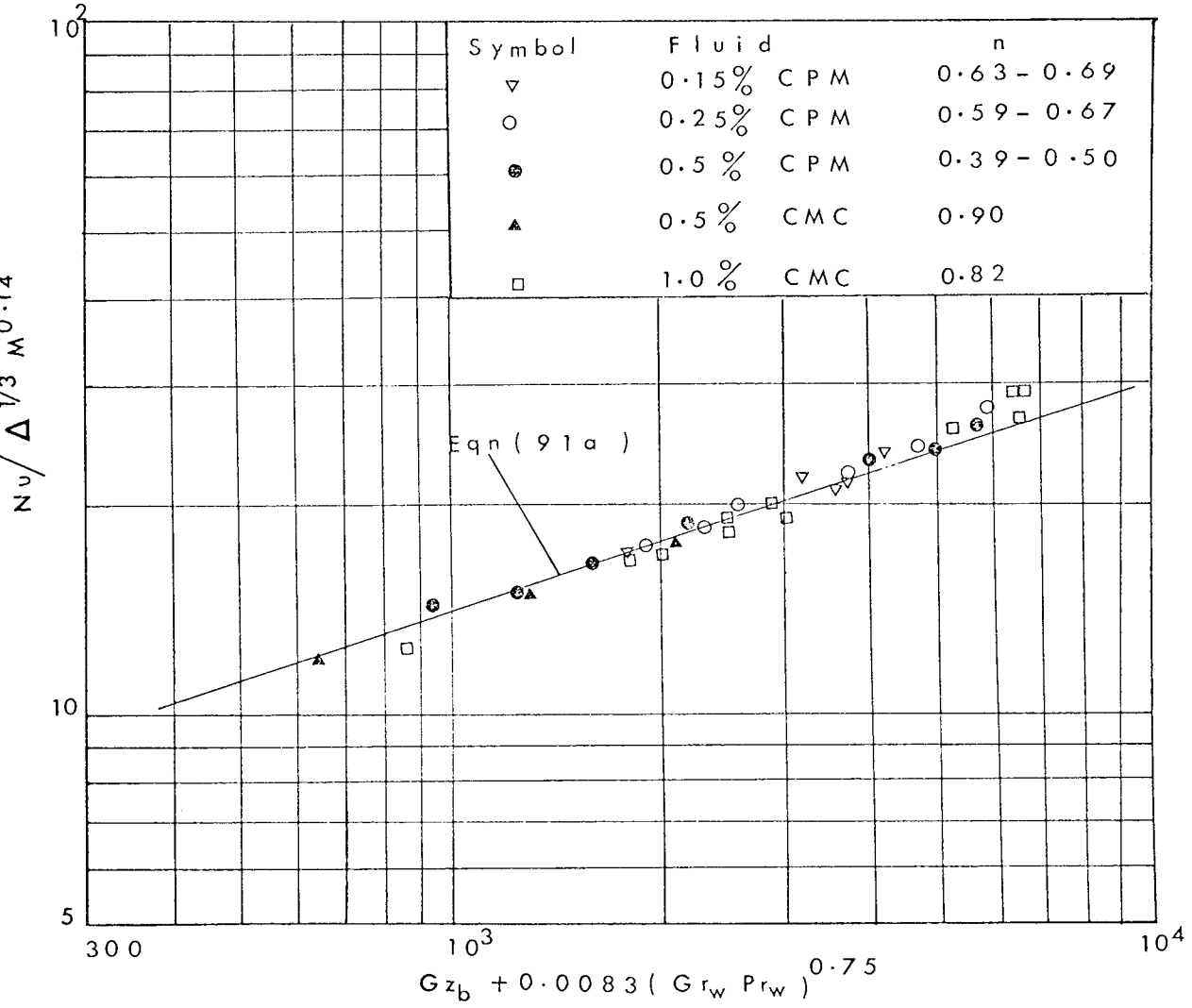

FIG 43 Nu - Gz CORRELATION --- NATURAL CONVECTION CORRECTION

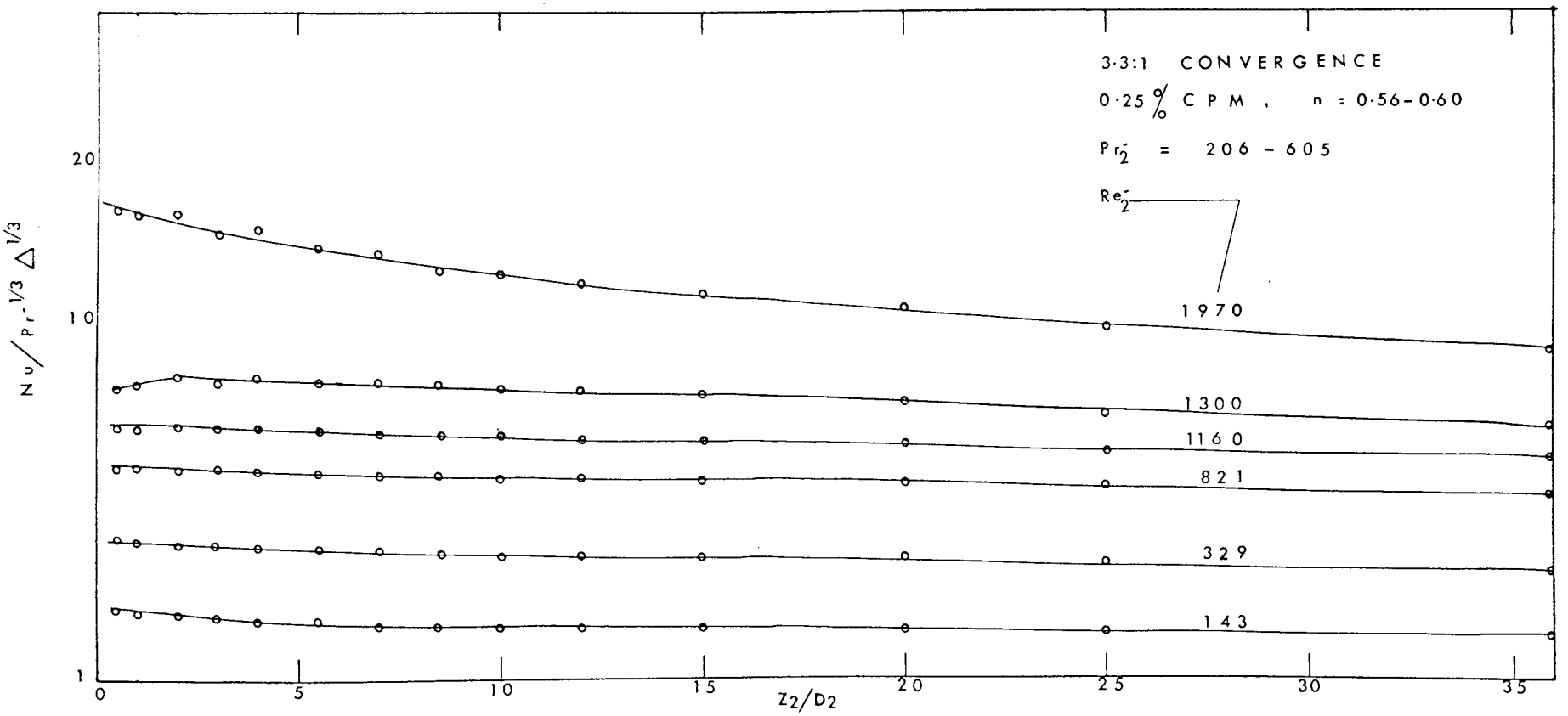

FIG. 44 AXIAL VARIATION OF HEAT TRANSFER COEFFICIENT

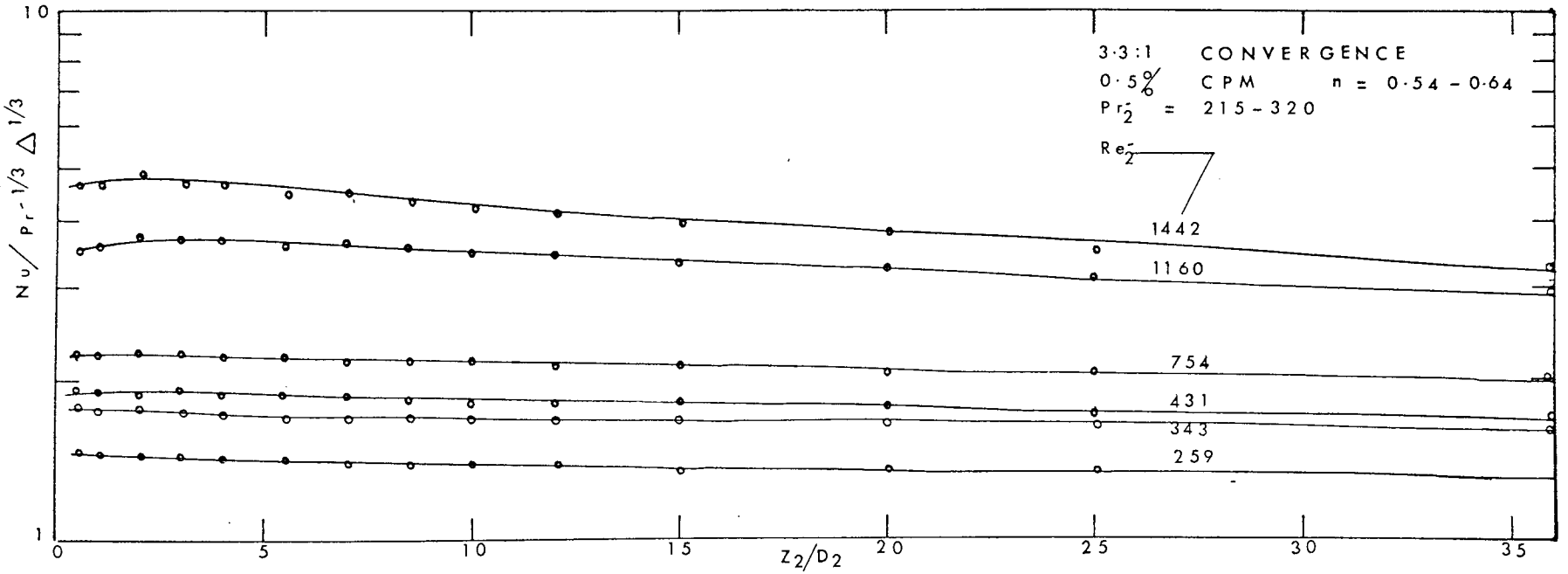

FIG.45 AXIAL VARIATION OF HEAT TRANSFER COEFFICIENT

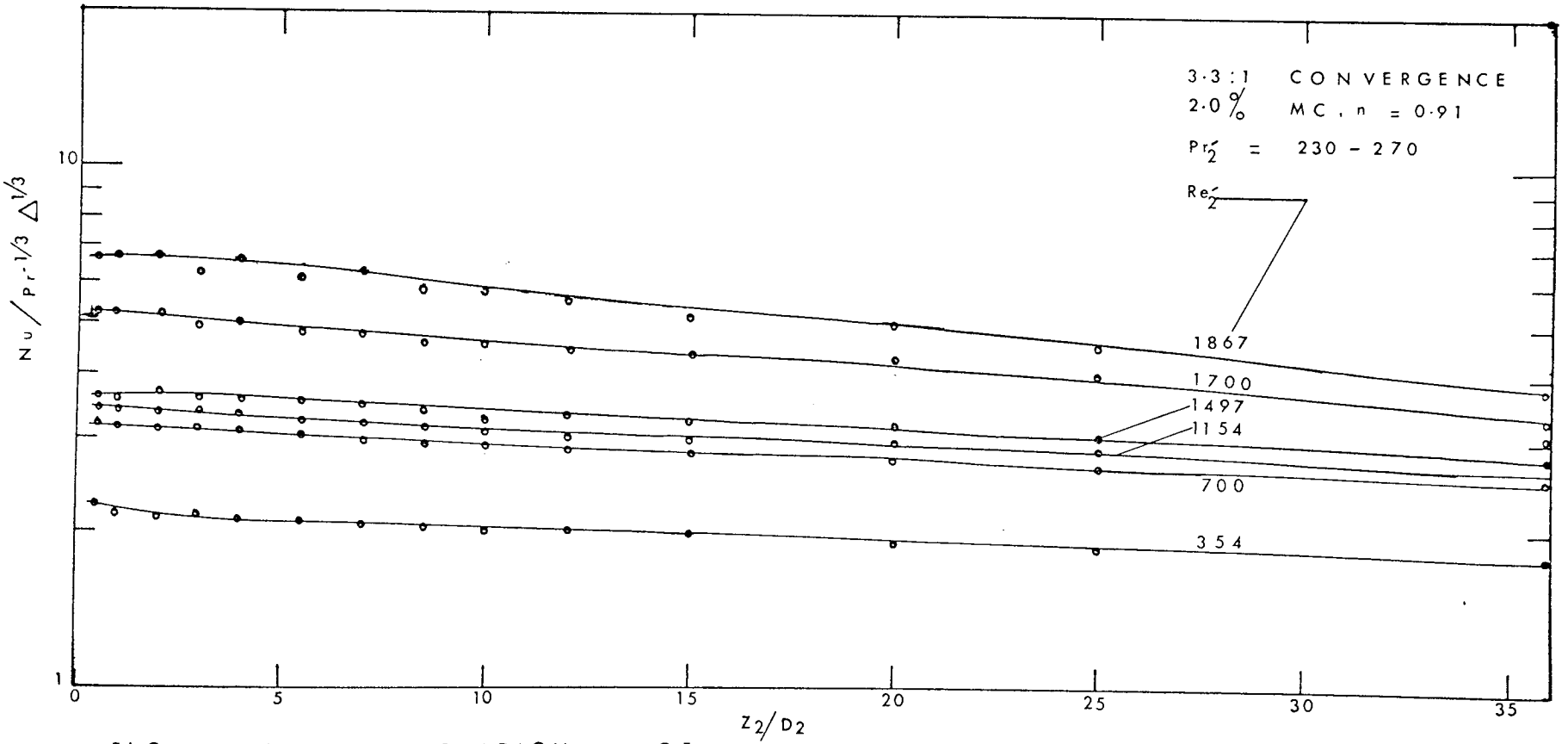

FIG. 46 AXIAL VARIATION OF HEAT TRANSFER COEFFICIENT

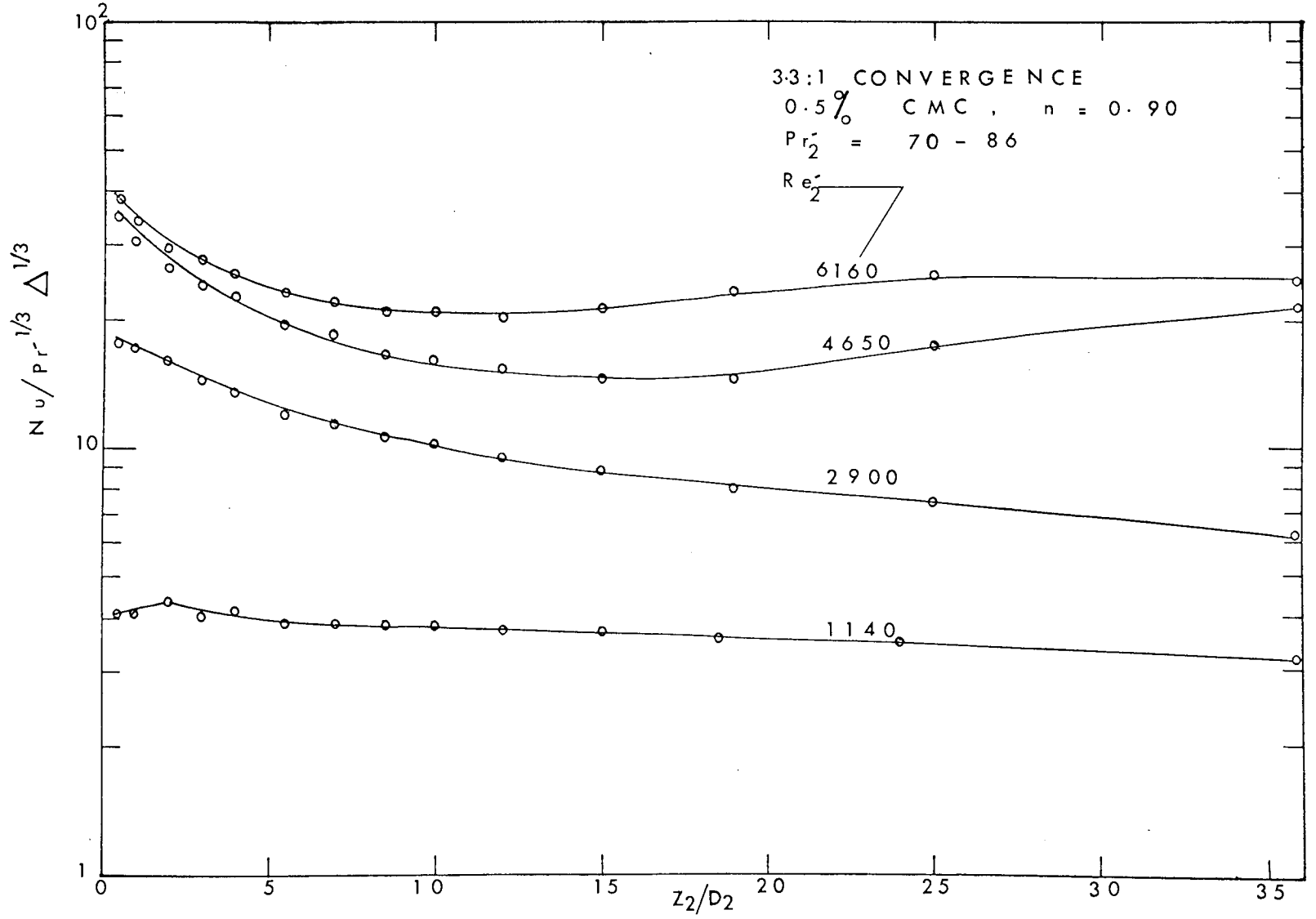

FIG. 47 AXIAL VARIATION OF HEAT TRANSFER COEFFICIENT

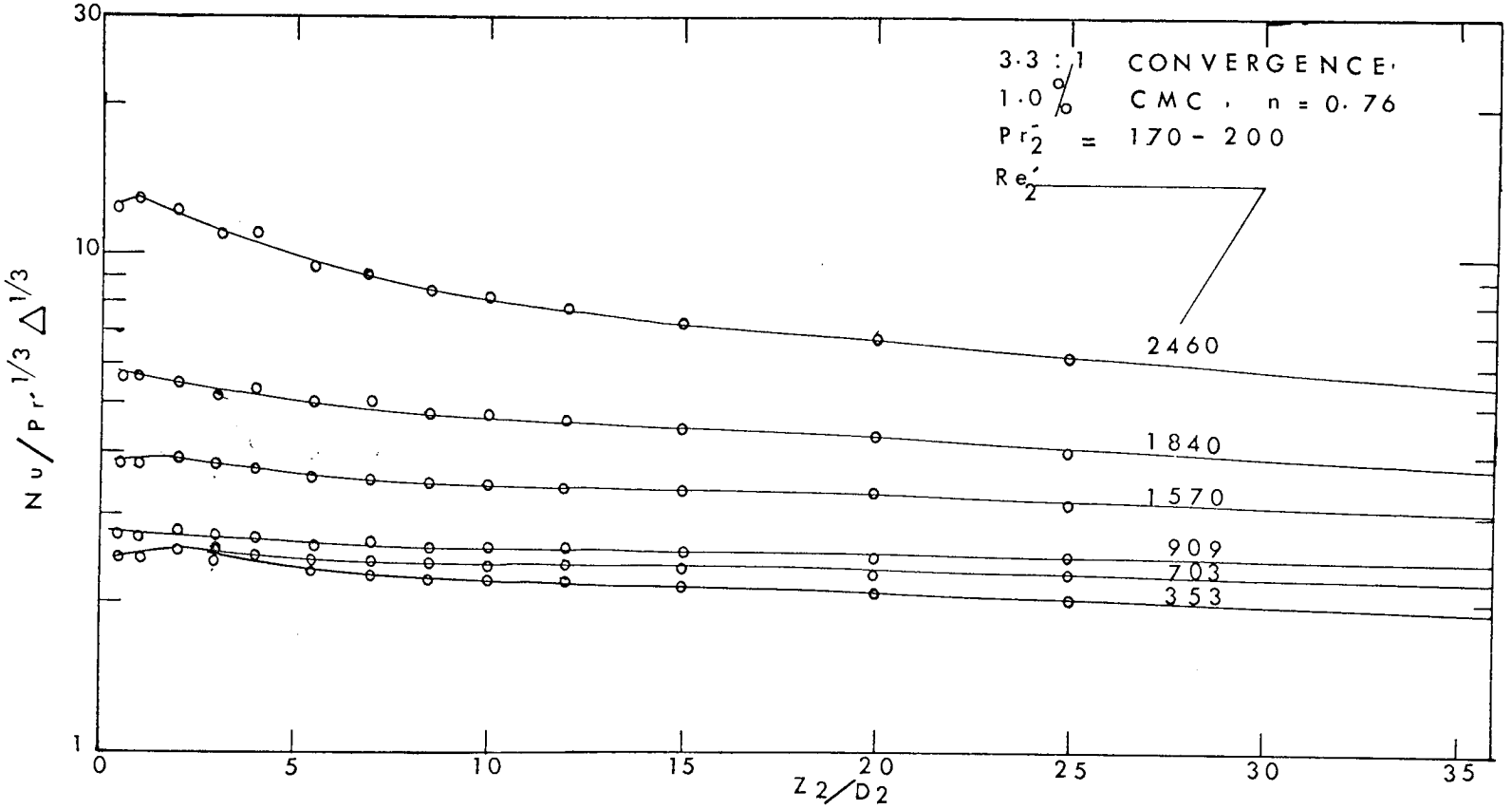

FIG. 48 AXIAL VARIATION OF HEAT TRANSFER COEFFICIENT

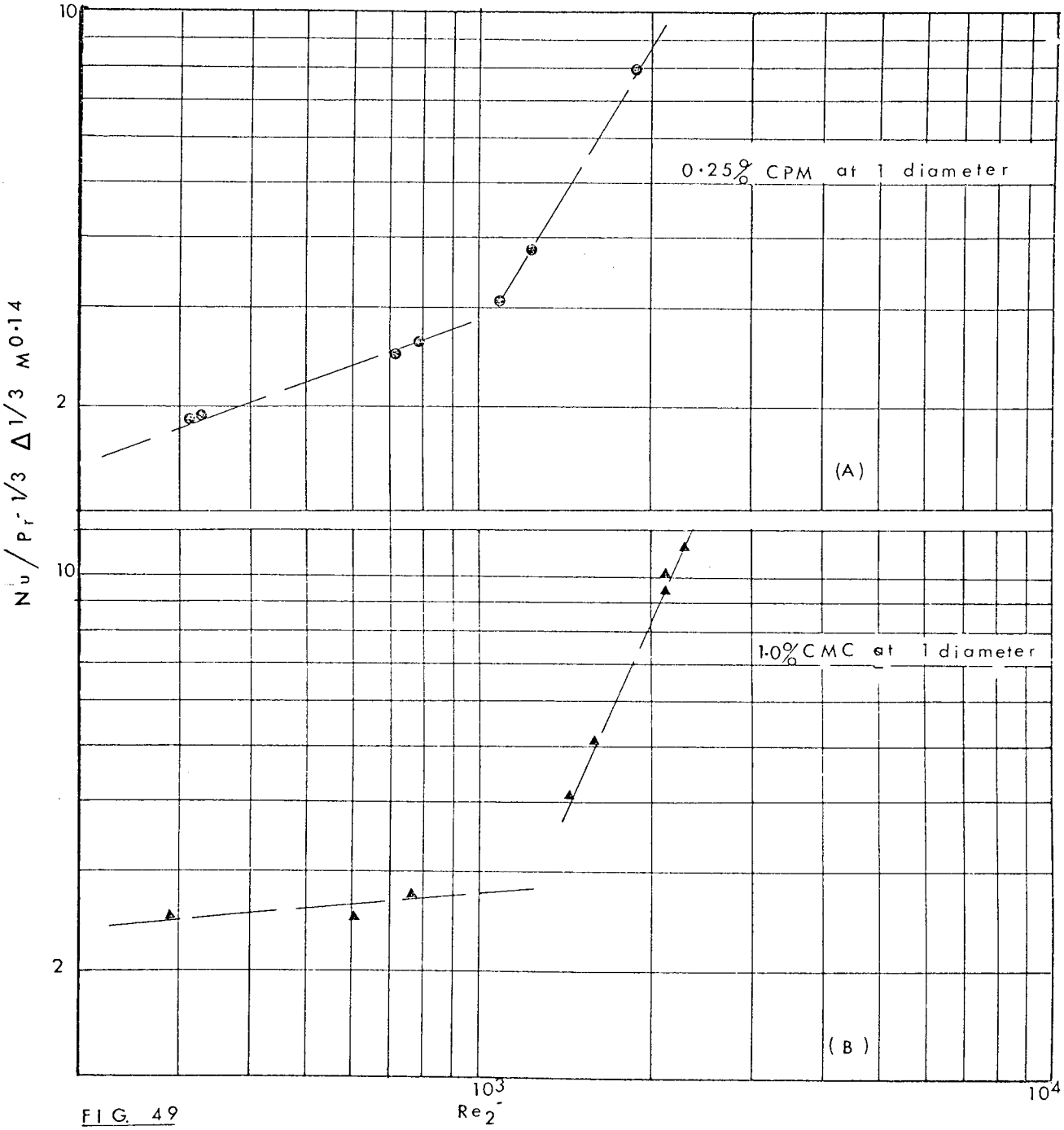

FIG. 49

VARIATION OF Nu WITH REYNOLDS NUMBER (3·3:1 CONVERGENCE)

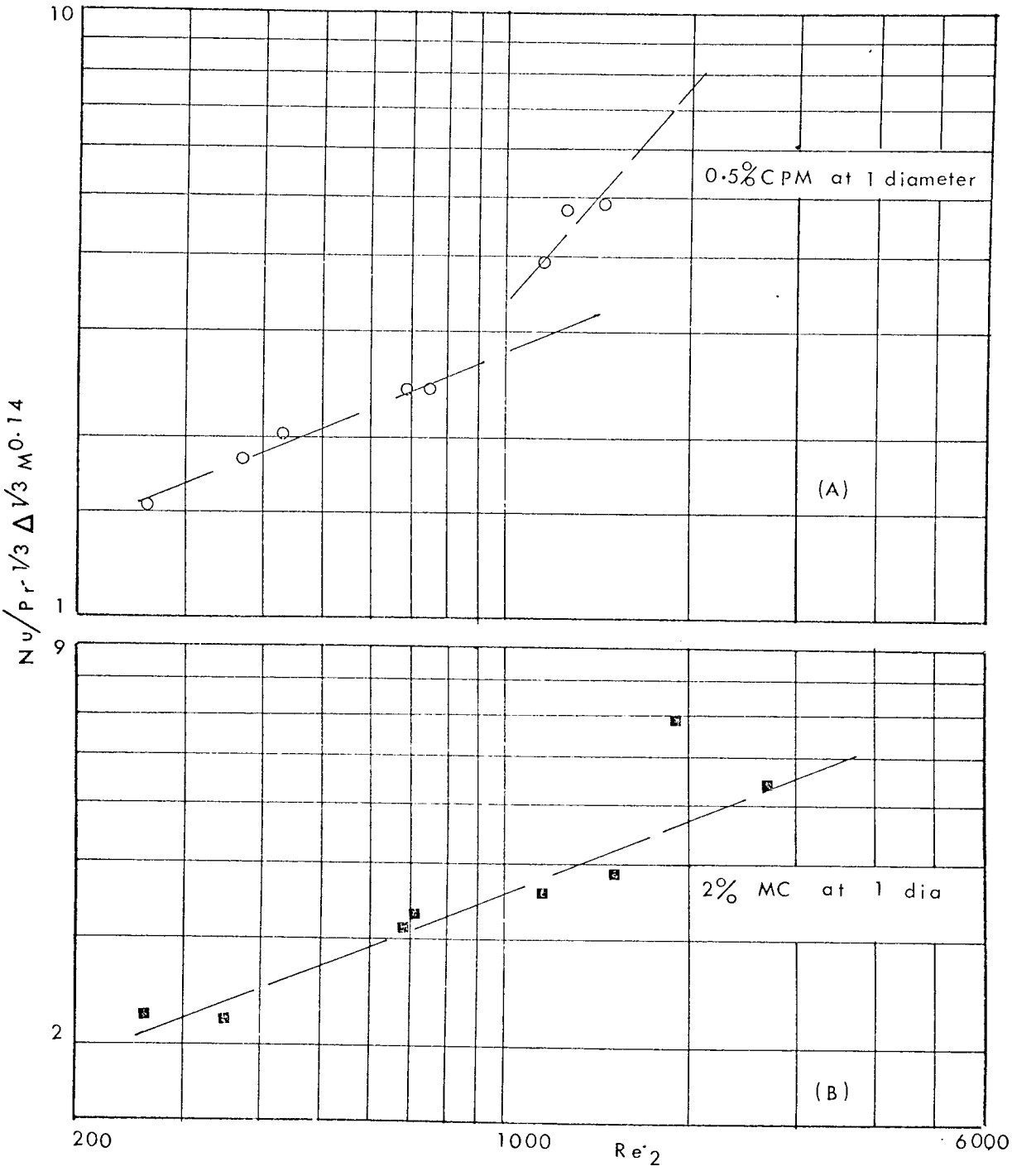

FIG. 50 VARIATION OF Nu WITH REYNOLDS NUMBER (3·3:1 CONVERGENCE)

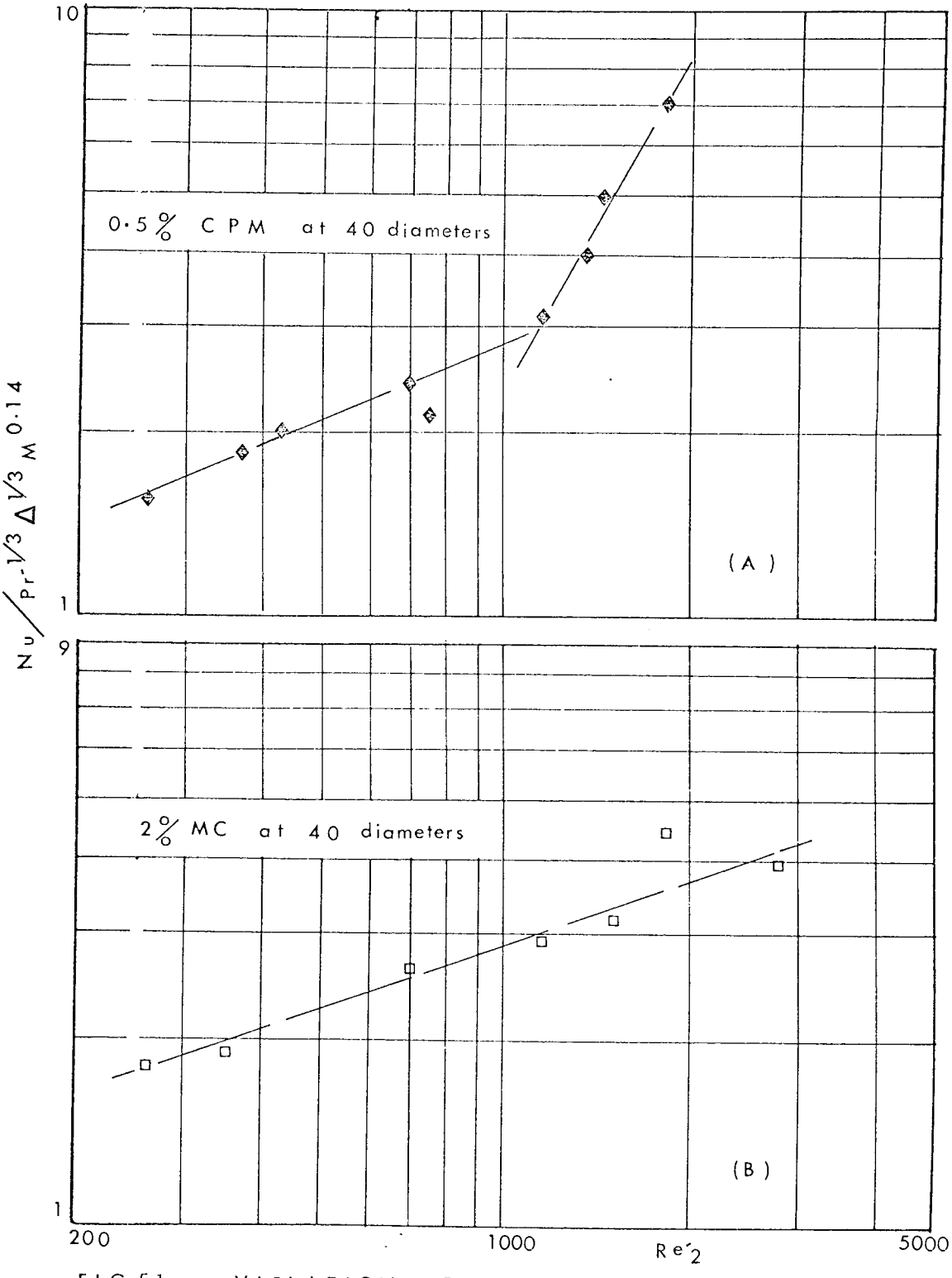

FIG.5.1 VARIATION OF Nu WITH REYNOLDS NUMBER (3·3 : 1 CONVERGENCE)

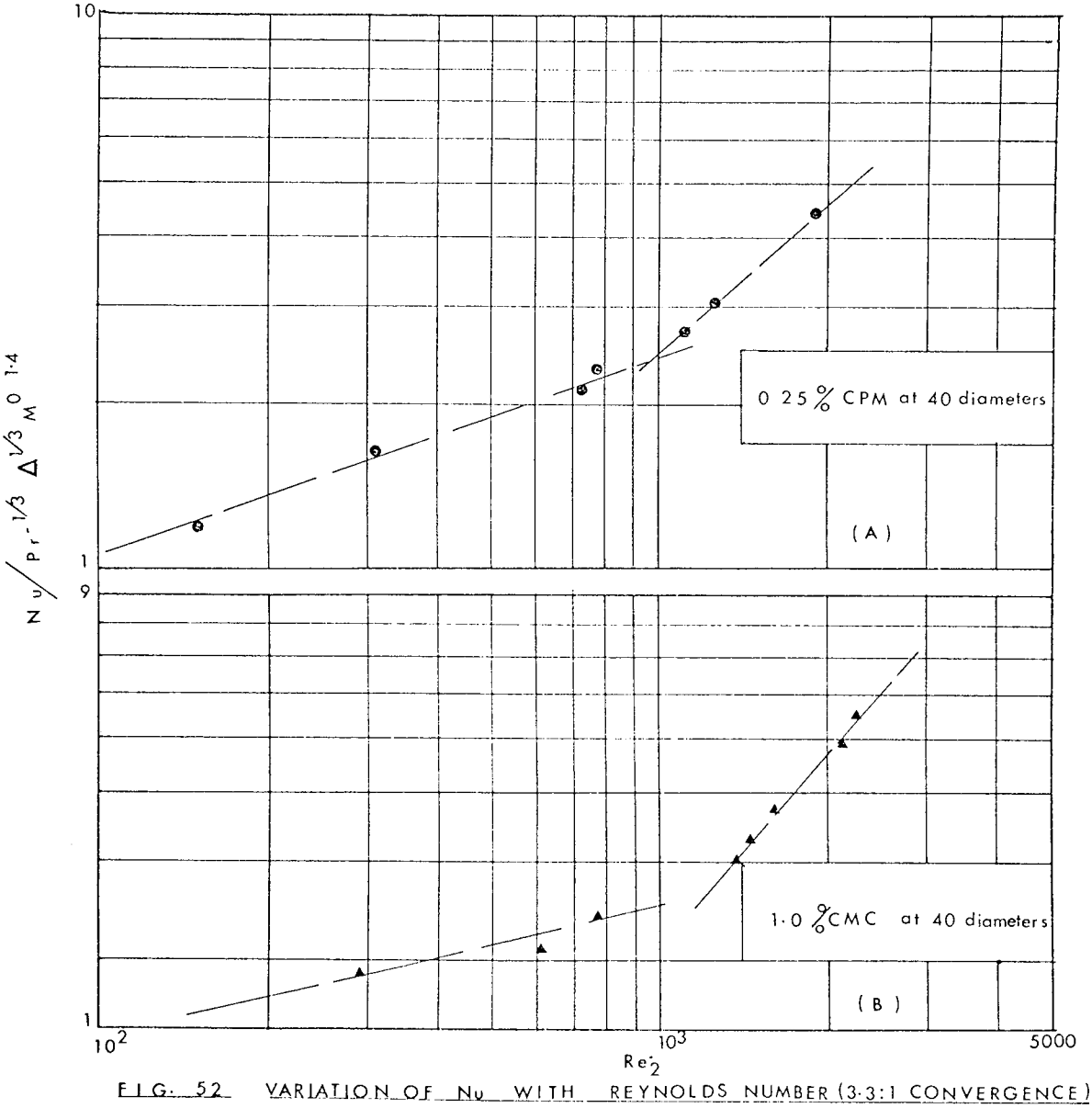

FIG. 52 VARIATION OF Nu WITH REYNOLDS NUMBER (3·3:1 CONVERGENCE)

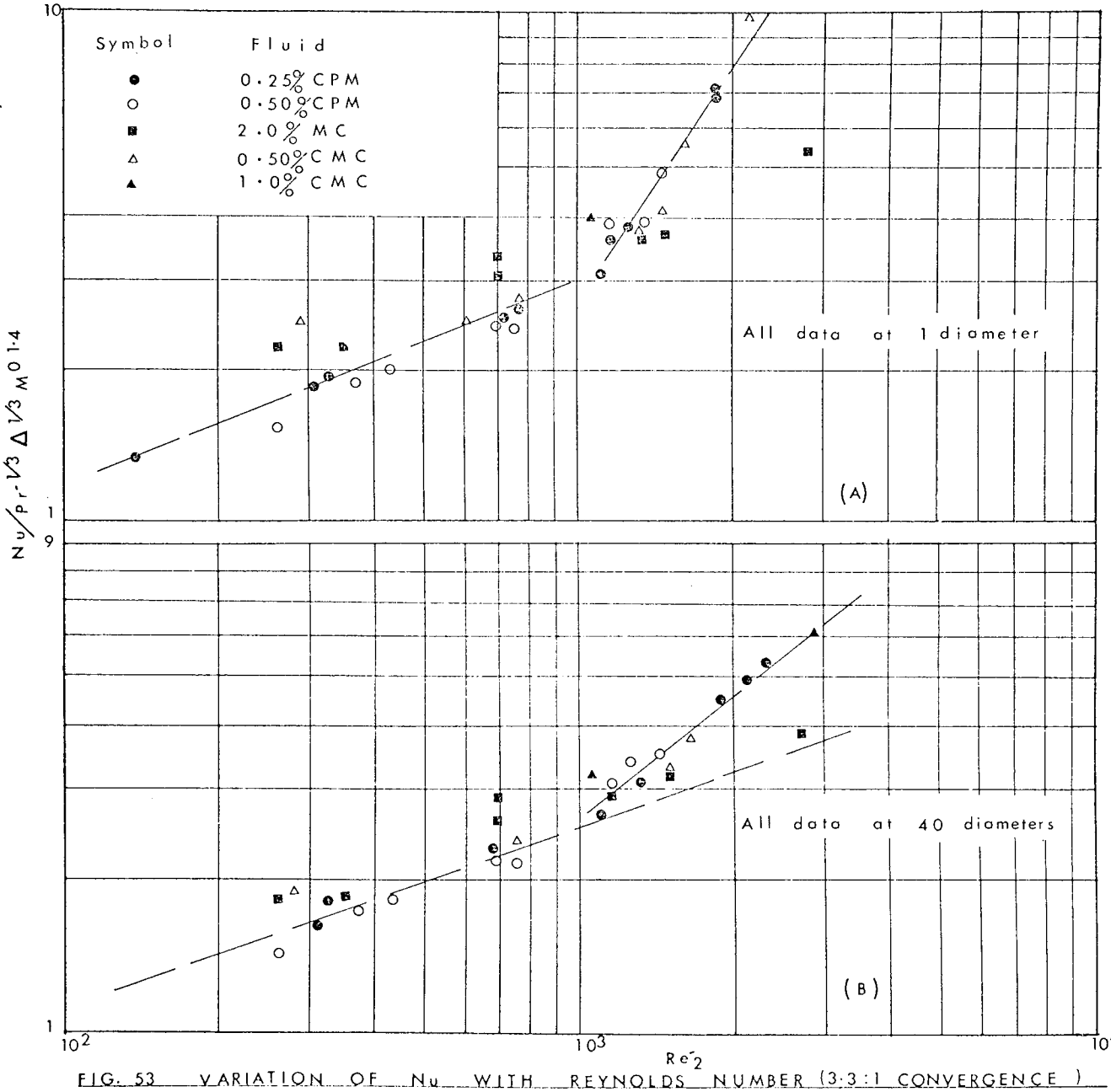

FIG. 53 VARIATION OF Nu WITH REYNOLDS NUMBER (3·3:1 CONVERGENCE)

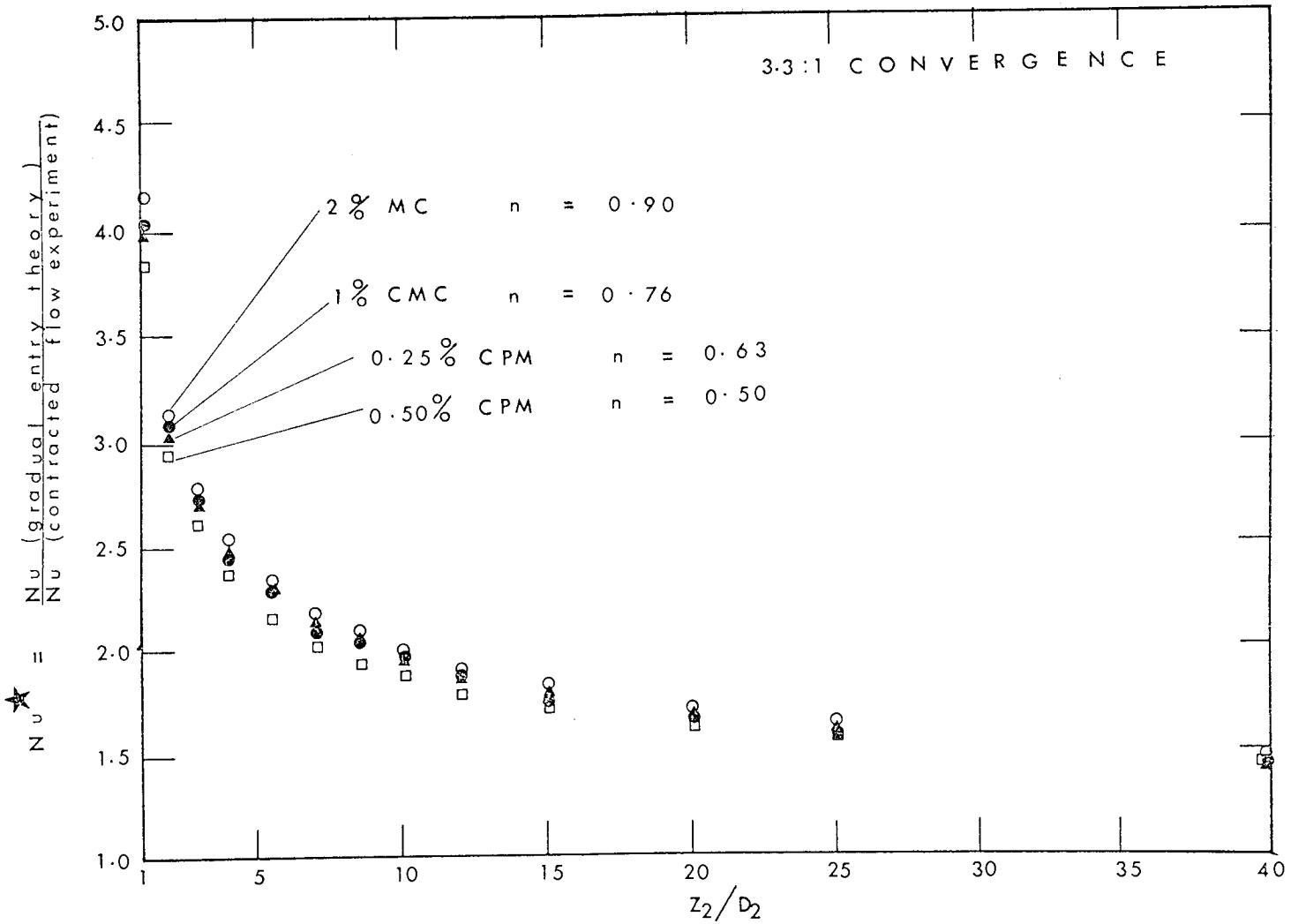

FIG. 54 AXIAL VARIATION OF Nu^* RATIO --- EFFECT OF 'n' (Pr_2) FOR $Re_2 > 1000$

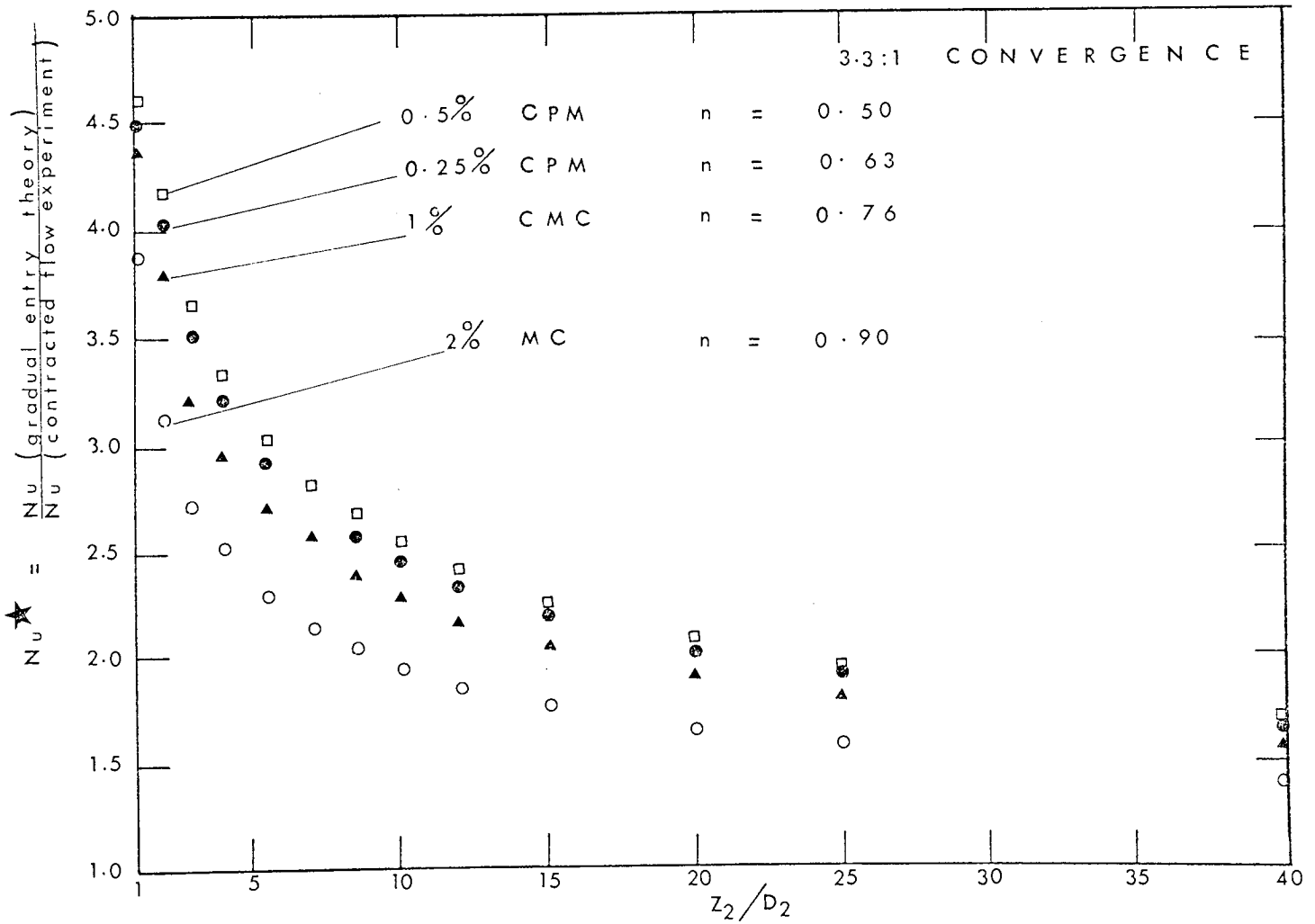

FIG. 55 AXIAL VARIATION OF Nu^* RATIO --- EFFECT OF 'n' (Pr_2) FOR $Re_2 < 1000$

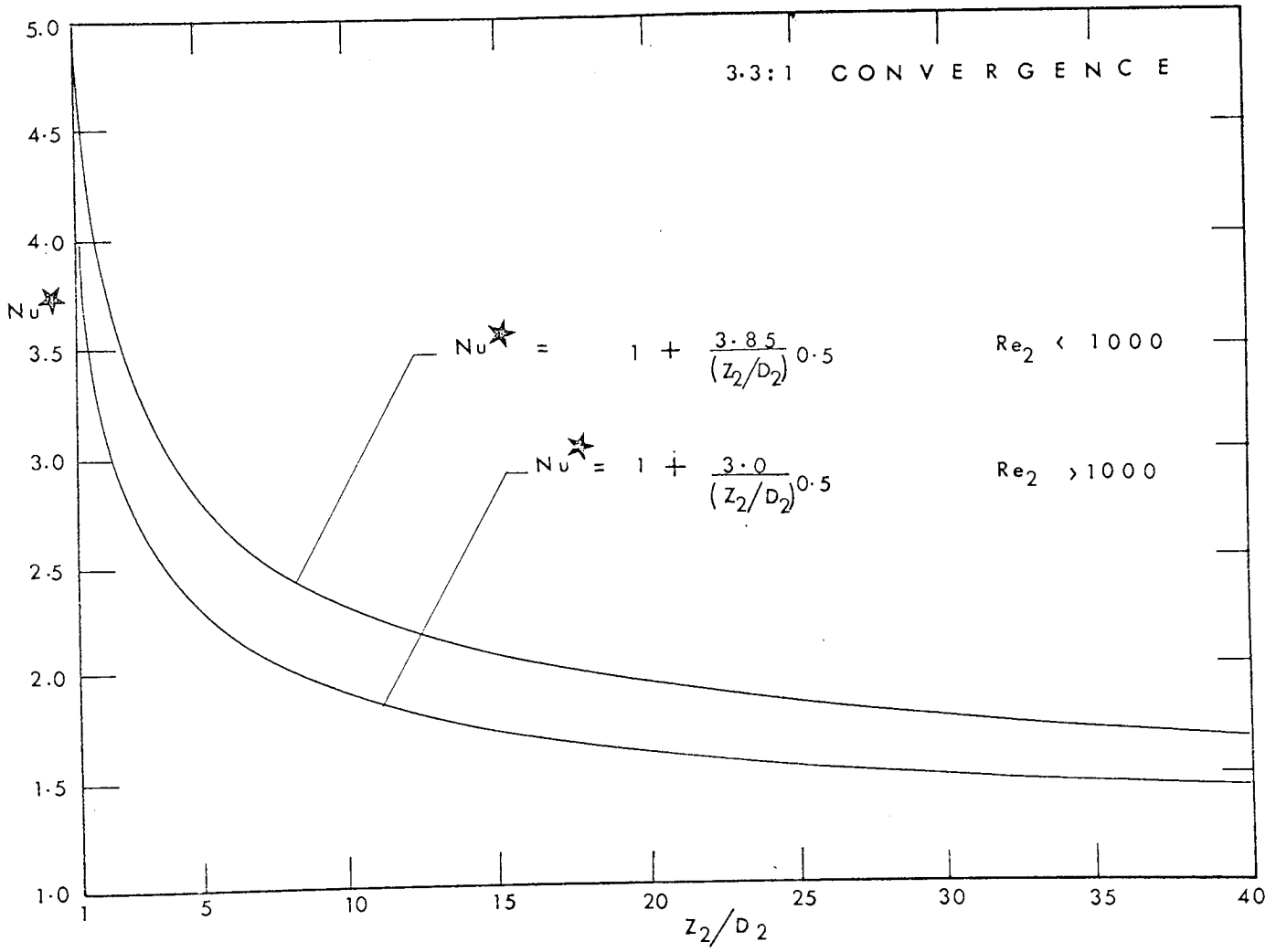

FIG. 56 $Nu^{\star}$ vs. Z_2/D_2 CORRELATION

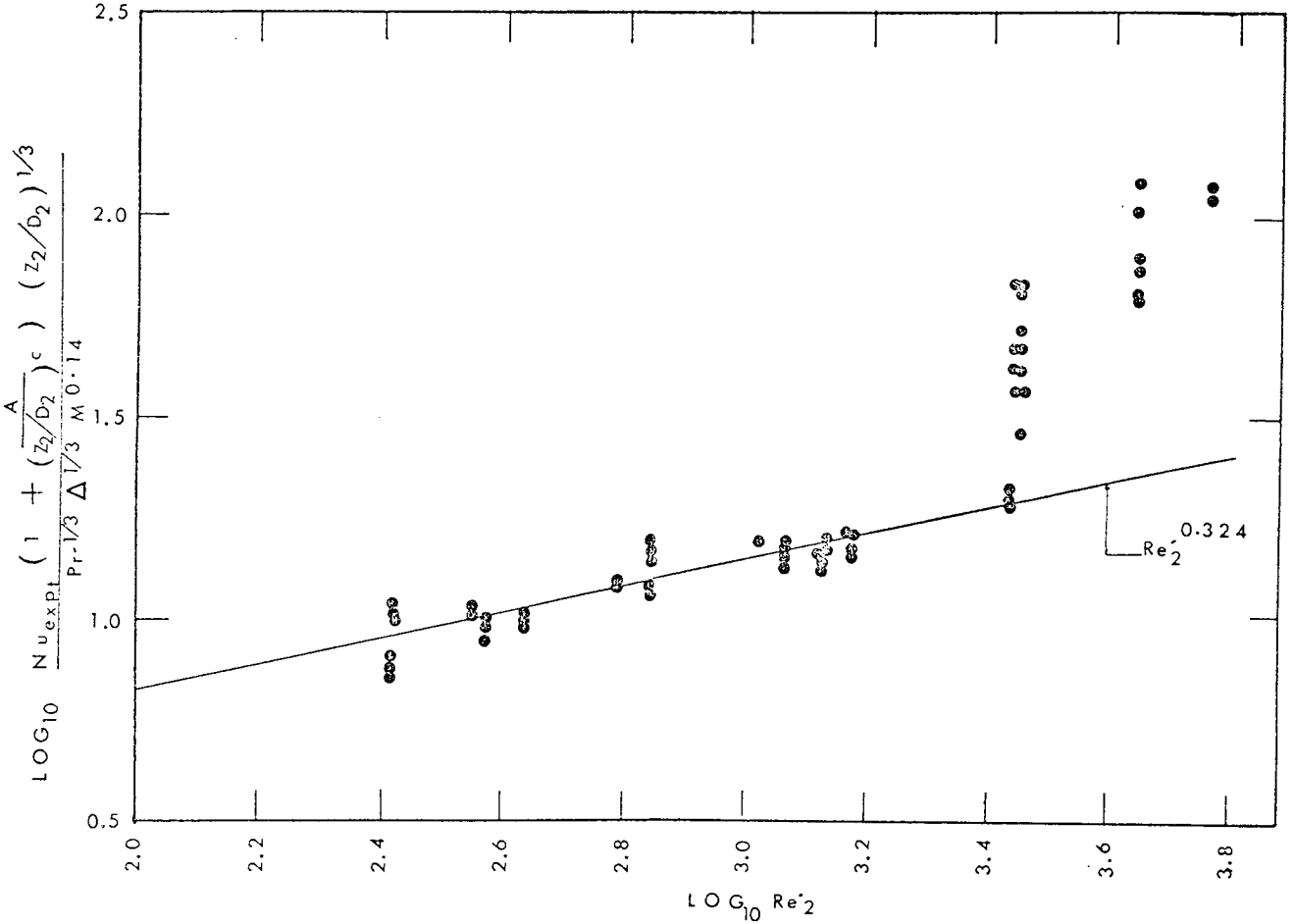

FIG. 57 $Nu/Pr^{-1/3} \Delta^{1/3} M^{0.14} f(Z/D)$ vs. Re'

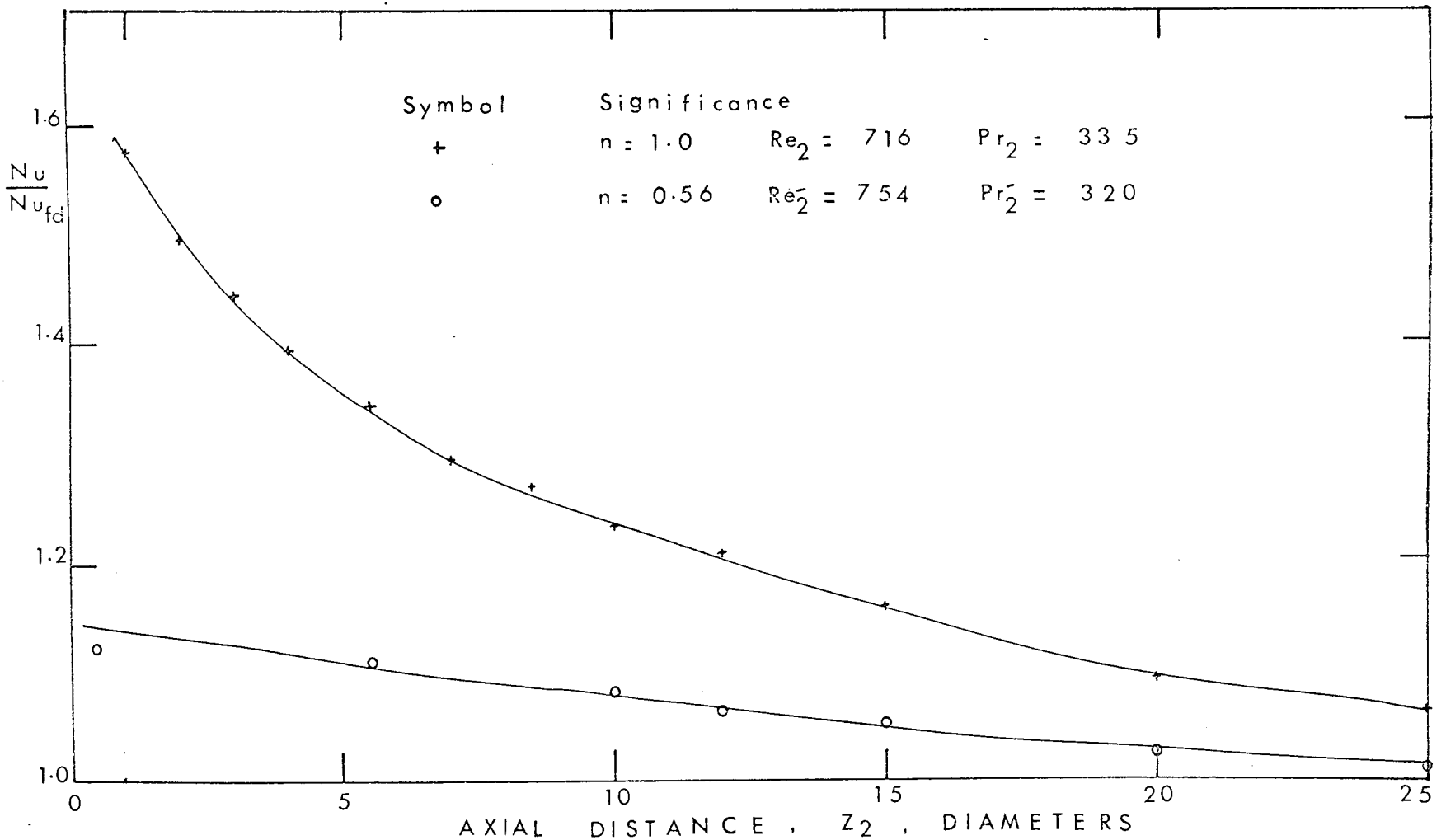

FIG· 5 8 COMPARISON BETWEEN NEWTONIAN AND NON-NEWTONIAN FLOW DEVELOPMENT DOWNSTREAM OF A 3·3:1 CONVERGENGE

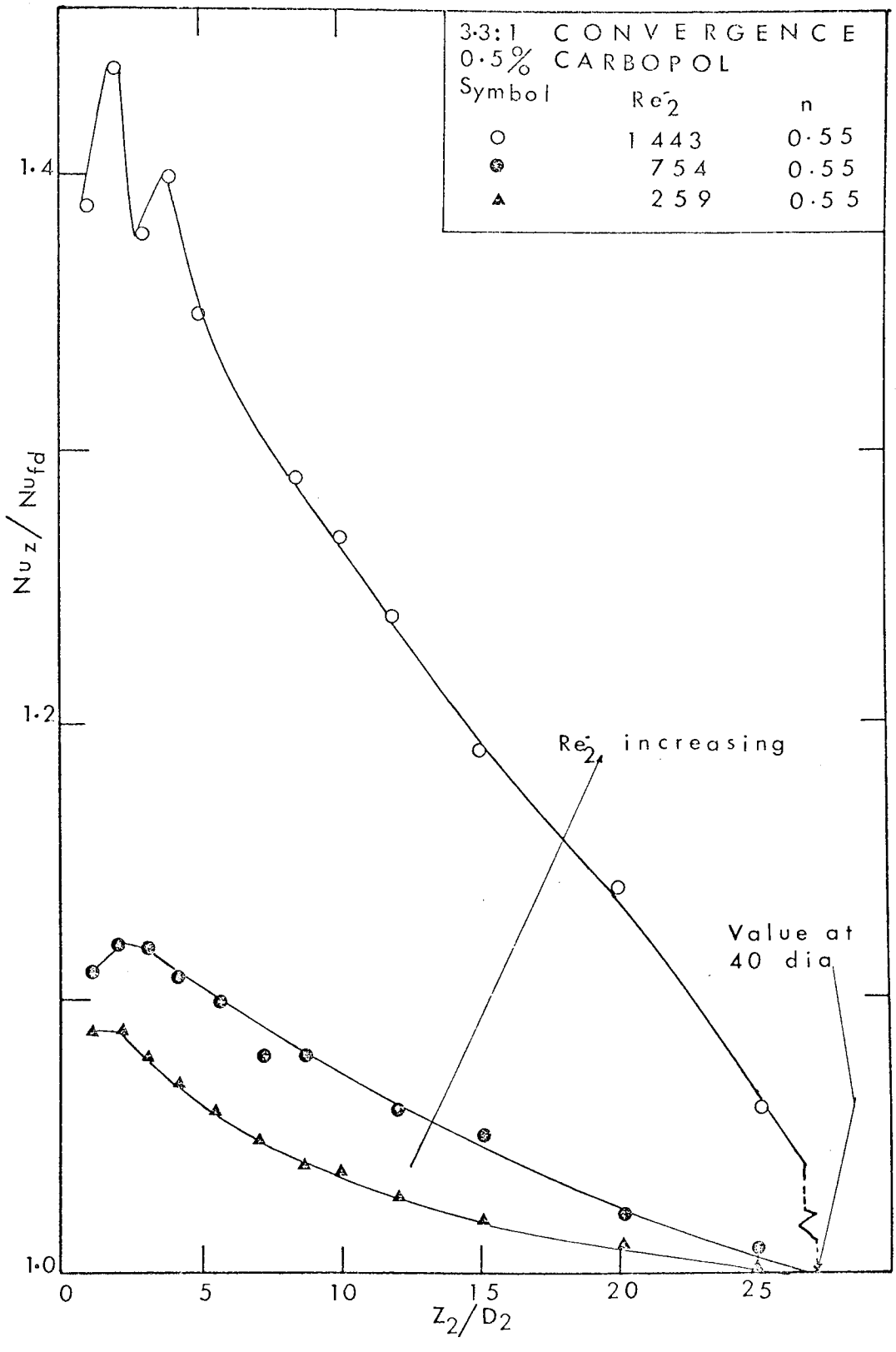

FIG. 59 EFFECT OF REYNOLDS NUMBER ON FLOW DEVELOPMENT

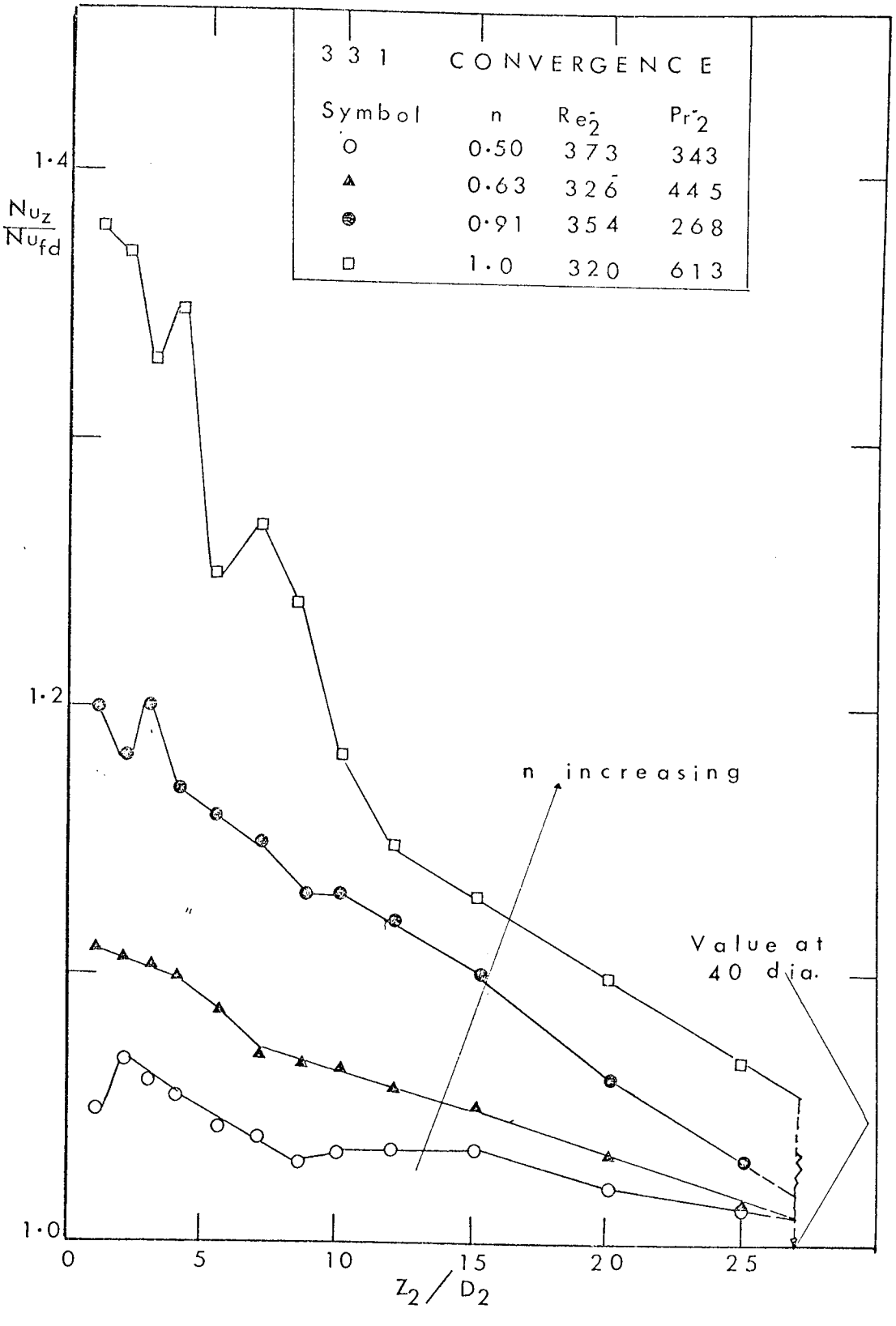

FIG. 60 EFFECT OF 'n' ON FLOW DEVELOPMENT

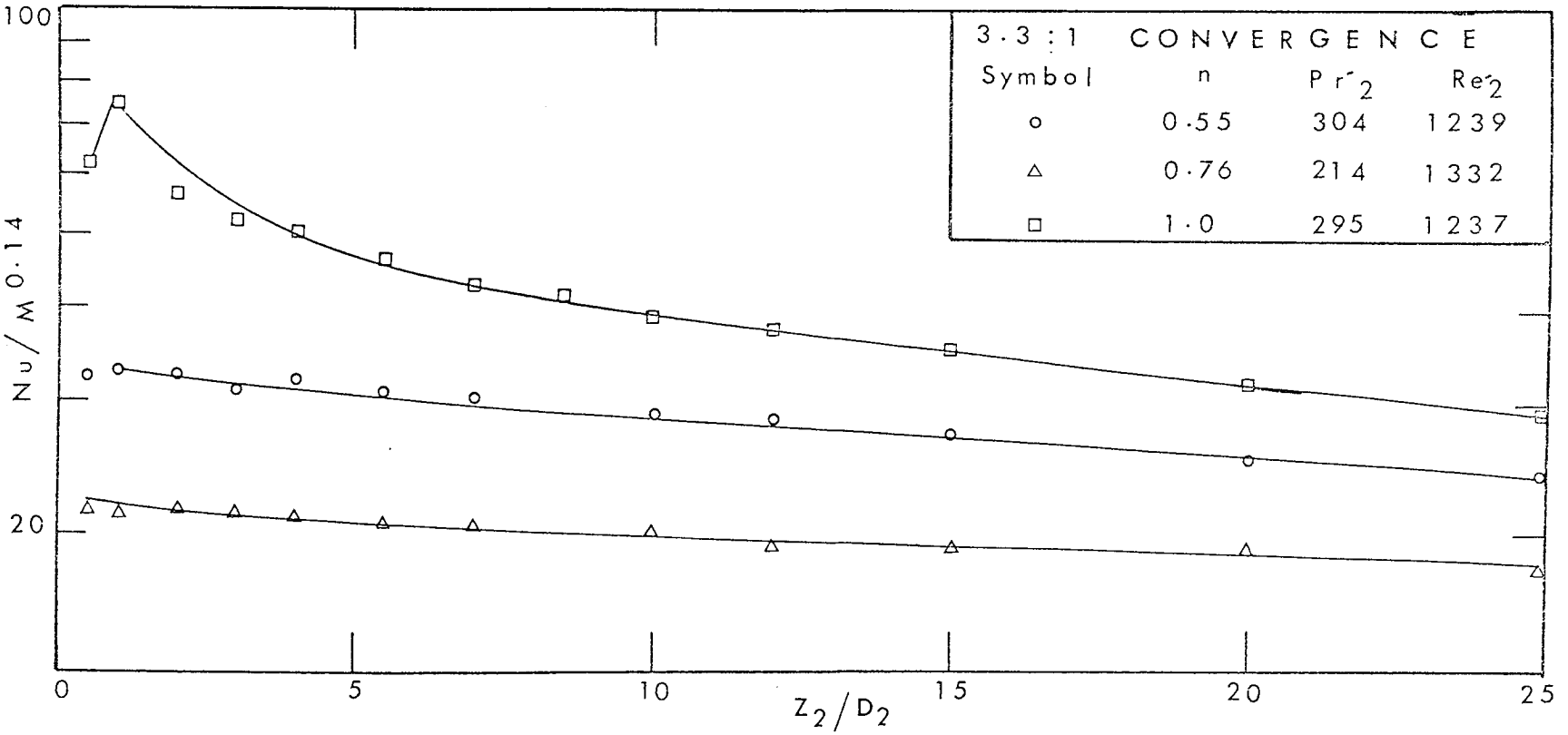

FIG. 61 EFFECT OF INDEX 'n' ON HEAT TRANSFER

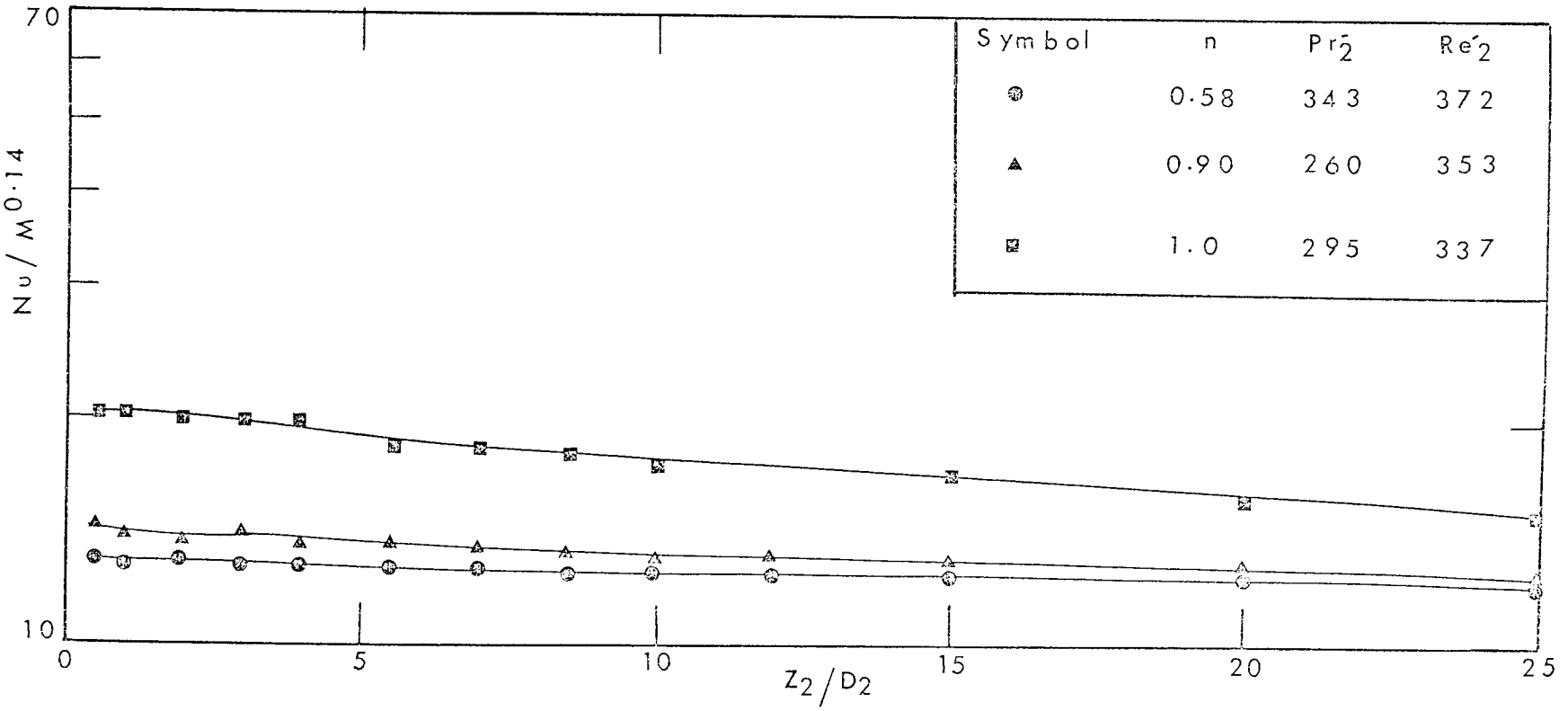

FIG. 62 EFFECT OF INDEX 'n' ON HEAT TRANSFER

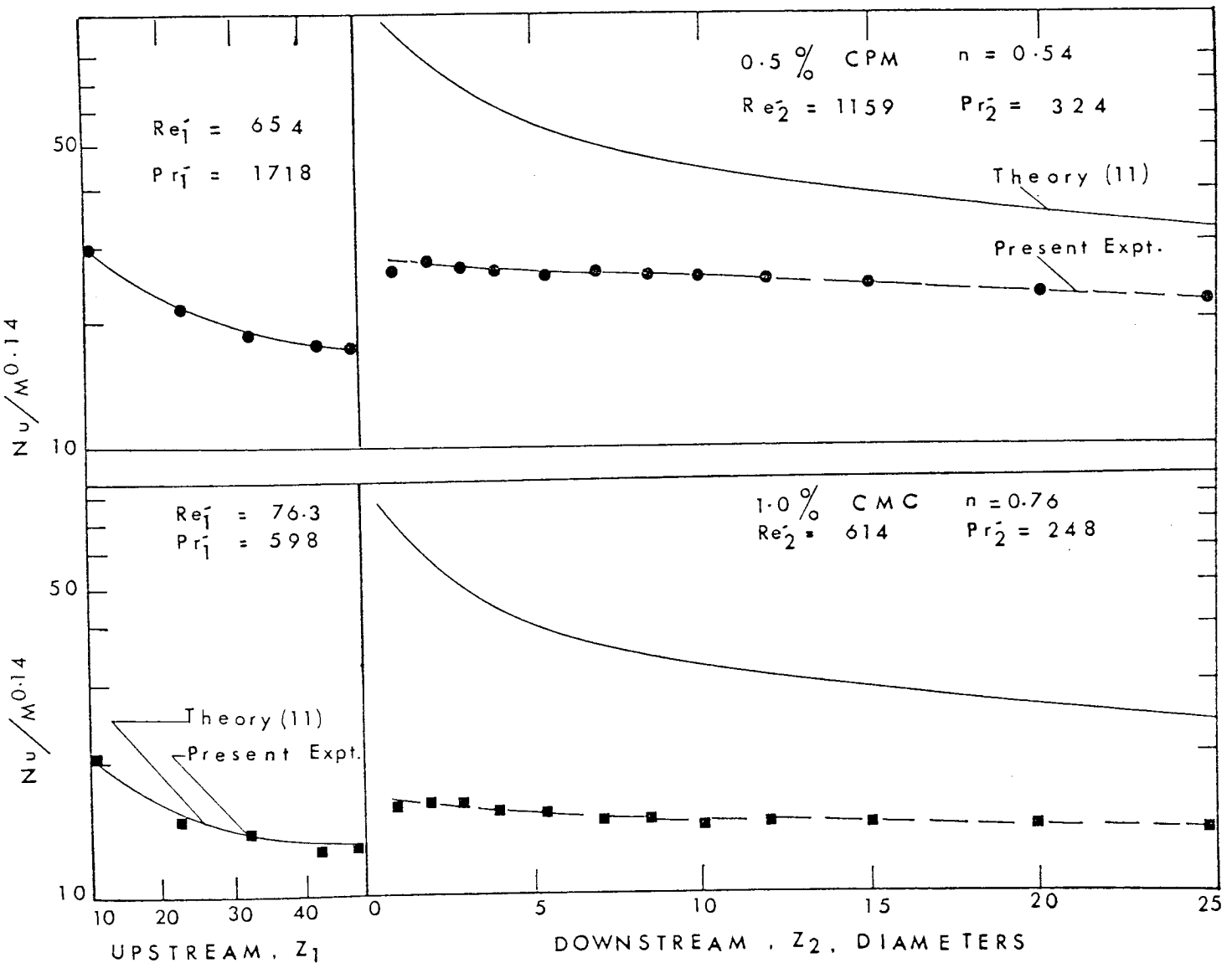

FIG. 63 NUSSELT NUMBER vs. AXIAL DISTANCE FOR A 3·3:1 CONVERGENCE COMPARISON WITH EXISTING CONTINUOUS TUBE THEORY

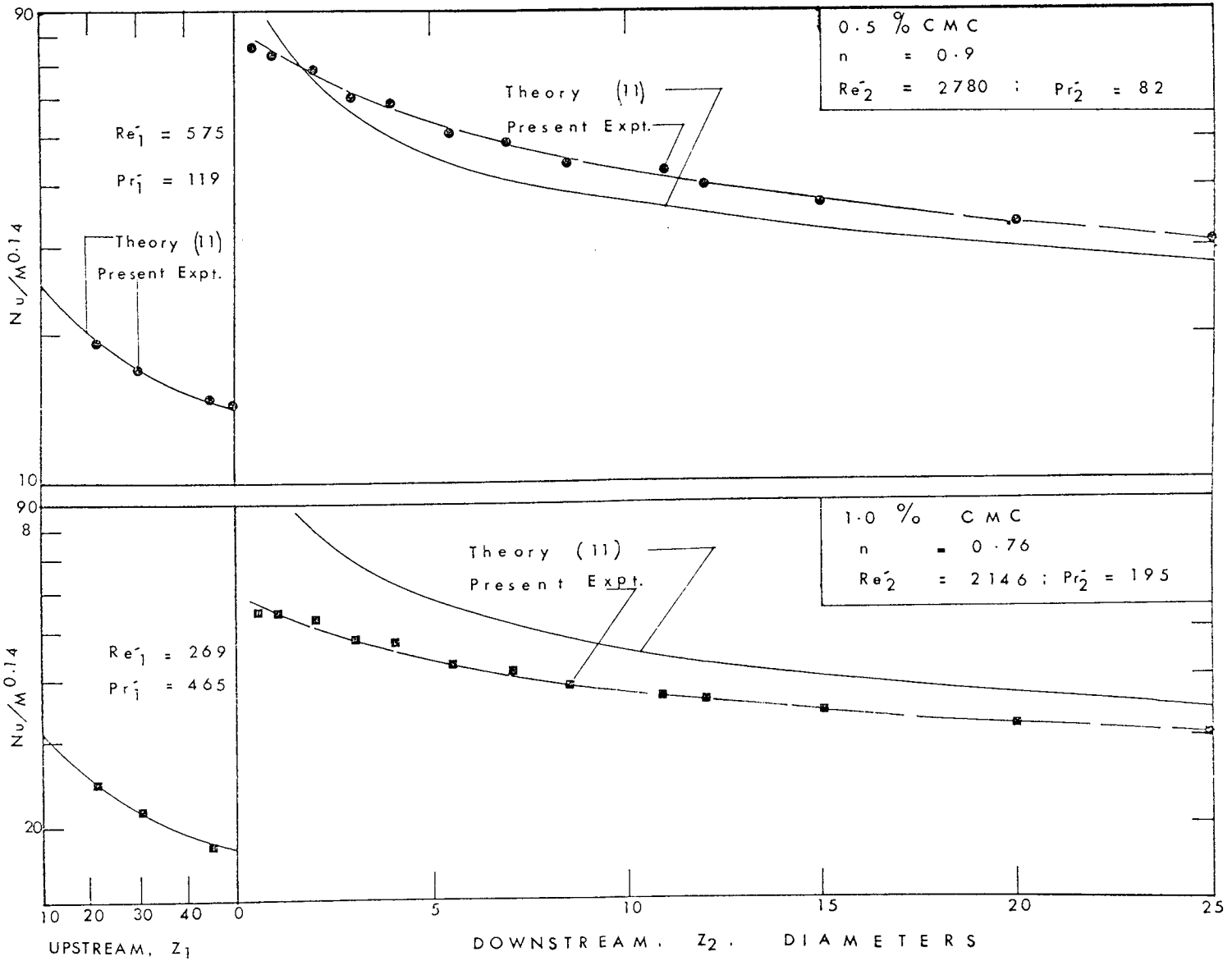

FIG. 64 NUSSELT NUMBER vs. AXIAL DISTANCE FOR A CONVERGENCE COMPARISON WITH EXISTING CONTINOUS TUBE THEORY

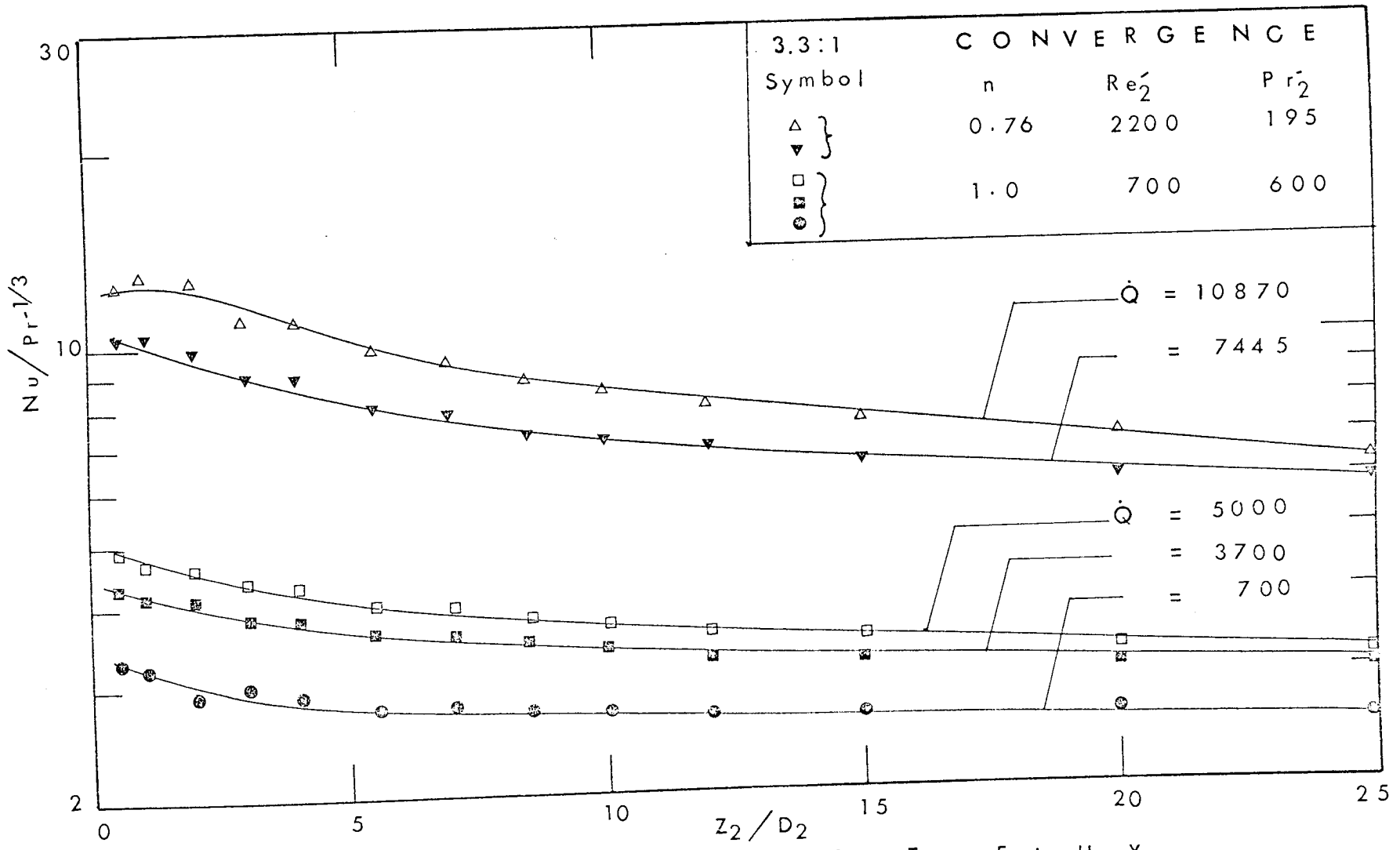

FIG. 65 EFFECT OF HEAT FLUX

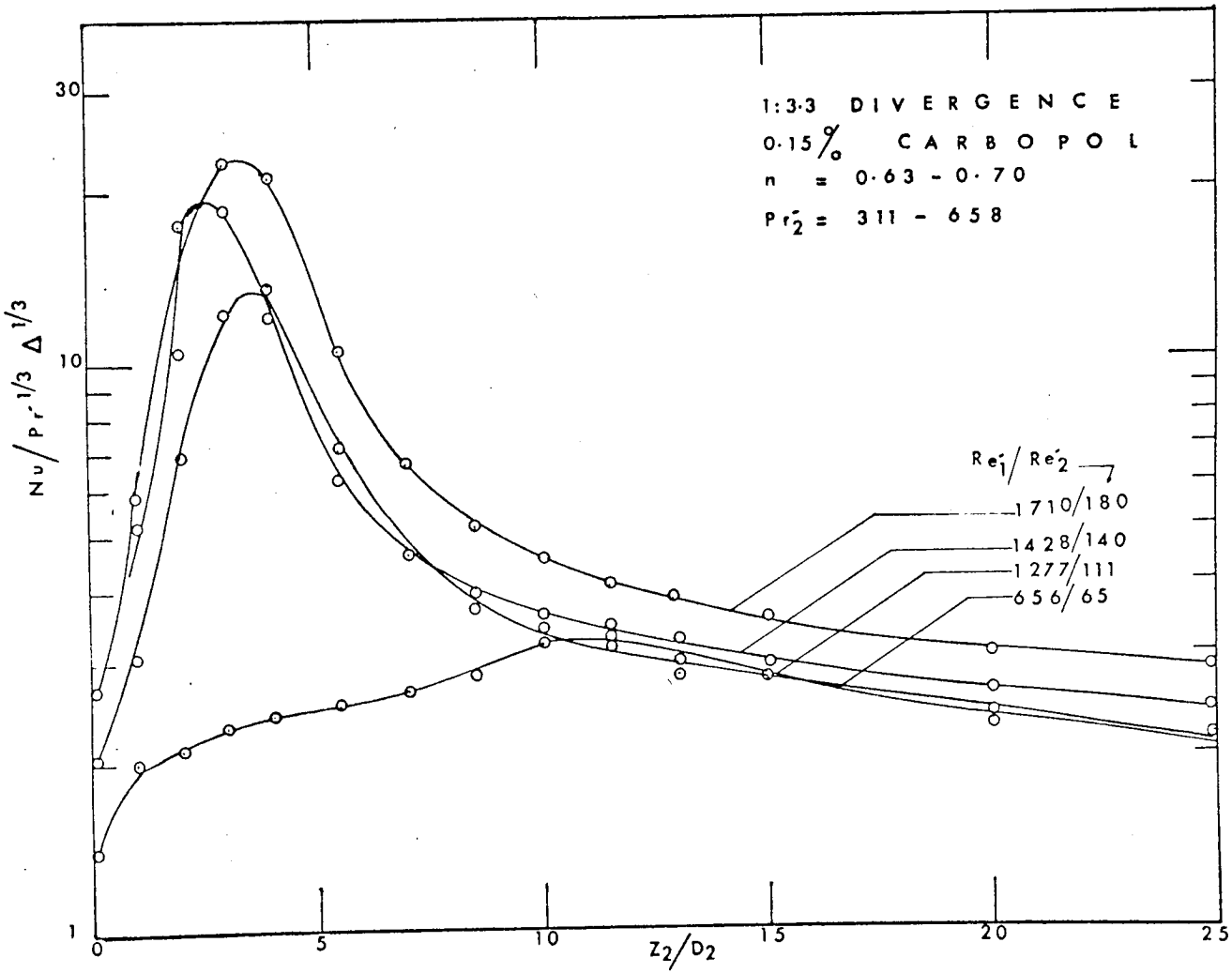

FIG. 66 AXIAL VARIATION OF HEAT TRANSFER COEFFICIENT

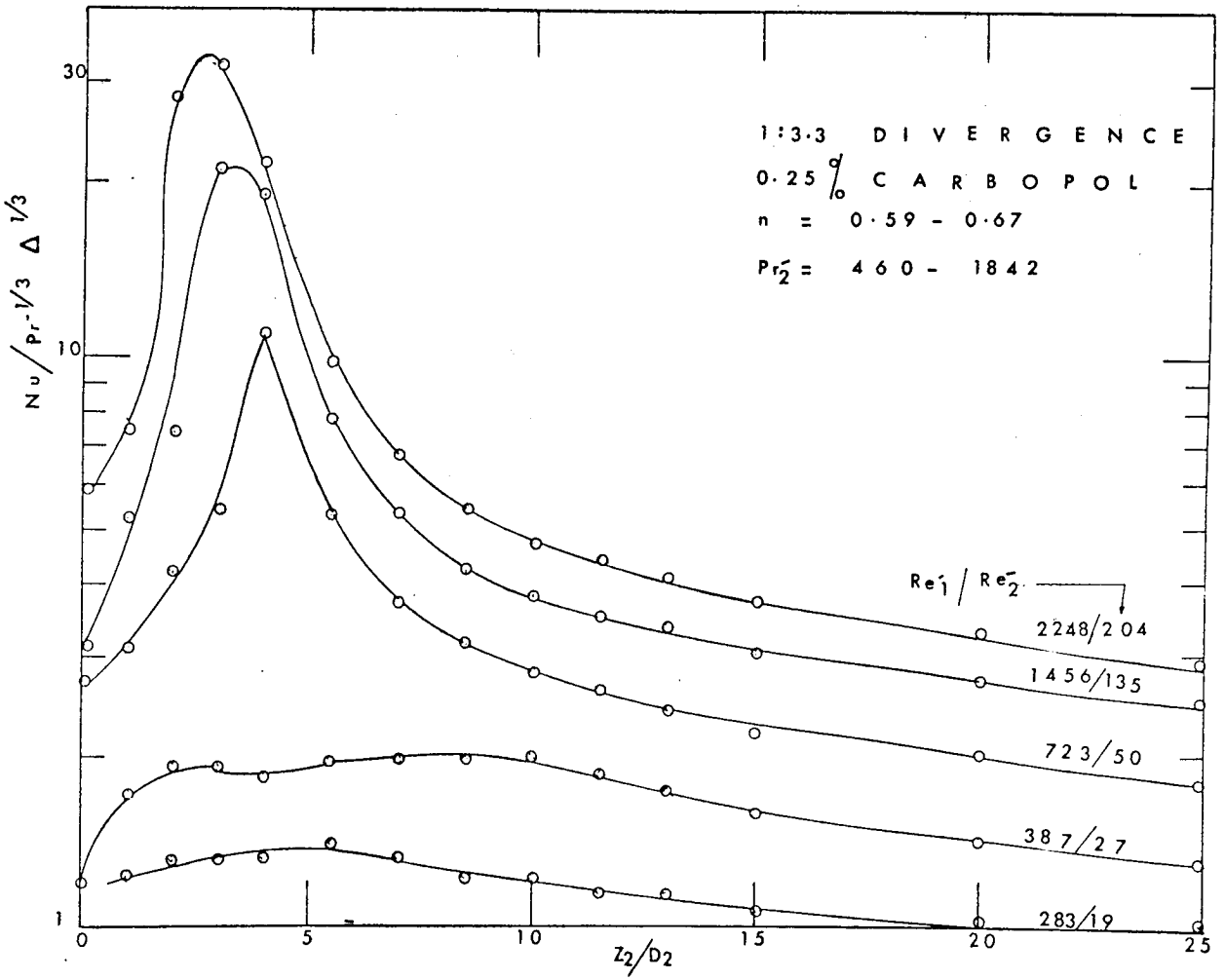

FIG. 67 AXIAL VARIATION OF HEAT TRANSFER COEFFICIENT

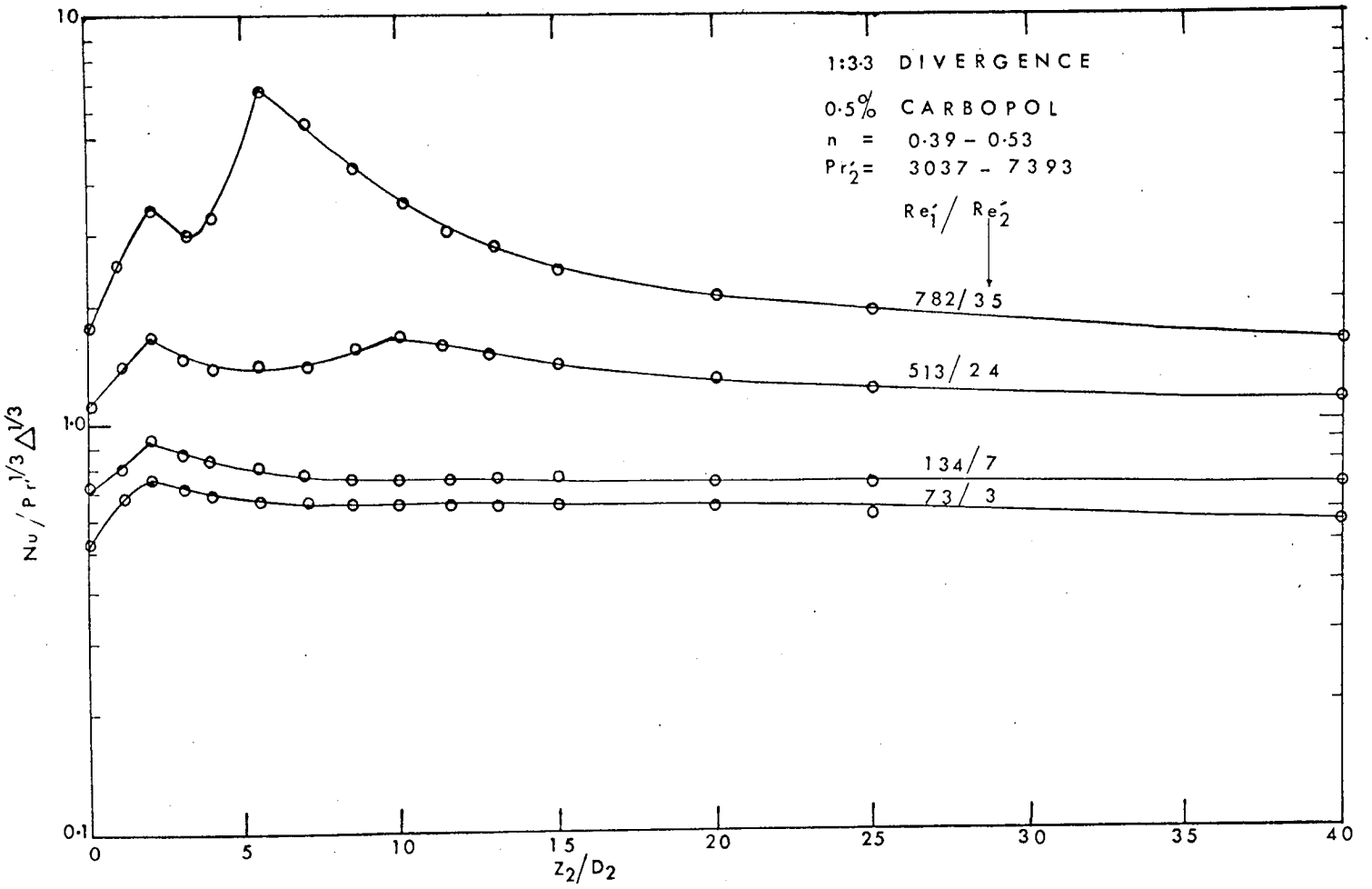

FIG. 68 AXIAL VARIATION OF HEAT TRANSFER COEFFICIENT

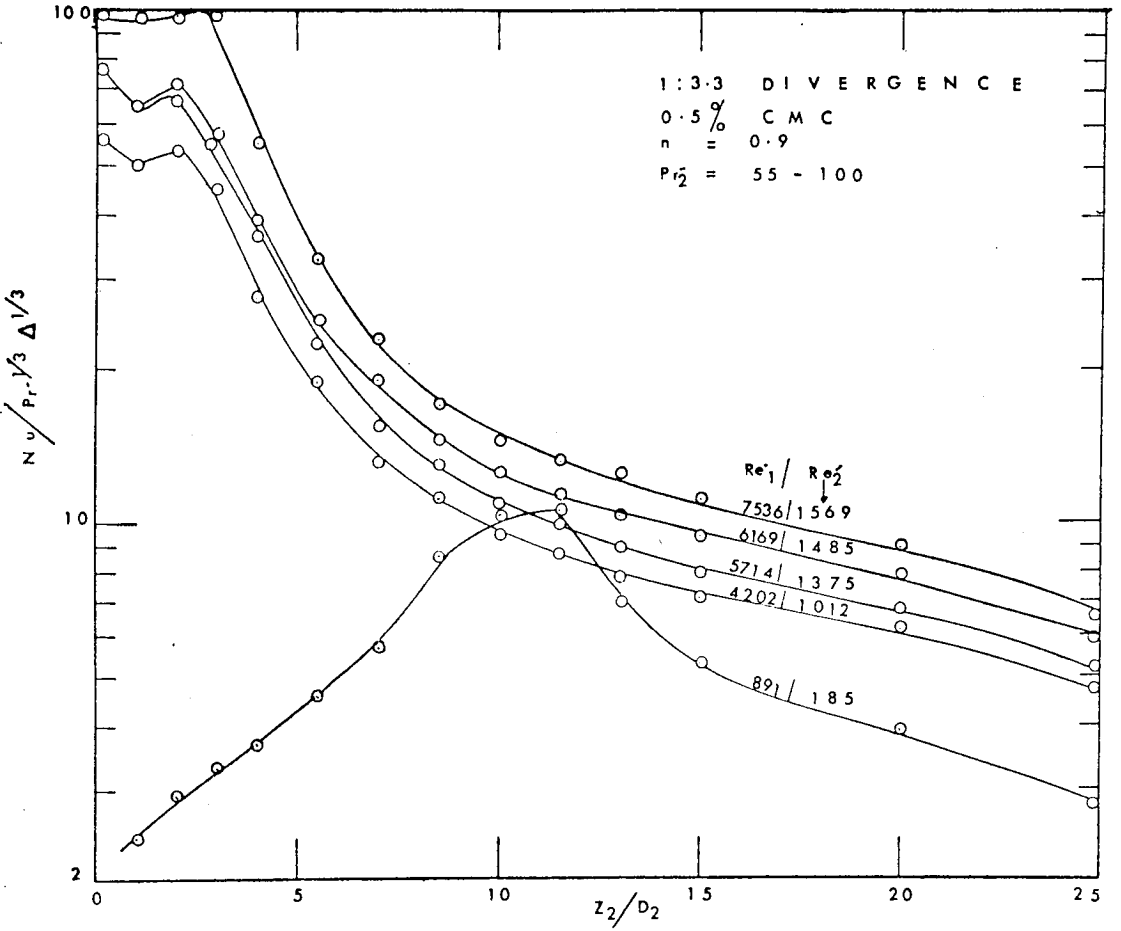

FIG. 69 AXIAL VARIATION OF HEAT TRANSFER COEFFICIENT

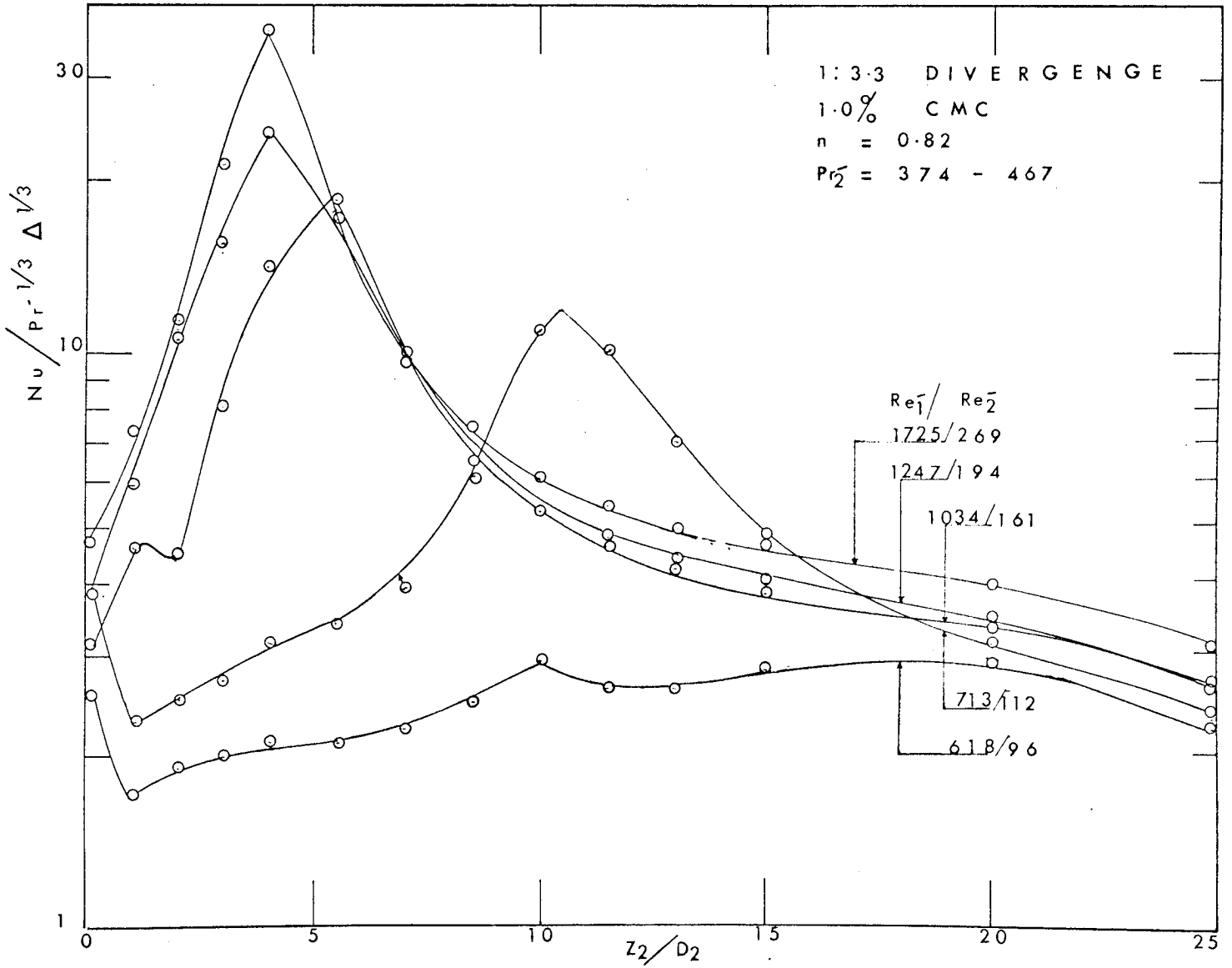

FIG. 70 AXIAL VARIATION OF HEAT TRANSFER COEFFICIENT

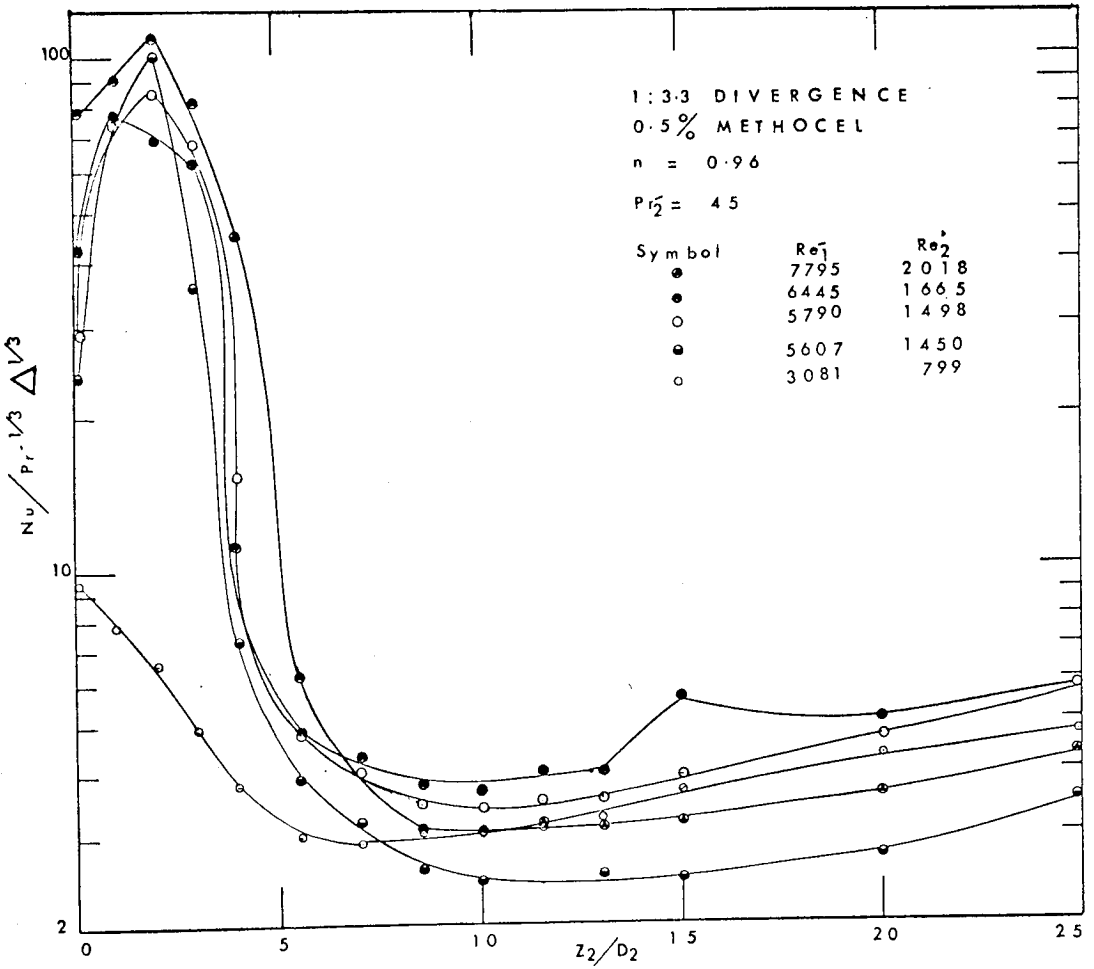

FIG 71. AXIAL VARIATION OF HEAT TRANSFER COEFFICIENT

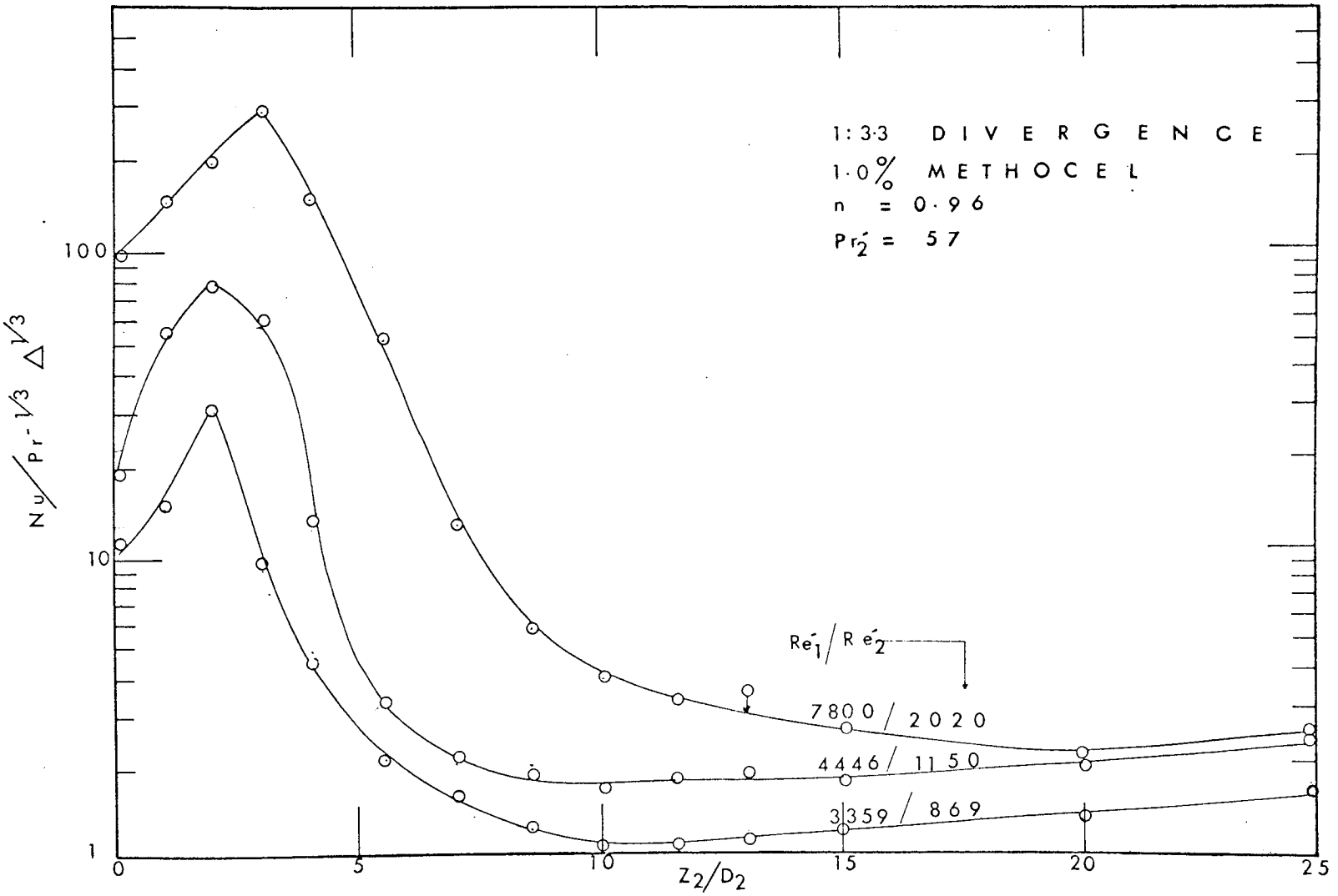

FIG. 72 AXIAL VARIATION OF HEAT TRANSFER COEFFICIENT

FIG. 73 EFFECT OF FREE CONVECTION ON POSITION OF MAXIMUM (MINIMUM) $\overline{Nu}$

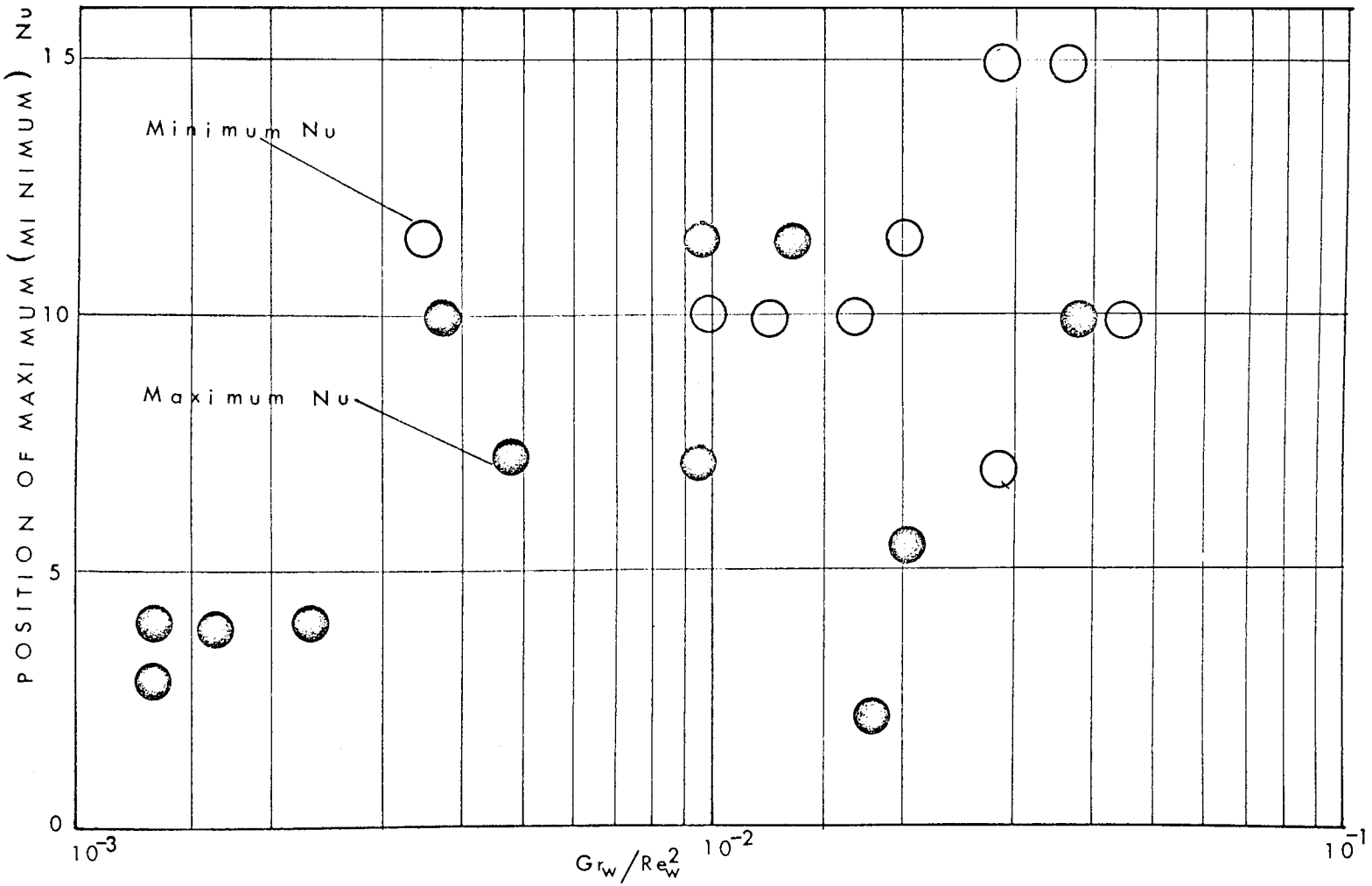

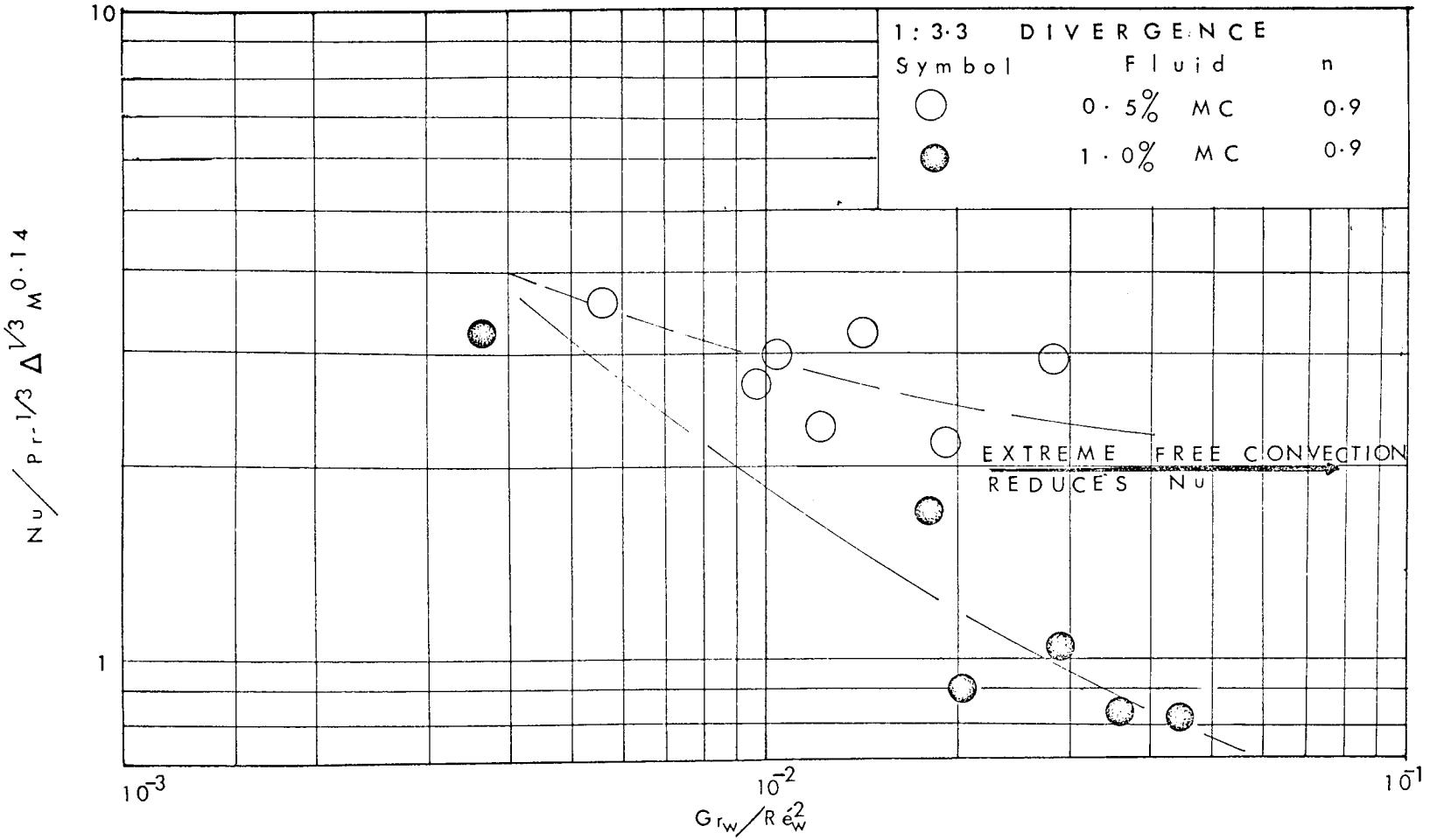

FIG. 74 THE REVERSE INFLUENCE OF FREE CONVECTION AT THE POSITION OF MINIMUM Nu

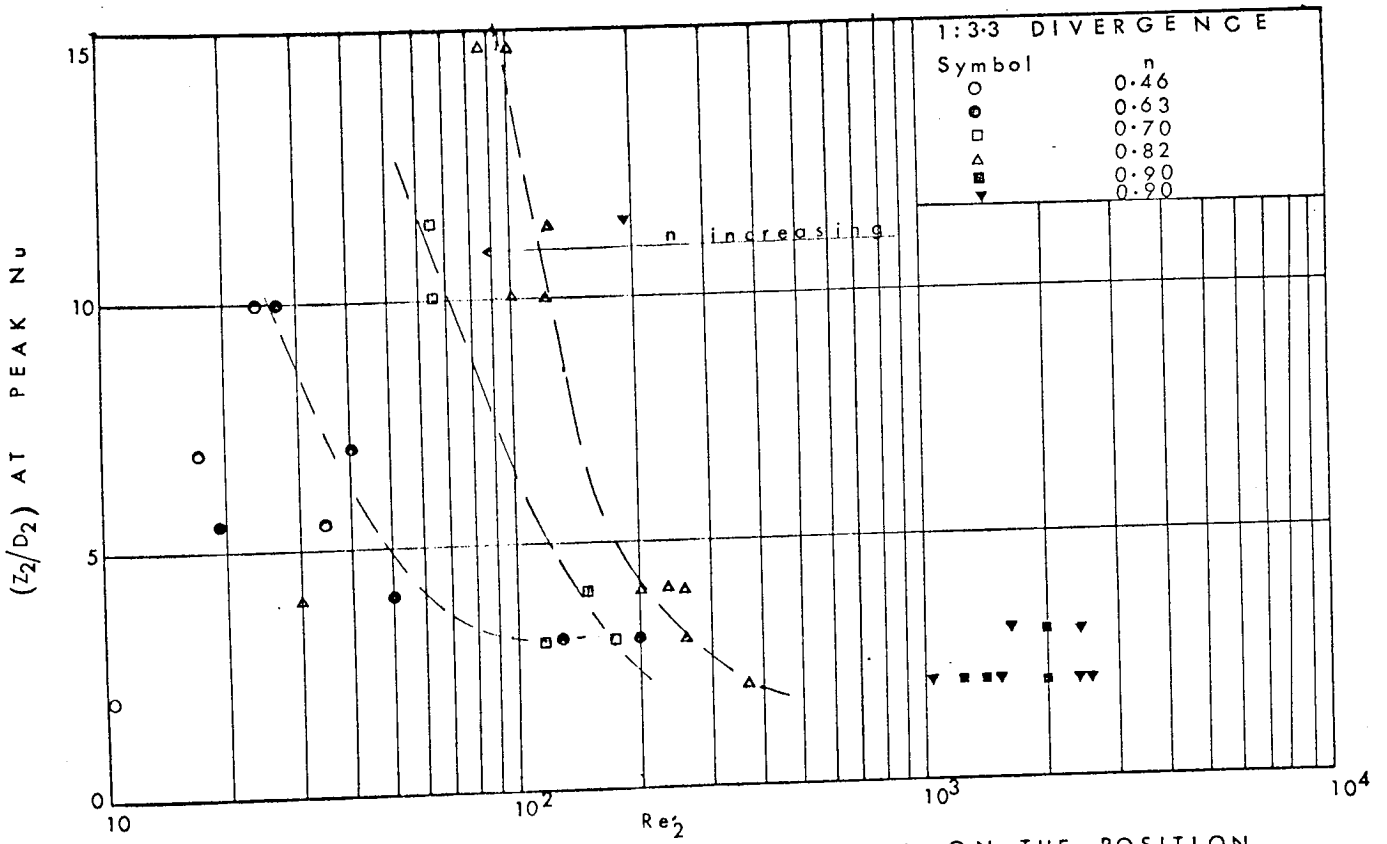

FIG. 75 EFFECT OF REYNOLDS NUMBER AND 'n' ON THE POSITION OF PEAK Nu

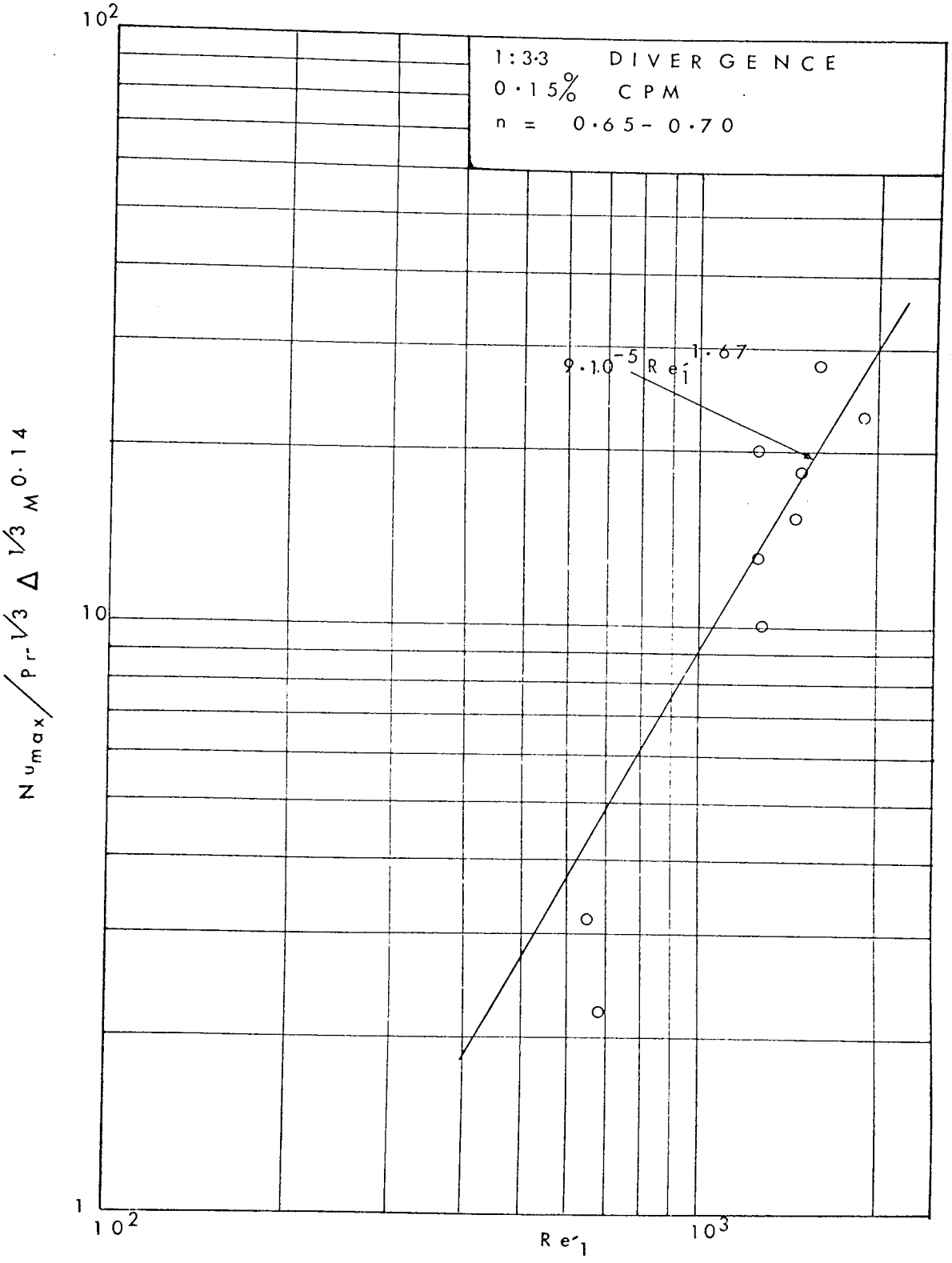

FIG. 76 Nu_{max} - Re'_1 CORRELATION

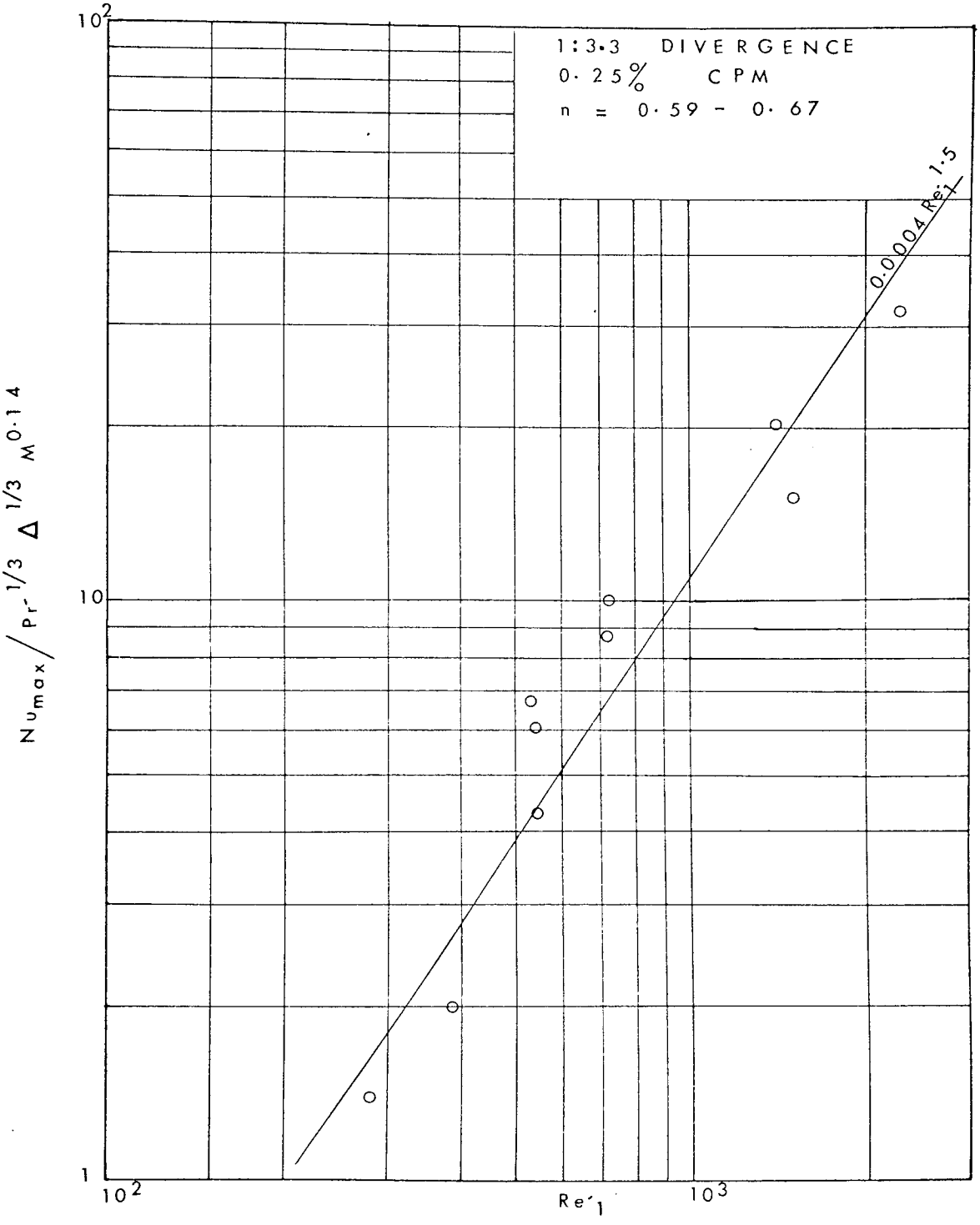

FIG. 77 $Nu_{max} - Re'_1$ CORRELATION

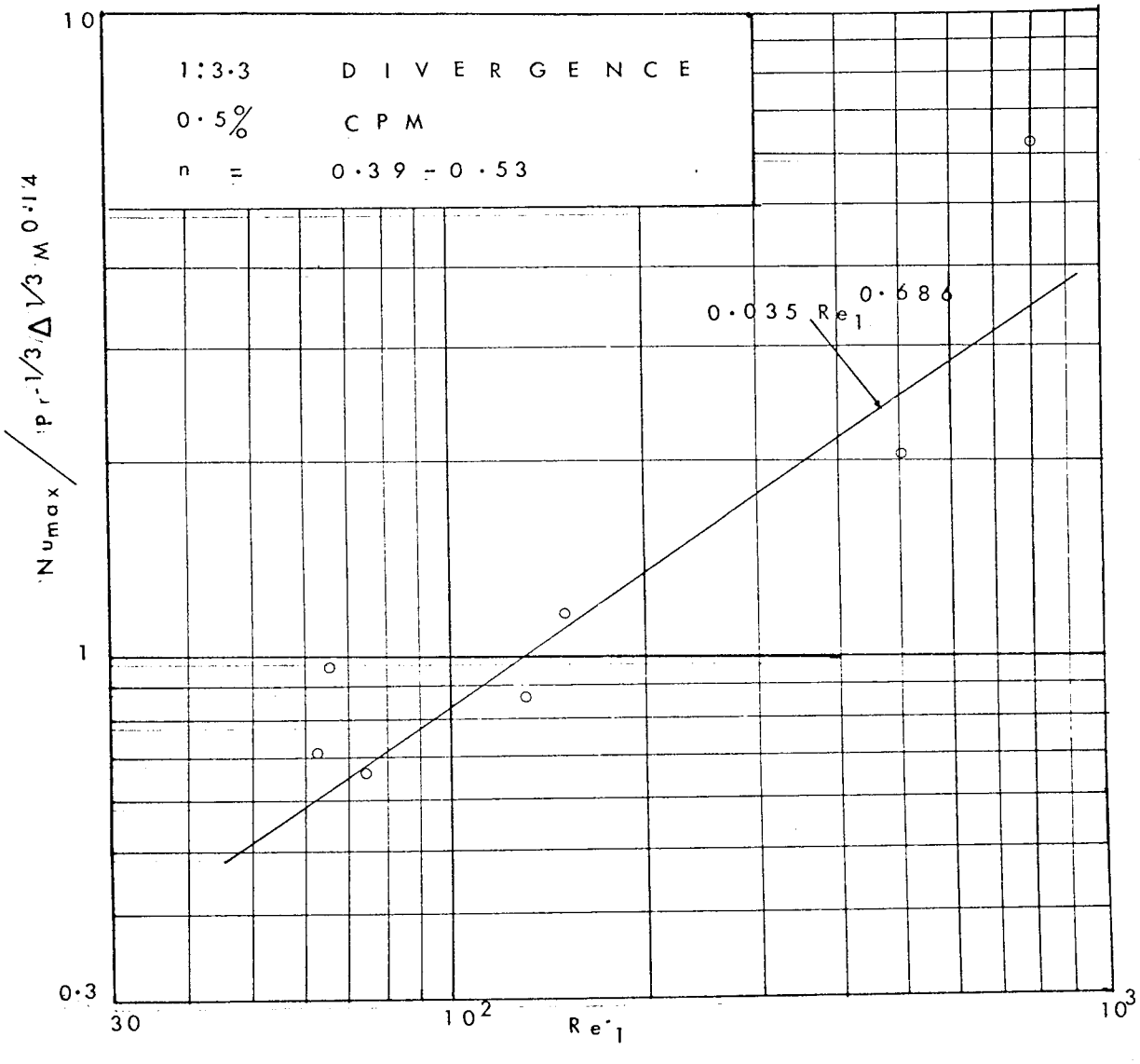

FIG. 78 Nu_{max} - Re'_1 CORRELATION

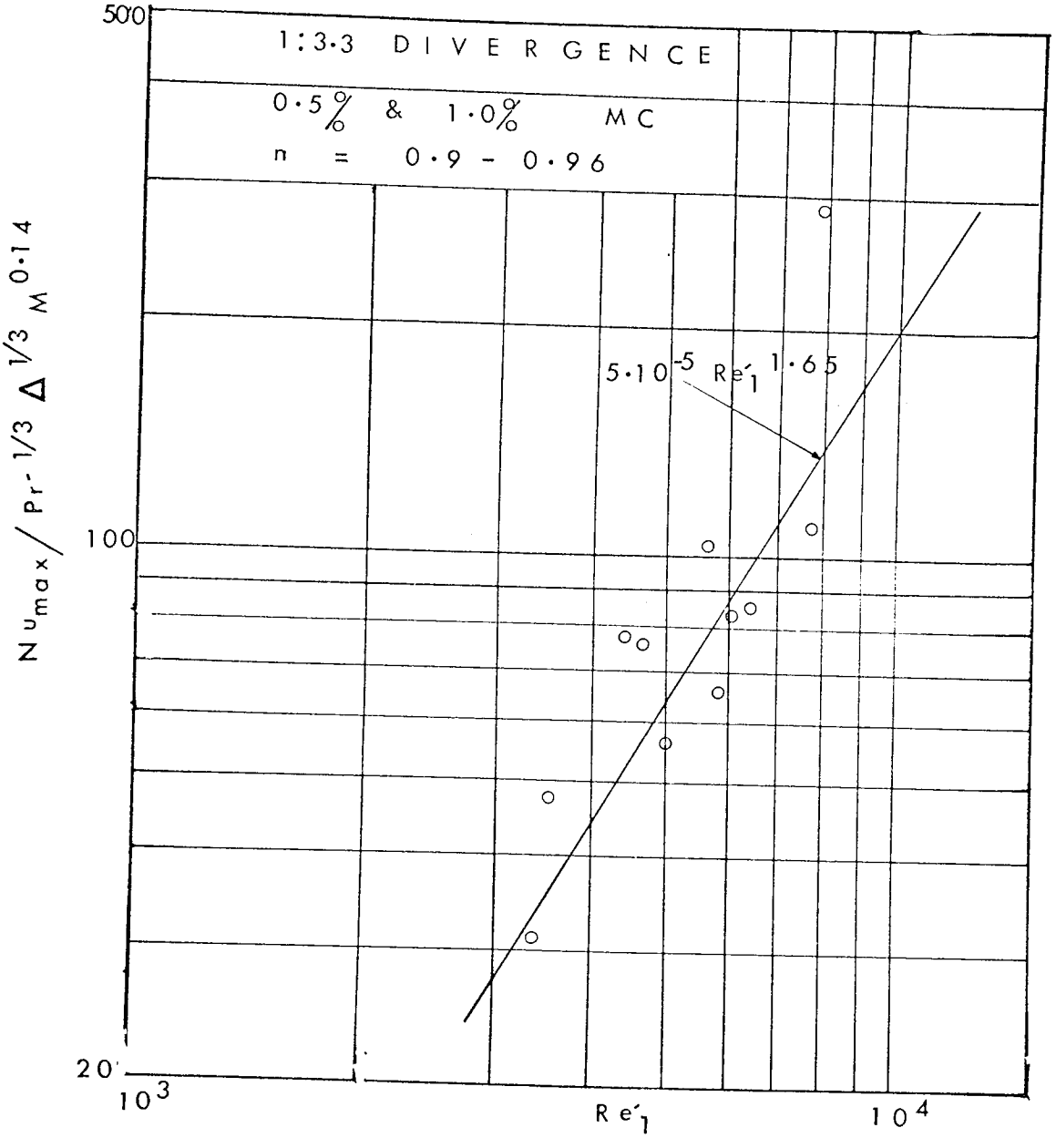

FIG. 79 Nu_{max} - Re'_1 CORRELATION

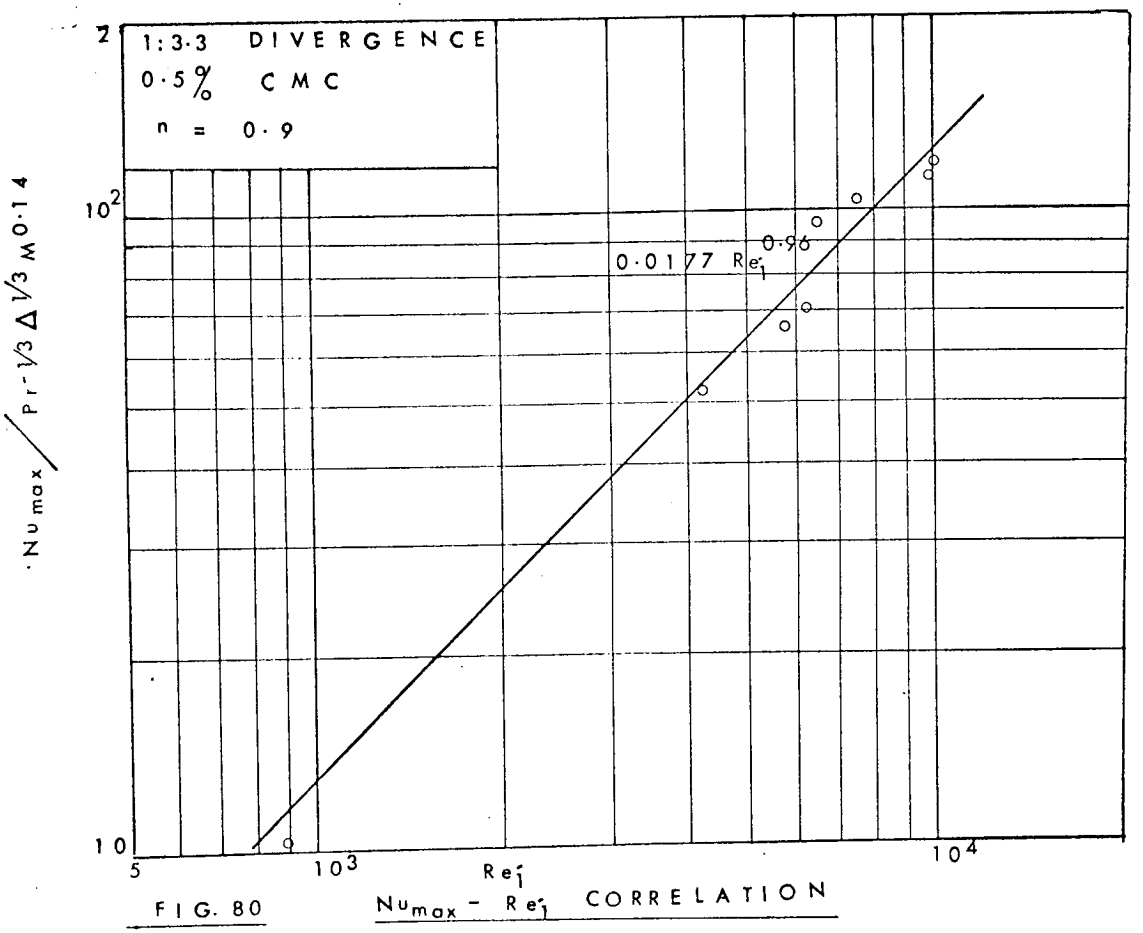

FIG. 80 Nu_{max} - Re_j CORRELATION

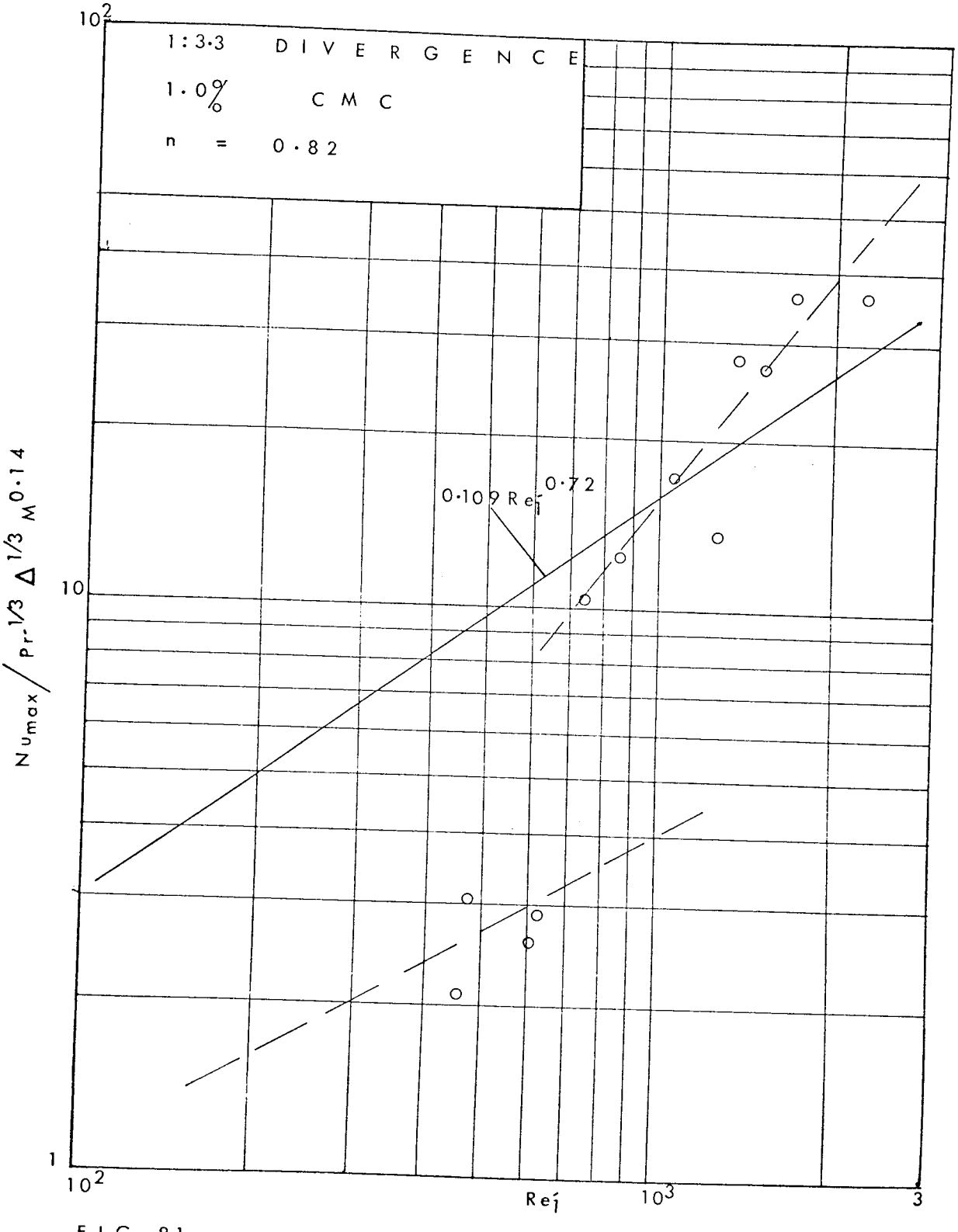

FIG. 81 Numax – Rej CORRELATION

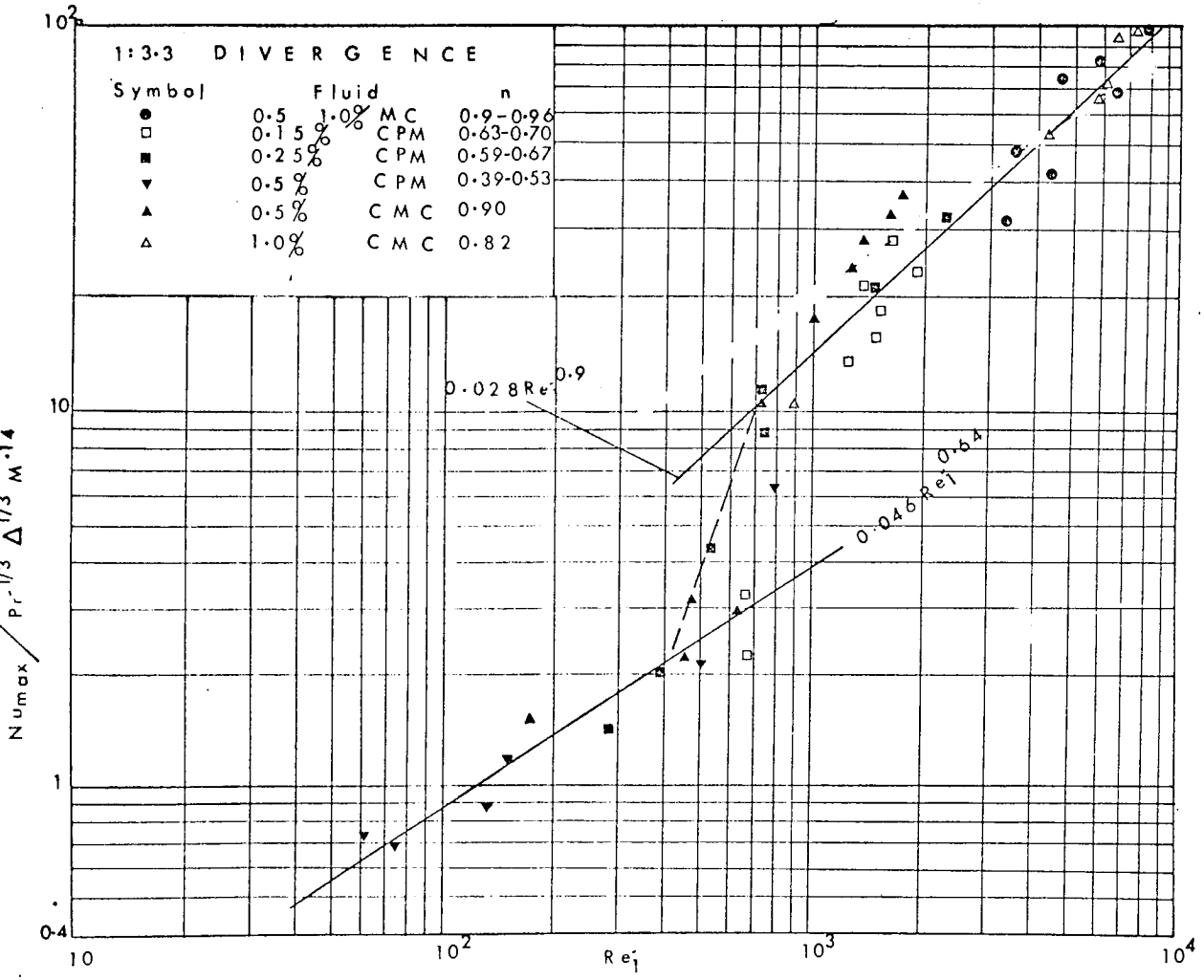

FIG. 82 Numax - Rej CORRELATION

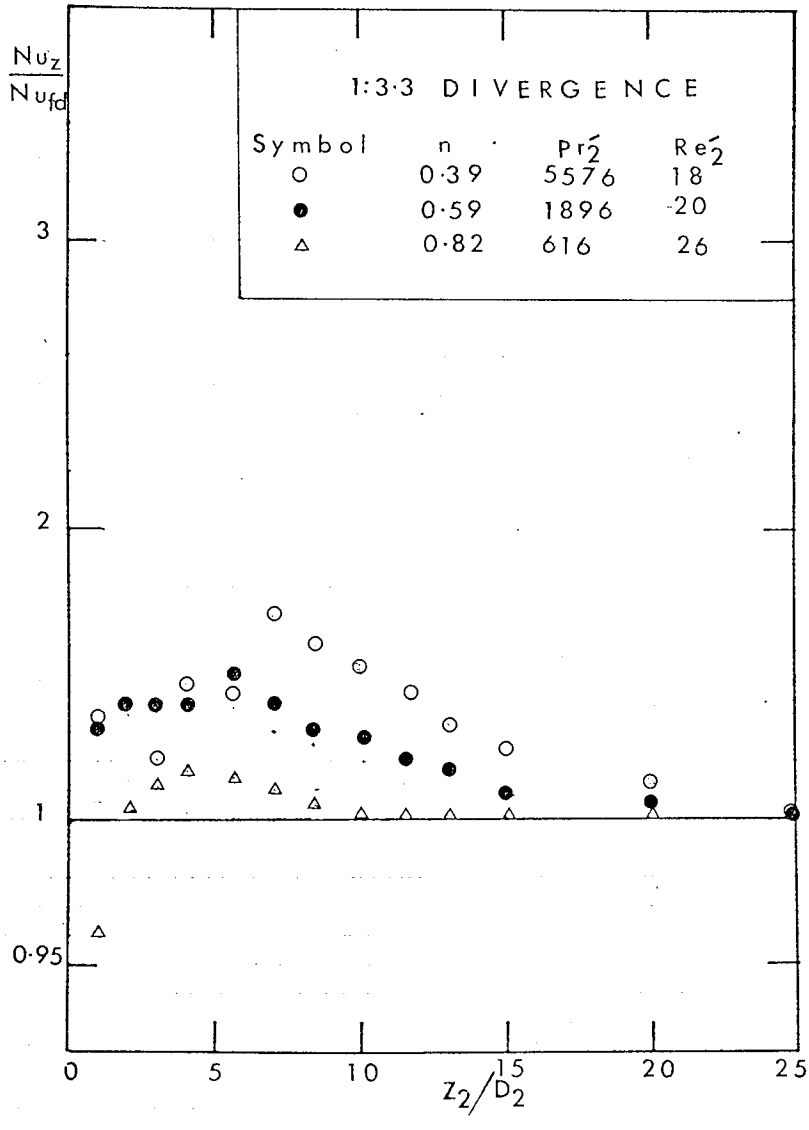

FIG 83 EFFECT OF INDEX 'n' ON FLOW DEVELOPMENT

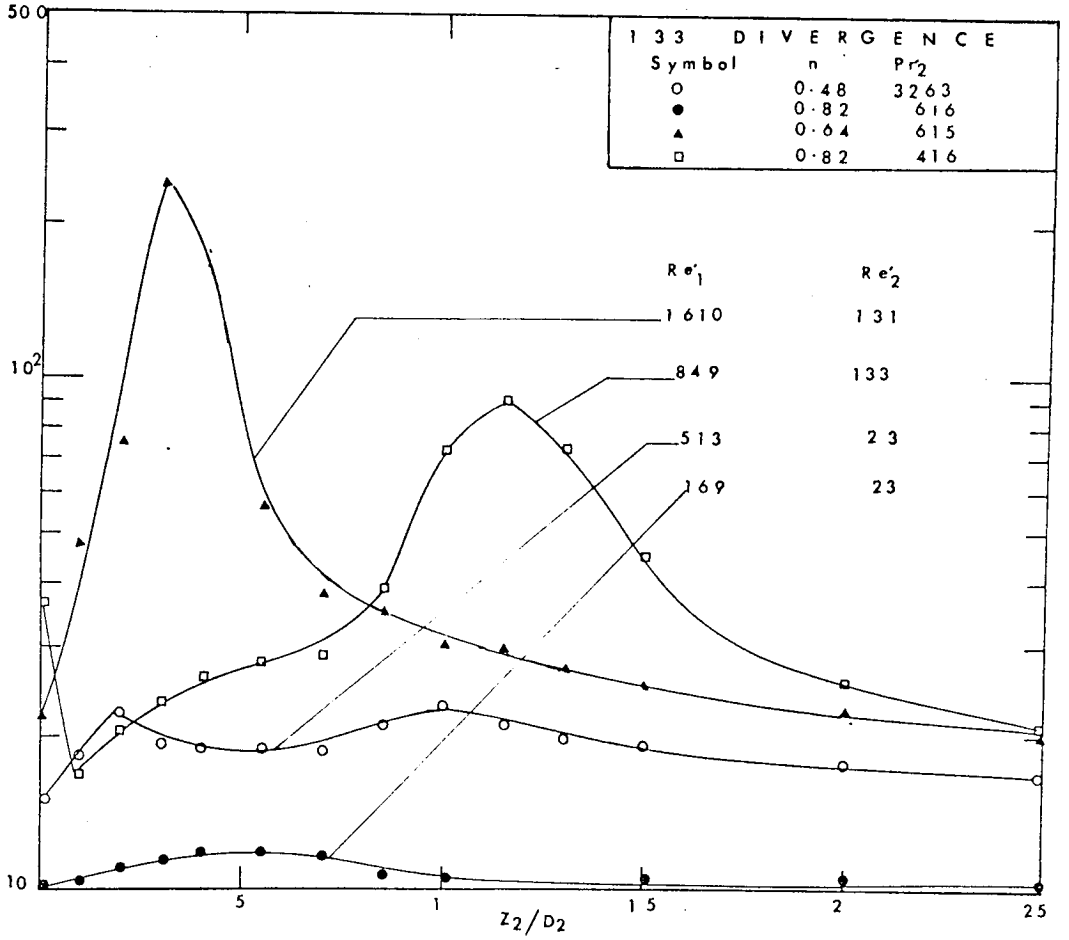

FIG 84 EFFECT OF 'n' ON HEAT TRANSFER

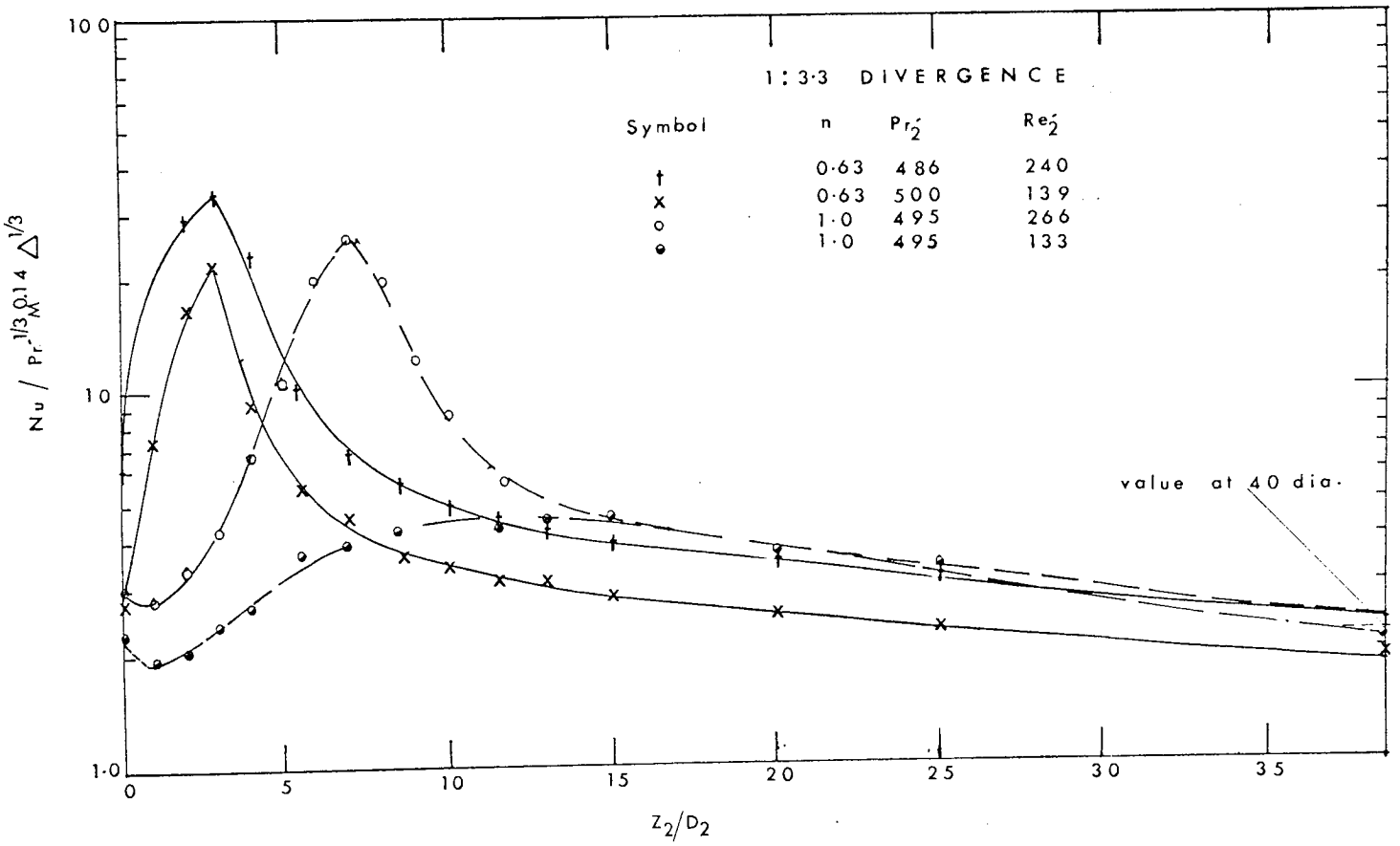

FIG. 85 COMPARISON OF NEWTONIAN AND NON-NEWTONIAN HEAT TRANSFER ----$Re_2' < 500$

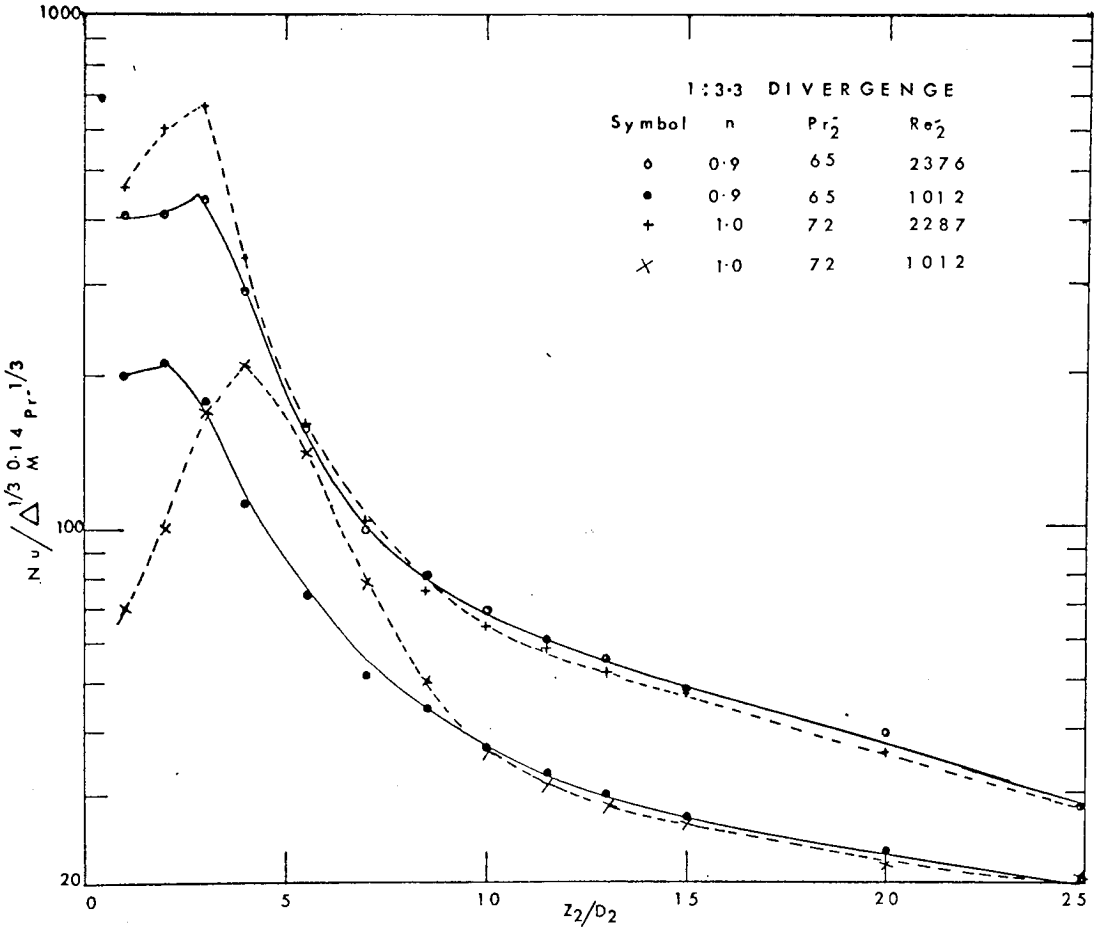

FIG. 86 COMPARISON OF NEWTONIAN AND NON-NEWTONIAN HEAT TRANSFER ---- $Re_2' > 500$

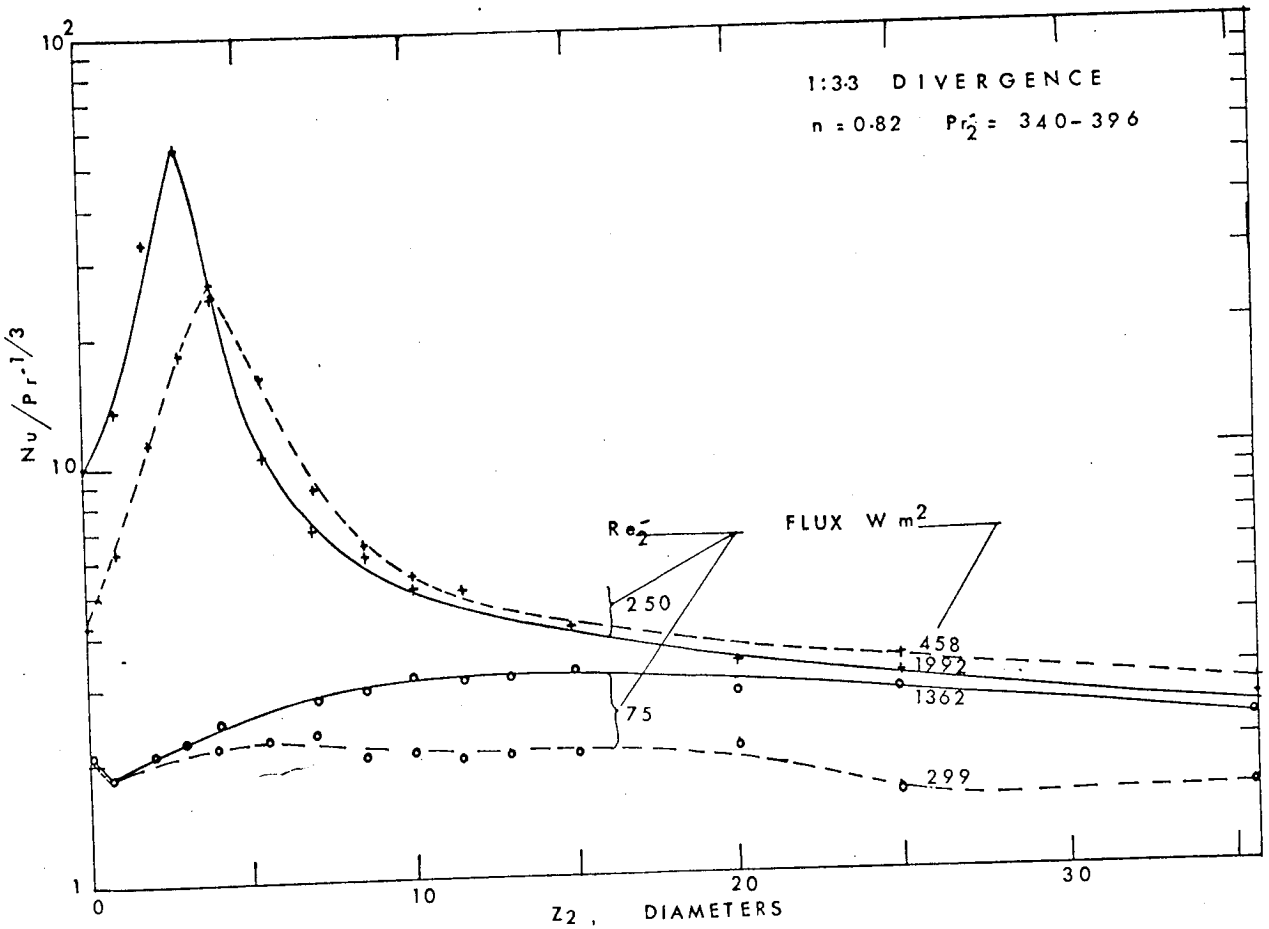

FIG. 87 EFFECT OF HEAT FLUX ON 1% CMC DATA

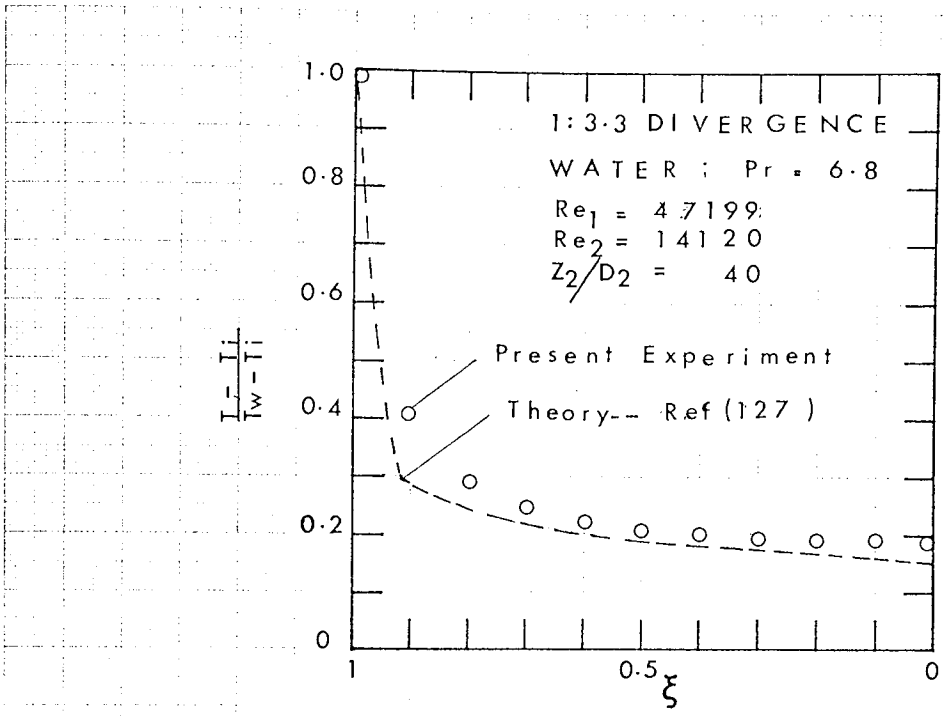

FIG. 88 RADIAL TEMPERATURE PROFILE

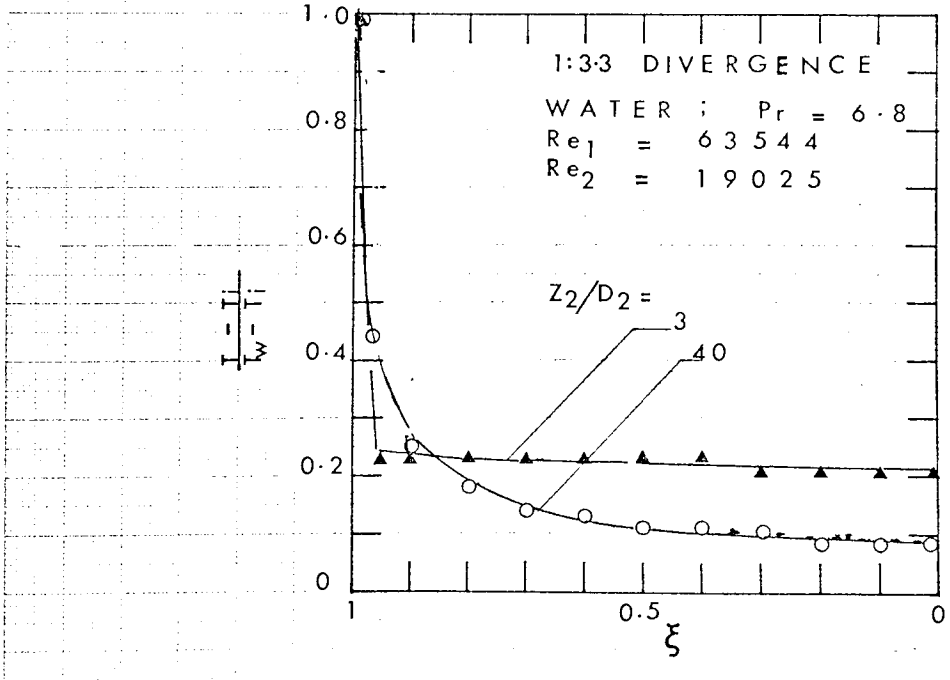

FIG. 89 RADIAL TEMPERATURE PROFILE

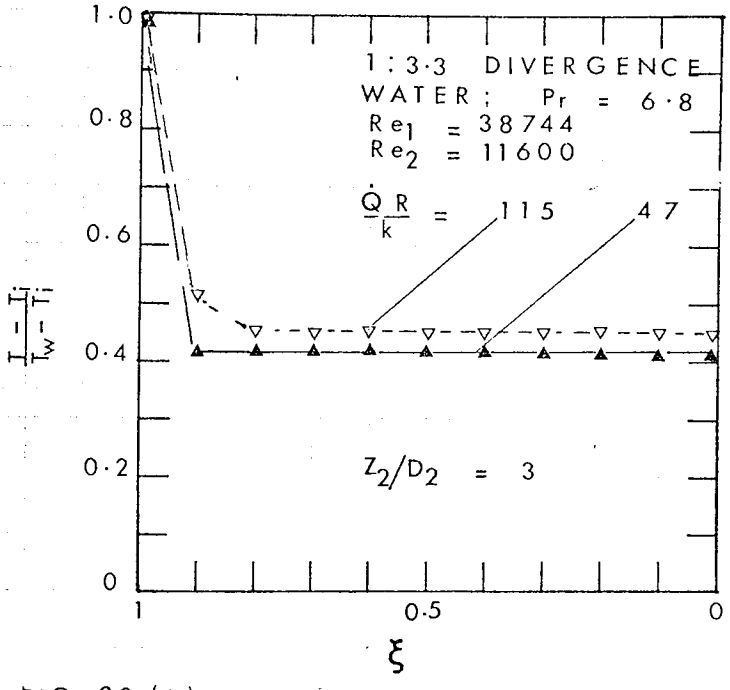

FIG. 90 (A)

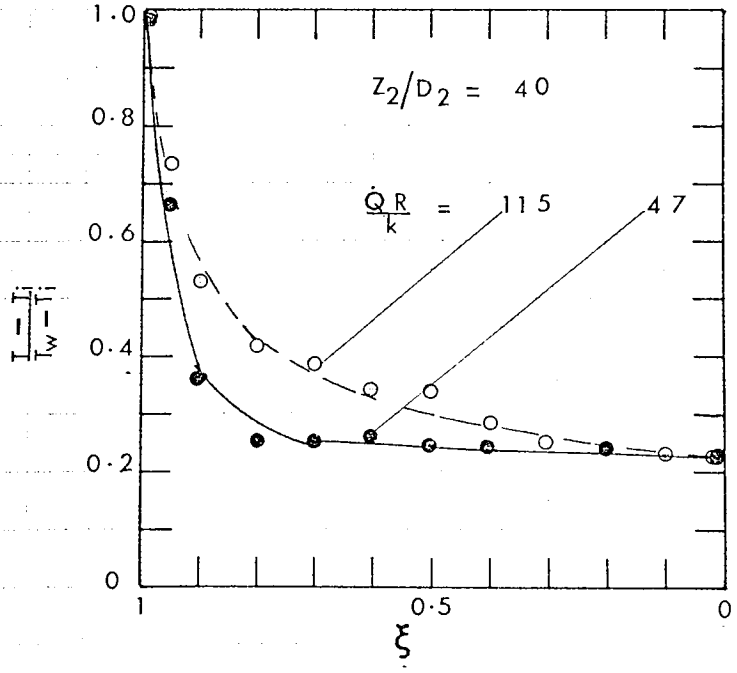

FIG 90 (B)

EFFECT OF HEAT FLUX ON RADIAL TEMPERATURE PROFILE.

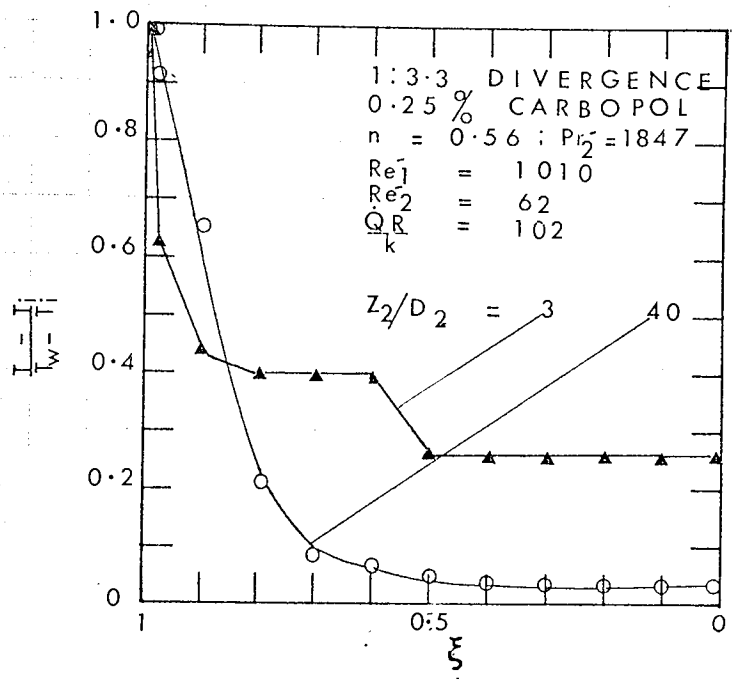

FIG. 91 RADIAL TEMPERATURE PROFILE

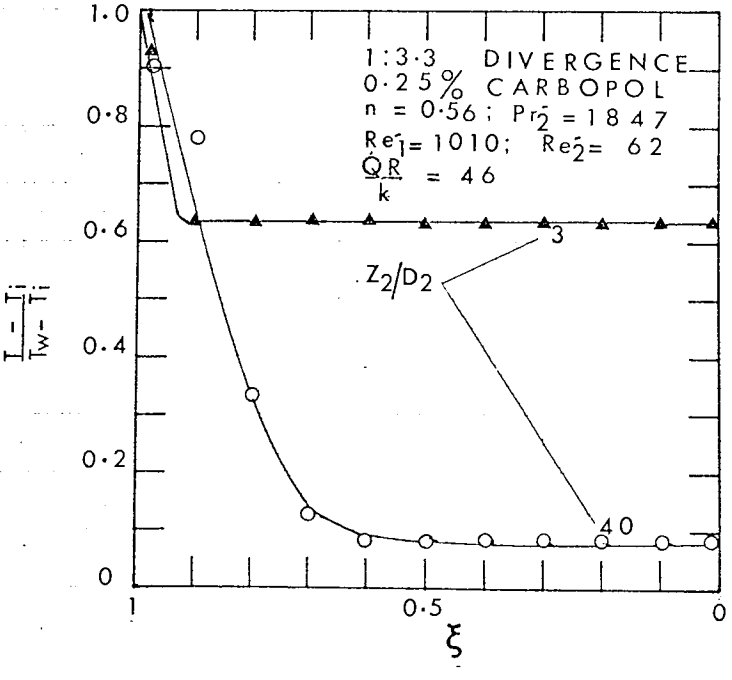

FIG. 92 RADIAL TEMPERATURE PROFILE

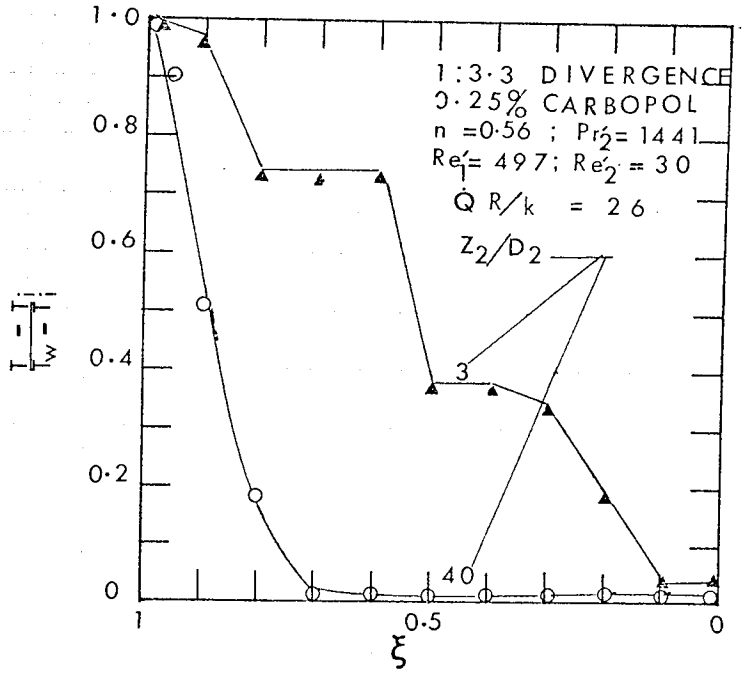

FIG. 93 RADIAL TEMPERATURE PROFILE

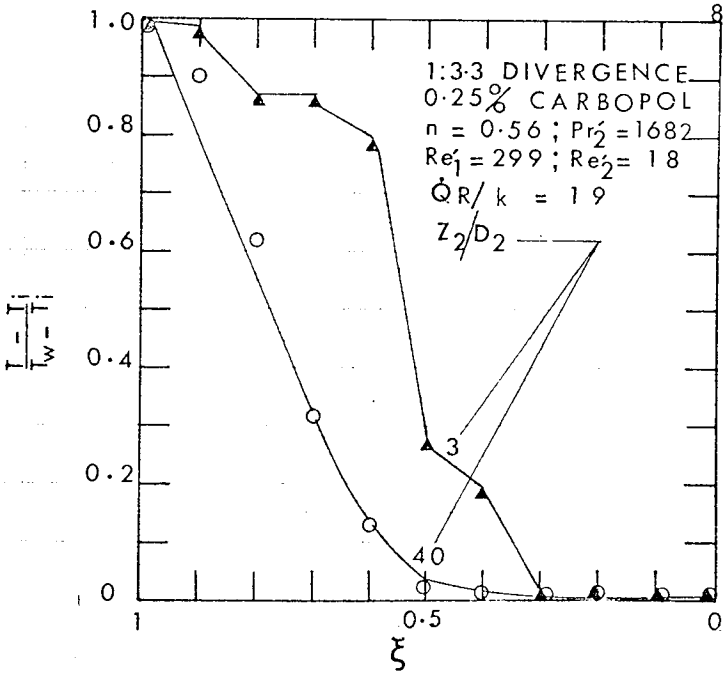

FIG. 94 RADIAL TEMPERATURE PROFILE

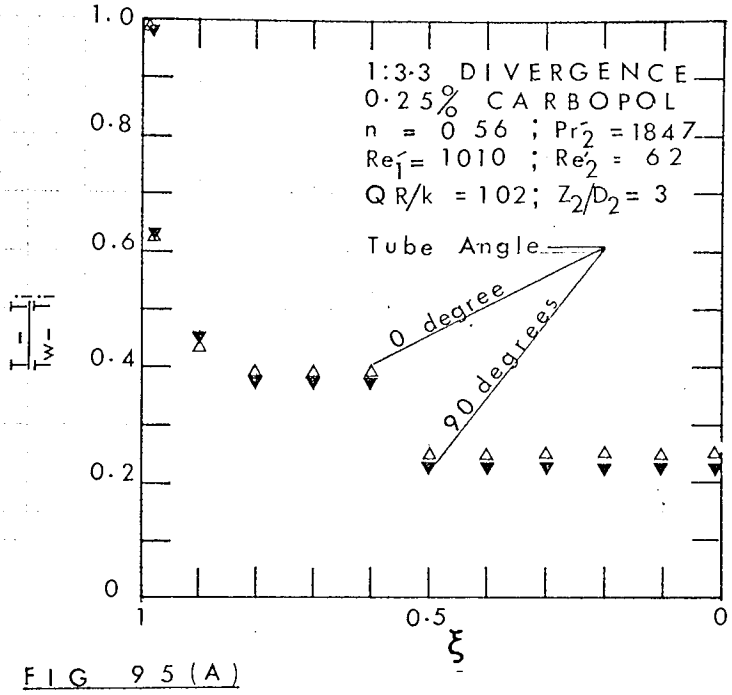

FIG 95 (A)

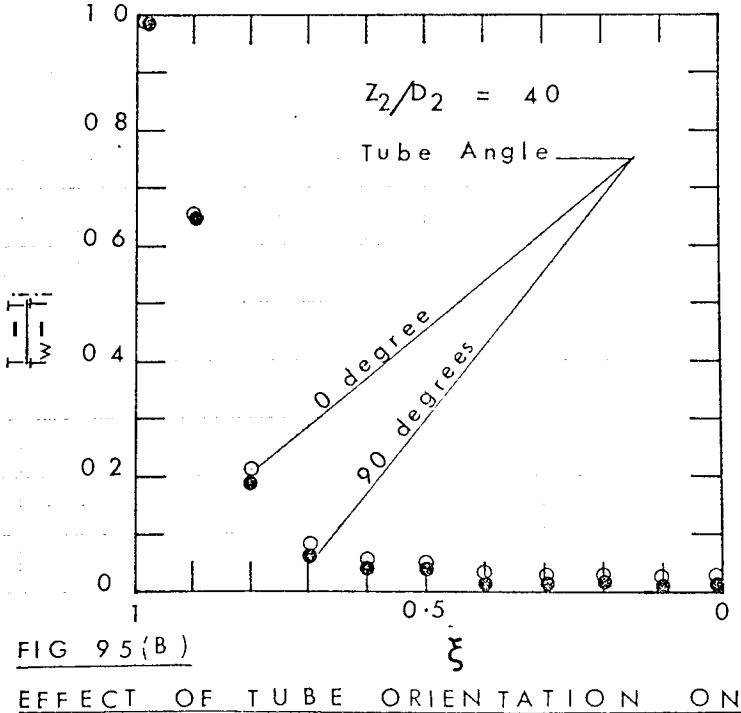

FIG 95(B)

EFFECT OF TUBE ORIENTATION ON RADIAL TEMPERATURE PROFILE

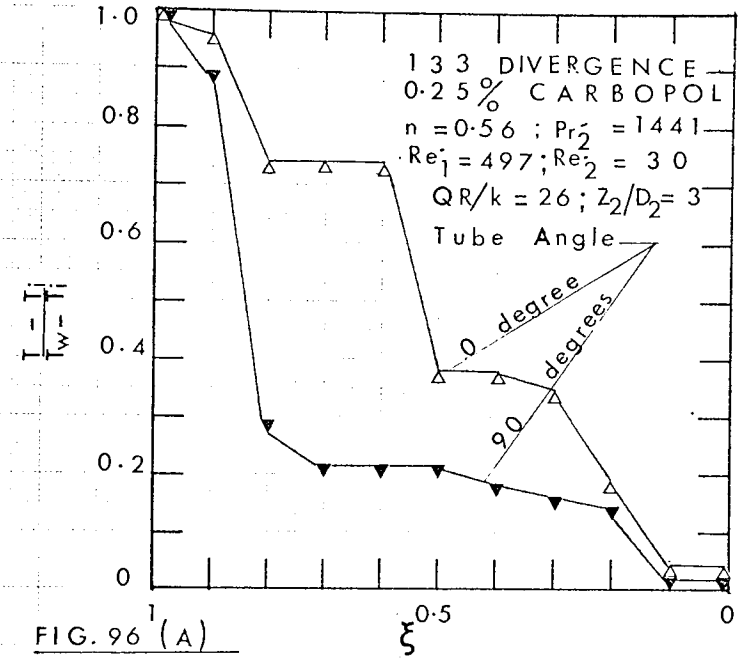

FIG. 96 (A)

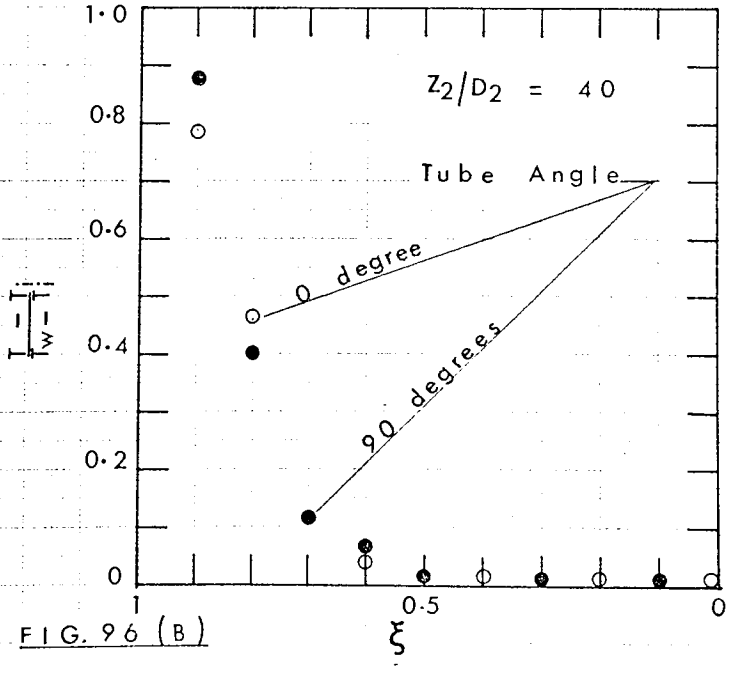

FIG. 96 (B)

EFFECT OF TUBE ORIENTATION ON RADIAL TEMPERATURE PROFILE

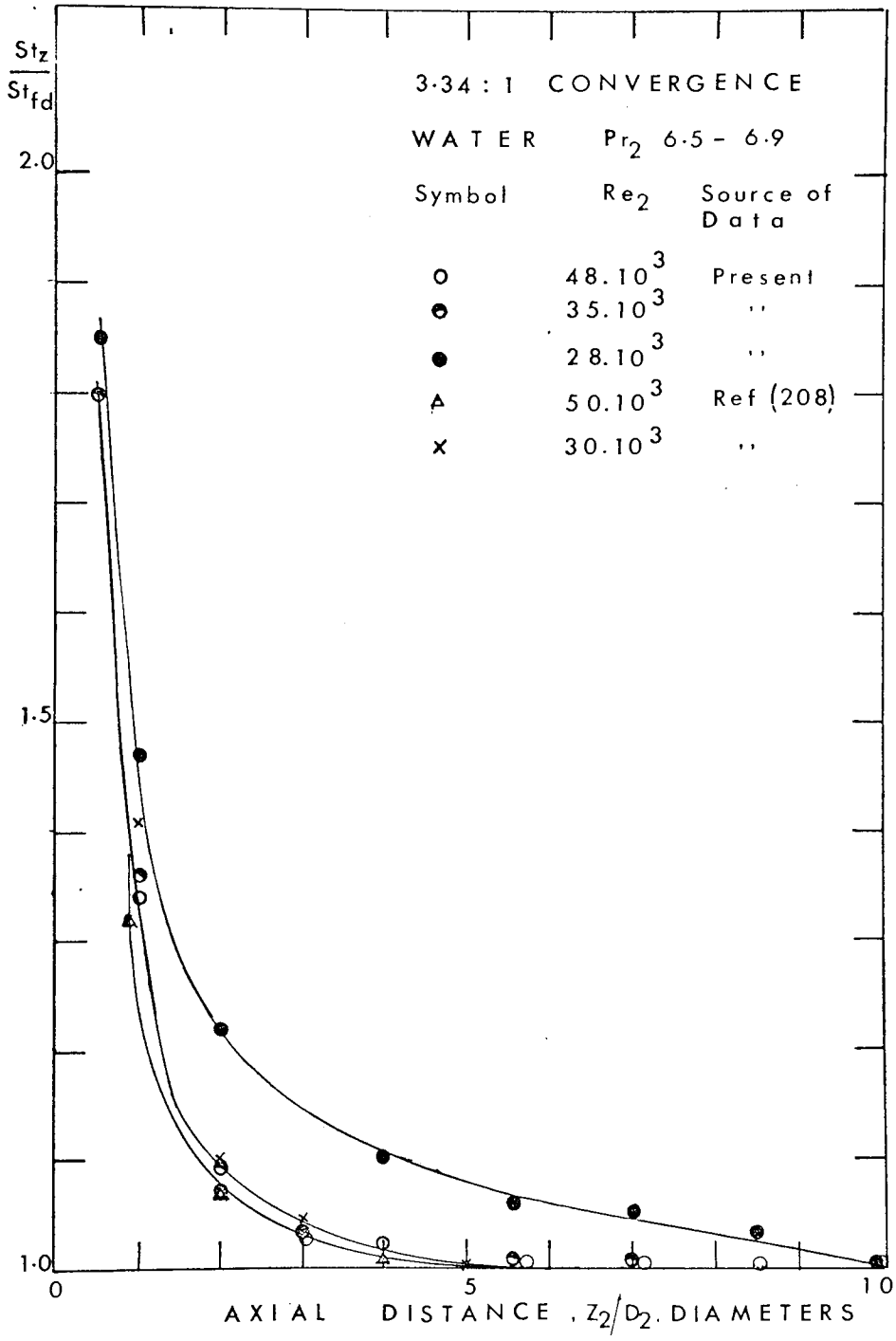

FIG. 97 AXIAL DISTRIBUTION OF STANTON NUMBER COMPARISON OF DATA

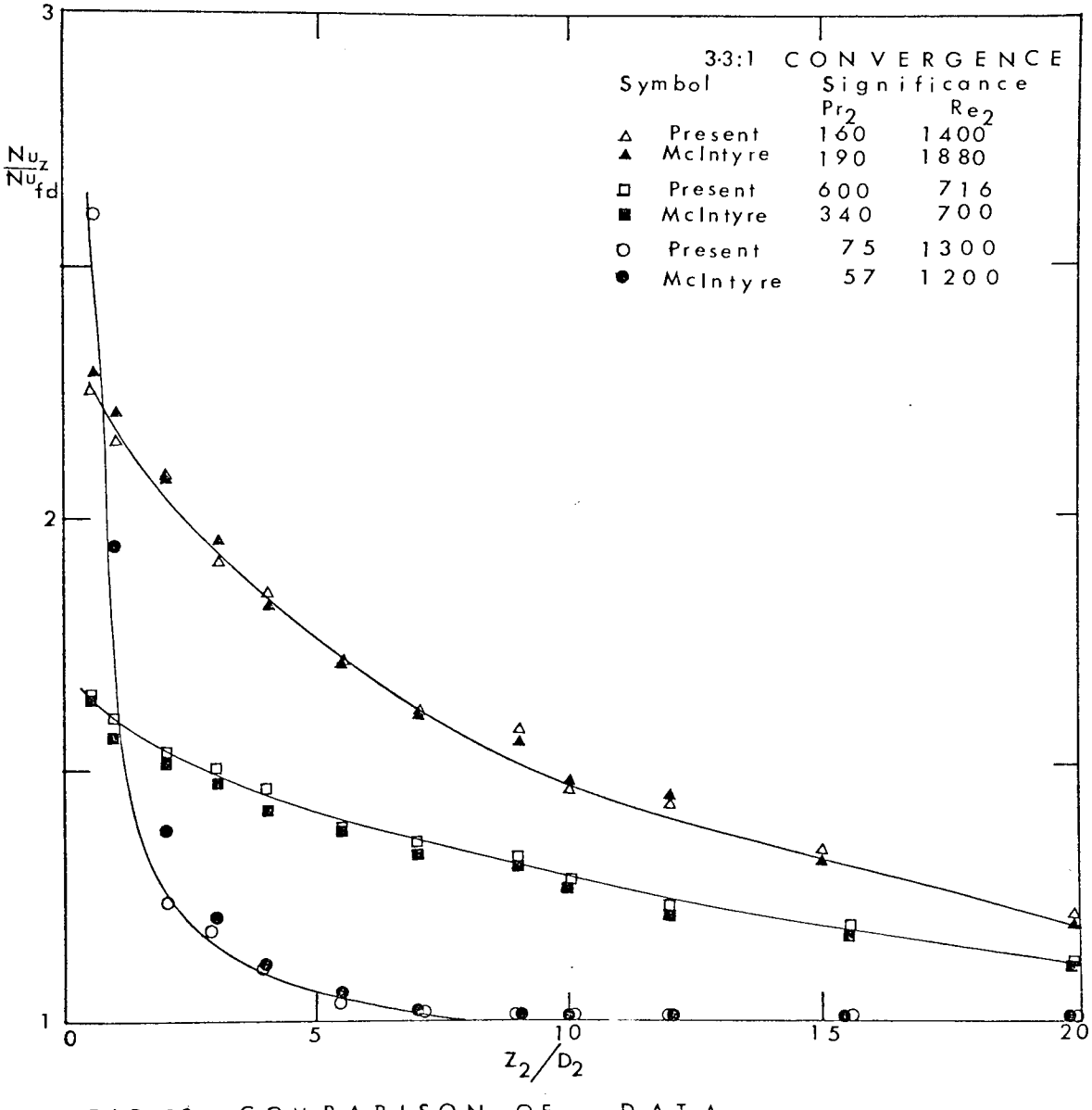

FIG. 98 COMPARISON OF DATA

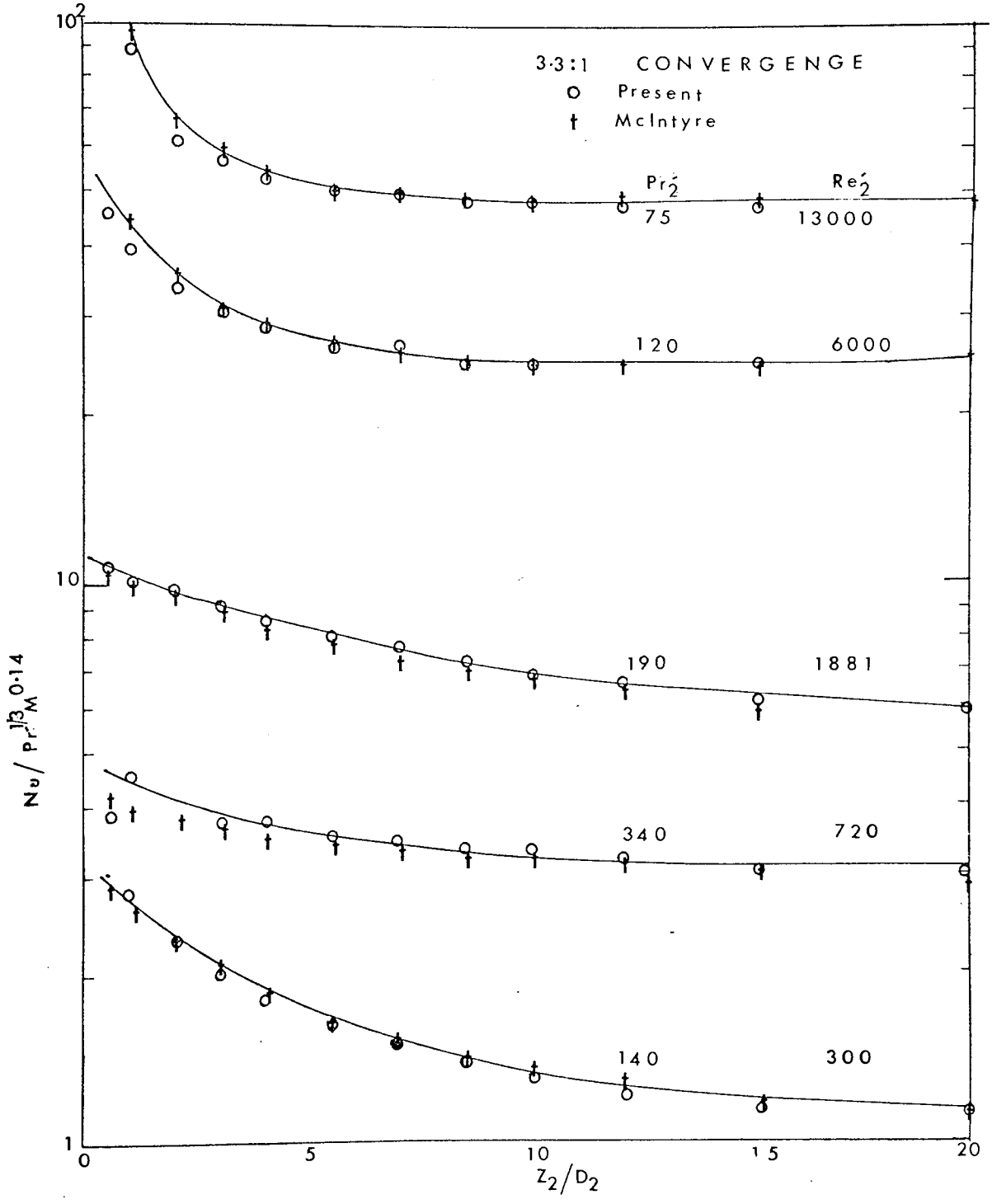

FIG·99 COMPARISON OF NEWTONIAN (GLYCOL) RESULTS

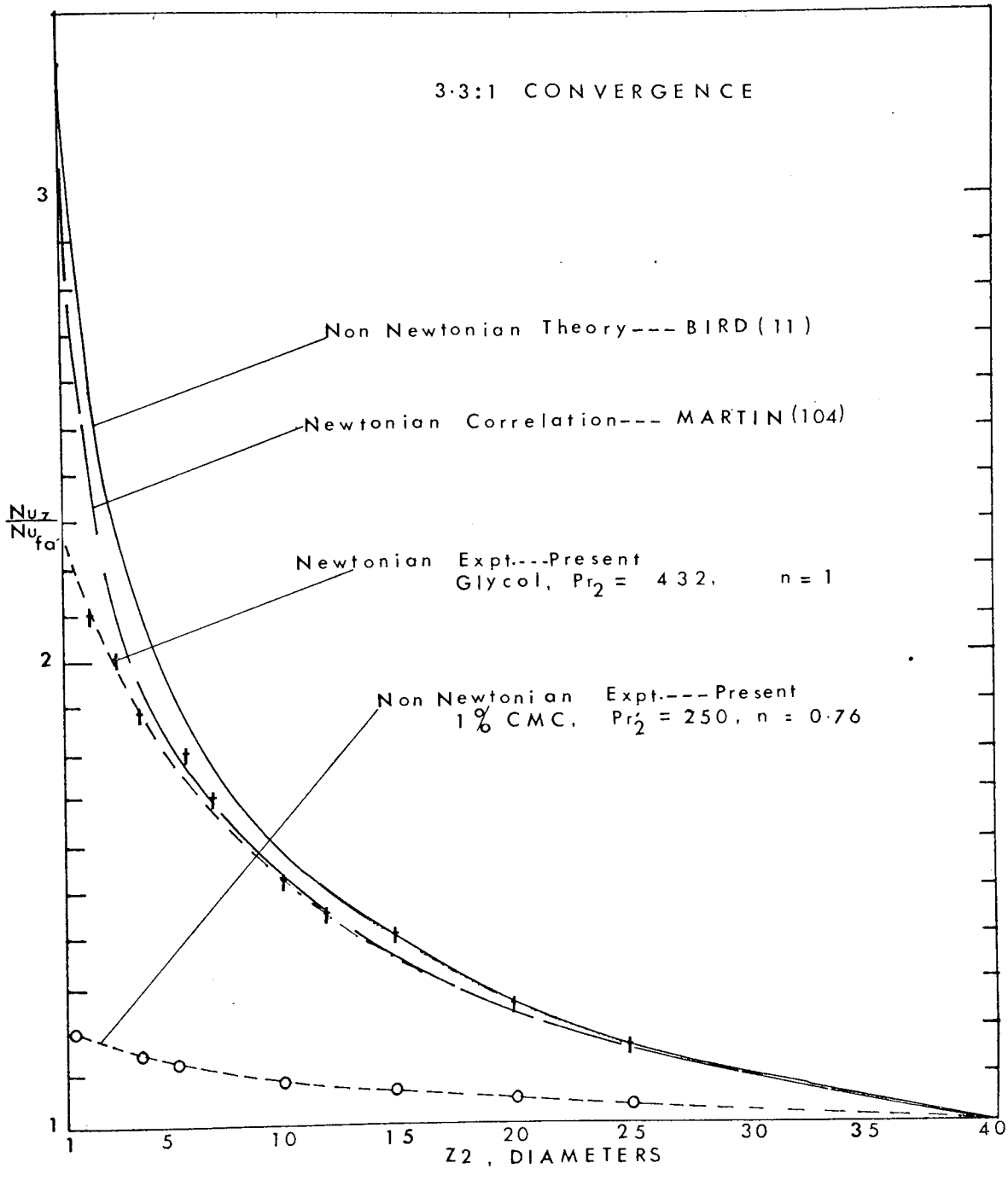

FIG. 100 AXIAL VARIATION OF LOCAL TO FULLY DEVELOPED NUSSELT NUMBER RATIO...COMPARISON OF DATA

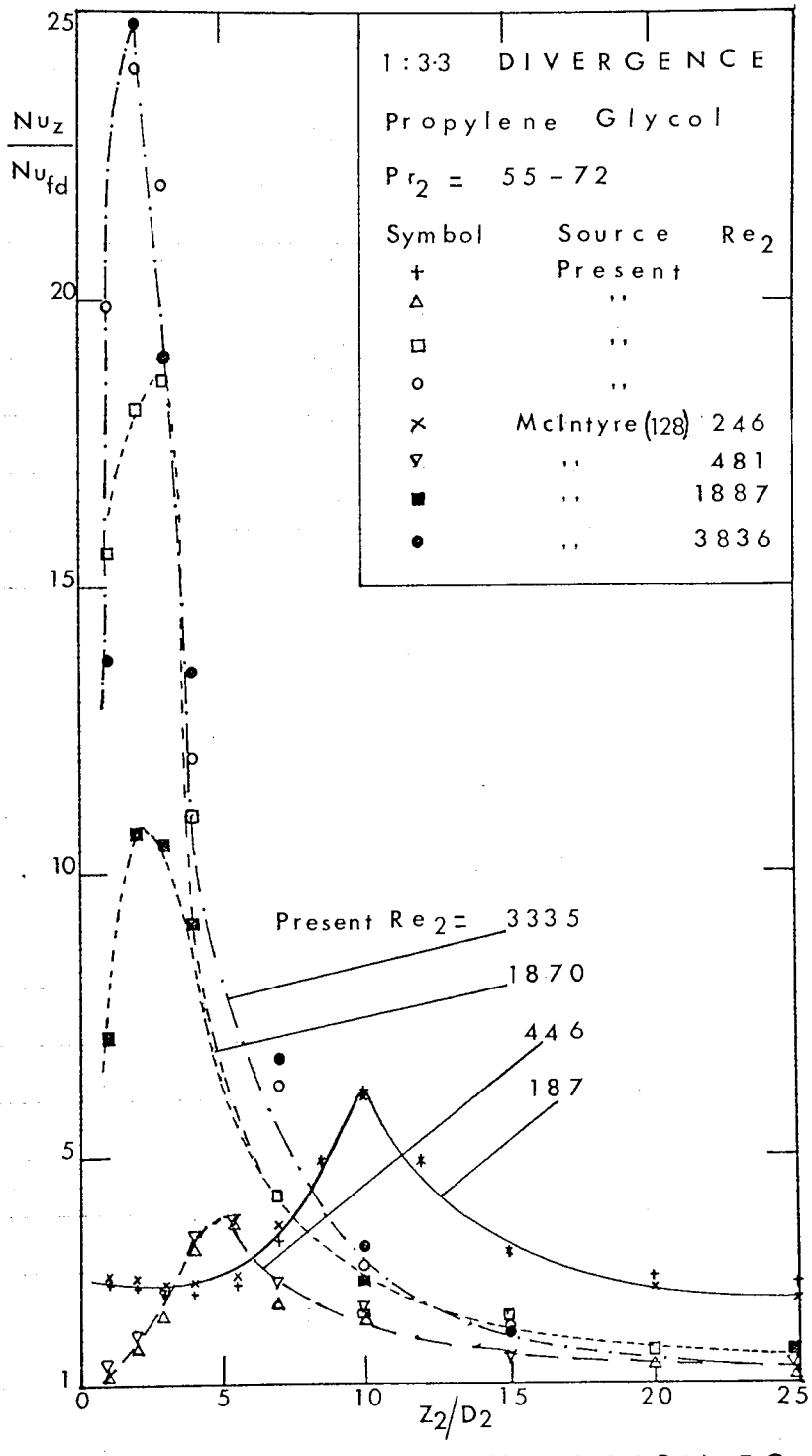

FIG.101 AXIAL VARIATION OF LOCAL TO FULLY DEVELOPED Nu RATIO COMPARISON OF DATA

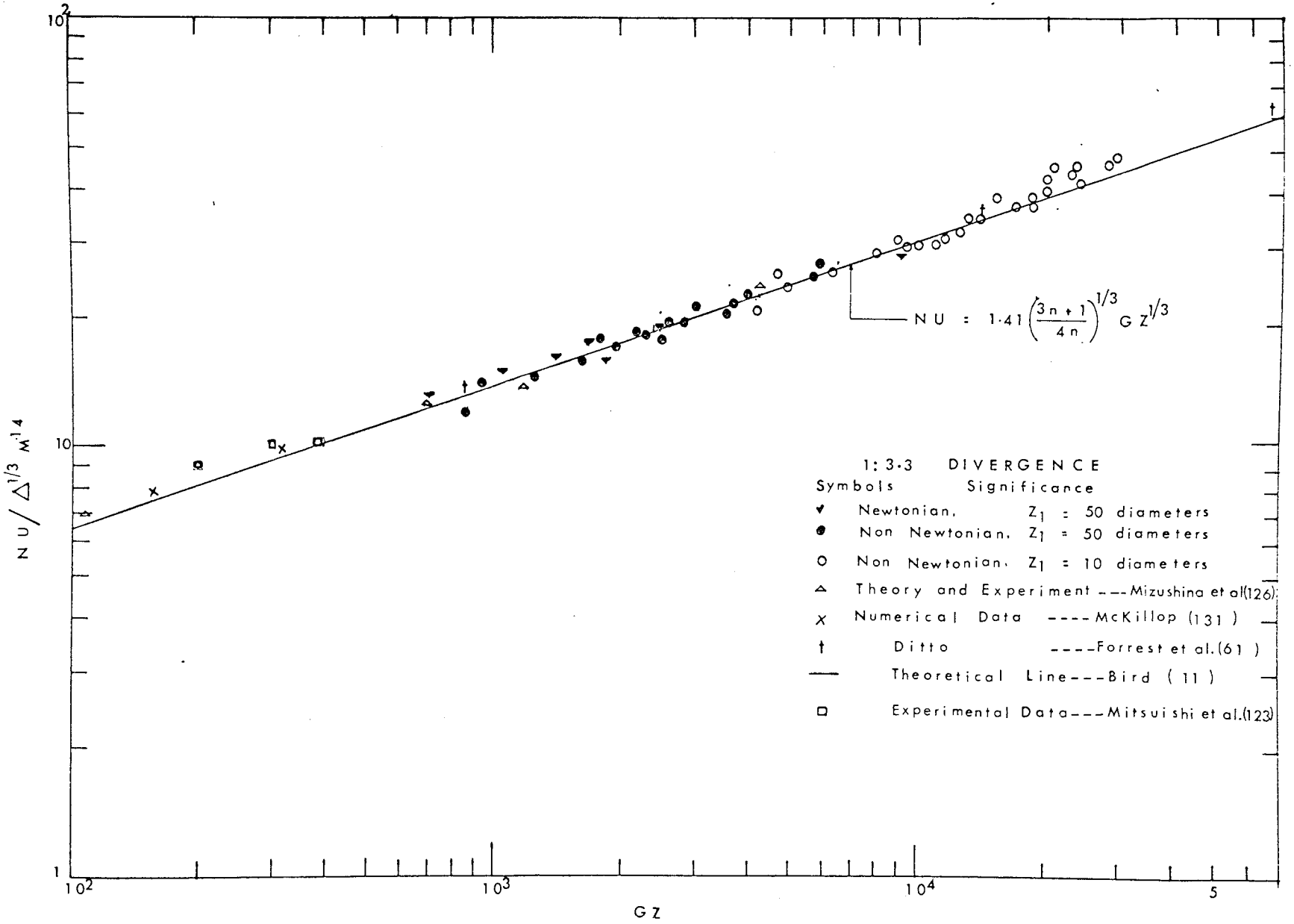

FIG. 102 NUSSELT - GRAETZ NUMBER CORRELATION OF UPSTREAM DATA COMPARISON OF DATA

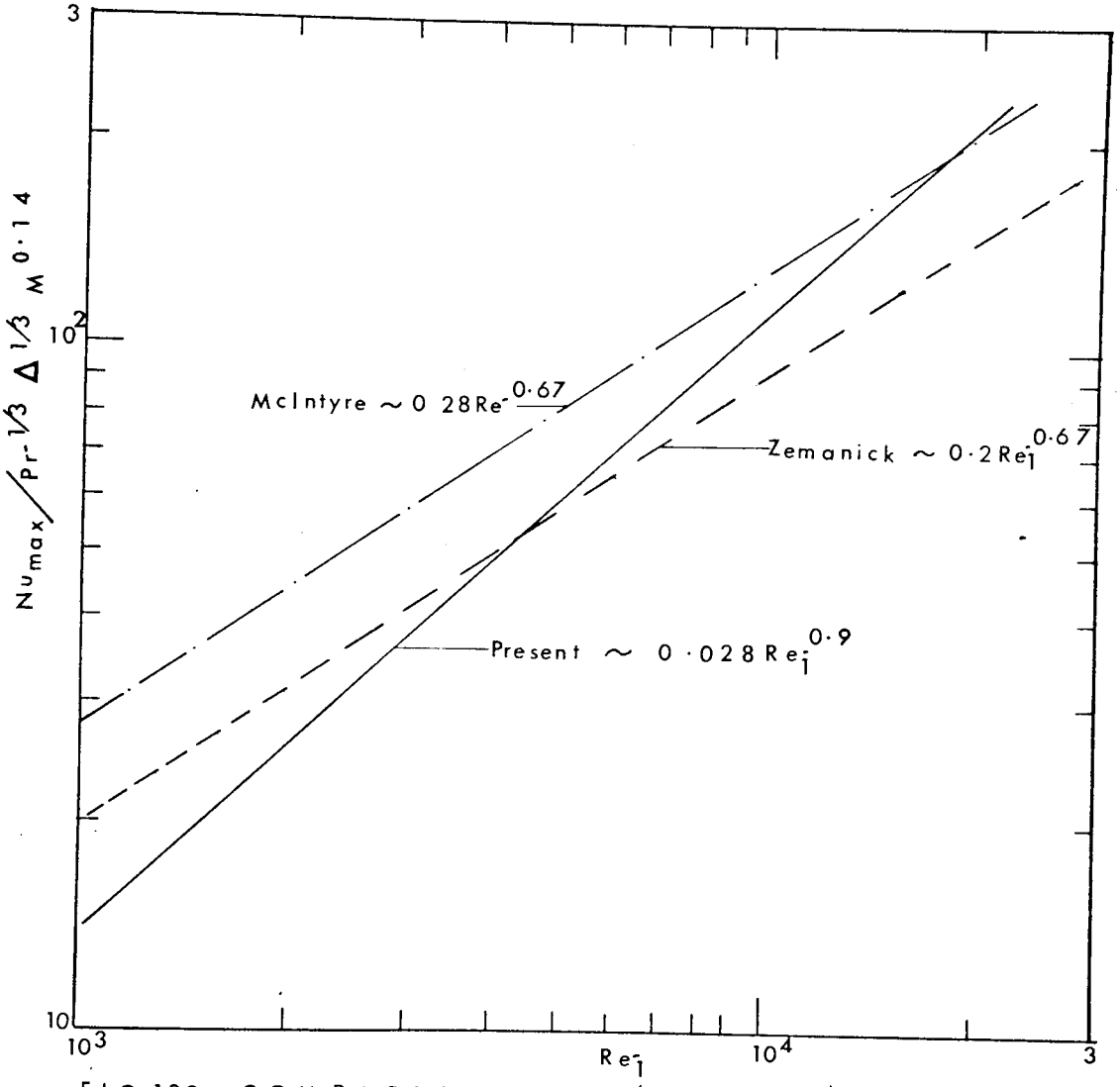

FIG. 103 COMPARISON OF ($Nu_{max} - Re_j$) CORRELATIONS

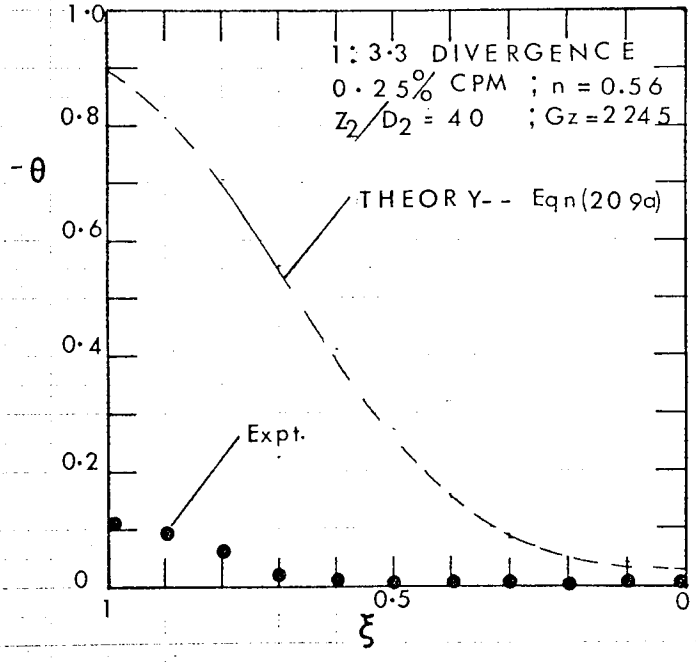

FIG. 104 COMPARISON OF DATA WITH THEORETICAL RADIAL TEMPERATURE PROFILE (NON-NEWTONIAN)

APPENDIX FOUR

NOTATION USED IN COMPUTER PROGRAM AND "PRINT-OUT"

A	Current	[A]
AVISC	Apparent Viscosity	[Ns/m^2]
B	Coefficient of thermal expansion	[$1/^oK$]
COEFF	Consistency coefficient (K_N)	[Ns^n/m^2]
CP	Specific heat capacity	[kJ/kg^oK]
DS	Density	[kg/m^3]
EN	Power law index (n)	[-]
FLO	Volume flow rate	[m^3/s]
FLUX	Wall heat flux	[W/m^2]
GR	Grashof number $(D^3 g\rho^2 (t_w - t_b)/\mu^2)$	[-]
GZ	Graetz number (W Cp/kL)	[-]
HL	Heat transfer coefficient	[$W/m^2\,^oK$]
K	Thermal conductivity	[$W/m\,^oK$]
KINS	Thermal conductivity of insulating material	[W/m^oK]
L	Length of pipe	[m]
LU	Unheated length of pipe	[m]
M	(Viscosity under bulk condition) / (Viscosity under wall condition)	[-]
NU	Nusselt number	[-]
PR	Prandtl number ($\mu Cp/k$)	[-]
PRG	Generalized Prandtl number ($\gamma\ Cp(U_m/D)^{n-1}(k)$)	[-]
Q	Net heat flux through pipe wall	[W/m^2]
QI	Total heat input to pipe wall, per unit length	[W/m]

QINS	Heat flow per unit length of insulation	[W/m]
QL	Net heat flux (loss) through insulation	[W/m^2]
R	Tube (inside) radius	[m]
RA	Radial depth of insulation	[m]
RE	Reynolds number ($\rho\ U_m D/\mu$)	[-]
REG	Generalized Reynolds number ($8U_m^{2-n}D^n\rho/K_N(6_n+2/n)^n$)	[-]
TAMB	Ambient temperature	[^oC]
TOUT	Bulk-fluid outlet temperature (measured)	[^oC]
TOTH	Estimated bulk-fluid outlet temperature	[^oC]
TPI	Inside tube wall temperature	[^oC]
TPO	Outside tube wall temperature	[^oC]
VEL	Mean velocity	[m/s]
X	Axial distance from start of heating	[m]
Y	Fluid consistency factor ($K_N 8^{n-1}(3n+1/4n)^n$)	[Ns^n/m^2]

NOTE:

(i) The numbers 1 and 2 used after a letter donate "upstream" and "downstream" tube sections respectively.

(ii) The letters I and X at the end of any notation generally denote "inside wall", and "bulk" conditions respectively.

(iii) The number 3 at the end of any notation means "raised to power $\frac{1}{3}$" e.g. GZX3 = $(GZX)^{\frac{1}{3}}$.

(iv) Other notations used in the program are self explanatory.

```
0007              MASTER(SECT2)
0008        C HEAT TRANSFER CALCULATIONS FOR TUBE WITH CHANGE OF SECTION USING
0009        C NON NEWTONIAN FLUIDS
0010        C DECLARE VARIABLES
0011              INTEGER  XX
0012              INTEGER G,GG,H,W,Z,JJ
0013              REAL        KX,KI,NUX,NUI,NUXFAC,NUIFAC,M,M14,NUM14,NFAC,L,
0014             1 NUIM14, JE
0015              REAL  PRX, RP,GP,GP4,NP3,NP3M14,GP4,NRP3,NRP3M4,NFP3,NFP3M4,
0016             1 NFRP3, NFRP3M, GZX, GZI, GX,NP4
0017              REAL GRIRE, GRIRE2, TK, TC,  TCI,TKI,TX1,TX2,TP3
0018              REAL AA, BB, COMP, RATIO
0019              REAL TIN,TOUT,FLO,A,TAMB,KP,KINS,RA,LU,EN,FACTOR,DELTA,VEL,DELSQ,
0020             1 SHEAR, FLUX1, FLUX2, TPC1
0021              DIMENSION GRIRE(2,100), GRIRE2(2,100), TK(2,100), TC(2,100),
0022             1 TCI(2,100),TKI(2,100),GX(2,100),NP4(2,100)
0023              DIMENSION RP(2,100), GP(2,100), GP4(2,100),
0024             1 NP3(2,100),NP3M14(2,100),GP4RP3(2,100),NRP3(2,100),NRP3M4(2,100),
0025             2 NFP3(2,100), NFP3M4(2,100), NFRP3(2,100), NFRP3M(2,100)

0026              DIMENSION CP(8), DS(8), BT(8)
0027              DIMENSION PRG(2,100)
0028              DIMENSION DSI(2,100)
0029              DIMENSION  KX(2,100),AVISCX(2,100),AVISCI(2,100),CPX(2,100),
0030             1DSX(2,100),TP0(2,100),TPI(2,100),X(2,100),QINS(2,100),QI(2,100),
0031             2 TX(2,100),REX(2,100),REI(2,100),PRX(2,100),PRI(2,100),REG(2,100),
0032             3 M(2,100),COEFFX(2,100),COEFFI(2,100),YX(2,100),YI(2,100),
0033             4 HLX(2,100),NUX(2,100),NUI(2,100),GZX(2,100),GZI(2,100),B(2,100),
0034             5 NUXFAC(2,100),NUIFAC(2,100),GZX3(2,100),GZI3(2,100),GZXPR1(2,100)
0035             6,GZXPR2(2,100),CONV1(2,100),CONV2(2,100),GRRE2(2,100),GRRE(2,100),
0036             7 JE(2,100),NUM14(2,100),NFAC(2,100),CALV(22),CALT(22),V(2),L(2),
0037             8 RO(2),RI(2),S(2),XX(2), M14(2,100), KI(2,100), GRX(2,100),
0038             9GRI(2,100),NUIM14(2,100), Q(2,100),  QL(2,100), CPI(2,100)
0039        C STORE CALIBRATION DATA (TEMP-MICROVOLTS )
0040        C
0041              CALT(1) = 10.0
0042              DO 3 JJ = 2,22
0043            3 CALT(JJ) = CALT(JJ- ) + 4.0
0044              CALV( ) = 431.0
0045              CALV(2) = 599.0
0046              CALV(3) = 773.0
0047              CALV(4) = 948.0
0048              CALV(5) = 1126.0
0049              CALV(6) = 1306.0
0050              CALV(7) = 1485.0
0051              CALV(8) = 1668.0
0052              CALV(9) = 1851.0
0053              CALV(10)= 2035.0
0054              CALV(11)=2222.0
0055              CALV(12)= 2410.0
0056              CALV(13)= 2599.0
0057              CALV(14)= 2790.0
0058              CALV(15)= 2982.0
0059              CALV(16)= 3173.0
0060              CALV(17)= 3367.0
0061              CALV(18)= 3565.0
0062              CALV(19)= 3761.0
0063              CALV(20)= 3961.0
0064              CALV(21)= 4161.0
0065              CALV(22)=4360.0
0066        C
0067        C     READ IN PROPERTY DATA
0068              READ(1,100) (CP(H), H=1,8), (DS(H), H=1,8), (BT(H), H=1,8)
0069          100 FORMAT(8E0.0,  8E0.0,  8E0.0 )
0070        C
0071        C START CALCULATIONS
0072        C READ IN NO. OF THERMOCOUPLE LOCATIONS
0073              READ(1,200) XX(1), XX(2)
0074          200 FORMAT(2I0)
0075        C READ IN EXPERIMENTAL DATA
0076            2 READ(1,300) TIN,TOUT,FLO,A,TAMB,KP,KINS,RA,COMP,LU,EN,AA,BB ,Z
0077          300 FORMAT(13E0.0, 1I0)
0078              READ(1,400) (V(G),G=1,2), (L(G), G=1,2 ), (RO(G), G=1,2 ), (RI(G),
0079             1 G=1,2 )
0080          400 FORMAT(8E0.0)
0081              READ(1,401) RATIO
0082          401 FORMAT (1E0.0)
0083              CALL CAL( TIN,CALV,CALT,TEMP)
0084              TIN = TEMP
0085              CALL CAL(TOUT,CALV,CALT,TEMP)
```

```
0086            TOUT = TEMP
0087          C READ IN TUBE TEMPERATURES AND LOCATIONS
0088            READ(1,500)  (X(1,G), G=1,6),  (X(2,G), G=1,17), (TPO(1,G), G=1,6
0089           1 ),  (TPO(2,G), G=1,17)
0090          500 FORMAT (46E0.0)
0091            WRITE(2, 901) TIN,TOUT,FLO,A,TAMB,KP,KINS,RA,COMP,LU,EN,AA,BB,Z
0092          901 FORMAT(1H1,3X,E8.4,3X,E8.4,3X,E8.4,3X,E8.4,3X,E8.6,3X,E8.4,3X,E8.4,3X,
0093           1 E8.4,3X,E8.4,3X,E8.4//3X,E8.4,3X,E8.4,3X,E12.9,3X,E12.9,3X,1I1 )
0094            WRITE(2, 902) V(1), V(2), L(1), L(2), RO(1), RO(2), RI(1), RI(2),
0095           1 XX(1), XX(2)
0096          902 FORMAT(///3X,E8.4,3X,E8.4,3X,E8.4,3X,E8.4,3X,E8.5,3X,E8.5,3X,
0097           1 E8.5, 3X,E8.5//3X, 7H XX1 = ,1I1, 3X, 7H XX2 = ,1I2 )
0098            DO 6 H=1,2
0099            KKK = XX(H)
0100            S(H) = RI(H) / RO(H)
0101            DO 7 G=1,KKK
0102            TPC = TPO(H,G)
0103            CALL CAL ( TPC, CALV, CALT, TEMP )
0104          7 TPO(H,G) = TEMP
0105          C
0106          C CALCULATE LOSS THROUGH INSULATION THEN LOCAL HEAT FLUX
0107          C
0108            KK = (XX(H)-1)
0109            DO 8 G =2,KK
0110            QINS(H,G) = 2.*3.1416*KINS*(TPO(H,G)-TAMB)/ALOG(RA/RO(H))
0111            NN = G-1
0112            MM = G+1
0113            DELSQ = ((TPO(H,MM)-TPO(H,G))/(X(H,MM)-X(H,G))-(TPO(H,G)-TPO(H,NN)
0114           1)/(X(H,G)-X(H,NN)))/((X(H,MM)-X(H,NN))*.5*(2.*RI(H))**2 )
0115            QI(H,G) = V(H)*A/L(H) +3.1416*KP*(RO(H)**2)*(1.-S(H)**2)*DELSQ-
0116           1 QINS(H,G)
0117          8 CONTINUE
0118            QINS(H,1) = QINS(H,2)
0119            QINS(H,KKK  ) = QINS(H,KK)
0120            QI(H,1) = QI(H,2)
0121            QI(H,KKK  ) = QI(H,KK)
0122          6 CONTINUE
0123          C
0124          C CALCULATE LOCAL FLUID (BULK) TEMPERATURES
0125            CALL INT( TIN,10,7,DS,VALUE )
0126            DSX(1,1) = VALUE
0127            CALL INT( TIN,10,7,CP,VALUE )
0128            CPX(1,1) = VALUE
0129            TX(1,1) = TIN-(2*3.1416*KINS*LU*(TIN-TAMB)/ALOG(RA/RO(1)))/
0130           1 (DSX(1,1)*FLO*CPX(1,1)*(1.0E 3) )
0131            TX1 = TX(1,1)
0132            CALL INT(TX1,10,7,CP,VALUE)
0133            CPX(1,1) = VALUE
0134            KK1 = XX(1)
0135            DO 9 H= 1,2
0136            KKK = XX(H)
0137            DO 66 G= 2,KKK
0138            IF (H.EQ.2.AND.G.EQ.2)  GO TO 11
0139          11 TX(2,1) = TX(1,KK1  )
0140            IF (H.EQ.2.AND.G.EQ.2)  GO TO 12
0141          12 CPX(2,1) = CPX(1,KK1  )
0142            TX(H,G) = (X(H,G)-X(H,(G-1)))*RI(H)*(QI(H,G)+QI(H,(G-1)))/(CPX(H,
0143           1 (G-1))*FLO*DSX(1,1)*(1.0E 5) ) +TX(H,(G-1) )
0144            GG = 0
0145          13 TX2 = TX(H,G)
```

```
0146                CALL INT(TX2,10,7,CP,VALUE)
0147                CPX(H,G) = VALUE
0148                TX(H,G) = (X(H,G)-X(H,(G-1))) *RI(H)*(QI(H,G)+QI(H,(G-1)))/((0.5*
0149               1 (CPX(H,(G-1)) +CPX(H,G)))*FLO*DSX(1,1)*(1.0E 5) ) + TX(H,(G-1))
0150                IF( GG-1) 14,15,15
0151             14 GG= GG+1
0152                GO TO 13
0153             15 CONTINUE
0154             66 CONTINUE
0155              9 CONTINUE
0156                TOTH = TX(2,XX(2) )
0157          C
0158                DELTA = (3.*EN + 1.)/(4.*EN)
0159                FACTOR = DELTA**0.333
0160          C OBTAIN LOCAL PROPERTIES AND CALCULATE INSIDE TUBE TEMPERATURES
0161          C
0162                DO 16 H=1,2
0163                KKK = XX(H)
0164                DO 17 G=1,KKK
0165                TX2 = TX(H,G)
0166                CALL INT(TX2,10,7,DS,VALUE)
0167                DSX(H,G) = VALUE
0168                TK(H,G) = (273.15 + TX(H,G) )/273.15
0169                KX(H,G) = -0.92247 + 2.8395*TK(H,G) - 1.8007*TK(H,G)**2 +
0170               1  0.52577*TK(H,G)**3 - 0.07344*TK(H,G)**4
0171                TC(H,G) = 1.0/(273.15 + TX(H,G) )
0172                COEFFX(H,G) = AA*EXP( BR*TC (H,G) )
0173                COEFFX(H,G) = COEFFX(H,G) * RATIO
0174                CALL INT(TX2,10,7,BT,VALUE)
0175                B(H,G) = VALUE
0176                TPI(H,G) =TPC(H,G)+((QI(H,G)+(S(H)**2)*QINS(H,G))/(4.*3.1416*KP))
0177               1*(1.-2.*(ALOG(1/S(H)))/(1.-S(H)**2))+(1.-S(H)**2)*QINS(H,G)/
0178               2(4.*3.1416*KP)
0179                TP3 = TPI(H,G)
0180                CALL INT(TP3, 10,7,CP,VALUE)
0181                CPI(H,G) = VALUE
0182                CALL INT(TP3,10,7,DS,VALUE)
0183                DSI(H,G) = VALUE
0184                TKI(H,G) = ( 273.15 + TPI(H,G))/273.15
0185                KI(H,G) = -0.92247 + 2.8395*TKI(H,G) - 1.8007*TKI(H,G)**2 +
0186               1  0.52577*TKI(H,G)**3 - 0.07344*TKI(H,G)**4
0187                TCI(H,G) = 1.0/(273.15 + TPI(H,G) )
0188                COEFFI(H,G) = AA*EXP( BR*TCI(H,G) )
0189                COEFFI(H,G) = COEFFI(H,G) * RATIO
0190          C
0191          C
0192          C CALCULATE REX,REI,REG,HLX,NUX,NUI,GRX,GRI,GZX,GZI,LOCALLY
0193                YX(H,G) =8.**(EN-1.)*COEFFX(H,G)*DELTA**EN*(1.0E-1)
0194                YI(H,G) =8.**(EN-1.)*COEFFI(H,G)*DELTA**EN*(1.0E-1)
0195                VEL = 10.0*FLO/(3.1416*RI(H)**2)
0196                SHEAR = 8.*VEL/(RI(H)*2.*(1.0E-2) )
0197                AVISCX(H,G) = COEFFI(H,G)*SHEAR**(EN-1.)*DELTA**(EN-1)*(1.0E-1)
0198                AVISCI(H,G) = COEFFI(H,G)*SHEAR**(EN-1.)*DELTA**(EN-1)*(1.0E-1)
0199                REX(H,G) = 2.0*DSX(H,G)*FLO/ (3.1416*AVISCI(H,G)*RI(H )*(1.0E-2) )
0200                REI(H,G) = 2.0*DSI(H,G)*FLO/ (3.1416*AVISCI(H,G)*RI(H )*(1.0E-2) )
0201                REG(H,G) = ((2.0*RI(H)*(1.0E-2))**EN*(VEL**(2.0-EN) )*DSX(H,G)*
0202               1(1.0E+3) ) /YI(H,G)
0203                PRG(H,G) =       (YI(H,G)*CPX(H,G)*(2*RI(H)*(1.0E-2)/VEL)**(1.0-EN)
0204               1  )*(1.0E+3) / KX(H,G)
0205                HLX(H,G)=QI(H,G)/(3.1416*2.*RI(H)*(TPI(H,G)-TX(H,G))*(1.0E-2) )
```

```
0206                NUX(H,G) = QI(H,G)/(3.1416*KX(H,G)*(TPI(H,G)-TX(H,G)))
0207                NUI(H,G) = QI(H,G)/(3.1416*KI(H,G)*(TPI(H,G)-TX(H,G)))
0208                GRX(H,G) = ((2.*RI(H))**3 )*(DSX(H,G)**2)*B(H,G)*(TPI(H,G)-TX(H,G)
0209               1 )*(9.806E-3)/(AVISCX(H,G)**2 )
0210                GRI(H,G) = ((2.*RI(H))**3 )*(DSI(H,G)**2)*B(H,G)*(TPI(H,G)-TX(H,G)
0211               1 )*(9.806E-3)/(AVISCI(H,G)**2 )
0212                PRX(H,G) = AVISCX(H,G)*CPX(H,G)/(KX(H,G)*(1.0E-3) )
0213                PRI(H,G) = AVISCI(H,G)*CPI(H,G)/(KI(H,G)*(1.0E-3) )
0214                GX(H,G) = DSX(H,G)*FLO /(3.1416*RI(H)**2*(1.0E-4) )
0215             17 CONTINUE
0216             16 CONTINUE
0217                WRITE(2,992) PRX(2,17), GRX(2,17),B(2,17),TPI(2,17),TX(2,17),
0218               1 AVISCX(2,17),DSX(2,17)
0219            992 FORMAT(//7X,9HPRX100 = ,F6.1,4X,9HGRX100 = ,F8.1,4X,9HB100    = ,
0220               1F8.1,4X, 9HTPI100 = ,F8.1//7X,9HTX100  = ,F8.1,4X,12HAVISCX100 = ,
0221               2E8.4,4X,9HDSX100 = ,E8.4 )
0222                G7X(1,1) = DSX(1,1)*FLO*CPX(1,1)/(KX(1,1)*1.00*RI(1)*(1.0E-5) )
0223                GZI(1,1) = DSX(1,1)*FLO*CPI(1,1)/(KI(1,1)*1.00*RI(1)*(1.0E-5) )
0224                GZX(2,1) = DSX(2,1)*FLO*CPX(2,1)/(KX(2,1)*1.00*RI(2)*(1.0E-5) )
0225                GZI(2,1) = DSX(2,1)*FLO*CPI(2,1)/(KI(2,1)*1.00*RI(2)*(1.0E-5) )
0226                GZXPR1(1,1) = GZX(1,1)+12.6*(PRI(1,1)*GRI(1,1)/  0.10 )**0.40
0227                GZXPR1(2,1) = GZX(2,1)+12.6*(PRI(2,1)*GRI(2,1)/  0.10 )**0.40
0228                DO 33 H = 1,2
0229                KKK = XX(H)
0230                DO 34 G = 2,KKK
0231                GZX(H,G) = DSX(H,G)*FLO*CPX(H,G)/(KX(H,G)*X(H,G)*2.*RI(H)*(1.0E-5)
0232               1 )
0233                GZI(H,G) = DSX(H,G)*FLO*CPI(H,G)/(KI(H,G)*X(H,G)*2.*RI(H)*(1.0E-5)
0234               1 )
0235                GZXPR1(H,G) = GZX(H,G)+12.6*(PRI(H,G)*GRI(H,G)/X(H,G) )**0.40
0236             34 CONTINUE
0237             33 CONTINUE
0238          C END OF MAIN CALCULATIONS
0239          C
0240          C
0241          C THE OUTPUT OF DATA NOW FOLLOWS  TO BE VARIED ACCORDING TO TESTS
0242          C
0243                WRITE(2,550)
0244             550 FORMAT(1H1,7X, 8HTEST NO. )
0245                DO 20 H =1,2
0246                KKK = XX(H)
0247                DO21G =1,KKK
0248                Q(H,G) = QI(H,G)/(0.06283*RI(H) )
0249                QL(H,G) = QINS(H,G)/(0.06283*RI(H) )
0250                FLUX1 = V(1)* A /(L(1)*0.06283*RI(1))
0251                FLUX2 = V(2)* A /(L(2)*0.06283*RI(2))
0252                M(H,G) = YX(H,G)/YI(H,G)
0253                M14(H,G) = M(H,G)**0.14
0254                NFAC(H,G) = NUX(H,G)/FACTOR
0255                NUM14(H,G) = NUX(H,G)/M14(H,G)
0256                NUXFAC(H,G) = NUX(H,G) / (M14(H,G)*FACTOR )
0257                NUIM14(H,G) = NUI(H,G)/M14(H,G)
0258                NUIFAC(H,G) = NUIM14( H,G)/FACTOR
0259                GZX3(H,G) = GZX(H,G)**0.333
0260                GZI3(H,G) = GZI(H,G)**0.333
0261                GZXPR2(H,G) = G7X(H,G) + 0.0083*(PRI(H,G)*GRI(H,G) )**0.75
0262                GRRE2(H,G) = GRI(H,G)/(REI(H,G)**2)
0263                GRRE(H,G) = GRI(H,G)/REI(H,G)
0264                JE(H,G) = HLX(H,G)*(PRX(H,G)**0.666 )/(GX(H,G)*CPX(H,G)*FACTOR*
0265               1 M14(H,G) )
```

```
0266                CONV1(H,G) = 1.75*FACTOR*GZXPR1(H,G)**0.333*M14(H,G)
0267                CONV2(H,G) = 1.75*GZXPR2(H,G)**0.333*M14(H,G)
0268                RP(H,G) = REX(H,G) * PRX(H,G)
0269                GP(H,G) = GRX(H,G)*PRX(H,G)
0270                GP4(H,G) = ((GRX(H,G)*PRX(H,G) )**0.25 )
0271                NP3(H,G) = NUX(H,G) / ( PRX(H,G)**0.333 )
0272                NP3M14(H,G) = NP3( H,G) /M14(H,G)
0273                NP4(H,G) = NUX(H,G)/(PRX(H,G)**0.400 )
0274                GP4RP3(H,G) = ((GRX(H,G)*PRX(H,G))**0.25) / ((REX(H,G)*PRX(H,G) )
0275               1 **0.333 )
0276                NRP3(H,G) = NUX(H,G) / ((REX(H,G)*PRX(H,G))**0.333 )
0277                NRP3M4(H,G) = NRP3(H,G) /M14(H,G)
0278                NFP3(H,G) = NP3(H,G) / FACTOR
0279                NFP3M4(H,G) = NP3M14(H,G)/FACTOR
0280                NFRP3(H,G) = NRP3(H,G) /FACTOR
0281                NFRP3M(H,G) = NRP3M4(H,G) /FACTOR
0282                WRITE(2,600) X(H,G), NUX(H,G)
0283              600 FORMAT(///7X, 5HX =  ,F6.1,4X,6HNU =  ,F7.2 )
0284                WRITE(2,700) REX(H,G),PRX(H,G),M(H,G),GRX(H,G),PRG(H,G),TPO(H,G),
0285               1 TPI(H,G),TX(H,G),Q(H,G),QL(H,G)
0286              700 FORMAT(2X,6HRE =  ,F7.1,4X,6HPR =  ,F6.1,4X,6HM =  ,F4.2,4X,
0287                 16HGR =  ,F8.1,4X,6HPRG = ,F6.1/2X,7HTPO =  ,F6.2,4X,7HTPI =  ,
0288                 2F6.2,4X,6HTX =  ,F6.2,4X,6HQ =  ,F7.1,4X,6HQL =  ,F6.1 )
0289                21 CONTINUE
0290                20 CONTINUE
0291                WRITE(2,800)
0292              800 FORMAT(1H1,7X, 8HTEST NO.,7X, 12HCOMPOSITION )
0293                WRITE(2,900) V(1),V(2),A,TIN,TOUT,TOTH,RI(1),RI(2),L(1),L(2),
0294               1 FLUX1,FLUX2,AVISCX(1,1)
0295              900 FORMAT (///7X, 6HV1 =  , F5.3, 4X, 6HV2 =  , F5.3, 4X, 6HA =  ,
0296                 1 F7.3, 4X, 7HTIN =  , F6.2, 4X,8HTOUT=  ,F6.2, 4X, 8HTOTH =  ,
0297                 2F6.2/7X,6HR1 =  ,F6.4,4X,6HR2 =  ,F6.4,4X,6HL1 =  ,F6.4,4X,6HL2 =
0298                 3 ,F6.4/7X,9HFLUX1 =  ,F7.1,4X,9HFLUX2 =  ,F7.1,4X,8HVISC =  ,F8.4)
0299                WRITE(2,950)
0300              950 FORMAT(///4X,11H   X       ,11H   HLX     ,11H   REG     ,11H   RE
0301                 1I     ,11H   GRI     ,11H   GZX     ,11H   GZI     ,11H   GZX3
0302                 2,11H   GZI3     )
0303                DO23H=1,2
0304                KKK = XX(H)
0305                DO24G=1,KKK
0306                WRITE(2,960) X(H,G),HLX(H,G),REG(H,G),REI(H,G),GRI(H,G),GZX(H,G),
0307               1GZI(H,G),GZX3(H,G),GZI3(H,G)
0308              960 FORMAT(///4X,F8.3,3X,E8.3,3X,E8.3,3X,E8.3,3X,E8.3,3X,E8.3,3X,
0309                 1 E8.3,3X, E8.3,3X,E8.3)
0310                24 CONTINUE
0311                23 CONTINUE
0312              C
0313              C     RESULTS RELEVANT TO DISCONTINUOUS TUBES
0314              C
0315                WRITE(2,970)
0316              970 FORMAT(1H1,4X,11HTEST NO.   ///4X,11H   X       ,11H   M14     ,11
0317                 1H   GP      ,11H   GP4     ,11H   N/P3    ,11H   RP      ,11H   GP
0318                 24/RP3 ,11H   N/RP3   ,11H   N/RP3M14)
0319                DO 25 H = 1,2
0320                KKK = XX(H)
0321                DO 26 G = 1,KKK
0322                WRITE(2,975) X(H,G), M14(H,G),GP(H,G),GP4(H,G),NP3(H,G),RP(H,G),
0323               1 GP4RP3(H,G),NRP3(H,G), NRP3M4(H,G)
0324              975 FORMAT(///4X,F8.3,3X,E8.3,3X,E8.3,3X,E8.3,3X,E8.3,3X,E8.3,3X,
0325                 1 E8.3,3X, E8.3,3X,E8.3)
```

```
0326                26 CONTINUE
0327                25 CONTINUE
0328          C
0329          C     RESULTS RELEVANT TO DISCONTINUOUS TUBES WITH NON NEWTONIAN FLUIDS
0330          C
0331                WRITE(2,976)
0332              976 FORMAT(1H1,4X,11HTEST NO.   ,5X,12HCOMPOSITION ///4X,11H    X
0333                1 ,11H   GRI/RE  ,11H   GRI/RE2 ,11H   NUX/NFAC,11H   NUI/NFAC,11H
0334                2  CONV1   ,11H   CONV2   ,11H   JE      ,11H   GZX     )
0335                DO 28 H = 1,2
0336                KKK = XX(H)
0337                DO 29 G = 1,KKK
0338                WRITE(2,977) X(H,G),GRRE(H,G),GRRE2(H,G),NUXFAC(H,G),NUIFAC(H,G),
0339               1CONV1(H,G),CONV2(H,G),JE(H,G),GZX(H,G)
0340              977 FORMAT(///4X,E8.3,3X,E8.3,3X,E8.3,3X,E8.3,3X,E8.3,3X,E8.3,3X,
0341                1 E8.3,3X, E8.3,3X,E8.3)
0342                29 CONTINUE
0343                28 CONTINUE
0344                WRITE(2,978)
0345              978 FORMAT(1H1,4X,11HTEST NO.   ///4X,11H    X       ,11H   GZX3    ,
0346                1 11H   GZI3    ,11H   N/P3F   ,11H   N/P3MF  ,11H   N/RP3F  ,11H
0347                2 N/RP3MF ,11H   YX      ,11H   N/P4    )
0348                DO 30 H = 1,2
0349                KKK = XX(H)
0350                DO 31 G = 1,KKK
0351                WRITE(2,980) X(H,G),GZX3(H,G),GZI3(H,G),NFP3(H,G),NFP3M4(H,G),
0352               1 NFRP3(H,G),NFRP3M(H,G), YX(H,G),NP4(H,G)
0353              980 FORMAT(///4X,E8.3,3X,E8.3,3X,E8.3,3X,E8.3,3X,E8.3,3X,E8.3,3X,
0354                1 E8.3,3X, E8.3,3X,E8.3 )
0355                31 CONTINUE
0356                30 CONTINUE
0357                WRITE(2,990) VEL,SHEAR,FACTOR
0358              990 FORMAT(///4X,10HVELOCITY =,1E8.2,4X,12HSHEAR RATE =,1E8.2,4X,8HFAC
0359                1TOR =,1E8.7 )
0360                IF(Z.EQ.1) GO TO 2
0361                STOP
0362                END
```

END OF SEGMENT, LENGTH 3898, NAME NONM

```
0363                SUBROUTINE CAL(AV,CV,CT,CONV)
0364                DIMENSION CV(22),  CT(22)
0365                REAL AV, CONV
0366                INTEGER U
0367                U = 1
0368               46 IF(AV - CV(U) ) 47,47,48
0369               48 U = U+1
0370                GO TO 46
0371               47 CONTINUE
0372                CONV = CT(U-1)+(AV-CV(U-1))*(CT(U)-CT(U-1))/(CV(U)-CV(U-1) )
0373                RETURN
0374                END
```

END OF SEGMENT, LENGTH   115, NAME CAL

```
0375          C     INTERPOLATION SUBROUTINE
```

```
0376          C     SUBROUTINE SUBPROGRAM
0377                SUBROUTINE INT(TW,TI,II,A,VALUE)
0378                DIMENSION  T(8), A(8)
0379                REAL TW, VALUE
0380                INTEGER TI, II, III, N
0381                III = II + 1
0382                DO 50N = 1,III
0383               50 T(N) = (N-1) *TI
0384                N = 1
0385               51 IF (TW - T(N) ) 52,52,53
0386               53 N = N + 1
0387                GO TO 51
0388               52 CONTINUE
0389                VALUE = A(N-1)+ (A(N)-A(N-1))*(TW-T(N-1))/(T(N)-T(N-1))
0390                RETURN
0391                END
```

END OF SEGMENT, LENGTH   153, NAME INT

```
0392                FINISH
```

TEST NO. 192 0.50% METHOCEL (60HG) n = 0.96

X = 0.0 NU = 144.05
RF = 8019.0 PR = 37.2 M = 1.02 GR = 102.6 PRG = 37.4
TPO = 23.19 TPI = 22.88 TX = 22.22 Q = 3821.3 QL = 1.4

X = 10.0 NU = 118.10
RF = 8094.8 PR = 36.8 M = 1.03 GR = 145.3 PRG = 37.2
TPO = 23.46 TPI = 23.15 TX = 22.24 Q = 3821.3 QL = 1.4

X = 50.0 NU = 122.85
RF = 8101.0 PR = 36.8 M = 1.03 GR = 140.4 PRG = 37.2
TPO = 23.46 TPI = 23.17 TX = 22.30 Q = 3821.4 QL = 1.4

X = 95.0 NU = 122.49 (DIVERGENCE)
RF = 8120.0 PR = 36.7 M = 1.03 GR = 142.1 PRG = 37.1
TPO = 23.55 TPI = 23.24 TX = 22.36 Q = 3821.5 QL = 1.5

X = 96.0 NU = 119.52
RF = 8126.4 PR = 36.7 M = 1.03 GR = 145.8 PRG = 37.0
TPO = 23.57 TPI = 23.26 TX = 22.36 Q = 3818.7 QL = 1.5

X = 100.0 NU = 130.10
RF = 8107.3 PR = 36.8 M = 1.03 GR = 133.3 PRG = 37.1
TPO = 23.51 TPI = 23.20 TX = 22.37 Q = 3818.7 QL = 1.5

X = 0.0 NU = 275.62
RF = 2064.3 PR = 43.2 M = 1.01 GR = 1583.1 PRG = 43.6
TPO = 22.76 TPI = 22.73 TX = 22.37 Q = 1061.1 QL = 0.1

X = 1.0 NU = 319.14
RF = 2061.0 PR = 43.2 M = 1.01 GR = 1363.3 PRG = 43.7
TPO = 22.72 TPI = 22.69 TX = 22.37 Q = 1061.1 QL = 0.1

X = 2.0 NU = 379.24
RF = 2057.8 PR = 43.3 M = 1.01 GR = 1144.6 PRG = 43.8
TPO = 22.67 TPI = 22.64 TX = 22.38 Q = 1061.8 QL = 0.1

X = 3.0 NU = 286.50
RF = 2064.2 PR = 43.2 M = 1.01 GR = 1525.5 PRG = 43.6
TPO = 22.76 TPI = 22.73 TX = 22.36 Q = 1062.0 QL = 0.2

X = 4.0 NU = 158.33
RF = 2085.4 PR = 42.7 M = 1.02 GR = 2839.9 PRG = 43.2
TPO = 23.06 TPI = 23.02 TX = 22.39 Q = 1070.3 QL = 0.4

X = 5.5 NU = 20.32
RF = 2414.4 PR = 36.9 M = 1.18 GR = 29236.2 PRG = 37.3
TPO = 27.31 TPI = 27.28 TX = 22.39 Q = 1054.6 QL = 3.4

X = 7.0 NU = 13.18
RF = 2641.0 PR = 33.7 M = 1.29 GR = 54052.3 PRG = 34.1
TPO = 29.98 TPI = 29.95 TX = 22.40 Q = 1056.0 QL = 5.3

X = 8.5 NU = 9.66
RF = 2885.8 PR = 30.9 M = 1.41 GR = 87453.6 PRG = 31.2
TPO = 32.66 TPI = 32.63 TX = 22.41 Q = 1049.1 QL = 7.2

X = 10.0 NU = 9.40
RF = 2907.0 PR = 30.7 M = 1.42 GR = 90461.6 PRG = 31.0
TPO = 32.88 TPI = 32.85 TX = 22.41 Q = 1052.5 QL = 7.3

X = 11.5 NU = 9.98
RF = 2862.6 PR = 31.1 M = 1.40 GR = 83940.7 PRG = 31.5
TPO = 32.41 TPI = 32.38 TX = 22.42 Q = 1055.7 QL = 7.0

X = 13.0 NU = 9.72
RF = 2885.8 PR = 30.9 M = 1.41 GR = 87390.5 PRG = 31.2
TPO = 32.66 TPI = 32.63 TX = 22.43 Q = 1053.4 QL = 7.2

X = 15.0 NU = 9.97
RF = 2866.8 PR = 31.1 M = 1.40 GR = 84516.8 PRG = 31.4
TPO = 32.46 TPI = 32.43 TX = 22.44 Q = 1054.0 QL = 7.0

X = 20.0 NU = 11.34
RF = 2753.1 PR = 32.4 M = 1.35 GR = 68275.4 PRG = 32.7
TPO = 31.25 TPI = 31.20 TX = 22.46 Q = 1055.0 QL = 6.2

X = 25.0 NU = 14.12
RF = 2604.0 PR = 34.2 M = 1.27 GR = 49298.2 PRG = 34.6
TPO = 29.56 TPI = 29.52 TX = 22.48 Q = 1056.3 QL = 5.0

X = 40.0 NU = 25.16
RF = 2463.0 PR = 35.4 M = 1.18 GR = 35054.2 PRG = 35.8
TPO = 25.42 TPI = 25.38 TX = 22.55 Q = 1059.4 QL = 2.8

X = 44.0 NU = 28.98
RF = 2392.5 PR = 35.7 M = 1.15 GR = 31455.0 PRG = 36.1
TPO = 24.66 TPI = 24.61 TX = 22.57 Q = 1060.2 QL = 2.5

TEST NO. 192 COMPOSITION 0.50% METHOCEL (60HG) n = 0.96

V1 = 1.497 V2 = 2.540 A = 206.740 TIN = 22.22 TOUT = 22.67 TOTH = 22.58
B1 = 0.8547 B2 = 2.8575 L1 = 1.7090 L2 = 2.7560
FLUX1 = 3822.8 FLUX2 = 1061.3 AVISC = *.5395E-02

X	HLX	REG	REI	GRI	GZX	GZI	GZX3	GZI3
.000E 00	.582E 04	.794E 04	.802E 04	.103E 03	.468E 06	.467E 06	.773E 02	.773E 02
.100E 02	.419E 04	.801E 04	.809E 04	.145E 03	.234E 05	.234E 05	.285E 02	.285E 02
.500E 02	.436E 04	.802E 04	.810E 04	.140E 03	.468E 04	.467E 04	.167E 02	.167E 02
.950E 02	.435E 04	.804E 04	.812E 04	.142E 03	.246E 04	.246E 04	.135E 02	.135E 02
.960E 02	.424E 04	.804E 04	.812E 04	.146E 03	.244E 04	.243E 04	.134E 02	.134E 02
.100E 03	.462E 04	.802E 04	.811E 04	.133E 03	.234E 04	.234E 04	.132E 02	.132E 02
.000E 00	.293E 04	.204E 04	.206E 04	.158E 04	.140E 06	.140E 06	.517E 02	.517E 02
.100E 01	.339E 04	.204E 04	.206E 04	.136E 04	.700E 05	.699E 05	.411E 02	.410E 02
.200E 01	.403E 04	.204E 04	.206E 04	.114E 04	.350E 05	.350E 05	.326E 02	.326E 02
.300E 01	.304E 04	.204E 04	.206E 04	.153E 04	.233E 05	.233E 05	.285E 02	.285E 02
.400E 01	.168E 04	.206E 04	.209E 04	.284E 04	.175E 05	.175E 05	.259E 02	.259E 02
.550E 01	.216E 03	.239E 04	.241E 04	.292E 05	.127E 05	.126E 05	.233E 02	.232E 02
.700E 01	.140E 03	.261E 04	.264E 04	.538E 05	.100E 05	.981E 04	.215E 02	.213E 02
.850E 01	.103E 03	.286E 04	.288E 04	.870E 05	.823E 04	.803E 04	.201E 02	.200E 02
.100E 02	.101E 03	.288E 04	.290E 04	.901E 05	.700E 04	.682E 04	.191E 02	.189E 02
.115E 02	.106E 03	.283E 04	.285E 04	.835E 05	.609E 04	.594E 04	.182E 02	.181E 02
.130E 02	.103E 03	.286E 04	.288E 04	.869E 05	.538E 04	.525E 04	.175E 02	.173E 02
.150E 02	.106E 03	.284E 04	.286E 04	.841E 05	.467E 04	.455E 04	.167E 02	.165E 02
.200E 02	.121E 03	.272E 04	.275E 04	.680E 05	.350E 04	.342E 04	.151E 02	.150E 02
.250E 02	.150E 03	.258E 04	.260E 04	.491E 05	.280E 04	.275E 04	.141E 02	.140E 02
.400E 02	.374E 03	.224E 04	.224E 04	.150E 05	.175E 04	.174E 04	.120E 02	.120E 02
.460E 02	.308E 03	.229E 04	.231E 04	.191E 05	.152E 04	.151E 04	.115E 02	.114E 02
.470E 02	.299E 03	.230E 04	.232E 04	.198E 05	.149E 04	.148E 04	.114E 02	.114E 02
.480E 02	.262E 03	.234E 04	.236E 04	.234E 05	.146E 04	.144E 04	.113E 02	.113E 02

TEST NO. 208 0·15% (W/W) CARBOPOL 934 n = 0·63

X = 0.0 NU = 113.32
RE = 1733.5 PR = 155.[illegible] M = 1.01 GR = 14.1 PRG = 177.9
TPO = 27.20 TPI = 26.76 TX = 25.44 Q = 5376.7 QL = 9.2

X = 10.0 NU = 48.76
RE = 1754.1 PR = 153.[illegible] M = 1.02 GR = 33.6 PRG = 175.8
TPO = 28.98 TPI = 28.54 TX = 25.46 Q = 5376.7 QL = 9.2

X = 50.0 NU = 25.19
RE = 1788.[illegible] PR = 150.[illegible] M = 1.04 GR = 67.9 PRG = 172.4
TPO = 31.94 TPI = 31.51 TX = 25.55 Q = 5372.8 QL = 13.6

(DIVERGENCE)

X = 95.0 NU = 20.15
RE = 1807.0 PR = 148.7 M = 1.05 GR = 87.0 PRG = 170.6
TPO = 33.53 TPI = 33.10 TX = 25.65 Q = 5371.0 QL = 16.0

X = 96.0 NU = 19.87
RE = 1808.0 PR = 148.6 M = 1.05 GR = 88.2 PRG = 170.5
TPO = 33.62 TPI = 33.19 TX = 25.65 Q = 5359.6 QL = 16.1

X = 100.0 NU = 20.76
RE = 1804.4 PR = 148.9 M = 1.05 GR = 84.1 PRG = 170.8
TPO = 33.31 TPI = 32.87 TX = 25.66 Q = 5359.6 QL = 16.1

X = 0.0 NU = 23.95
RE = 140.1 PR = 573.7 M = 1.04 GR = 171.4 PRG = 658.0
TPO = 31.54 TPI = 31.50 TX = 25.66 Q = 1496.7 QL = 4.2

X = 1.0 NU = 45.95
RE = 137.6 PR = 584.3 M = 1.02 GR = 86.2 PRG = 670.1
TPO = 28.76 TPI = 28.71 TX = 25.67 Q = 1496.7 QL = 4.2

X = 2.0 NU = 155.98
RE = 135.6 PR = 592.7 M = 1.01 GR = 24.8 PRG = 679.7
TPO = 26.62 TPI = 26.58 TX = 25.68 Q = 1504.8 QL = 2.7

X = 3.0 NU = 164.64
RE = 135.6 PR = 592.8 M = 1.01 GR = 23.4 PRG = 679.9
TPO = 26.58 TPI = 26.53 TX = 25.68 Q = 1498.1 QL = 2.7

X = 4.0 NU = 98.31
RE = 136.1 PR = 590.5 M = 1.01 GR = 39.4 PRG = 677.2
TPO = 27.16 TPI = 27.11 TX = 25.69 Q = 1495.6 QL = 3.1

X = 5.5 NU = 53.88
RE = 137.2 PR = 585.9 M = 1.02 GR = 73.0 PRG = 671.9
TPO = 28.33 TPI = 28.29 TX = 25.70 Q = 1493.3 QL = 3.9

X = 7.0 NU = 40.47
RE = 138.0 PR = 582.5 M = 1.02 GR = 98.4 PRG = 668.1
TPO = 29.20 TPI = 29.15 TX = 25.71 Q = 1492.8 QL = 4.5

X = 8.5 NU = 34.35
RE = 138.5 PR = 580.1 M = 1.03 GR = 116.8 PRG = 665.3
TPO = 29.82 TPI = 29.78 TX = 25.72 Q = 1492.4 QL = 5.0

X = 10.0 NU = 31.49
RE = 138.9 PR = 578.7 M = 1.03 GR = 128.2 PRG = 663.7
TPO = 30.20 TPI = 30.16 TX = 25.73 Q = 1492.4 QL = 5.3

X = 11.5 NU = 29.76
RE = 139.1 PR = 577.7 M = 1.03 GR = 136.2 PRG = 662.5
TPO = 30.47 TPI = 30.42 TX = 25.74 Q = 1492.7 QL = 5.4

X = 13.0 NU = 27.57
RE = 139.5 PR = 576.2 M = 1.03 GR = 147.7 PRG = 660.8
TPO = 30.85 TPI = 30.80 TX = 25.75 Q = 1492.0 QL = 5.7

X = 15.0 NU = 25.60
RE = 139.8 PR = 574.7 M = 1.04 GR = 160.0 PRG = 659.1
TPO = 31.25 TPI = 31.21 TX = 25.77 Q = 1491.8 QL = 6.0

X = 20.0 NU = 22.66
RE = 140.5 PR = 571.9 M = 1.04 GR = 182.8 PRG = 655.9
TPO = 31.99 TPI = 31.94 TX = 25.80 Q = 1491.3 QL = 6.5

X = 25.0 NU = 20.71
RE = 141.1 PR = 569.6 M = 1.05 GR = 201.6 PRG = 653.2
TPO = 32.59 TPI = 32.55 TX = 25.83 Q = 1490.9 QL = 7.0

X = 40.0 NU = 16.57
RE = 142.7 PR = 563.0 M = 1.06 GR = 259.2 PRG = 645.7
TPO = 34.32 TPI = 34.33 TX = 25.94 Q = 1489.5 QL = 8.2

X = 46.0 NU = 19.71
RE = 141.5 PR = 567.[illegible] M = 1.05 GR = 235.[illegible] PRG = 650.9
TPO = [illegible] TPI = [illegible] TX = [illegible] Q = [illegible] QL = [illegible]

TEST NO. 208 COMPOSITION 0.15 % CARBOPOL (CPM) 934 n = 0.63

V1 = 2.005 V2 = 3.006 A = 246.560 TIN = 25.44 TOUT = 26.16 TOTH = 25.99
R1 = 0.8547 R2 = 2.8575 I1 = 1.7090 I2 = 2.7560
FIDX1 = 5386.6 FIDX2 = 1497.9 AVISC = *.2270E-01

X	HIX	REG	REI	GRI	GZX	GZI	GZX3	GZI3
.000E 00	.405E 04	.151E 04	.173E 04	.141E 02	.422E 06	.471E 06	.747E 02	.746E 02
.100E 02	.174E 04	.153E 04	.175E 04	.336E 02	.211E 05	.210E 05	.275E 02	.275E 02
.500E 02	.902E 03	.156E 04	.179E 04	.677E 02	.422E 04	.416E 04	.161E 02	.160E 02
.950E 02	.721E 03	.158E 04	.180E 04	.866E 02	.222E 04	.218E 04	.130E 02	.129E 02
.960E 02	.711E 03	.158E 04	.180E 04	.878E 02	.220E 04	.216E 04	.130E 02	.129E 02
.100E 03	.743E 03	.157E 04	.180E 04	.838E 02	.211E 04	.208E 04	.128E 02	.127E 02
.000E 00	.257E 03	.122E 03	.140E 03	.171E 03	.126E 06	.125E 06	.500E 02	.497E 02
.100E 01	.492E 03	.120E 03	.137E 03	.860E 02	.631E 05	.627E 05	.397E 02	.396E 02
.200E 01	.167E 04	.118E 03	.136E 03	.248E 02	.316E 05	.315E 05	.315E 02	.315E 02
.300E 01	.176E 04	.118E 03	.136E 03	.234E 02	.210E 05	.210E 05	.275E 02	.275E 02
.400E 01	.105E 04	.119E 03	.136E 03	.394E 02	.158E 05	.157E 05	.250E 02	.250E 02
.550E 01	.577E 03	.120E 03	.137E 03	.729E 02	.115E 05	.114E 05	.225E 02	.224E 02
.700E 01	.433E 03	.120E 03	.138E 03	.982E 02	.902E 04	.894E 04	.208E 02	.207E 02
.850E 01	.368E 03	.121E 03	.139E 03	.117E 03	.743E 04	.735E 04	.195E 02	.194E 02
.100E 02	.337E 03	.121E 03	.139E 03	.128E 03	.631E 04	.624E 04	.184E 02	.184E 02
.115E 02	.319E 03	.121E 03	.139E 03	.136E 03	.549E 04	.543E 04	.176E 02	.175E 02
.130E 02	.295E 03	.122E 03	.139E 03	.147E 03	.486E 04	.480E 04	.169E 02	.168E 02
.150E 02	.274E 03	.122E 03	.140E 03	.160E 03	.421E 04	.415E 04	.161E 02	.160E 02
.200E 02	.243E 03	.123E 03	.140E 03	.182E 03	.316E 04	.311E 04	.146E 02	.146E 02
.250E 02	.222E 03	.123E 03	.141E 03	.201E 03	.252E 04	.248E 04	.136E 02	.135E 02
.400E 02	.178E 03	.124E 03	.142E 03	.258E 03	.158E 04	.155E 04	.116E 02	.115E 02
.460E 02	.211E 03	.123E 03	.141E 03	.214E 03	.137E 04	.135E 04	.111E 02	.110E 02
.470E 02	.205E 03	.124E 03	.141E 03	.221E 03	.134E 04	.132E 04	.110E 02	.109E 02
.480E 02	.201E 03	.124E 03	.142E 03	.226E 03	.131E 04	.129E 04	.109E 02	.108E 02

TEST NO. 227 0.25% CARBOPOL 934 n = 0.67

X = 0.0 NU = 141.97
RE = 2541.7 PR = 146.0 M = 1.01 GR = 12.0 PRG = 164.8
TPO = 27.16 TPI = 26.75 TX = 25.75 Q = 5050.4 QL = 9.0

X = 10.0 NU = 54.70
RE = 2569.5 PR = 145.2 M = 1.02 GR = 31.8 PRG = 163.1
TPO = 28.76 TPI = 28.35 TX = 25.77 Q = 5050.4 QL = 9.0

X = 50.0 NU = 29.14
RE = 2609.8 PR = 142.9 M = 1.03 GR = 61.7 PRG = 160.5
TPO = 31.07 TPI = 30.66 TX = 25.83 Q = 5047.5 QL = 12.5

(DIVERGENCE)

X = 95.0 NU = 22.64
RE = 2635.0 PR = 141.5 M = 1.04 GR = 81.2 PRG = 158.9
TPO = 32.53 TPI = 32.12 TX = 25.90 Q = 5045.5 QL = 14.6

X = 96.0 NU = 22.46
RE = 2635.8 PR = 141.5 M = 1.04 GR = 81.9 PRG = 158.9
TPO = 32.57 TPI = 32.16 TX = 25.90 Q = 5039.5 QL = 14.7

X = 100.0 NU = 23.14
RE = 2632.7 PR = 141.6 M = 1.04 GR = 79.3 PRG = 159.1
TPO = 32.39 TPI = 31.98 TX = 25.90 Q = 5039.5 QL = 14.7

X = 0.0 NU = 48.45
RE = 233.1 PR = 478.5 M = 1.02 GR = 116.2 PRG = 537.4
TPO = 28.67 TPI = 28.62 TX = 25.90 Q = 1411.8 QL = 3.8

X = 1.0 NU = 61.01
RE = 232.2 PR = 480.3 M = 1.01 GR = 91.6 PRG = 539.4
TPO = 28.11 TPI = 28.07 TX = 25.91 Q = 1411.8 QL = 3.8

X = 2.0 NU = 230.62
RE = 229.7 PR = 485.5 M = 1.00 GR = 23.9 PRG = 545.3
TPO = 26.53 TPI = 26.49 TX = 25.91 Q = 1424.6 QL = 2.7

X = 3.0 NU = 262.14
RE = 229.6 PR = 485.7 M = 1.00 GR = 21.0 PRG = 545.5
TPO = 26.47 TPI = 26.42 TX = 25.92 Q = 1419.1 QL = 2.7

X = 4.0 NU = 177.75
RE = 230.0 PR = 484.9 M = 1.01 GR = 31.0 PRG = 544.6
TPO = 26.71 TPI = 26.67 TX = 25.92 Q = 1418.8 QL = 2.9

X = 5.5 NU = 80.17
RE = 231.5 PR = 481.9 M = 1.01 GR = 69.5 PRG = 541.2
TPO = 27.62 TPI = 27.58 TX = 25.93 Q = 1416.6 QL = 3.5

X = 7.0 NU = 54.10
RE = 232.7 PR = 479.2 M = 1.02 GR = 104.1 PRG = 538.3
TPO = 28.42 TPI = 28.38 TX = 25.94 Q = 1415.8 QL = 4.1

X = 8.5 NU = 44.18
RE = 233.6 PR = 477.4 M = 1.02 GR = 128.5 PRG = 536.2
TPO = 28.98 TPI = 28.93 TX = 25.94 Q = 1415.6 QL = 4.5

X = 10.0 NU = 38.53
RE = 234.3 PR = 476.0 M = 1.02 GR = 148.3 PRG = 534.6
TPO = 29.42 TPI = 29.38 TX = 25.95 Q = 1415.3 QL = 4.8

X = 11.5 NU = 35.39
RE = 234.8 PR = 475.0 M = 1.03 GR = 162.1 PRG = 533.5
TPO = 29.73 TPI = 29.69 TX = 25.96 Q = 1415.3 QL = 5.0

X = 13.0 NU = 32.90
RE = 235.2 PR = 474.1 M = 1.03 GR = 175.1 PRG = 532.5
TPO = 30.02 TPI = 29.98 TX = 25.97 Q = 1415.1 QL = 5.2

X = 15.0 NU = 30.11
RE = 235.8 PR = 472.9 M = 1.03 GR = 192.4 PRG = 531.1
TPO = 30.40 TPI = 30.36 TX = 25.98 Q = 1414.8 QL = 5.5

X = 20.0 NU = 26.47
RE = 236.8 PR = 470.9 M = 1.03 GR = 220.9 PRG = 528.8
TPO = 31.05 TPI = 30.98 TX = 26.00 Q = 1414.4 QL = 5.9

X = 25.0 NU = 23.80
RE = 237.7 PR = 469.0 M = 1.04 GR = 247.8 PRG = 526.8
TPO = 31.61 TPI = 31.57 TX = 26.02 Q = 1414.0 QL = 6.3

X = 40.0 NU = 20.00
RE = 239.5 PR = 465.5 M = 1.05 GR = 300.0 PRG = 522.8
TPO = 32.73 TPI = 32.68 TX = 26.09 Q = 1413.2 QL = 7.1

X = 44.0 NU = 19.4

TEST NO. 227 COMPOSITION 0.25% CARBOPOL (CPM) 934

V1 = 1.944 V2 = 2.942 A = 238.880 TIN = 25.75 TOUT= 26.13 TOTH = 26.13
R1 = 0.8547 R2 = 2.8575 L1 = 1.7090 L2 = 2.7560
FLUX1 = 5060.0 FLUX2 = 1420.3 AVISC = *.2150E-01

X	HIX	REG	REI	GRI	GZX	GZI	GZX3	GZI3
.000E 00	.508E 04	.226E 04	.254E 04	.120E 02	.586E 06	.585E 06	.833E 02	.832E 02
.100E 02	.196E 04	.229E 04	.257E 04	.318E 02	.293E 05	.291E 05	.307E 02	.307E 02
.500E 02	.104E 04	.232E 04	.261E 04	.616E 02	.586E 04	.579E 04	.180E 02	.179E 02
.950E 02	.811E 03	.235E 04	.263E 04	.809E 02	.308E 04	.304E 04	.145E 02	.144E 02
.960E 02	.805E 03	.235E 04	.263E 04	.816E 02	.305E 04	.301E 04	.145E 02	.144E 02
.100E 03	.829E 03	.234E 04	.263E 04	.790E 02	.293E 04	.289E 04	.143E 02	.142E 02
.000E 00	.519E 03	.208E 03	.233E 03	.116E 03	.175E 06	.174E 06	.557E 02	.556E 02
.100E 01	.654E 03	.207E 03	.232E 03	.915E 02	.876E 05	.871E 05	.442E 02	.442E 02
.200E 01	.247E 04	.205E 03	.230E 03	.239E 02	.438E 05	.437E 05	.351E 02	.351E 02
.300E 01	.281E 04	.204E 03	.230E 03	.209E 02	.292E 05	.292E 05	.307E 02	.307E 02
.400E 01	.190E 04	.205E 03	.230E 03	.310E 02	.219E 05	.219E 05	.279E 02	.279E 02
.550E 01	.859E 03	.206E 03	.231E 03	.695E 02	.159E 05	.159E 05	.251E 02	.250E 02
.700E 01	.580E 03	.207E 03	.233E 03	.104E 03	.125E 05	.124E 05	.231E 02	.231E 02
.850E 01	.473E 03	.208E 03	.233E 03	.128E 03	.103E 05	.102E 05	.217E 02	.216E 02
.100E 02	.413E 03	.209E 03	.234E 03	.148E 03	.876E 04	.869E 04	.206E 02	.205E 02
.115E 02	.379E 03	.209E 03	.235E 03	.162E 03	.762E 04	.755E 04	.196E 02	.196E 02
.130E 02	.353E 03	.209E 03	.235E 03	.175E 03	.674E 04	.667E 04	.188E 02	.188E 02
.150E 02	.323E 03	.210E 03	.236E 03	.192E 03	.584E 04	.578E 04	.180E 02	.179E 02
.200E 02	.284E 03	.211E 03	.236E 03	.220E 03	.438E 04	.433E 04	.163E 02	.162E 02
.250E 02	.255E 03	.212E 03	.237E 03	.247E 03	.350E 04	.346E 04	.151E 02	.151E 02
.400E 02	.214E 03	.213E 03	.239E 03	.299E 03	.219E 04	.216E 04	.130E 02	.129E 02
.460E 02	.200E 03	.214E 03	.240E 03	.323E 03	.190E 04	.187E 04	.124E 02	.123E 02
.470E 02	.201E 03	.214E 03	.240E 03	.322E 03	.186E 04	.183E 04	.123E 02	.122E 02
.480E 02	.198E 03	.214E 03	.240E 03	.322E 03	.182E 04	.179E 04	.122E 02	.121E 02

TEST NO. 235 0.5% CARBOPOL 934 n = 0.53

X = 0.0 NU = 124.94
RE = 74.3 PR = 801.2 M = 1.00 GR = 0.2 PRG = 978.8
TPO = 25.93 TPI = 25.79 TX = 25.39 Q = 1771.1 QL = 9.0

X = 10.0 NU = 29.17
RE = 75.1 PR = 792.9 M = 1.01 GR = 0.7 PRG = 968.7
TPO = 27.27 TPI = 27.12 TX = 25.43 Q = 1771.1 QL = 9.0

X = 50.0 NU = 15.62
RE = 76.0 PR = 783.1 M = 1.02 GR = 1.3 PRG = 956.7
TPO = 28.87 TPI = 28.72 TX = 25.56 Q = 1769.3 QL = 11.4
(DIVERGENCE)

X = 95.0 NU = 12.43
RE = 76.5 PR = 777.2 M = 1.03 GR = 1.7 PRG = 949.5
TPO = 29.82 TPI = 29.68 TX = 25.71 Q = 1767.8 QL = 12.8

X = 96.0 NU = 12.45
RE = 76.5 PR = 777.2 M = 1.03 GR = 1.7 PRG = 949.4
TPO = 29.82 TPI = 29.68 TX = 25.71 Q = 1769.0 QL = 12.8

X = 100.0 NU = 12.29
RE = 76.6 PR = 776.7 M = 1.03 GR = 1.7 PRG = 948.9
TPO = 29.89 TPI = 29.75 TX = 25.73 Q = 1769.0 QL = 12.8

X = 0.0 NU = 9.59
RE = 4.2 PR = 4234.8 M = 1.04 GR = 2.6 PRG = 5173.6
TPO = 30.54 TPI = 30.52 TX = 25.73 Q = 492.5 QL = 6.2

X = 1.0 NU = 10.94
RE = 4.2 PR = 4253.2 M = 1.03 GR = 2.3 PRG = 5196.1
TPO = 29.96 TPI = 29.94 TX = 25.74 Q = 492.5 QL = 6.2

X = 2.0 NU = 12.60
RE = 4.2 PR = 4269.4 M = 1.03 GR = 2.0 PRG = 5216.0
TPO = 29.44 TPI = 29.43 TX = 25.75 Q = 497.0 QL = 5.9

X = 3.0 NU = 11.13
RE = 4.2 PR = 4255.1 M = 1.03 GR = 2.2 PRG = 5198.4
TPO = 29.89 TPI = 29.87 TX = 25.76 Q = 490.8 QL = 6.2

X = 4.0 NU = 10.83
RE = 4.2 PR = 4250.7 M = 1.03 GR = 2.3 PRG = 5193.1
TPO = 30.02 TPI = 30.01 TX = 25.77 Q = 491.7 QL = 6.3

X = 5.5 NU = 10.82
RE = 4.2 PR = 4249.8 M = 1.03 GR = 2.3 PRG = 5192.0
TPO = 30.04 TPI = 30.03 TX = 25.78 Q = 492.3 QL = 6.3

X = 7.0 NU = 10.62
RE = 4.2 PR = 4246.8 M = 1.03 GR = 2.3 PRG = 5188.3
TPO = 30.13 TPI = 30.12 TX = 25.80 Q = 491.8 QL = 6.3

X = 8.5 NU = 10.84
RE = 4.2 PR = 4248.8 M = 1.03 GR = 2.3 PRG = 5190.7
TPO = 30.07 TPI = 30.05 TX = 25.81 Q = 492.4 QL = 6.3

X = 10.0 NU = 10.70
RE = 4.2 PR = 4246.5 M = 1.03 GR = 2.3 PRG = 5187.9
TPO = 30.13 TPI = 30.12 TX = 25.83 Q = 492.0 QL = 6.3

X = 11.5 NU = 10.69
RE = 4.2 PR = 4245.6 M = 1.03 GR = 2.3 PRG = 5186.8
TPO = 30.16 TPI = 30.14 TX = 25.84 Q = 492.3 QL = 6.4

X = 13.0 NU = 10.45
RE = 4.2 PR = 4241.9 M = 1.03 GR = 2.4 PRG = 5182.3
TPO = 30.27 TPI = 30.25 TX = 25.86 Q = 492.0 QL = 6.4

X = 15.0 NU = 10.13
RE = 4.2 PR = 4236.7 M = 1.04 GR = 2.5 PRG = 5176.0
TPO = 30.42 TPI = 30.41 TX = 25.88 Q = 491.8 QL = 6.6

X = 20.0 NU = 10.10
RE = 4.2 PR = 4234.0 M = 1.04 GR = 2.5 PRG = 5172.7
TPO = 30.49 TPI = 30.48 TX = 25.93 Q = 491.9 QL = 6.6

X = 25.0 NU = 9.63
RE = 4.2 PR = 4225.0 M = 1.04 GR = 2.6 PRG = 5161.7
TPO = 30.76 TPI = 30.74 TX = 25.98 Q = 491.6 QL = 6.8

X = 40.0 NU = 9.11
RE = 4.2 PR = 4210.0 M = 1.04 GR = 2.8 PRG = 5143.4
TPO = 31.18 TPI = 31.17 TX = 26.14 Q = 491.3 QL = 7.1

TEST NO. 235 COMPOSITION 0.5% cpm n = 0.53

V1 = 1.153 V2 = 1.740 A = 141.740 TIN = 25.39 TOUT = 25.64 TOTH = 26.22
R1 = 0.8547 R2 = 2.8575 L1 = 1.7090 L2 = 2.7560
FLUX1 = 1780.7 FLUX2 = 498.4 AVISC = +.1172E 00

X	HLX	REG	RET	GRI	GZX	GZI	GZX3	GZI3
.000E 00	.447E 04	.608E 02	.743E 02	.158E 00	.935E 05	.934E 05	.452E 02	.452E 02
.100E 02	.104E 04	.614E 02	.751E 02	.691E 00	.467E 04	.465E 04	.167E 02	.166E 02
.500E 02	.559E 03	.622E 02	.760E 02	.133E 01	.935E 03	.927E 03	.975E 01	.973E 01
.950E 02	.445E 03	.626E 02	.765E 02	.170E 01	.492E 03	.487E 03	.788E 01	.785E 01
.960E 02	.446E 03	.626E 02	.765E 02	.170E 01	.487E 03	.482E 03	.785E 01	.782E 01
.100E 03	.440E 03	.627E 02	.766E 02	.173E 01	.467E 03	.463E 03	.774E 01	.772E 01
.000E 00	.103E 03	.344E 01	.420E 01	.259E 01	.279E 05	.276E 05	.302E 02	.301E 02
.100E 01	.117E 03	.342E 01	.418E 01	.226E 01	.140E 05	.138E 05	.240E 02	.239E 02
.200E 01	.135E 03	.341E 01	.417E 01	.196E 01	.698E 04	.692E 04	.191E 02	.190E 02
.300E 01	.119E 03	.342E 01	.418E 01	.221E 01	.466E 04	.461E 04	.167E 02	.166E 02
.400E 01	.116E 03	.342E 01	.418E 01	.228E 01	.349E 04	.346E 04	.151E 02	.151E 02
.550E 01	.116E 03	.343E 01	.418E 01	.229E 01	.254E 04	.251E 04	.136E 02	.136E 02
.700E 01	.114E 03	.343E 01	.419E 01	.233E 01	.200E 04	.197E 04	.126E 02	.125E 02
.850E 01	.116E 03	.343E 01	.419E 01	.229E 01	.164E 04	.163E 04	.118E 02	.117E 02
.100E 02	.115E 03	.343E 01	.419E 01	.232E 01	.140E 04	.138E 04	.112E 02	.111E 02
.115E 02	.115E 03	.343E 01	.419E 01	.232E 01	.121E 04	.120E 04	.106E 02	.106E 02
.130E 02	.112E 03	.343E 01	.419E 01	.238E 01	.107E 04	.106E 04	.102E 02	.102E 02
.150E 02	.109E 03	.344E 01	.420E 01	.246E 01	.931E 03	.921E 03	.974E 01	.971E 01
.200E 02	.108E 03	.344E 01	.420E 01	.248E 01	.698E 03	.691E 03	.885E 01	.882E 01
.250E 02	.103E 03	.344E 01	.421E 01	.262E 01	.558E 03	.552E 03	.822E 01	.819E 01
.400E 02	.977E 02	.345E 01	.422E 01	.281E 01	.349E 03	.345E 03	.703E 01	.700E 01
.460E 02	.942E 02	.346E 01	.423E 01	.293E 01	.303E 03	.300E 03	.671E 01	.668E 01
.470E 02	.942E 02	.346E 01	.423E 01	.294E 01	.297E 03	.293E 03	.666E 01	.663E 01
.480E 02	.938E 02	.346E 01	.423E 01	.295E 01	.291E 03	.287E 03	.661E 01	.659E 01

TEST NO. 281
n = 0.90 0.5% (W/W) SODIUM CARBOXYMETHYL CELLULOSE

X = 0.0 NU = 37.19
RE = 932.3 PR = 73.7 M = 1.02 GR = 38.1 PRG = 75.7
TPO = 21.82 TPI = 21.71 TX = 20.65 Q = 1385.4 QL = 5.5

X = 10.0 NU = 24.55
RE = 944.0 PR = 72.7 M = 1.04 GR = 59.2 PRG = 74.8
TPO = 22.38 TPI = 22.27 TX = 20.67 Q = 1385.4 QL = 5.5

X = 50.0 NU = 14.27
RE = 970.0 PR = 70.8 M = 1.06 GR = 108.1 PRG = 72.7
TPO = 23.62 TPI = 23.51 TX = 20.77 Q = 1383.7 QL = 7.3

X = 95.0 NU = 11.18 (DIVERGENCE)
RE = 988.3 PR = 69.4 M = 1.08 GR = 144.0 PRG = 71.4
TPO = 24.47 TPI = 24.36 TX = 20.87 Q = 1381.5 QL = 8.6

X = 96.0 NU = 11.61
RE = 985.9 PR = 69.6 M = 1.08 GR = 138.6 PRG = 71.5
TPO = 24.36 TPI = 24.25 TX = 20.87 Q = 1387.7 QL = 8.4

X = 100.0 NU = 12.13
RE = 983.0 PR = 69.8 M = 1.07 GR = 132.0 PRG = 71.7
TPO = 24.22 TPI = 24.11 TX = 20.88 Q = 1387.7 QL = 8.4

X = 0.0 NU = 14.27
RE = 201.4 PR = 101.9 M = 1.06 GR = 1791.9 PRG = 104.7
TPO = 23.39 TPI = 23.38 TX = 20.88 Q = 377.8 QL = 3.8

X = 1.0 NU = 11.11
RE = 204.6 PR = 100.3 M = 1.07 GR = 2376.7 PRG = 103.1
TPO = 24.11 TPI = 24.10 TX = 20.89 Q = 377.8 QL = 3.8

X = 2.0 NU = 13.76
RE = 202.1 PR = 101.5 M = 1.06 GR = 1909.3 PRG = 104.3
TPO = 23.55 TPI = 23.54 TX = 20.89 Q = 385.2 QL = 3.4

X = 3.0 NU = 15.64
RE = 200.8 PR = 102.2 M = 1.05 GR = 1655.0 PRG = 105.1
TPO = 23.24 TPI = 23.22 TX = 20.90 Q = 384.6 QL = 3.2

X = 4.0 NU = 17.55
RE = 199.7 PR = 102.8 M = 1.05 GR = 1458.6 PRG = 105.6
TPO = 22.99 TPI = 22.98 TX = 20.91 Q = 384.4 QL = 3.0

X = 5.5 NU = 21.69
RE = 198.0 PR = 103.7 M = 1.04 GR = 1163.0 PRG = 106.5
TPO = 22.61 TPI = 22.60 TX = 20.92 Q = 384.9 QL = 2.8

X = 7.0 NU = 26.89
RE = 196.6 PR = 104.4 M = 1.03 GR = 925.2 PRG = 107.3
TPO = 22.29 TPI = 22.28 TX = 20.93 Q = 384.7 QL = 2.6

X = 8.5 NU = 41.03
RE = 194.7 PR = 105.4 M = 1.02 GR = 596.7 PRG = 108.3
TPO = 21.84 TPI = 21.83 TX = 20.94 Q = 385.9 QL = 2.2

X = 10.0 NU = 49.17
RE = 194.1 PR = 105.7 M = 1.02 GR = 494.9 PRG = 108.7
TPO = 21.70 TPI = 21.69 TX = 20.95 Q = 385.7 QL = 2.1

X = 11.5 NU = 49.96
RE = 194.1 PR = 105.7 M = 1.02 GR = 488.1 PRG = 108.7
TPO = 21.70 TPI = 21.69 TX = 20.96 Q = 386.2 QL = 2.1

X = 13.0 NU = 32.86
RE = 195.7 PR = 104.8 M = 1.02 GR = 753.0 PRG = 107.7
TPO = 22.09 TPI = 22.08 TX = 20.97 Q = 384.9 QL = 2.4

X = 15.0 NU = 25.03
RE = 197.3 PR = 104.0 M = 1.03 GR = 1004.9 PRG = 106.9
TPO = 22.45 TPI = 22.44 TX = 20.99 Q = 384.8 QL = 2.7

X = 20.0 NU = 18.36
RE = 199.8 PR = 102.7 M = 1.04 GR = 1406.9 PRG = 105.6
TPO = 23.01 TPI = 23.00 TX = 21.02 Q = 384.5 QL = 3.1

X = 25.0 NU = 12.55
RE = 203.9 PR = 100.6 M = 1.07 GR = 2145.0 PRG = 103.4
TPO = 23.96 TPI = 23.94 TX = 21.06 Q = 383.7 QL = 3.7

X = 40.0 NU = 13.03
RE = 203.9 PR = 100.6 M = 1.06 GR = 2081.6 PRG = 103.4
TPO = 23.96 TPI = 23.94 TX = 21.14 Q = 383.8 QL = 3.7

TEST NO. 281 COMPOSITION 0.5% (W|W) SODIUM CARBOXYMETHYL CELLULOSE (CMC)
n = 0.90

V1 = 1.014 V2 = 1.523 A = 125.900 TIN = 20.65 TOUT= 21.29 TOTH = 21.22
R1 = 0.8547 R2 = 2.8575 L1 = 1.7090 L2 = 2.7560
FLUX1 = 1391.0 FLUX2 = 387.5 AVISC = *.1065E-01

X	HLX	REG	REI	GRI	GZX	GZI	GZX3	GZI3
.000E 00	.131E 04	.907E 03	.932E 03	.380E 02	.108E 06	.108E 06	.474E 02	.474E 02
.100E 02	.868E 03	.918E 03	.944E 03	.592E 02	.539E 04	.537E 04	.175E 02	.175E 02
.500E 02	.505E 03	.944E 03	.969E 03	.108E 03	.108E 04	.107E 04	.102E 02	.102E 02
.950E 02	.396E 03	.962E 03	.987E 03	.144E 03	.567E 03	.562E 03	.826E 01	.824E 01
.960E 02	.411E 03	.959E 03	.985E 03	.138E 03	.561E 03	.556E 03	.823E 01	.821E 01
.100E 03	.429E 03	.956E 03	.982E 03	.132E 03	.539E 03	.534E 03	.812E 01	.810E 01
.000E 00	.151E 03	.196E 03	.201E 03	.179E 04	.322E 05	.320E 05	.317E 02	.316E 02
.100E 01	.118E 03	.199E 03	.204E 03	.237E 04	.161E 05	.160E 05	.252E 02	.251E 02
.200E 01	.146E 03	.197E 03	.202E 03	.191E 04	.806E 04	.800E 04	.200E 02	.199E 02
.300E 01	.166E 03	.195E 03	.201E 03	.169E 04	.557E 04	.554E 04	.175E 02	.174E 02
.400E 01	.186E 03	.194E 03	.200E 03	.146E 04	.403E 04	.401E 04	.159E 02	.158E 02
.550E 01	.230E 03	.193E 03	.198E 03	.116E 04	.293E 04	.292E 04	.143E 02	.143E 02
.700E 01	.285E 03	.191E 03	.197E 03	.925E 03	.230E 04	.229E 04	.132E 02	.132E 02
.850E 01	.434E 03	.189E 03	.195E 03	.596E 03	.190E 04	.189E 04	.123E 02	.123E 02
.100E 02	.520E 03	.189E 03	.194E 03	.495E 03	.161E 04	.161E 04	.117E 02	.117E 02
.115E 02	.529E 03	.189E 03	.194E 03	.488E 03	.140E 04	.140E 04	.112E 02	.112E 02
.130E 02	.348E 03	.190E 03	.196E 03	.753E 03	.124E 04	.124E 04	.107E 02	.107E 02
.150E 02	.265E 03	.192E 03	.197E 03	.100E 04	.107E 04	.107E 04	.102E 02	.102E 02
.200E 02	.194E 03	.194E 03	.200E 03	.141E 04	.806E 03	.801E 03	.928E 01	.927E 01
.250E 02	.133E 03	.198E 03	.204E 03	.214E 04	.644E 03	.640E 03	.862E 01	.860E 01
.400E 02	.138E 03	.198E 03	.204E 03	.208E 04	.403E 03	.400E 03	.737E 01	.735E 01
.460E 02	.114E 03	.201E 03	.207E 03	.259E 04	.350E 03	.347E 03	.703E 01	.701E 01
.480E 02	.106E 03	.202E 03	.208E 03	.283E 04	.335E 03	.332E 03	.694E 01	.691E 01

TEST NO. 238 0·5% (W/W) CARBOPOL 934 n = 0·55

X = 0.0 NU = 80.33
RE = 88.2 PR = 1277.1 M = 1.01 GR = 6.4 PRG = 1558.3
TPO = 26.80 TPI = 26.77 TX = 25.69 Q = 934.4 QL = 5.5

X = 10.0 NU = 34.29
RE = 89.2 PR = 1262.6 M = 1.02 GR = 15.5 PRG = 1520.9
TPO = 28.29 TPI = 28.26 TX = 25.72 Q = 934.4 QL = 5.5

X = 30.0 NU = 22.45
RE = 90.1 PR = 1249.1 M = 1.03 GR = 24.2 PRG = 1504.6
TPO = 29.69 TPI = 29.66 TX = 25.78 Q = 933.4 QL = 4.5 (CONVERGENCE)

X = 46.0 NU = 19.25
RE = 90.6 PR = 1242.5 M = 1.03 GR = 28.6 PRG = 1496.6
TPO = 30.38 TPI = 30.35 TX = 25.83 Q = 932.9 QL = 5.0

X = 47.0 NU = 18.79
RE = 90.7 PR = 1241.4 M = 1.04 GR = 29.3 PRG = 1495.4
TPO = 30.49 TPI = 30.46 TX = 25.83 Q = 932.4 QL = 5.0

X = 48.0 NU = 18.71
RE = 90.7 PR = 1241.2 M = 1.04 GR = 29.4 PRG = 1495.1
TPO = 30.51 TPI = 30.49 TX = 25.83 Q = 932.4 QL = 5.0

X = 0.5 NU = 31.80
RE = 1525.3 PR = 246.7 M = 1.02 GR = 12.2 PRG = 297.1
TPO = 28.93 TPI = 28.67 TX = 25.83 Q = 3231.4 QL = 8.2

X = 1.0 NU = 32.31
RE = 1524.8 PR = 246.8 M = 1.02 GR = 12.0 PRG = 297.2
TPO = 28.89 TPI = 28.63 TX = 25.83 Q = 3231.4 QL = 8.2

X = 2.0 NU = 32.26
RE = 1524.8 PR = 246.8 M = 1.02 GR = 12.0 PRG = 297.2
TPO = 28.89 TPI = 28.63 TX = 25.84 Q = 3226.6 QL = 8.2

X = 3.0 NU = 30.90
RE = 1525.8 PR = 246.6 M = 1.02 GR = 12.4 PRG = 297.0
TPO = 28.98 TPI = 28.72 TX = 25.84 Q = 3190.3 QL = 8.3

X = 4.0 NU = 31.79
RE = 1525.3 PR = 246.7 M = 1.02 GR = 12.2 PRG = 297.1
TPO = 28.93 TPI = 28.67 TX = 25.84 Q = 3227.5 QL = 8.2

X = 5.5 NU = 30.40
RE = 1526.6 PR = 246.5 M = 1.02 GR = 12.6 PRG = 296.9
TPO = 29.04 TPI = 28.78 TX = 25.84 Q = 3207.1 QL = 8.4

X = 7.0 NU = 30.05
RE = 1527.1 PR = 246.4 M = 1.02 GR = 12.8 PRG = 296.8
TPO = 29.09 TPI = 28.83 TX = 25.84 Q = 3214.6 QL = 8.5

X = 8.5 NU = 28.88
RE = 1528.4 PR = 246.2 M = 1.02 GR = 13.3 PRG = 296.5
TPO = 29.20 TPI = 28.94 TX = 25.84 Q = 3205.2 QL = 8.6

X = 10.0 NU = 28.75
RE = 1528.6 PR = 246.1 M = 1.02 GR = 13.4 PRG = 296.5
TPO = 29.22 TPI = 28.96 TX = 25.84 Q = 3212.3 QL = 8.7

X = 12.0 NU = 28.40
RE = 1529.1 PR = 246.1 M = 1.02 GR = 13.6 PRG = 296.4
TPO = 29.27 TPI = 29.01 TX = 25.85 Q = 3215.4 QL = 8.7

X = 15.0 NU = 26.33
RE = 1532.0 PR = 245.6 M = 1.03 GR = 14.7 PRG = 295.8
TPO = 29.51 TPI = 29.25 TX = 25.85 Q = 3209.2 QL = 9.1

X = 20.0 NU = 25.23
RE = 1533.8 PR = 245.3 M = 1.03 GR = 15.4 PRG = 295.5
TPO = 29.67 TPI = 29.41 TX = 25.85 Q = 3211.3 QL = 9.3

X = 25.0 NU = 23.90
RE = 1536.1 PR = 244.9 M = 1.03 GR = 16.3 PRG = 295.0
TPO = 29.87 TPI = 29.61 TX = 25.86 Q = 3210.3 QL = 9.6

X = 40.0 NU = 22.52
RE = 1538.9 PR = 244.5 M = 1.03 GR = 17.4 PRG = 294.5
TPO = 30.11 TPI = 29.85 TX = 25.87 Q = 3210.3 QL = 10.0

X = 97.0 NU = 19.98
RE = 1545.3 PR = 243.4 M = 1.03 GR = 19.8 PRG = 293.2
TPO = 30.67 TPI = 30.41 TX = 25.91 Q = 3210.7 QL = 10.8

TEST NO. 238 COMPOSITION 0.5% CARBOPOL (CPM) 934 n = 0.55

V1 = 2.382 V2 = 1.517 A = 194.820 TIA = 25.69 TOUT= 25.94 TOTH = 25.93
R1 = 2.8575 R2 = 0.8547 L1 = 2.7560 L2 = 1.7040
FLUX1 = 937.9 FLUX2 = 3220.3 AVISC = .1820E 00

X	HLX	REG	REI	GRI	G2X	G2I	G2X3	G2I3
.000E 00	.860E 03	.732E 02	.881E 02	.644E 01	.177E 06	.176E 06	.559E 02	.559E 02
.100E 02	.367E 03	.740E 02	.891E 02	.154E 02	.884E 04	.879E 04	.206E 02	.206E 02
.300E 02	.240E 03	.748E 02	.900E 02	.241E 02	.295E 04	.292E 04	.143E 02	.143E 02
.460E 02	.206E 03	.752E 02	.905E 02	.285E 02	.192E 04	.190E 04	.124E 02	.124E 02
.470E 02	.201E 03	.753E 02	.905E 02	.292E 02	.188E 04	.186E 04	.123E 02	.123E 02
.480E 02	.200E 03	.753E 02	.906E 02	.294E 02	.184E 04	.182E 04	.122E 02	.122E 02
.500E 00	.114E 04	.127E 04	.152E 04	.121E 02	.591E 06	.587E 06	.836E 02	.834E 02
.100E 01	.116E 04	.127E 04	.152E 04	.119E 02	.296E 06	.294E 06	.663E 02	.662E 02
.200E 01	.116E 04	.127E 04	.152E 04	.119E 02	.148E 06	.147E 06	.527E 02	.525E 02
.300E 01	.111E 04	.127E 04	.152E 04	.123E 02	.985E 05	.978E 05	.460E 02	.459E 02
.400E 01	.114E 04	.127E 04	.152E 04	.121E 02	.739E 05	.734E 05	.418E 02	.417E 02
.550E 01	.109E 04	.127E 04	.153E 04	.126E 02	.537E 05	.533E 05	.376E 02	.375E 02
.700E 01	.108E 04	.127E 04	.153E 04	.128E 02	.422E 05	.419E 05	.347E 02	.346E 02
.850E 01	.103E 04	.127E 04	.153E 04	.133E 02	.348E 05	.345E 05	.325E 02	.324E 02
.100E 02	.103E 04	.127E 04	.153E 04	.134E 02	.296E 05	.293E 05	.308E 02	.307E 02
.120E 02	.102E 04	.127E 04	.153E 04	.136E 02	.246E 05	.244E 05	.290E 02	.289E 02
.150E 02	.943E 03	.127E 04	.153E 04	.147E 02	.197E 05	.195E 05	.269E 02	.268E 02
.200E 02	.904E 03	.127E 04	.153E 04	.154E 02	.148E 05	.146E 05	.245E 02	.244E 02
.250E 02	.856E 03	.128E 04	.153E 04	.163E 02	.118E 05	.117E 05	.227E 02	.226E 02
.400E 02	.807E 03	.128E 04	.154E 04	.174E 02	.739E 04	.732E 04	.194E 02	.194E 02
.970E 02	.716E 03	.128E 04	.154E 04	.198E 02	.305E 04	.301E 04	.145E 02	.144E 02
.990E 02	.646E 03	.129E 04	.155E 04	.219E 02	.298E 04	.295E 04	.144E 02	.143E 02
.100E 03	.646E 03	.129E 04	.155E 04	.219E 02	.295E 04	.292E 04	.144E 02	.143E 02

TEST NO. 261

X = 0.0	NU = 36.81						
RE = 27.2	PR = 1599.8	M = 1.02	GR = 7.8	PRG = 1866.4			
TPO = 23.71	TPI = 23.68	TX = 20.99	Q = 1045.0	QL = 6.0			
X = 10.0	NU = 23.83						
RE = 27.5	PR = 1582.1	M = 1.03	GR = 12.5	PRG = 1845.8			
TPO = 25.26	TPI = 25.23	TX = 21.09	Q = 1045.0	QL = 6.0			
X = 30.0	NU = 15.85						
RE = 27.9	PR = 1557.0	M = 1.04	GR = 19.5	PRG = 1816.5			
TPO = 27.51	TPI = 27.48	TX = 21.27	Q = 1043.4	QL = 7.6			
X = 46.0	NU = 13.41						
RE = 28.1	PR = 1543.0	M = 1.05	GR = 23.7	PRG = 1800.2			
TPO = 28.78	TPI = 28.75	TX = 21.41	Q = 1042.5	QL = 8.5			
X = 47.0	NU = 13.43						
RE = 28.1	PR = 1543.0	M = 1.05	GR = 23.7	PRG = 1800.1			
TPO = 28.78	TPI = 28.75	TX = 21.42	Q = 1042.8	QL = 8.5			
X = 48.0	NU = 13.33						
RE = 28.2	PR = 1542.2	M = 1.05	GR = 23.9	PRG = 1799.3			
TPO = 28.84	TPI = 28.81	TX = 21.43	Q = 1042.8	QL = 8.5			
X = 0.5	NU = 14.50						
RE = 399.6	PR = 363.4	M = 1.05	GR = 10.9	PRG = 423.9			
TPO = 28.69	TPI = 28.40	TX = 21.43	Q = 3579.6	QL = 17.8			
X = 1.0	NU = 14.32						
RE = 399.8	PR = 363.2	M = 1.05	GR = 11.0	PRG = 423.7			
TPO = 28.78	TPI = 28.49	TX = 21.43	Q = 3579.6	QL = 17.8			
X = 2.0	NU = 14.42						
RE = 399.9	PR = 363.1	M = 1.05	GR = 11.1	PRG = 423.6			
TPO = 28.80	TPI = 28.51	TX = 21.43	Q = 3613.2	QL = 17.9			
X = 3.0	NU = 14.38						
RE = 399.9	PR = 363.1	M = 1.05	GR = 11.1	PRG = 423.6			
TPO = 28.82	TPI = 28.53	TX = 21.44	Q = 3613.2	QL = 17.9			
X = 4.0	NU = 14.36						
RE = 400.0	PR = 363.0	M = 1.05	GR = 11.1	PRG = 423.5			
TPO = 28.84	TPI = 28.55	TX = 21.44	Q = 3618.0	QL = 17.9			
X = 5.5	NU = 14.15						
RE = 400.3	PR = 362.8	M = 1.05	GR = 11.3	PRG = 423.2			
TPO = 28.93	TPI = 28.64	TX = 21.44	Q = 3608.2	QL = 18.1			
X = 7.0	NU = 14.16						
RE = 400.3	PR = 362.7	M = 1.05	GR = 11.3	PRG = 423.2			
TPO = 28.96	TPI = 28.66	TX = 21.45	Q = 3619.4	QL = 18.1			
X = 8.5	NU = 13.90						
RE = 400.6	PR = 362.4	M = 1.05	GR = 11.5	PRG = 422.8			
TPO = 29.07	TPI = 28.78	TX = 21.45	Q = 3606.4	QL = 18.3			
X = 10.0	NU = 13.90						
RE = 400.7	PR = 362.4	M = 1.05	GR = 11.5	PRG = 422.8			
TPO = 29.09	TPI = 28.80	TX = 21.46	Q = 3614.5	QL = 18.3			
X = 12.0	NU = 13.77						
RE = 400.9	PR = 362.2	M = 1.05	GR = 11.6	PRG = 422.6			
TPO = 29.16	TPI = 28.86	TX = 21.46	Q = 3611.5	QL = 18.4			
X = 15.0	NU = 13.71						
RE = 401.0	PR = 362.1	M = 1.05	GR = 11.7	PRG = 422.4			
TPO = 29.20	TPI = 28.91	TX = 21.47	Q = 3613.3	QL = 18.5			
X = 20.0	NU = 13.45						
RE = 401.4	PR = 361.7	M = 1.05	GR = 12.0	PRG = 422.0			
TPO = 29.36	TPI = 29.06	TX = 21.48	Q = 3612.3	QL = 18.7			
X = 25.0	NU = 13.24						
RE = 401.8	PR = 361.4	M = 1.05	GR = 12.2	PRG = 421.6			
TPO = 29.49	TPI = 29.20	TX = 21.50	Q = 3612.0	QL = 18.9			
X = 40.0	NU = 13.01						
RE = 402.2	PR = 360.9	M = 1.06	GR = 12.5	PRG = 421.0			
TPO = 29.67	TPI = 29.37	TX = 21.54	Q = 3612.0	QL = 19.1			
X = 97.0	NU = 11.86						
RE = 404.7	PR = 358.5	M = 1.06	GR = 14.0	PRG = 418.3			
TPO = 30.58	TPI = 30.29	TX = 21.70	Q = 3611.0	QL = 20.5			
X = 99.0	NU = 11.56						
RE = 405.2	PR = 358.1	M = 1.06	GR = 14.2	PRG = 417.8			
TPO = 30.76	TPI = 30.47	TX = 21.71	Q = 3611.0	QL = 20.8			

0·25% CARBOPOL 934

n = 0·60

(CONVERGENCE)

TEST NO. 261 COMPOSITION 0.25% (W/W) CARBOPOL 934 n = 0.60

V1 = 2.525 V2 = 1.618 A = 205.960 TIN = 20.99 TOUT = 21.68 TOTH = 21.71
R1 = 2.8575 R2 = 0.8547 L1 = 2.7560 L2 = 1.7090
FLUX1 = 1051.0 FLUX2 = 3631.1 AVISC = .2314E 00

X	HLX	RFG	REI	GRI	GZX	GZI	GZX3	GZI3
.000E 00	.390E 03	.233E 02	.272E 02	.784E 01	.683E 05	.678E 05	.407E 02	.406E 02
.100E 02	.252E 03	.236E 02	.275E 02	.124E 02	.341E 04	.338E 04	.150E 02	.150E 02
.300E 02	.168E 03	.239E 02	.279E 02	.195E 02	.114E 04	.112E 04	.104E 02	.104E 02
.460E 02	.142E 03	.241E 02	.281E 02	.236E 02	.742E 03	.728E 03	.903E 01	.898E 01
.470E 02	.142E 03	.241E 02	.281E 02	.236E 02	.726E 03	.713E 03	.897E 01	.891E 01
.480E 02	.141E 03	.241E 02	.281E 02	.238E 02	.711E 03	.698E 03	.890E 01	.885E 01
.500E 00	.514E 03	.343E 03	.399E 03	.108E 02	.228E 06	.224E 06	.608E 02	.605E 02
.100E 01	.507E 03	.343E 03	.399E 03	.110E 02	.114E 06	.112E 06	.483E 02	.480E 02
.200E 01	.511E 03	.343E 03	.399E 03	.110E 02	.570E 05	.560E 05	.383E 02	.381E 02
.300E 01	.509E 03	.343E 03	.399E 03	.110E 02	.380E 05	.373E 05	.335E 02	.333E 02
.400E 01	.509E 03	.343E 03	.399E 03	.111E 02	.285E 05	.280E 05	.304E 02	.303E 02
.550E 01	.501E 03	.343E 03	.400E 03	.112E 02	.207E 05	.204E 05	.274E 02	.272E 02
.700E 01	.502E 03	.343E 03	.400E 03	.113E 02	.163E 05	.160E 05	.253E 02	.251E 02
.850E 01	.492E 03	.343E 03	.400E 03	.115E 02	.134E 05	.132E 05	.237E 02	.235E 02
.100E 02	.492E 03	.343E 03	.400E 03	.115E 02	.114E 05	.112E 05	.224E 02	.223E 02
.120E 02	.488E 03	.344E 03	.400E 03	.116E 02	.950E 04	.933E 04	.211E 02	.210E 02
.150E 02	.486E 03	.344E 03	.400E 03	.117E 02	.760E 04	.746E 04	.196E 02	.195E 02
.200E 02	.477E 03	.344E 03	.401E 03	.119E 02	.570E 04	.559E 04	.178E 02	.177E 02
.250E 02	.469E 03	.344E 03	.401E 03	.121E 02	.456E 04	.447E 04	.165E 02	.164E 02
.400E 02	.461E 03	.345E 03	.401E 03	.124E 02	.285E 04	.279E 04	.141E 02	.140E 02
.970E 02	.420E 03	.347E 03	.404E 03	.139E 02	.117E 04	.115E 04	.105E 02	.105E 02
.990E 02	.410E 03	.347E 03	.404E 03	.143E 02	.115E 04	.113E 04	.105E 02	.104E 02
.100E 03	.414E 03	.347E 03	.404E 03	.141E 02	.114E 04	.112E 04	.104E 02	.103E 02

TEST NO. 267 1% (W/W) SODIUM CARBOXYMETHYLCELLULOSE n = 0.76

X = 0.0 NU = 128.36
RE = 203.3 PR = 451.4 M = 1.03 GR = 43.1 PRG = 487.0
TPO = 21.54 TPI = 21.49 TX = 20.26 Q = 1666.9 QL = 4.0

X = 10.0 NU = 30.39
RE = 223.9 PR = 409.7 M = 1.13 GR = 221.7 PRG = 442.1
TPO = 25.57 TPI = 25.52 TX = 20.33 Q = 1666.9 QL = 4.0

X = 30.0 NU = 19.54
RE = 240.2 PR = 381.7 M = 1.21 GR = 400.1 PRG = 411.9
TPO = 28.58 TPI = 28.53 TX = 20.47 Q = 1664.9 QL = 6.2

(CONVERGENCE)

X = 46.0 NU = 16.56
RE = 249.0 PR = 368.1 M = 1.25 GR = 511.1 PRG = 397.2
TPO = 30.13 TPI = 30.08 TX = 20.58 Q = 1664.3 QL = 7.3

X = 47.0 NU = 16.69
RE = 255.6 PR = 358.7 M = 1.29 GR = 603.0 PRG = 387.0
TPO = 31.27 TPI = 31.22 TX = 20.59 Q = 1652.6 QL = 8.1

X = 48.0 NU = 16.43
RE = 249.2 PR = 367.9 M = 1.25 GR = 512.6 PRG = 397.0
TPO = 30.16 TPI = 30.11 TX = 20.59 Q = 1652.6 QL = 8.1

X = 0.5 NU = 24.29
RE = 1859.9 PR = 164.8 M = 1.17 GR = 48.0 PRG = 177.8
TPO = 27.73 TPI = 27.27 TX = 20.59 Q = 5732.2 QL = 11.7

X = 1.0 NU = 24.21
RE = 1860.9 PR = 164.7 M = 1.17 GR = 48.2 PRG = 177.7
TPO = 27.76 TPI = 27.29 TX = 20.59 Q = 5732.2 QL = 11.7

X = 2.0 NU = 24.80
RE = 1857.7 PR = 165.0 M = 1.17 GR = 47.5 PRG = 178.0
TPO = 27.69 TPI = 27.22 TX = 20.60 Q = 5806.9 QL = 11.6

X = 3.0 NU = 23.60
RE = 1868.7 PR = 164.0 M = 1.18 GR = 49.9 PRG = 177.0
TPO = 27.93 TPI = 27.47 TX = 20.60 Q = 5709.1 QL = 12.0

X = 4.0 NU = 23.98
RE = 1866.5 PR = 164.2 M = 1.18 GR = 49.4 PRG = 177.2
TPO = 27.89 TPI = 27.42 TX = 20.60 Q = 5781.1 QL = 11.9

X = 5.5 NU = 23.05
RE = 1876.4 PR = 163.3 M = 1.18 GR = 51.6 PRG = 176.2
TPO = 28.11 TPI = 27.65 TX = 20.60 Q = 5739.7 QL = 12.2

X = 7.0 NU = 23.19
RE = 1876.3 PR = 163.3 M = 1.18 GR = 51.5 PRG = 176.2
TPO = 28.11 TPI = 27.64 TX = 20.61 Q = 5770.2 QL = 12.2

X = 8.5 NU = 22.44
RE = 1885.2 PR = 162.6 M = 1.19 GR = 53.5 PRG = 175.4
TPO = 28.31 TPI = 27.85 TX = 20.61 Q = 5741.0 QL = 12.5

X = 10.0 NU = 22.55
RE = 1885.1 PR = 162.6 M = 1.19 GR = 53.5 PRG = 175.4
TPO = 28.31 TPI = 27.84 TX = 20.61 Q = 5765.8 QL = 12.5

X = 12.0 NU = 21.84
RE = 1894.9 PR = 161.7 M = 1.19 GR = 55.7 PRG = 174.5
TPO = 28.53 TPI = 28.07 TX = 20.62 Q = 5752.2 QL = 12.8

X = 15.0 NU = 21.29
RE = 1903.7 PR = 161.0 M = 1.20 GR = 57.7 PRG = 173.7
TPO = 28.73 TPI = 28.27 TX = 20.62 Q = 5754.3 QL = 13.1

X = 20.0 NU = 20.60
RE = 1915.5 PR = 160.0 M = 1.21 GR = 60.4 PRG = 172.6
TPO = 29.00 TPI = 28.53 TX = 20.63 Q = 5753.7 QL = 13.5

X = 25.0 NU = 20.23
RE = 1922.4 PR = 159.4 M = 1.21 GR = 62.0 PRG = 172.0
TPO = 29.16 TPI = 28.69 TX = 20.64 Q = 5754.3 QL = 13.8

X = 40.0 NU = 18.89
RE = 1949.3 PR = 157.2 M = 1.23 GR = 68.4 PRG = 169.6
TPO = 29.76 TPI = 29.29 TX = 20.68 Q = 5753.2 QL = 14.7

X = 97.0 NU = 16.58
RE = 2009.1 PR = 152.5 M = 1.26 GR = 83.5 PRG = 164.5
TPO = 31.07 TPI = 30.64 TX = 20.80 Q = 5753.1 QL = 16.6

X = 99.0 NU = 15.37
RE = 2041.3 PR = 150.1 M = 1.28 GR = 92.3 PRG = 161.9
TPO = 31.77 TPI = 31.30 TX = 20.80 Q = 5708.0 QL = 17.7

91.7 PRG = 162.1
GR = QL = 17.7

TEST NO. 267 COMPOSITION 1% (W/W) SODIUM CARBOXY METHYL CELLULOSE (CELLOFAS 850)

n = 0.76

V1 = 3.188 V2 = 2.041 A = 259.360 TIN = 20.26 TOUT = 20.83 TOTH = 20.80
R1 = 2.8575 R2 = 0.9547 L1 = 2.7560 L2 = 1.7090
FLUX1 = 1671.0 FLUX2 = 5768.0 AVISC = *.6517E-01

X	HLX	RFG	REI	GRI	GZX	GZI	GZX3	GZI3
.000E 00	.136E 04	.188F 03	.203E 03	.430E 02	.144E 06	.144E 06	.522E 02	.522E 02
.100E 02	.321E 03	.208F 03	.224E 03	.221E 03	.721E 04	.711E 04	.193E 02	.192E 02
.300E 02	.207E 03	.223F 03	.240E 03	.399E 03	.240E 04	.235E 04	.134E 02	.133E 02
.460E 02	.175F 03	.231E 03	.248E 03	.509E 03	.157E 04	.153F 04	.116E 02	.115E 02
.470F 02	.155F 03	.237F 03	.255E 03	.600E 03	.153E 04	.149E 04	.115E 02	.114E 02
.480F 02	.174F 03	.231F 03	.249E 03	.510E 03	.150E 04	.146E 04	.114E 02	.113E 02
.500E 00	.859F 03	.172F 04	.186E 04	.478E 02	.481E 06	.473E 06	.780E 02	.776E 02
.100F 01	.856E 03	.172F 04	.186E 04	.480E 02	.241E 06	.237E 06	.620E 02	.616E 02
.200F 01	.877E 03	.172F 04	.185E 04	.473E 02	.120E 06	.118F 06	.492E 02	.489E 02
.300F 01	.831E 03	.173F 04	.187E 04	.497E 02	.802E 05	.788E 05	.430E 02	.427F 02
.400E 01	.848E 03	.173E 04	.186E 04	.492E 02	.602E 05	.591E 05	.390E 02	.388E 02
.550E 01	.815F 03	.174F 04	.187E 04	.514E 02	.438E 05	.430F 05	.351E 02	.349E 02
.700E 01	.820E 03	.174E 04	.187E 04	.514E 02	.344E 05	.338E 05	.324E 02	.322E 02

.850E 01	.547F 03	.919F 03	.990E 03	.401E 02	.170E 05	.167E 05	.256E 02	.255E 02
.100E 02	.548E 03	.919F 03	.990E 03	.403E 02	.144E 05	.142E 05	.243E 02	.241E 02
.120E 02	.543E 03	.921F 03	.992E 03	.408E 02	.120E 05	.118E 05	.228E 02	.227E 02
.150E 02	.535E 03	.923F 03	.994E 03	.416E 02	.961E 04	.943E 04	.212E 02	.211E 02
.200E 02	.522F 03	.928E 03	.999E 03	.431E 02	.721E 04	.707E 04	.193E 02	.191E 02
.250E 02	.516F 03	.930F 03	.100E 04	.437E 02	.577E 04	.566E 04	.179E 02	.178E 02
.400E 02	.506E 03	.934F 03	.101E 04	.452E 02	.360E 04	.353E 04	.153E 02	.152E 02
.970E 02	.450F 03	.958F 03	.103E 04	.539E 02	.149E 04	.145E 04	.114E 02	.113E 02
.990E 02	.456F 03	.958F 03	.103E 04	.538F 02	.146E 04	.142F 04	.113E 02	.112E 02
.100E 03	.434F 03	.966F 03	.104E 04	.573F 02	.144E 04	.141E 04	.113E 02	.112E 02